APPLICATION OF COUMARIN DERIVATIVES IN DNA-ASSOCIATED STUDY: MUTATION DETECTION, SITE-SPECIFIC LABELING, PHOTOINDUCED INTERSTRAND CROSS-LINKS AND LIGATION REACTIONS

by

Huabing Sun

A Dissertation Submitted in

Partial Fulfillment of the

Requirements for the Degree of

Doctor of Philosophy

In Chemistry

at

The University of Wisconsin-Milwaukee

May 2015

ABSTRACT
APPLICATION OF COUMARIN DERIVATIVES IN DNA-ASSOCIATED STUDY: MUTATION DETECTION, SITE-SPECIFIC LABELING, PHOTOINDUCED INTERSTRAND CROSS-LINKS AND LIGATION REACTIONS

by

Huabing Sun

The University of Wisconsin-Milwaukee, 2015
Under the Supervision of Professor Xiaohua Peng

Coumarin derivatives have been widely utilized as cross-linking agents in polymer science, being fluoroprobes in biochemistry and as medicines in pharmacy. But the coumarin's fluorogenic properties and reactivities in DNA were rarely reported and unclear, which limits its bioapplications due to possible side reactions towards biomolecules. In this thesis, we investigated the activity of coumarin moiety towards natural DNA and expanded its application in DNA-associated study. We have found that coumarin derivatives can serve as perfect DNA cross-linking agents, as alkylation agents for site-specific labeling, and fluoroprobes for single nucleotide polymorphism (SNP) analysis, which provided a novel insight of biotoxicity of coumarin in biological system and a novel bioanalytical tool.

First, sequence-dependent DNA-templated fluorogenic "click" reaction has been developed for SNP detection. Oligonucleotide (ODN) probes containing nonfluorescent alkyne-modified coumarin or azide group at the terminal sites efficiently hydride with the matched ODN template, a tumor-associated p53 gene with single nucleotide transition from dT to dC. The alkyne and azide groups at the adjacent position provided effective concentration for fluorogenic "click" reaction which generated substantial fluorescence signal. However, no obvious fluorescence was observed for noncomplementary DNA

templates. In this way, coumarin-based fluorogenic “click” reaction can be used for SNP analysis. In addition, the coumarin derivatives with the bromo group were employed as alkylation agents for site-specifically labeling dT in natural DNA, affording highly fluorescent ODNs for bioanalysis.

Second, we have found that the coumarin moieties induced quantitative photoreversible DNA interstrand cross-link (ICL) formation with dT allowing for real-time monitoring DNA cross-linking process via fluorescence assay. Photoinduced [2+2] cycloaddition between coumarin moiety and thymidine upon 350 nm irradiation generated DNA ICLs with formation of *syn*- and *anti*-cyclobutane adducts, which can be reversed into the single stranded ODNs with 254 nm photoirradiation. ICL formation completely quenched the fluorescence of coumarin, which, for the first time, enables fast and real-time detection of DNA cross-linking and photoreversibile process via fluorescence spectroscopy.

Finally, rearrangement of the kinetic-controlled ligation products to the thermo-controlled ICL products was observed during photoswitchable process. In addition, light-sensitive and sequence-specific photorelease of coumarin moieties from ODN strand was discovered. Further study showed that the G:C base pairs and 350 nm irradiation played a central role in the reaction.

TABLE OF CONTENTS

Abstract ii

Table of Contents iv

List of Figures viii

List of Tables xii

List of Abbreviations xiii

Acknowledgements xv

CHAPTER PAGE

1. **Introduction** 1

1.1. Coumarin and Its Derivatives 1

1.2. The Applications of Coumarin 3

1.2.1. Fluorescent Chemosensors 3

1.2.2. Pharmacotherapy and Cross-Linking Agents 6

1.2.3. Application of Coumarin in DNA 9

1.3. DNA-Templated Reactions 11

1.3.1. DNA Synthesis and Modification 11

1.3.2. DNA Interstrand Cross-Link Reaction 16

1.3.3. DNA Ligation Reactions 20

1.3.4. Potential Application of Coumarin in DNA 23

1.4. References 26

2. **Template-Directed Fluorogenic Click Reaction: DNA Interstrand Cross-Linking, Oligonucleotide Ligation, and Single Nucleotide Discrimination** .. 30

2.1. Introduction 30

2.2. ODN Probes for Fluorogenic Reaction 33

2.2.1. Preparation of the ODNs Containing Alkyne-Modified Coumarin . 33

2.2.2. Thermal Stability Study 36

2.3. Fluorogenic DNA Interstrand Cross-Linking via Click Reaction 37

2.3.1. Efficiency of Click Reaction 37

2.3.2. Detection of ICL via Fluorescence Assay 39

2.3.3. Selectivity of Fluorogenic DNA Interstrand Cross-Linking 41

2.4. Single Nucleotide Discrimination via the Fluorogenic Click Ligation Reaction 42

2.4.1. Optimization of Probes 42

2.4.2. Single Nucleotide Discrimination 50

2.5. Preparation of PNA Monomers 53

2.6. Future Study: Copper-Free Click Reaction 55

2.7. Experimental Section 56

2.8. References 73

2.9. Appendices A: Characterization of Compounds 77

3. **Site-Specific Fluorescence Labeling of Natural DNA** 88

3.1. Introduction 88

3.2. Synthesis of Fluorescent Tags for DNA Labeling 89

3.3. Reactivity of Labeling Agents towards Nuclic Acids 91

3.4. Optimization of the Reaction Condition for DNA Labeling 93

3.5. Sequence-Depentent DNA Labeling 94

3.6. Future Study 95

3.7. Experimental Section 96

3.8. References 102

3.9. Appendices B: Characterization of Compounds 104

4. **Photo-Reversible DNA Interstrand Cross-Linking by Coumarin** 114

4.1. Introduction 114

4.2. Coumarin-Containing ODNs for ICL Study 116

4.2.1. Synthesis of Coumarin Derivatives 116

4.2.2. Preparation of the ODNs 118

4.2.3. Thermal Stability Study 119

4.3. Structure Determination of Coumarin-dT Adducts 120

4.3.1. LC-MS Analysis for Monomer Reaction 120

4.3.2. [2+2] Cycloaddition between **1** and dT 123

4.4. The Effects of Linker and Flanking Sequences on ICL 124

4.4.1. Linker Effect on Cross-Linking Efficiency 124

4.4.2. Flanking Sequence-Dependent Cross-Link Formation 126

4.5. ICL Detection via Fluorescence Assay 129

4.5.1. Design Principle 129

4.5.2. Fluorescence Assay for Monitoring ICL Formation 131

4.6. Photoreversible DNA Cross-Linking 135

4.7. Mutation Detection 137

4.8. The Effect of Incorporation Site on ICL Formation 139

4.9. Experimental Section 141

4.10. References 154

5. **Rearrangement of Coumarin-Induced DNA Intrastrand Cross-Linking to Interstrand Cross-Linking** 159

5.1. Introduction 159

5.2. Synthesis of ODNs Containing Coumarin Moieties 159

5.3. The Effects of dT Position and Linker on the ICL Efficiency 161

5.4. Coumarin-Induced ICL and Ligation Reaction 164

5.5. Rearrangement and Photorelease of the Coumarin Moiety 167

5.5.1. Rearrangement during Photoswitchable Process 167

5.5.2. Photorelease Reaction 170

5.6. Experimental Section 171

5.7. References 174

5.8. Appendices C: Characterization of Compounds 175

Curriculum Vitae 177

LIST OF FIGURES

Figure 1-1. The structures of coumarin and its derivatives 1

Figure 1-2. Synthesis of the coumarins via Perkin reaction (a) and Pechmann condensation (b) 2

Figure 1-3. Energy diagram of fluorescence (a) and intramolecular charge transfer (b) 4

Figure 1-4. Chemosensors and the detection of Hg^{2+} (a), pH (b), and H_2O_2 (c)..... 5

Figure 1-5. Metabolism (a) and pharmacology (b) of coumarins 6

Figure 1-6. Photodimerization and cleavage of coumarin 8

Figure 1-7. Photoreversible crosslink of the polyoxazoline containing coumarin . 9

Figure 1-8. Coumarin-based fluorogenic click reactions..... 10

Figure 1-9. Preparation of fluorescent ODNs via the fluorogenic reaction..... 11

Figure 1-10. Preparation of ODNs via DNA solid-phase synthesis 13

Figure 1-11. Linkages and reactions for ODNs post-conjugation 15

Figure 1-12. DNA interstrand cross-link agents 17

Figure 1-13. DNA interstrand cross-links with modified DNA constructs 18

Figure 1-14. Examples of DNA templated ligation reactions 21

Figure 1-15. Selectively post-labeling natural DNA with coumarins..... 25

Figure 2-1. Detection of p53 mutations via a fluorogenic “click” reaction 33

Figure 2-2. The synthesis of alkyne-modified coumarin phosphoramidite **7** 34

Figure 2-3. Synthesis of ODNs containing the azide group 34

Figure 2-4. The fluorogenic ICL reaction between ODN **4** and ODN **5** 39

Figure 2-5. Monitoring fluorogenic ICL reaction via fluorescence assay 40

Figure 2-6. Single-nucleotide-specific "click" cross-linking reaction 42

Figure 2-7. The selectivity of "click" ligation reactions using probe ODN **4** 44

Figure 2-8. Sequence-specific fluorogenic "click" ligation reaction for probes ODN **8** and ODN **10** in the presence of templates **12a-d**..... 47

Figure 2-9. Optimizations of the "click" ligation reaction conditions 48

Figure 2-10. Fluorogenic "click" ligation reaction between ODN **10** and ODN **11** in the presence of template **12a** 49

Figure 2-11. Detection of tumor's mutated nucleic acids via fluorogenic ligation reaction 50

Figure 2-12. Fluorescence spectra of ICL and ligation products..... 52

Figure 2-13. Synthesis of PNA and structure of duplex formed by PNA and DNA 54

Figure 2-14. Synthesis of azide-based PNA monomer 55

Figure 2-15. Synthesis of coumarin-based PNA monomer 55

Figure 2-16. Synthesis of coumarin-based biarylazacyclooctynone 56

Figure 3-1. N3-alkylation of thymidine and uridine..... 89

Figure 3-2. Preparation of alkylation agents **3** and **8** 90

Figure 3-3. N3-akylation of thymidine with **3** and **8** 92

Figure 3-4. Excitation and emission spectra of T, **3** and **10** 93

Figure 3-5. Fluorescence spectra of resulting ODNs under different conditions .. 94

Figure 3-6. Fluorescence spectra of resulting ODNs after the labeling for ODN-**A12**, **T12**, **G12**, and **T12** 95

Figure 3-7. Preparation of alkylation agent **14** for detection of H_2O_2 96

Figure 4-1. Preparation of phosphoramidites **8**-**13** 117

Figure 4-2. LC-MS analysis of photochemical reaction of **1** and nucleosides 123

Figure 4-3. Cycloaddition between **1** and dT, and fluorescence emission spectra of **1** and products. 124

Figure 4-4. PAGE analysis of ICL formation for ds DNA-**1**-**6** 125

Figure 4-5. List of ds DNAs used in the study 127

Figure 4-6. Fluorescence intensity of **4** when flanked by different bases 127

Figure 4-7. Cyclic voltammogram of coumarin **4** 128

Figure 4-8. PAGE analysis of ICL generation for ds DNA-**1**, **4**, and **7**-**9** 129

Figure 4-9. Fluorescence spectra of ds DNA-**4** before and after photoirradiation . 130

Figure 4-10. ICL formation rate of ds DNA-**4** via fluorescence assay..... 132

Figure 4-11. ICL formation rate of ds DNA-**7** via fluorescence assay..... 133

Figure 4-12. ICL formation rate of ds DNA-**8** via fluorescence assay..... 134

Figure 4-13. ICL formation rate of ds DNA-**9** via fluorescence assay..... 134

Figure 4-14. Photoreversible process for ds DNA-**4** over three cycles 136

Figure 4-15. Photoreversible process for ds DNA-**7** over three cycles 136

Figure 4-16. PAGE analysis of ICL formation for ds DNA-**11a-d** 137

Figure 4-17. Decreased fluorescence intensity at 385 nm for ds DNA-**11a-d**..... 138

Figure 4-18. PAGE analysis of ICL formation and cleavage of ds DNA-**10**, **12**, and **13** 140

Figure 5-1. Synthesis of the phosphoramidites **4-6** 160

Figure 5-2. Double stranded DNAs used in this study 161

Figure 5-3. PAGE analysis of distance-dependent ICL formation 163

Figure 5-4. PAGE analysis of ICL and ligation reactions for ds DNA-**13**/**14**..... 165

Figure 5-5. PAGE analysis of ICL and ligation reactions for ds DNA-**15**/**16** 166

Figure 5-6. Cross-link yields during photoreversible process for ds DNA-**13-16**.. 169

Figure 5-7. Photorelease reaction of **3** for ds DNA-**15**/**16**..... 171

LIST OF TABLES

Table 2-1. Oligodeoxynucleotides used in the study 35

Table 2-2. Duplex thermal stability 37

Table 2-3. Duplex melting temperatures (Tm) of ODN probes 45

Table 4-1. List of coumarin-containing ODNs 118

Table 4-2. Melting temperatures of ds DNA-**1**-**6**..... 120

Table 4-3. ICL formation rates for ds DNA-**1**-**6**..... 126

Table 4-4. Rate of ICL formation or cleavage for ds DNA-**4**, and **7**-**9**..... 132

Table 4-5. Rate of ICL formation or cleavage for ds DNA-**11a**-**d** 139

Table 4-6. Rate of ICL formation or cleavage for ds DNA-**10**, **12**, and **13** 141

Table 5-1. ICL reaction rates for ds DNA-**7**-**12** 163

Table 5-2. Rates of cross-link formation or cleavage for ds DNA-**13**-**16** 167

LIST OF ABBREVIATIONS

A	Adenosine
ATP	Adenosine triphosphate
C	Cytidine
CPG	Crushed porous glass
DCC	*N*,*N* -Dicyclohexylcarbodiimide
DIPEA	*N*,*N*-Diisopropylethylamine
DNA	2'-Deoxyribonucleic acid
DMF	Dimethylaminomethylene
DMSO	Dimethyl sulfoxide
DMTr	4′,4′-Dimethoxytrityl
ds DNA	Double-stranded DNA
EDTA	Ethylenediaminotetraacetic acid
ESI	Electrospray
EtOAc	Ethyl acetate
EtOH	Ethanol
Fmoc	Fluorenylmethyloxycarbonyl
G	Guanosine
HATU	*O*-(Azabenzotriazol-1-yl)-*N*,*N*,*N'*,*N'*-tetramethyluronium hexafluorophosphate
HBTU	*O*-(Benzotriazol-1-yl)-*N*,*N*,*N'*,*N'*-tetramethyluronium hexafluorophosphate
HRMS	High-resolution mass spectrometry
k	Reaction rate constant
MALDI-TOF	Matrix-assisted laser desorption/ionization – time of flight
MeCN	Acetonitrile

MeOH	Methanol
MS	Mass spectrometry
NMR	Nuclear magnetic resonance
NHS	*N*-Hydroxysuccinimide
Pac	Phenoxyacetyl
PNA	Peptide nucleic acid
^{i}Pr	Isopropyl
qPCR	Quantitative polymerase chain reaction
RNA	Ribonucleic acid
T	Thymidine
TBAF	Tert-n-butylammonium fluoride
TEA	Triethylamine
THF	Tetrahydrofuran
T_m	Melting temperature
TMS	Trimethylsilyl
TPP	Triphenylphosphine
U	Uridine
UV	Ultraviolet

ACKNOWLEDGMENTS

First of all, I would like to thank my advisor, Prof. Xiaohua Peng, for her kind support and thoughtful supervision. Her profound knowledge, excellent advice and professional training have helped me to become a better researcher and taught me the value of persistence for truth and nature of chemistry. Thanks to my previous advisors, Prof. Jing Li and Prof. Fuzhen Tian, for their nice training and kind help. I really appreciate the nice support and help from my committee members: Prof. Andy Pacheco, Prof. Alan Schwabacher, Prof. Alexander Arnold, and Prof. Mark Dietz. Thank Prof. Yinsheng Wang (University of California at Riverside) and Prof. J. Craig Blain (Harvard University) for their kind collaboration.

It is my great pleasure to be one member of Prof. Peng's Lab, which offers perfect opportunities to learn novel bio-techniques and interdisciplinary research from interesting discussions with talented coworkers. Thanks to Dr. Sheng Cao, Dr. Wenbing Chen, Dr. Yanyan Han, and Yibin Wang for kind assistance during my study and life; Mohammad Mojibul Haque, Heli Fan, and Hyeyoung Eom as good collaborators for their contribution to synthesize coumarin derivatives; Yunyan Kuang as a good collaborator for professional training of biotechniques; undergraduate students, without listing their name due to afraidness of missing someone, for their help in lab.

Sincere gratitude to staffs, lecturers and professors in the department of Chemistry & Biochemistry, I could not successfully complete my graduate studies without their support and help. Generous financial support from our department and University helping me a lot in expanding my opinions in biochemical issues is greatly acknowledged.

Last but not the least, special thanks to my family for their unconditionally support in these years: my parents, Shenglei Sun and Huanchun Zhang, taught me studious, optimistic, kind and social personalities being highly valuable in my life; my wife, Heli Fan, provided trust and great support all the time; and my son, Fan Sun, is training me to be a responsible father and gives me endless energy.

(Huabing Sun, Jan 2015 at UW-Milwaukee)

Chapter 1. Introduction

1.1. Coumarin and Its Derivatives

Coumarins, known as benzo-α-pyrones, were first isolated from Tonka beans in 1820s and first prepared by William Henry Perkin in 1868.[1-2] The non-substituted coumarin shows weak fluorescence, but its derivatives with suitable substitutions exhibit strong fluorescence with high fluorescence quantum yield and large Stokes shift.[3-5] For example, installation of an electron-withdrawing group at the position-3 and/or an electron-donating group at the position-7 can greatly enhance the fluorescence of the coumarin moiety.[6] Moreover, the coumarin can be substituted at varied positions, such as the position-3, 4, 6, 7, and 8. Usually, the coumarin with an electron-donating hydroxyl group at the positon-7 was considered as the parent of many coumarin analogues (Figure 1-1).

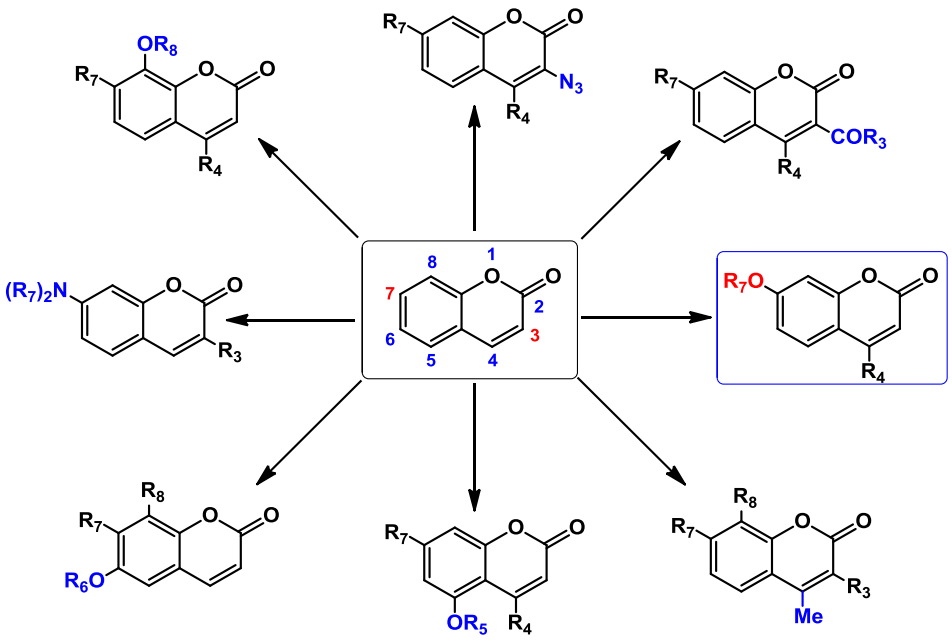

Figure 1-1. The structures of coumarin and its derivatives.

Initially, the coumarin was synthesized using the Perkin reaction via the aldol condensation of salicylaldehyde and acetic anhydride in the presence of sodium acetate as a base catalyst (Figure 1-2).[7] Later, the Pechmann condensation of resorcinol and malic acid/ethyl acetoacetate provided another more economical and efficient method for synthesis of coumarin and its derivatives. Condensation starts with electrophilic attack of the activated carbonyl group at the ortho position of benzene ring under acidic conditions. Then, esterification/transesterification and dehydration occurs yielding the coumarin moiety (Figure 1-2).[8-9] Most coumarin analogues in our studies were prepared via Pechmann condensation.

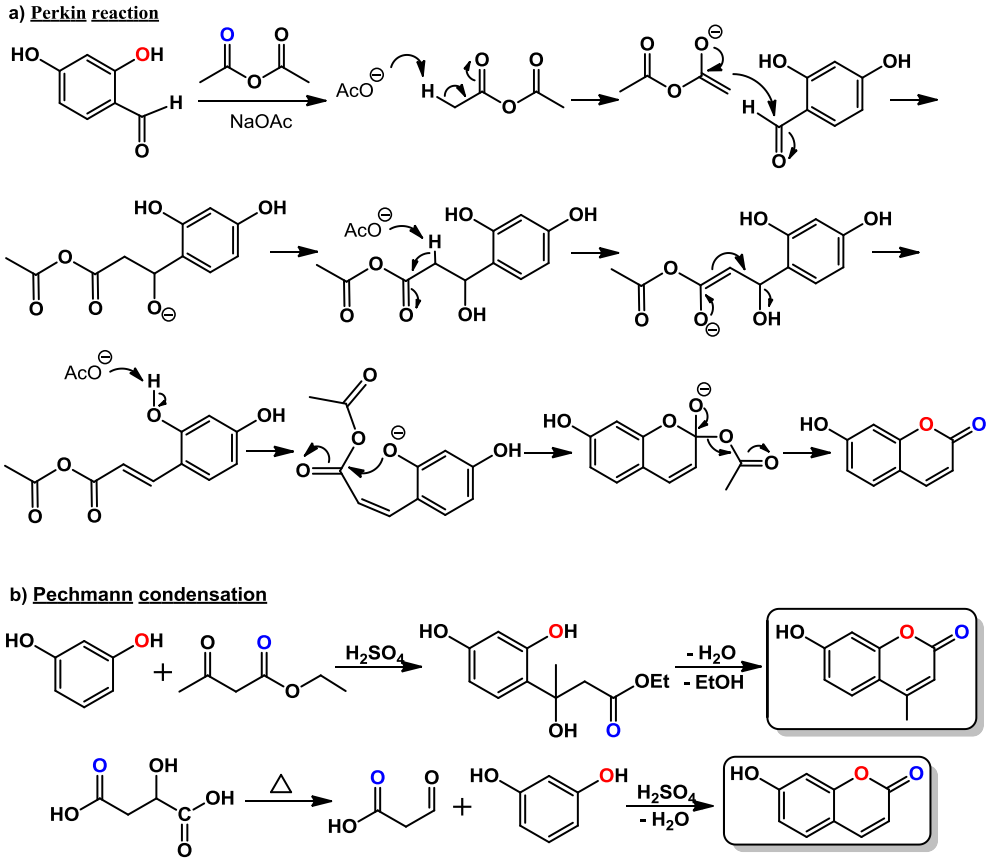

Figure 1-2. Synthesis of the coumarins via Perkin reaction (a) and Pechmann condensation (b).

1.2. The Applications of Coumarin

Due to the excellent photo-properties and photo-reactivities, coumarin and its analogues have found wide applications. They have been used as fluorophores, chemosensors, pharmacotherapy drugs, and cross-linking agents.

1.2.1. Fluorescent Chemosensors

The fluorescence of coumarin can be tuned by introducing different substituents with varied electron-donating/withdrawing abilities, which is widely used in design of coumarin derivatives. The substituents-dependent fluorescence properties of the coumarin moiety may result from intramolecular charge transfer.[10] It is well-known that π- π^* transitions can form the excited states via excitation from the HOMO (the highest occupied molecular orbital) to the LUMO (the lowest unoccupied molecular orbital). Then the internal conversion of the excited states to lower energy states occurs with loss of heat energy. Subsequently, the excited state would return to the ground state by emission of a photon as the form of fluorescence (Figure 1-3a). The emitted photon (light) with less energy has a longer wavelength, which can be distinguished from the excitation light. Usually, transitions of coumarin are related to the intra-molecular charge transfer from the benzene ring to the pyranone moiety. As shown in Figure 1-3b, an electron donating group at the position-7 and/or an electron-withdrawing group (-COOH) at the position-3 can promote the process, thereby enhancing the fluorescence intensity of coumarin.[11]

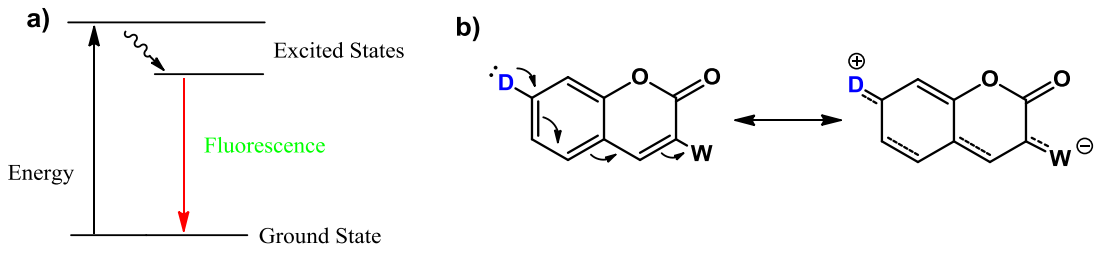

Figure 1-3. Energy diagram of fluorescence (a) and intramolecular charge transfer (b).

Coumarin derivatives serve as the fluorescent chemosensors for various metal ions including Hg (II), Cu (II), Ni (II), Zn (II), Fe (III), Al (III), Ca (II), Cr (III), and Ag (I), pH of the solution, and detection of biochemical agents such as hydrogen peroxide, nitric oxide, and nitroxide.[12-17] For example, chemosensors for detection of Hg^{2+} ions have been reported using Hg (II) ions-induced desulfurization reaction to afford fluorescent coumarin analogue (Figure 1-4a).[12] The non-conjugated chemosensor 2-hydroxy *cis*-comarinic acid **1** is weakly fluorescent, but can be converted to a highly fluorescent coumarin **2** which undergoes Hg^{2+}-catalyzed desulfurization-lactonization cascade.[12] This fluorescent sensor showed a non-fluorescent background, good selectivity and fast sensitivity towards Hg^{2+} (Figure 1-4a). Additionally, coumarin derivatives acted as pH-responsive fluorescent sensors. For example, compound **3** serves as a pH-dependent probe.[15] The pH-responsive photophysical properties of **3** result from the phenol moiety which is in an equilibrium between the protonated and deprotonated phenolate forms at different pH, while an electron-withdrawing group (e.g. -Cl) at the 6-position of coumarin reduces the pK_a value of **3** to the desired level. Moreover, the lipophilicity of the probe can be fine-tuned via introducing ammonium salts of carboxylic acids. The excitation intensity as well as the fluorescence intensity depended on pH value of solution (Figure 1-4b). A protonated form of **3** was produced at a low pH value, which

showed weaker fluorescent intensity than a deprotonated form generated under basic condition. In this way, it can be used as pH-responsive probes.

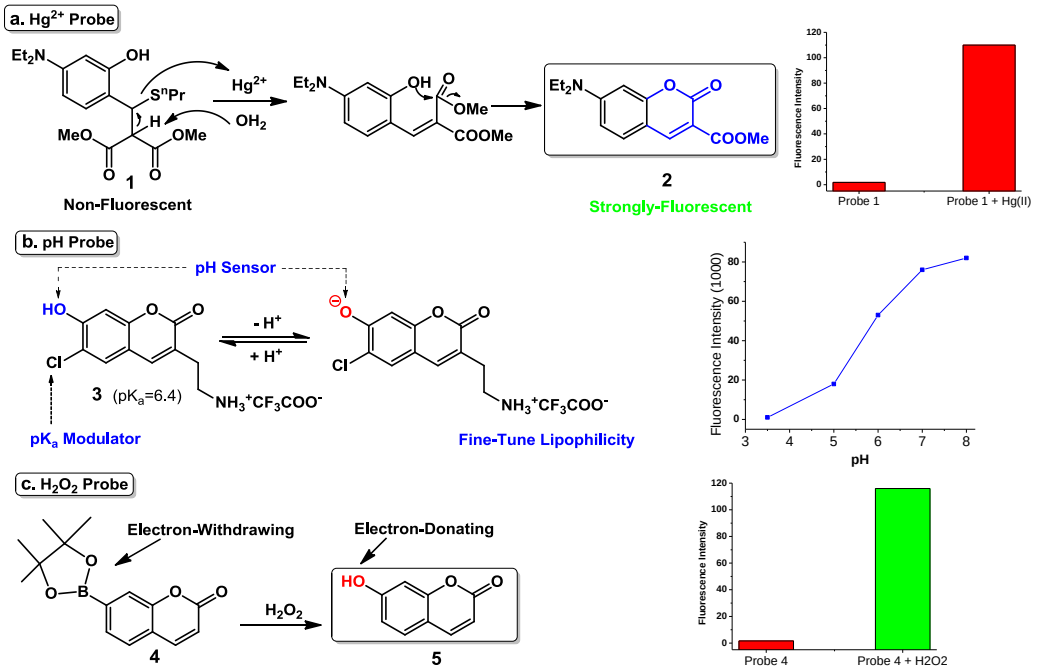

Figure 1-4. Chemosensors and the detection of Hg^{2+} (a), pH (b), and H_2O_2 (c).

Recently, coumarin-derived fluorescent chemosensors with minimal toxicity have been applied in the detection of biochemical agents, such as hydrogen peroxide, nitric oxide, nitroxide, and hydroxyl radicals.[16, 17] Introduction of an electron-withdrawing boronate group at the position-7 in probe **4** quenches the fluorescence of coumarin, while the boronate group can be selectively converted to an electron-donating hydroxyl group in the presence of hydrogen peroxide which greatly enhances the fluorescence intensity and the quantum yield of the coumarin moiety.[16] This water-soluble probe **4** showed good selectivity for hydrogen peroxide over other reactive oxygen species. About 100-fold enhancement of the fluorescence intensity was observed with **4** after reaction with hydrogen peroxide (Figure 1-4c).

1.2.2. Pharmacotherapy and Cross-Linking Agents

Recent studies showed that the coumarin derivatives have good pharmacological properties and photoreactivities. Thus, they are widely used as therapeutic agents or cross-linking agents in material science.

First of all, coumarin showed lower toxicity than other related compounds. They are moderately toxic to the liver and kidneys with a median lethal dose of 275 mg/kg. The coumarin derivatives have been widely used in foods, beverages, cosmetics, and tobacco.[18] They can be metabolized in body by a specific cytochrome P-450 system with hydroxylation majorly at the position-7 or 3 (Figure 1-5a). The yielded product 3-hydroxycoumarin can be further nonenzymatically metabolized to water-soluble o-hydroxyphenyl lactic acid and o-hydroxyphenylacetic acid via ring splitting.[19]

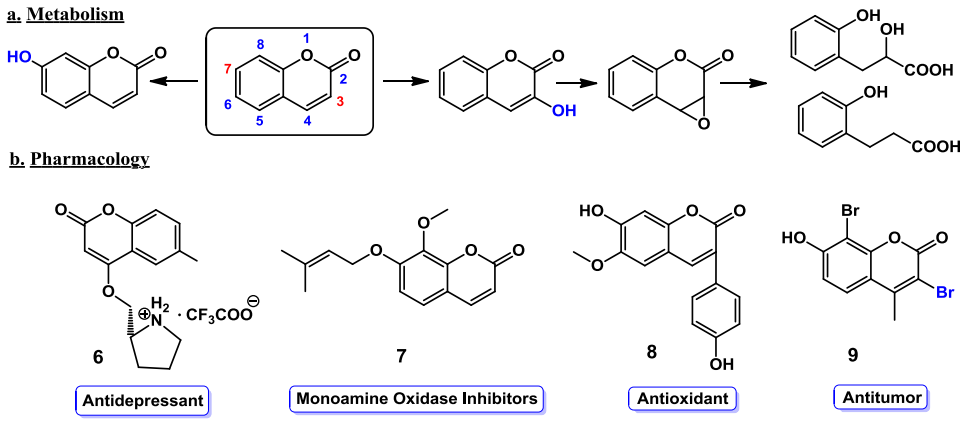

Figure 1-5. Metabolism (a) and pharmacology (b) of coumarins.

Besides low toxicity, coumarin analogues exhibit a broad spectrum of pharmacological properties, such as antidepressant, antimicrobial, antioxidant, anti-inflammatory, and anti-tumor activity (Figure 1-5b).[20-22] For example, coumarin derivatives can inhibit endogerous generation of reactive nitrogen species and reactive oxygen species with one

or more unpaired electrons. These reactive oxidants have important functions in physiological concentrations, such as cell signaling, inducing mitogenic response and defense against infection caused by microorganisms.[20] However, the excessive free radicals levels may lead to oxidative stress which causes damages to lipids, proteins and DNA. Coumarin derivatives exhibiting antioxidant properties have the capacity to reduce these harmful effects. For instance, nitric oxide serves as a molecular messenger, but overproduction of nitric oxide can cause disorder in central nervous system, resulting in depressant. The acetic acid salt derivative of coumarin **6** acts as the inhibitor of nitric oxide synthase, therefore controlling generation of nitric oxide.[20] Compound **6** can clinically use as anti-depressant. Coumarin derivatives also serve as monoamine oxidase inhibitors for treatment of Parkinson's disease. Suitable monoamine oxidase helps to maintain neuron firing rates in the body, but monoamine oxidase over normal level can generate toxic hydroxyl radicals leading to the neurodegenerative disorders such as Parkinson's disease. Compound **7** can efficiently inhibit excessive generation of monoamine oxide, thereby being used for treatment of Parkinson's disease.[21] Coumarins consisting of benzopyrone rings, such as coumarin **8**, have also shown antioxidant properties via reducing generation and stimulating the scavenging of oxidative species.[21] Interestingly, coumarins that act as protein kinase 2 inhibitors showed anti-tumor activites.[21] Protein kinase 2 known as pleiotropic enzymes controls a broad series of bioevents such as cell cycle regulation, gene expression, and RNA and protein synthesis. Studies demonstrated that its overexpression in a variety of tumors contributes to uncontrolled growth of tumors cells. Coumarin **9** can form strong electrostatic interactions with protein kinase 2 leading to loss of its bioactivity.[22] Thus, compound **9**

acts as selective inhibitors of protein kinase 2 and efficiently reduces growth rate of tumors.

The coumarins also show good photo-optical properties and have been applied in polymer science and bio-study, especially photoreversible (photodimerization and photocleavage) research.[23] Coumarin dimerization occurs upon photoirradiation with a wavelength of more than 300 nm forming the *syn*- and *anti*-dimers via [2 + 2] cycloaddition reaction. Formation of the *syn*- and *anti*-dimers depends on the concentration of coumarin and the polarity of solvents (Figure 1-6). Usually, coumarin at high concentrations would favorably be at the excited singlet state, which can react with the coumarin at the ground-state to yield *syn*-dimmer, while low concentrations would favor the triplet state to produce *anti*-dimer. In addition, the singlet state is favored in polar solvents, leading to generation of *syn*-dimmer, while nonpolar solvents or existence of photosensitizers such as benzophenone would result in *anti*-dimer.[24] Moreover, the formed cyclobutane dimers can be symmetrically cleaved into coumarin monomer via photoscission reaction upon photo-irradiation at 254 nm. The dimmers with stable structures (five- or six-membered rings) attached to the cyclobutane, would be cleaved into the original monomers, preserving the stable structure. While asymmetric cleavage would occur for dimers without stable rings, resulting from either steric or other possible repulsions among neighbors.[25]

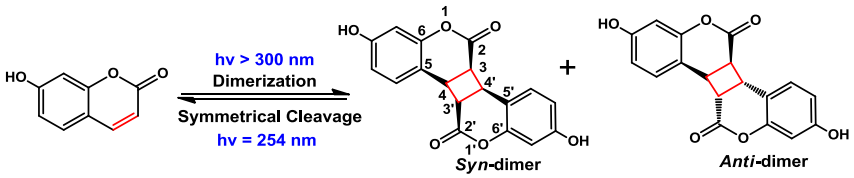

Figure 1-6. Photodimerization and cleavage of coumarin.

The coumarin with intrinsic fluorescence and photoreversible properties has wide applications.[25] They have been used for size-tunable study via photo-cross-linking and cleavage of coumarin, formulation of nanoparticles, and drug delivery via photoclevage of the dimers. Photo-cross-linkable polymers containing coumarin as side chain are used as liquid crystalline polymers for information storage devices, nonlinear optical devices, and television and computer displays. The photosensitive polyoxazoline containing

coumarins can dimerize to form polyoxazoline gels upon photo irradiation at 350 nm, while the cross-linked polymer can be split into single strands after irradiation at 253 nm. The cross-linked polymer films cannot dissolve in methanol, but become soluble after 253 nm irradiation (Figure 1-7).[26] Photoresponsive biopolymers, such as polypeptides containing coumarins, have been used for the chemical synthesis of biodegradable cross-linked materials.[27]

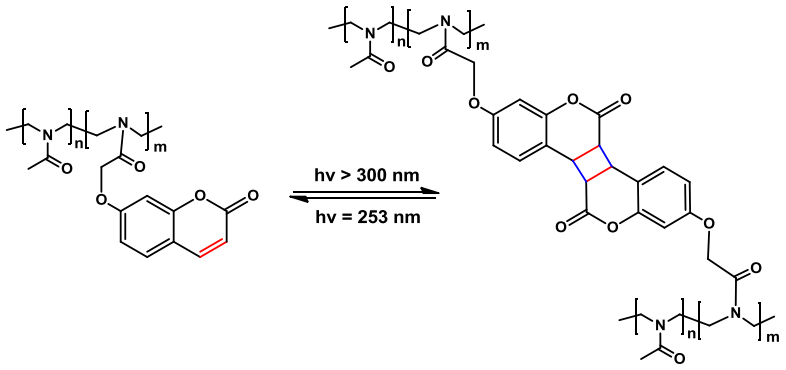

Figure 1-7. Photoreversible crosslink of the polyoxazoline containing coumarin.

1.2.3. Application of Coumarin in DNA

Coumarin-derived fluorophores have also found wide application in the field of nucleic acid chemistry. They are used as biosensors, phototriggers, and fluorescence tags for sequencing, DNA structure determination, and bio-kinetic analysis. Coumarin fluorophore can be covalently bound to DNA via a number of biochemical or cost-effective chemical methods. Recently, coumarin-based fluorogenic “click” reaction has been proved to be an important postsynthetic DNA labeling method which showed high efficiency under mild reaction conditions and produced the distinct fluorescence. It has been widely applied in the emerging area of cell biology and functional proteomics.[28] Non-fluorescent coumarin derivatives are employed in fluorogenic “click” reactions which generate substantial fluorescent signal with formation of triazole complexes. It is well-known that installation of an electron-withdrawing group at the 3-position and/or an

electron-donating group at the 7-position greatly increase the fluorescence intensity of coumarin moiety. On the other hand, substitution by the functional group with opposite electroproperties would quench its fluorescence. Based on this principle, two coumarin-based fluorogenic "click" reactions were developed. One employs an alkyne-modified coumarin **10** and the other uses an azide-modified coumarin **12**. Compound **10** contains the electron-withdrawing alkynyl group at the position-7 which quenches the fluorescence of the coumarin, while the electron-donating triazole moiety is formed after "click" reaction which restores the fluorescence of the coumarin moiety **11** (Figure 1-8).[29] In the other method, compound **12** with an electron-rich azide group at the position-3 is not fluorescent but undergoes "click" reaction to generate a highly fluorescent product **13**. The greatly enhanced fluorescence intensity of **13** results from formation of the triazole moiety which has decreased electron density in comparison with azide group (Figure 1-8).[30]

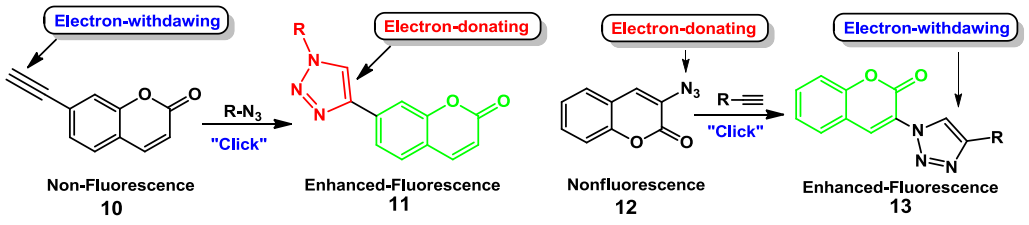

Figure 1-8. Coumarin-based fluorogenic click reactions.

These fluorogenic "click" reactions have been widely applied in construction of fluorescently tagged oligodeoxyribonucleotides (ODNs). In particular, 3-azidocoumarin **12** attracted much attention in this field because it can react with any alkyn-modified nucleotides to produce a fluorescent product. The alkyn-modified nucleosides can be easily incorporated in ODN via solid-phase DNA synthesis. For example, the alkyne-

modified uridine nucleosides (**14**) can be easily converted into the corresponding phosphoramidites which are readily incorporated into ODNs at single or multiple site (s) via standard solid-phase DNA synthesis.[31] The ODNs containing alkyne reporters react with non-fluorescent 7-hydoxyl-3-azidocoumarin in the presence of catalyst Cu (I) to yield the ODNs with high fluorescence (Figure 1-9).

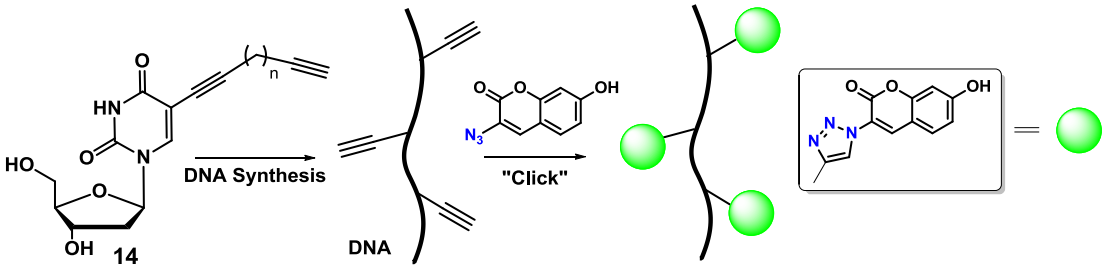

Figure 1-9. Preparation of fluorescent ODNs via the fluorogenic reaction.

1.3. DNA-Templated Reactions

1.3.1. DNA Synthesis and Modification

DNA-templated reactions of modified ODN probes have been widely used in nucleic acid sensing, small-molecule discovery, and reaction discovery via effective-molarity-based method.[32-33] Several natural or artificial methods exist to create chemically unmodified gene sequences, including DNA replication in nature, polymerase chain reaction, and gene synthesis. Great efforts have been made for improving the ODN bio/chemical properties by introducing novel groups to ODNs. Two common approaches, direct incorporation of chemical modifications into ODNs via solid-phase synthesis or post-synthetic conjugation with functional reporter groups, were employed for construction of ODNs with various chemical functional groups.

The first one involves direct incorporation of the modified nucleoside phosphoramidites bearing the designed functional groups via solid-phase DNA synthesis, in which ODNs are bound on the surface of glass bead with pores and prepared via step-by-step reactions in the solutions. This method showed great advantage of easily removing excess un-reacted agents or byproducts from the desired ODNs via washing. ODN synthesis is performed via the stepwise addition of free nucleotide residue at the 5'-terminus of ODN via synthetic cycles.[34] Usually, one ODN synthetic cycle consists of four steps: detritylation, coupling, capping, and oxidation (Figure 1-10). Detritylation, also known as de-blocking, is to remove the dimethoxytrityl (DMTr) in the solid bead-bound ODN using an acid (2% trichloroacetic acid) to generate the reactive residue, a free hydroxyl group at the 5-terminus. The formed DMTr cation with a color of orange-red was used for quantification of the last synthesis cycle. Then, the phosphoramidite is activated by 1*H*-tetrazole and subsequently reacts with the 5'-hydroxy group in the solid bead-bound ODN. The phosphite triester linkage is formed in the process. Followed by the coupling reaction, the capping reaction is performed by permanently blocking the unreacted 5'-hydroxy group using a mixture of 1-methylimidazole and acetic anhydride. This step prevents formation of deletion sequences. Finally, the tricoordinated phosphite triester linkage is oxidized to a more stable tetracoordinated phosphate trimester using a solution of iodine/water/pyridine. The ODN product contains a dimethoxytrityl (DMTr) protected 5'-hydroxy group that undergoes further synthetic cycles for elongation of the ODN chain. The designed modified phosphoramidites with DMTr group can be incorporated into flexible positions.

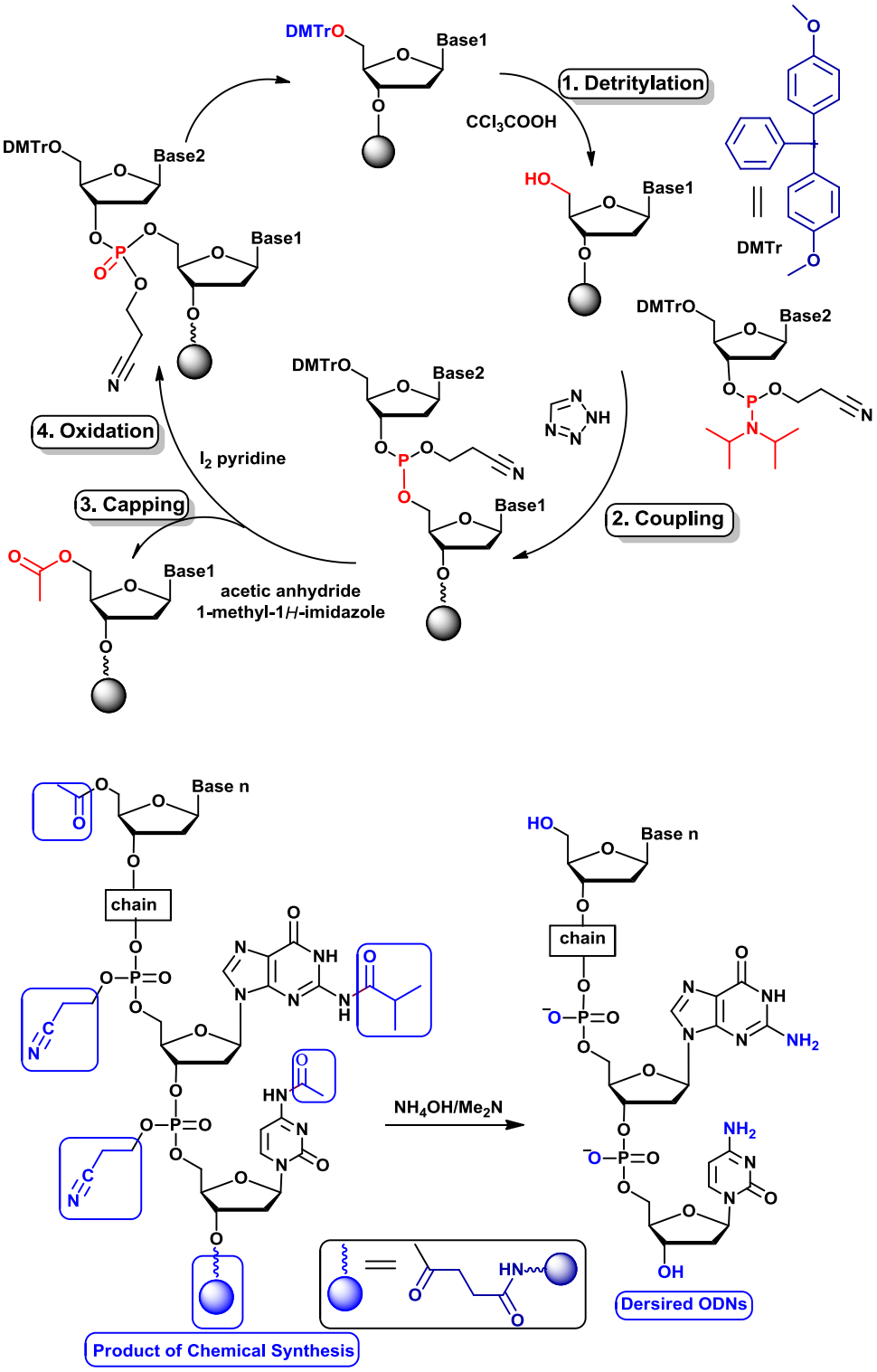

Figure 1-10. Preparation of ODNs via DNA solid-phase synthesis.

The ODNs produced by solid-phase synthesis contain various protecting groups, such as 2-cyanoethyl groups at the phosphate moieties and the acyl groups at the A, G, and C.[35] Following by solid-phase synthesis, the ODNs are usually deprotected, cleaved from the solid support, and purified. Normally, the ammonia solutions are employed for cleaving the bounded ODNs from solid support. Meanwhile, all protecting groups are removed yielding the desired ODNs (Figure 1-10). After the cleavage and deprotection, the desired ODNs are purified via two major methods, denaturing polyacrylamide gel electrophoresis (PAGE) or high performance liquid chromatography (HPLC). The purified ODNs can be characterized by mass spectrum, such as matrix-assisted laser desorption/ionization time-of-flight mass spectrometry (MALDI-TOF).

The post-synthetic conjugation method was also used for preparation of modified ODNs. It is particularly useful when the designed functional groups are not compatible with DNA solid-phase synthesis or post-treatment conditions. This method involves two steps: first, the ODNs containing a reporter group was synthesized via solid-phase synthesis; second, coupling of the ODNs with the designed functional residues to form the target ODNs. Several chemical linkages or highly efficient chemical reactions, such as amide, thiourea, thioethers, and thiazolidines linkages, Diels-Alder and Huisgen dipolar cycloadditions, and Staudinger ligations reactions, have been developed/used for facile construction of modified ODNs with the desired biochemical properties.[36]

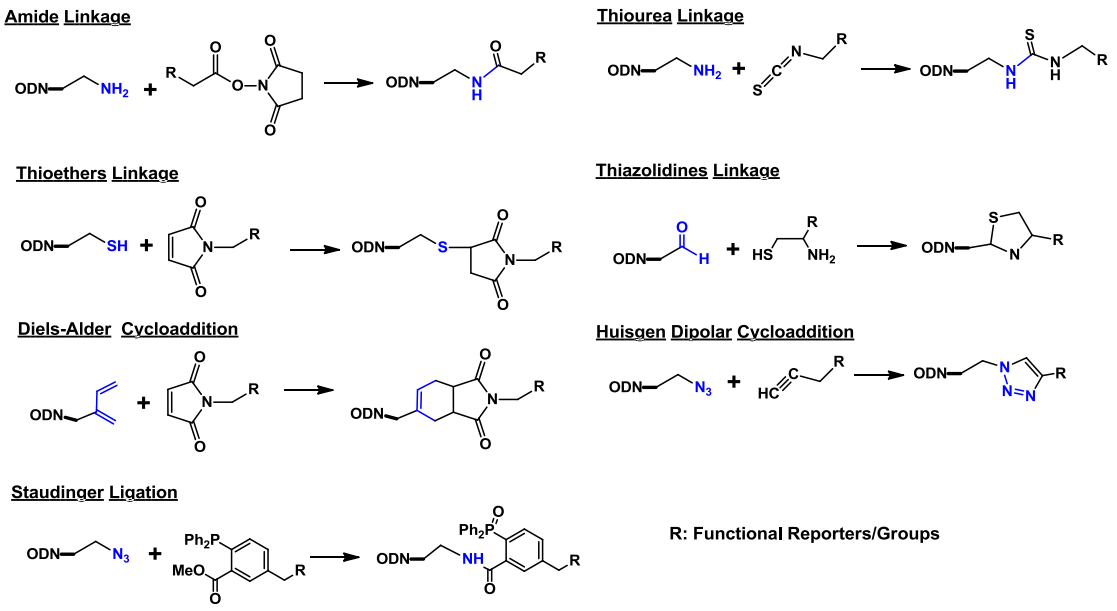

Figure 1-11. Linkages and reactions for ODNs post-conjugation.

The amide and thiourea linkages can be generated via chemical reactions between the amino group in ODNs and the carbodiimide-activated carboxylic and isothiocyanate groups (Figure 1-11). The reaction is highly efficient. However, the pH-dependent amino groups and carbodiimide-activated intermediates may lead to low reactivity and side reactions under acidic conditions. The sulfur-containing linkages, for instance thioethers and thiazolidines, can be prepared via the reaction of thiol groups with the active maleimide or vinyl sulfone or 1,2-aminothiol reporters (Figure 1-11). Side reactions may also occur especially with biomolecules containing thiol groups. In addition, hydrolysis of thiazolidine linkages can occur at the acidic environment by the reaction of 1, 2-aminothiol with an aldehyde moiety. Recently, “click” reactions, such as Diels-Alder and Huisgen dipolar cycloadditions, and Staudinger ligations were developed for ODNs post-conjugation (Figure 1-11). The Diels-Alder cycloadditions involve reaction of the diene in ODNs with an electron-donating group and a dienophile bearing an electron-withdrawing group. The Huisgen 1, 3-dipolar cycloadditions and Staudinger ligation

reactions between an azide and an alkyne or the phosphane group can form triazole and aza-ylide linkages. These have been widely used for construction of ODNs with special biochemical properties.

1.3.2. DNA Interstrand Cross-Linking Reaction

The modified ODNs with chemically functional groups have been widely utilized in the DNA-templated reactions, in which complementary ODNs hybridize via hydrogen bonds to form a DNA duplex, so that the reactive groups of ODNs can be confined to the same region in space affording highly effective concentration for the reactions.[37] DNA-templated reactions enable the efficient biochemical reaction occurring with a much lower concentration (nM-μM) than non-templated chemical synthesis (M). In general, DNA interstrand cross-link (ICL) reaction and ligation reaction are two most important DNA-templated reactions which receive lots of attention in biochemistry.

DNA ICL reactions refer to the reactions capable of forming the covalent chemical bonds between the two strands of a DNA double helix. Usually, the ICL reaction can be achieved by various exogenous cross-linking agents or functional reporters introduced in the modified ODNs. In genetics, the formed covalent bonds cannot be cleaved by enzymes. If not repaired, DNA ICLs can block the DNA strand separation and interrupt DNA replication finally leading to cell death.[38] Many exogenous DNA cross-linking agents have been clinically used in the cancer therapy. For example, bifunctional alkylating agents such as the nitrogen mustards (**15**) and *cis*-diamminedichloroplatinum (II) (**16**) can react with the N7 of the guanine to yield interstrand cross-links (Figure 1-12). Photoreactive psoralen (**17**) can cross-link the thymidine via [2 + 2] cycloaddition when irradiated with UV light >300 nm. Psoralens have been used for treatment of

psoriasis, vitiligo and cutaneous T-cell lymphoma.[39] Recently, H_2O_2-responsive anticancer prodrugs targeting the unique biochemical alterations such as high level of reactive oxygen species in cancer cells have been discovered. These agents exhibit therapeutic activity and selectivity.[40] For example, our group has developed several novel H_2O_2-activated anticancer prodrugs containing electron-withdrawing boronate esters (**18** and **19**). These compounds are inactive towards DNA but can be triggered by H_2O_2 to release active species: quinone methides or nitrogen mustards that directly form DNA ICL products (Figure 1-12).[41-42]

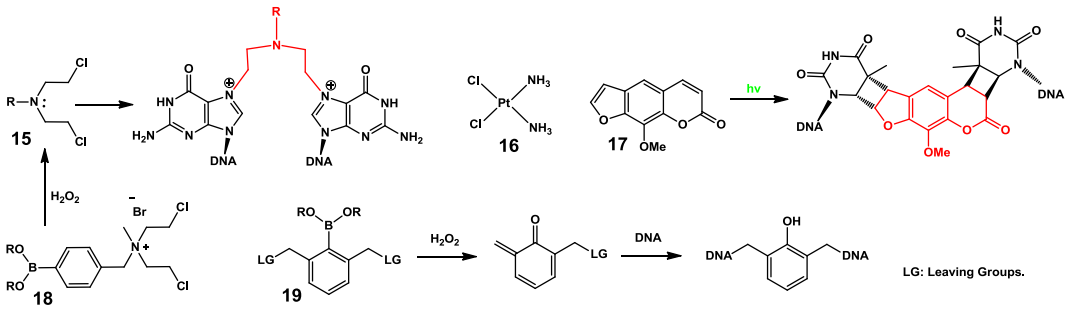

Figure 1-12. DNA interstrand cross-link agents.

For most bifunctional DNA alkylating agents, the ICL formation requires much excessive DNA cross-linking agents (most more than 100 times) but leading to low ICL yields (most < 50%), several side reactions and DNA damages. Cross-linking also occurs in the same strand to form the monoadducts and intrastrand cross-links.[43] Cross-linking between DNA and protein is also possible.

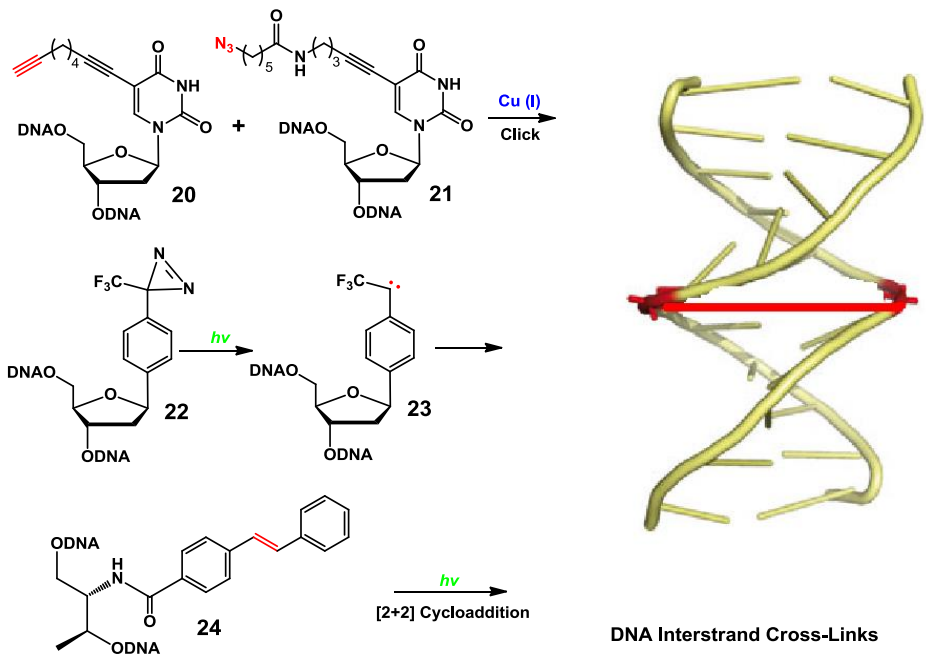

Figure 1-13. DNA interstrand cross-links with modified DNA constructs.

DNA-templated reactions overcome the problems discussed above: a) only equivalent modified DNA constructs are required to enable the efficient ICL reactions with high cross-linking yields; b) less side reactions are observed and good selectivity is achieved. A number of modified ODNs consist of different functional groups which can produce the efficient ICL reaction via various chemistry, such as click chemistry, photo-generated radicals or carbens, and photo-induced cycloaddition.[44-47] Among these, "click" chemistry has been widely applied for covalently cross-linking complementary DNA strands through formation of triazole linkages.[44] A number of alkyne- or azide-modified nucleotides have been developed for DNA-associated "click" reactions.[45] For example, various terminal alkynes or azide groups are introduced in 2'-deoxyuridine, which was incorporated into ODNs via solid-phase DNA synthesis and ODNs post-conjugation respectively (Figure 1-13). Highly efficient "click" reactions have been achieved using these alkyne-containing (**20**) and azide-modified (**21**) ODNs leading to quantitative formation of DNA ICL products. These DNA-templated "click" reactions are complete

within 15 min. The diazirine-based nucleoside analogues were also incorporated in ODNs which allowed efficient interstrand cross-linking upon photoirradiation.[46] The aryl-(trifluoromethyl) diazirine-modified nucleoside analogue **22** is particularly useful for this purpose. They can be successfully incorporated into ODNs via solid-phase synthesis. Photoirradiation causes loss of the nitrogen gas generating a carbene **23** which is highly reactive towards a variety of functional groups even the inert aliphatic C-H bonds. The ODNs containing **22** produce very stable DNA interstrand cross-links (Figure 1-13). DNA ICLs are also generated via [2 + 2] photocycloaddition reaction. For example, the artificial base pairs of two p-stilbazoles **24** introduced in the base paring positions of two complementary DNA strands efficiently produced DNA cross-linking products upon light irradiation at 340 nm. The photo-cross-linking reaction can finish within 3 min yielding two diastereomers due to free rotation of the vinyl group.[47] The cross-linked duplex was highly stable (Figure 1-13). The DNA cross-linking reactions by modified DNA constructs showed high efficiency. They have been applied in various fields including detection of nucleic acid-nucleic acid and protein-nucleic acid interactions, DNA repair, gene regulation, reversible control of DNA hybridization, phototherapy, and DNA-based nanomaterials.[44-45] Although DNA-templated ICL reactions using two complementary ODN strands are simple and highly efficient, they usually require two modified ODNs which limits their applications in natural DNA study such as the detection of mutation, sequencing and translating DNA sequences. These problems can be overcome by DNA-templated ligation reaction.

1.3.3. DNA Ligation Reactions

DNA-templated chemical ligation reactions are defined as joining two short DNA fragments by chemical reactions in the presence of a long complementary DNA template.[37] In biology, DNA ligase which can biocatalyze formation of phosphodiester linkers between 3'-hydroxyl and 5'-phosphoryl groups is used for DNA bio-ligation reactions, such as the polymerase chain reaction (PCR). Unlike the interstrand cross-link reactions using two ODN strands, DNA-templated ligation reactions consist of three ODN strands including a long natural DNA template being complementary with the other two probe strands to modulate the effective molarity of the two reactants, and two short ODN strands with reactive groups at the terminal positions participating in the chemical reaction.[37] DNA hybridization among three strands can form the DNA duplex confining the reactive groups at the internal positions in space. This can create a very high effective molarity of reactants, resulting in efficient reactions with accelerated reaction rates by several orders of magnitude.

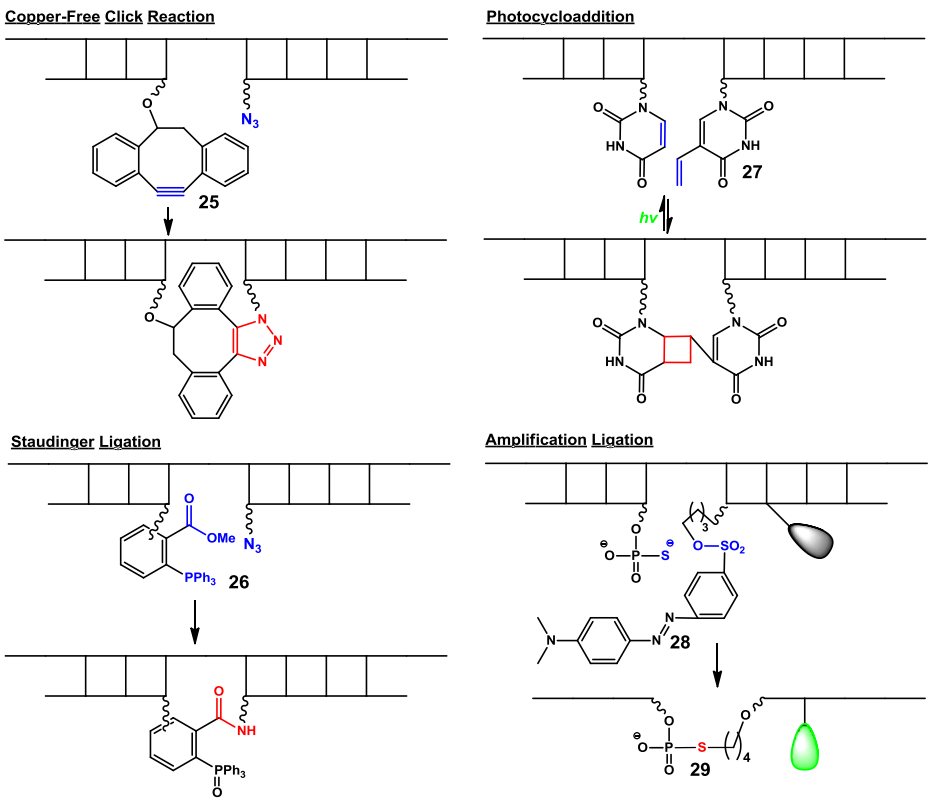

Figure 1-14. Examples of DNA templated ligation reactions.

Many biocompatible reactions have been employed in DNA-templated ligation, such as copper-free click reactions, Staudinger ligation, and photocycloaddition.[48-51] Among these, DNA-templated copper-free alkyne-azide [3 + 2] cycloaddition reaction is very efficient and fast (Figure 1-14). The most prominent copper-free "click" reaction is the strain-promoted azide-alkyne [3 + 2] cycloaddition (SPAAC) reaction using a cyclooctyne moiety and an azido group which is first developed by Bertozzi.[48] The SPAAC reaction showed high efficiency and orthogonality without using the toxic Cu (I) which allows wide *in vivo* applications. Initially, the dibenzocyclooctyne **25** was employed in SPAAC reaction.[49] Compound **25** was introduced at the 5-terminus of ODN via solid-phase DNA synthesis, while the azide moiety was incorporated at the 3'-terminus of ODN via post-conjugation. In the presence of a matched template, the

SPAAC reaction occurs to afford the stable ligation product with high efficiency. The reaction is complete within 5 min. Recently, the Staudinger ligation has been employed for ligating ODN strands. For example, the reaction between a triaryl phosphine bearing an electrophilic trap and an azide group yields an stable amide linkage efficiently forming ODN ligation products (Figure 1-14).[50] Both azides and the triaryl phosphine with the methyl ester **26** are introduced in ODNs through post-conjugation methods because they are not compatible with the conditions used in solid-phase DNA synthesis. With formation of DNA duplex via hybridization, the aza-ylide is generated to react with the ester forming a five-membered ring. After hydrolysis, the stable amide linkage is formed in the ligation product. Sometimes, the natural ODNs can also serve as the reactants in the ligation reaction.

Apart from "click" chemistry and Staudinger reaction, photo-induced [2 + 2] cycloaddition is also used for DNA ligation. The C5-C6 double bond of pyrimidines is often involved in the DNA-templated photo-induced [2 + 2] cycloaddition reactions. Fujimoto developed a highly efficient reversible photoligation using 5-vinyl-2'-deoxyuridine (**27**) and 2'-deoxyuridine with no side reactions (Figure 1-14).[51] The 5-vinyl-2'-deoxyuridine (**27**) can be incorporated in ODNs via automated DNA synthesis. The photocycloaddition of 5-vinyl-2'-deoxyuridine and the natural dU in the internal positions of the longer ODN template is almost quantitative upon irradiation at 366 nm. The formed product can be photo-cleaved to the original strands via 302 nm photo-irradiation. The ligation products are longer than the starting ODNs and would bind more tightly with ODN template than the two starting probe strands via hydrogen bonds, which prevent dissociation of the ligated product from the template. Therefore the template

loses its catalytic ability and one template only produces one ligated product. Recently, the ligation reactions capable of achieving template turnover have been developed. Kool group reported that the nucleophilic phosphorothioate group at the 5'-terminus can react with the dabsylate group **28** at the 3-terminus to form the butanediol-linker **29** (Figure 1-14). [52] Formation of the linker **29** destabilizes the duplex formed by ligated products and the template, which is favorable for releasing the free template for further ligation reactions. Therefore, this method yields generation of multiple ligated products with one DNA template. Moreover, the dabsylate group **28** can quench the fluorescence of the fluorophore conjugated in the flanking base, but the fluorescence can be restored after loss of the dabsylate group in the ligation reactions. Thus, the ligation reaction involving a dabsylate group can produce 92-fold amplification of fluorescence signals without using enzymes, additional chemical reagents, or thermal cycling.

1.3.4. Potential Application of Coumarin in DNA

Although DNA-templated organic reactions have been well studied and various functional groups have been introduced in ODNs for such purpose, the biological application of these reactions is still limited due to several unsolved problems, such as the challenge in real-time detection and amplification of the formed products and the challenge in signal amplification due to low-abundance of DNA targets in biological system. We expect that these challenges can be overcome by development of fluorogenic DNA-templated reactions capable of fluorescence signal amplification. As the coumarin moieties show substituent-dependent tunable fluorescence, we became interested in DNA-templated coumarin-based fluorogenic reactions. Such reactions use non-fluorescent coumarin precursors as reporters which undergo a certain chemical reaction

to produce a highly fluorescent product. They are expected to expand the biological applications of DNA-templated reaction, such as for developing simple methods for real-time detection of single nucleotide polymorphism (SNP) and for highly sensitive fluorescence-labeling. Although lots of methods have been developed for sequence-specific DNA detection using fluorescence assays, most of them have low sensitivity and involve stringent washing of unreacted probe which are costly and/or time-consuming. The coumarin-based fluorogenic reaction with low/no background will avoid removal of the unreacted probes (Chapter 2), which allows development of simple and easy methods for real-time SNP detection.

On the other hand, the DNA-templated reaction is highly efficient which offers an excellent way for studying organic molecules' reactivities towards DNA. The coumarins have been widely utilized as drugs, biomolecular reporters, and components in bio-nanomaterials. However, its reactivity towards biomolecules is still unclear which may induce unrecognized side reactions in bioapplications. We fully investigate the reactivity of the coumarin moiety towards four DNA components by using DNA-templated chemical reaction. Such study provides a novel understanding about biochemical properties of coumarins in cells (Chapter 4 and 5). In addition, we discovered a bromo-substituted coumarin derivative (**30**) that reacts with dT under physiological conditions. The reactions between coumarin derivative **30** and dT in natural DNA can afford the DNA conjugates with several fluorescent coumarin reporters (Chapter 3). This allowed us to develop a novel method capable of labeling natural DNA with multiple fluorophores by taking the advantages of the good chemical reactivity of coumarin derivatives with dT, which greatly increase its analytical sensitivity. Most current DNA labeling methods just

allow one fluorescent reporter being conjugated to one natural ODN strand leading to low sensitivity.

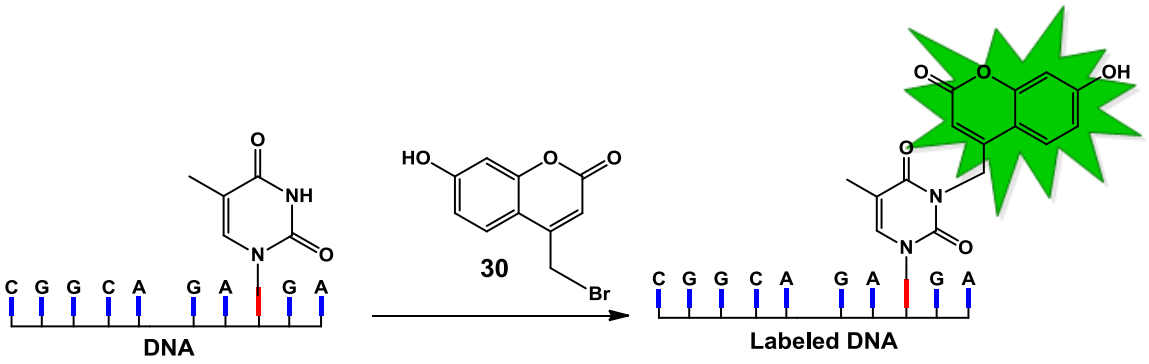

Figure 1-15. Selectively post-labeling natural DNA with coumarins.

1.4. References

[1] Vogel, A. Preparation of benzoic acid from tonka beans and from the flowers of melilot or sweet clover. *Annals of Physics* **1820**, *64*, 161-166.

[2] Perkin, W. H. On the artificial production of coumarin and formation of its homologues. *Journal of the Chemical Society* **1868**, *21*, 53-63.

[3] Lakowicz, J. R. *Principles of Fluorescence Spectroscopy*. Kluwer Academic/Plenum Publishers: New York, NY, USA, **1999**, *Chapter 3*, 280.

[4] Valeur, B. *Molecular Fluorescence: Principles and Aplications*. Wiley-Verlag Chemie GmbH: Weinheim, Germany, **2001**, *Chapter 3*, 79.

[5] Krystkowiak, E., Dobek, K., Burdziński, G., Maciejewski, A., Radiationless deactivation of 6-aminocoumarin from the S1-ICT state in nonspecifically interacting solvents. *Photochem. Photobiol. Sci.* **2012**, *11*, 1322-1330.

[6] Kaholek, M., Hrdlovič, P. Characteristics of excited states of 3-substituted coumarin derivatives and transfer of electronic energy to N-oxyl radicals. *J. Photochem. Photobiol. A Chem.* **1999**, *127*, 45-55.

[7] Kinza Aslam, K., Khosa, M. K., Jahan, N., Nosheen, S. Short communication: synthesis and applications of coumarin. *Pak J Pharm Sci.* **2010**, *23*, 449-454.

[8] Pechmann, H. V. Neue bildungsweise der cumarine. synthese des daphnetins. *Berichte der deutschen chemischen Gesellschaft.* **1884**, *17*, 929-936.

[9] Corrie, J. E. T. A convenient synthesis of *N*-(7-dimethylamino-4-methylcoumarin-3-yl)-maleimide incorporating a novel variant of the Pechmann reaction. *J. Chem. Soc. Perkin Trans. I* **1990**, *7*, 2151-2152.

[10] Donovalová, J., Cigáň, M., Stankovičová, H., Gašpar, J., Danko, M., Gaplovský, A., Hrdlovič, P. Spectral properties of substituted coumarins in solution and polymer matrices. *Molecules* **2012**, *17*, 3259-3276.

[11] Bangar, R. B., Varandajaran, T. S. Substituent and solvent effects on the twisted intramolecular charge transfer of three new 7-(diethylamino)coumarin-3-aldehyde derivatives. *J. Phys. Chem.* **1994**, *98*, 8903-8905.

[12] Jiang, W., Wang, W. A selective and sensitive "turn-on" fluorescent chemodosimeter for Hg^{2+} in aqueous media via Hg^{2+} promoted facile desulfurization-lactonization reaction. *Chem. Commun.* **2009**, *26*, 3913-3915.

[13] Li, H., Cai, L., Li, J., Hu, Y., Zhou, P., Zhang, J. Novel coumarin fluorescent dyes: synthesis, structural characterization and recognition behavior towards Cu (II) and Ni (II). *Dyes Pigments* **2011**, *91*, 309-316.

[14] Li, H., Gao, S., Xi, Z. A colorimetric and "turn-on" fluorescent chemosensor for Zn (II) based on coumarin Schiff-base derivative. *Inorg. Chem. Commun.* **2009**, *12*, 300-303.

[15] Lee, M., Gubernator, N. G., Sulzer, D., Sames, D. Development of pH-responsive fluorescent false neurotransmitters. *J. Am. Chem. Soc.* **2010**, *132*, 8828-8830.

[16] Du, L., Li, M., Zheng, S., Wang, B. Rational design of a fluorescent hydrogen peroxide probe based on the umbelliferone fluorophore. *Tetrahedron Lett.* **2008**, *49*, 3045-3048.

[17] Feuster, E. K., Glass, T. E. Detection of amines and unprotected amino acids in aqueous conditions by formation of highly fluorescent iminium ions. *J. Am. Chem. Soc.* **2003**, *125*, 16174-16175.

[18] Lake, B. G. Coumarin metabolism, toxicity & carcinogenicity: relevance for human risk assessement. *Food & Chemical Toxicology* **1999**, *37*, 423-453.

[19] Egan, D., O'Kennedy, R., Moran, E., Cox, D., Prosser, E., Thornes, R. D. The pharmacology, metabolism, analysis, and applications of coumarin and coumarin-related compounds. *Drug Metab Rev.* **1990**, *22*, 503-529.

[20] Chimenti, F., Bizzarri, B., Bolasco, A., Secci, D., Chimenti, P., Granese, A., Carradori, S., Rivanera, D., Zicari, A., Scaltrito, M. M., Sisto, F. Synthesis, selective anti-Helicobacter pylori activity, and cytotoxicity of novel N-substituted-2-oxo-2H-1-benzopyran-3-carboxamides. *Bioorg. Med. Chem. Lett.* **2010**, *20*, 4922-4926.

[21] Kostova, I., Bhatia, S., Grigorov, P., Balkansky, S., Parmar, V. S., Prasad, A. K., Saso, L. Coumarins as antioxidants. *Curr Med Chem*. **2011**, *18*, 3929-3951.

[22] Huang, X. Y., Shan, Z. J., Zhai, H. L., Su, L., Zhang, X. Y. Study on the anticancer activity of coumarin derivatives by molecular modeling. *Chem. Biol. Drug Des.* **2011**, *78*, 651-658.

[23] Trenor, S. R., Shultz, A. R., Love, B. J., Long, T. E. Coumarins in polymers: from light harvesting to photo-cross-linkable tissue scaffolds. *Chem. Rev.* **2004**, *104*, 3059-3077.

[24] Lewis, F. D., Barancyk, S. V. Lewis acid catalysis of photochemical reactions. 8. Photodimerization and cross-cycloaddition of coumarin *J. Am. Chem. Soc.* **1989**, *111*, 8653-8661.

[25] Yonezawa, N., Yoshida, T., Hasegawa, M. Symmetric and asymmetric photocleavage of the cyclobutane rings in head-to-head coumarin dimers and their lactone-opened derivatives. *J. Chem. Soc., Perkin Trans. 1* **1983**, 1083-1086.

[26] Chujo, Y., Sada, K., Saegusa, T. Polyoxazoline having a coumarin moiety as a pendant group. Synthesis and photogelation. *Macromolecules* **1990**, *23*, 2693-2697.

[27] Yamamoto, H., Kitsuki, T., Nishida, A., Asada, K., Ohkawa, K. Photoresponsive peptide and polypeptide systems. 13. Photoinduced cross-linked gel and biodegradation properties of copoly (l-lysine) containing ε-7-coumaryloxyacetyl-l-lysine residues. *Macromolecules* **1999**, *32*, 1055-1061.

[28] Le Droumaguet, C., Wang, C., Wang, Q. Fluorogenic click reaction. *Chem Soc Rev.* **2010**, *39*, 1233-1239.

[29] Zhou, Z., Fahrni, C. J. A fluorogenic probe for the copper (I)-catalyzed azide-alkyne ligation reaction: modulation of the fluorescence emission via $^{3}(n,\pi^*)-^{1}(\pi,\pi^*)$ inversion. *J. Am. Chem. Soc.* **2004**, *126*, 8862-8863.

[30] Sivakumar, K., Xie, F., Cash, B. M., Long, S., Barnhill, H. N., Wang, Q. A fluorogenic 1,3-dipolar cycloaddition reaction of 3-azidocoumarins and acetylenes. *Org. Lett.* **2004**, *6*, 4603-4606.

[31] Gierlich, J., Burley, G. A., Gramlich, P. M., Hammond, D. M., Carell, T. Click chemistry as a reliable method for the high-density postsynthetic functionalization of alkyne-modified DNA. *Org. Lett.* **2006**, *8*, 3639-3642.

[32] Xu, Y., Kool, E. T. Rapid, selective selenium-mediated autoligation of DNA strands. *J. Am. Chem. Soc.* **2000**, *122*, 9040-9041.

[33] Mattes, A., Seitz, O. Mass-spectrometric monitoring of a PNA-based ligation reaction for the multiplex detection of DNA single-nucleotide polymorphisms. *Angew. Chem. Int. Ed.* **2001**, *40*, 3178-3181.

[34] Reese, C. B. The chemical synthesis of oligo- and poly-nucleotides by the phosphotriester approach. *Tetrahedron* **1978**, *34*, 3143-3179.

[35] Beaucage, S. L., Iyer, R. P. Advances in the synthesis of oligonucleotides by the phosphoramidite approach. *Tetrahedron* **1992**, *48*, 2223-2311.

[36] Singh, Y., Murata, P., Defrancq, E. Recent developments in oligonucleotide conjugation. *Chem. Soc. Rev.* **2010**, *39*, 2054-2070.

[37] Li, X., Liu, D. R. DNA-templated organic synthesis: nature's strategy for controlling chemical reactivity applied to synthetic molecules. *Angew. Chem. Int. Ed.* **2004**, *43*, 4848-4870.

[38] Noll, D. M., Mason, T. M., Miller, P. S. Formation and repair of interstrand cross-links in DNA. *Chem. Rev.* **2006,** *106*, 277-301.

[39] Rajski, S. R., Williams, R. M. DNA cross-linking agents as antitumor drugs. *Chem. Rev.* **1998**, *98*, 2723-2795.

[40] Kuang, Y., Balakrishnan, K., Gandhi, V., Peng, X. Hydrogen peroxide inducible DNA cross-linking agents: targeted anticancer prodrugs. *J. Am. Chem. Soc.* **2011**, *133*, 19278-19281.

[41] Chen, W., Han, Y., Peng, X. Aromatic nitrogen mustard-based prodrugs: activity, selectivity, and the mechanism of DNA cross-linking. *Chem. Eur. J.* **2014**, *20*, 7410-7418.

[42] Cao, S., Wang, Y., Peng, X. The leaving group strongly affects H_2O_2-induced DNA cross-linking by arylboronates. *J. Org. Chem.* **2014**, *79*, 501-508.

[43] Rudd, G. N., Hartley, J. A., Souhami, R. L. Persistence of cisplatin-induced DNA interstrand crosslinking in peripheral blood mononuclear cells from elderly and young individuals. *Cancer Chemother. Pharmacol.* **1995**, *35*, 323-326.

[44] Kocalka, P., El-Sagheer, A. H., Brown, T. Rapid and efficient DNA strand cross-linking by click chemistry. *ChemBioChem.* **2008**, *9*, 1280-1285.

[45] Haque, M. M., Peng, X. DNA-associated click chemistry. *Sci. China, Chem.* **2014**, *57*, 215-231.

[46] Qiu, Z.; Lu, L.; Jian, X.; He, C. A diazirine-based nucleoside analogue for efficient DNA interstrand photocross-linking. *J. Am. Chem. Soc.* **2008**, *130*, 14398-14399.

[47] Kashida, H., Doi, T., Sakakibara, T., Hayashi, T., Asanuma, H. *p*-Stilbazole moieties as artificial base pairs for photo-cross-linking of DNA duplex. *J. Am. Chem. Soc.* **2013**, *135*, 7960-7966.

[48] Jewetta, J. C., Bertozzi, C. R. Cu-free click cycloaddition reactions in chemical biology. *Chem. Soc. Rev.* **2010**, 39, 1272-1279.

[49] Shelbourne, M., Chen, X., Brown, T., El-Sagheer, A. H. Fast copper-free click DNA ligation by the ring-strain promoted alkyne-azide cycloaddition reaction. *Chem. Commun.* **2011**, *47*, 6257-6259.

[50] Kohn, M., Breinbauer, R. The Staudinger ligation-a gift to chemical biology. *Angew. Chem. Int. Ed.* **2004**, *43*, 3106-3116.

[51] Fujimoto, K., Matsuda, S., Takahashi, N., Saito, I. Template-directed photoreversible ligation of deoxyoligonucleotides via 5-vinyldeoxyuridine. *J. Am. Chem. Soc.* **2000,** *122*, 5646-5647.

[52] Abe, H., Kool, E. T. Destabilizing universal linkers for signal amplification in self-ligating probes for RNA. *J. Am. Chem. Soc.* **2004**, *126*, 13980-13986.

Chapter 2. Template-Directed Fluorogenic Click Reaction: DNA Interstrand Cross-Linking, Oligonucleotide Ligation, and Single Nucleotide Discrimination[1]

2.1. Introduction

The abnormal behaviors of tumor cells are demonstrated resulting from mutations in key regulatory genes. Therefore, fast and facile detection of mutated gene is highly important for early diagnosis and treatment of cancer diseases.[2-5] Several methods have been developed to monitor gene mutations, for example DNA chip analysis,[6] denaturing high-performance liquid chromatography analysis,[7] hetereoduplex analysis,[8] and those have been applied in hospital laboratories, such as the single-strand conformational polymorphism and restriction fragment length polymorphism analyses.[9-11] Recently, rapid and simple methods based on DNA melting curve analysis have been developed.[12-15] However, most existing technologies rely on allele-specific hybridization. Hybridization alone is a non-covalent binding event between the target DNA and a complementary oligonucleotide probe. This is a transient event that requires stringent conditions, barely exhibits sufficient selectivity in distinguishing matched from single-base mismatched DNA targets, and cannot be used in cells. One of the most common strategies currently used to engender high selectivity in sequence detection is the use of DNA-ligation reactions (e.g. ligases).[16] Many DNA-templated chemical reactions have been utilized for sensing DNA or RNA sequences, which can achieve single nucleotide discrimination.[17-18] The advantages offered by chemical ligation techniques is the feasibility of performing

reactions with DNA-analogues on RNA templates, and/or within living cells, and allowing direct read-outs of the formed products.[19-20]

One important issue in the design of DNA-diagnostic chemical reactions is the detection of the formed product. Gel electrophoresis and HPLC-based separation techniques have most frequently been used as the precise yet time-consuming means of reaction monitoring. Mass spectroscopy has been demonstrated to enable rapid and accurate detection of reaction products. However, these methods are off-line methods. These limitations have motivated the development of simpler fluorescence-based assays with molecular beacons, binary probes, forced intercalation of thiazole orange probes, and base-discriminating fluorescent probes. Fluorescence assay enables real-time measurements, and provides advantages as far as ease, sensitivity, and speed of detection.[21] The major disadvantage of fluorescence assay is the background signal that arises from a number of sources.[22] For example, fluorescence occurs from partially labeled molecular beacons (possessing the fluorophore, but not the quencher), a small amount of "open" hairpin structures in the absence of the target, and the inefficiency of the quencher to totally deactivate the dye fluorescence.[23] To obtain *in-situ* and real-time information on the DNA-templated chemical reactions and to eliminate residual fluorescence, it is expected that the reporters used should be non-fluorescent, but can generate a fluorescent product upon DNA-templated chemical reaction. In this work, we used the copper(I)-catalyzed azide-alkyne cycloaddition (CuAAC) to develop a fluorogenic "click" ligation reaction which is capable of single nucleotide discrimination and can be used for detecting tumor's mutated genes.

The CuAAC reaction, the most prominent example of click chemistry attracts particular attention for DNA-templated reaction and a variety of biological application because the "click" chemistry is a regioselective and bioorthogonal reaction that is clean, fast, high-yielding, and operated in aqueous solution.[24-25] Brown and coworkers first applied the "click" reaction for template-directed DNA ligation and covalent intramolecular DNA circularization and catenation.[26] Later, our group has utilized the "click" reaction for developing a highly efficient chemical ligation for quantitative conjugation of peptide nucleic acid (PNA) with DNA.[27] The PNA click ligation is sequence-specific and capable of single nucleotide discrimination.

Recently, fluorogenic "click" reactions between non-fluorescent alkynes and azides to form a substantial turn-on fluorescent signal upon formation of triazole complexes have been optimized. These reactions have been widely used in bioconjugation labeling and fluorogenic probing.[28-34] However, the fluorogenic "click" reaction as one of the important click reactions has not been used in the template-dependent reaction for DNA single nucleotide discrimination. We envisaged a very simple method of detecting tumor's mutated nucleic acids by using the fluorogenic "click" reaction. In this chapter, ODNs containing non-fluorescent alkyne-modified coumarin or azide group were employed as the probes for DNA-templated ligation and interstrand cross-linking and for detection of SNPs in p53 tumor suppressor gene. The fluorogenic "click" reaction occurred only in the presence of tumor-associated genetic sequences p53 gene with one base mutation which produced strongly fluorescent products (Figure 2-1).

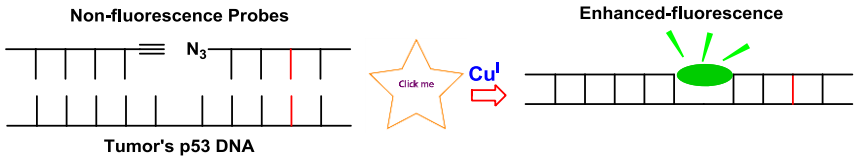

Figure 2-1. Detection of p53 mutations via a fluorogenic "click" reaction.

2.2. ODN Probes for Fluorogenic Reaction

2.2.1. Preparation of the ODNs Containing Alkyne-Modified Coumarin

The goal of the study is to develop a simple and effective method to detect tumor's mutated nucleic acids by using the fluorogenic "click" reaction. Such method will allow easy, fast, sensitive, and real-time detection of specific nucleic acid sequences without stringent washing conditions or background signal from un-reacted probes. This requires the design of non-fluorescent DNA probes that can be covalently bound together via a CuAAC reaction to produce an enhanced fluorescence signal. The use of non-fluorescent probes will ensure a low background or zero background. The covalent attachment between two probes will produce a permanent signal and avoid the stringent conditions for washing un-reacted probes. Initially, we chose coumarin derivatives as fluorogenic reporters because their fluorescence intensity can be tuned by varying the electronic properties of the substituents at the aromatic rings.[35] Furthermore, they are easy to prepare and are biocompatible. It is known that coumarin analogues having an alkyne group at the position-7 or those carrying an azido group at the position-3 are non-fluorescent but can undergo "click" reaction to generate a fluorescent product via formation of a triazole moiety.[35] As the azide group is not compatible with solid-phase DNA synthesis via phophoramidite chemistry due to the Staudinger reaction (see chapter 1), we used an alkyne-modified coumarin as the reporter which was incorporated at the 5'-terminus of DNA probes. Therefore, 7-ethynyl-4-hydroxymethylchromen-2-one (**6**) and its phosphoramidite building block **7** have been prepared (Figure 2-2). As described by Fahrni and co-worker, 7-ethynyl-4-

hydroxymethylchromen-2-one (**6**) was synthesized starting from ethyl acetoacetate.[36] PAC phosphoramidites have been employed for synthesizing ODNs containing alkyne-modified coumarin because a very mild deprotection condition is used which can avoid decomposition of the functionalized DNA probes.

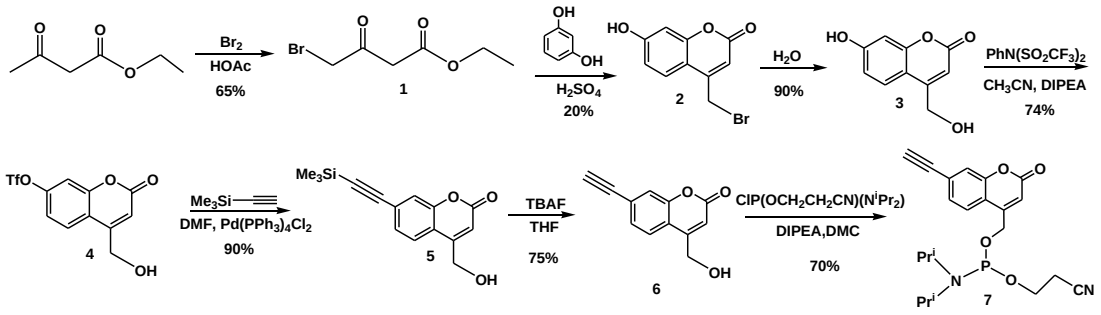

Figure 2-2. Synthesis of alkyne-modified coumarin phosphoramidite **7**.

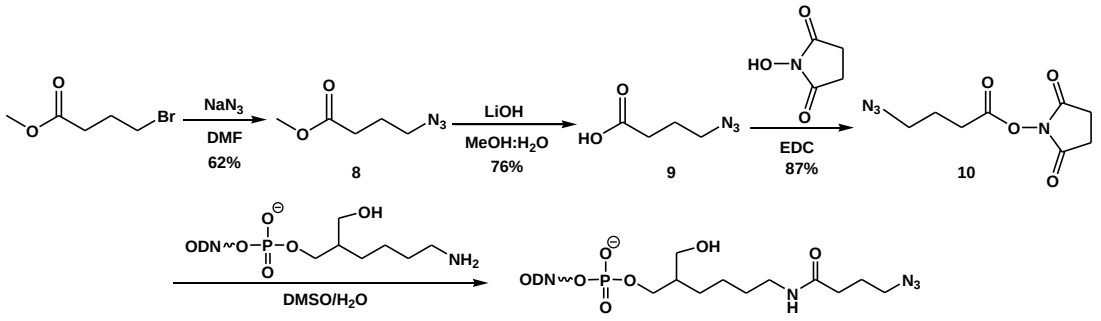

Figure 2-3. Synthesis of ODNs containing the azide group.

We followed the procedure described by Brown and coworkers to synthesize ODNs containing azide group in the 3'-terminus.[26] Incorporation of azide group was done by the reaction of succinimidyl-4-azidobutyrate (**10**) and 3'-amino-modifier C7-ODNs (Figure 2-3). Compound **10** was prepared starting from methyl 4-bromobutanoate. All ODNs have been purified by 20% denaturing PAGE. ODNs containing alkyne-modified coumarin or azide group have been confirmed by mass spectrometry (Table 2-1).

Table 2-1. Oligodeoxynucleotides used in the study.

Entry	ODN sequence	Mass (Calcd.)	Mass (Found)[d]
ODN **1**	3′-dCGGAGGCCAAGT		n.d.
ODN **2**	3′-dACTTGGCCTCCG		n.d.
[a]ODN **3**	3′-d**NH$_2$**ACTTGGCCTCCG		n.d.
[b]ODN **4**	3′-d**Z**ACTTGGCCTCCG	3917.5	3916.9
[c]ODN **5**	3′-dCGGAGGCCAAGT**6**	3957.5	3957.4
[c]ODN **6**	3′-dCGGAGACCAAGT**6**	3941.5	3941.6
[a]ODN **7**	3′-d**NH$_2$**CTTGGCCT		n.d.
[b]ODN **8**	3′-d**Z**CTTGGCCT	2696.7	2696.6
[a]ODN **9**	3′-d**NH$_2$**CTTGGCCTC		n.d.
[b]ODN **10**	3′-d**Z**CTTGGCCTC	2985.9	2985.9
[c]ODN **11**	3′-dCGTACCCGCCGT**6**	3844.4	3844.0
ODN **12a-d**	3′-dTACCCGGAG**X**CCAAG TACGGCGGGTACGTCCT **12a**: **X** = G; **12b**: **X** = A; **12c**: **X** = T; **12d**: **X** = C		n.d.
ODN **13**	3′-dAGGCCAAGT		n.d.
ODN **14a-d**	3′-dGAG**X**CCAAGT **14a**: **X** = G; **14b**: **X** = A; **14c**: **X** =T; **14d**: **X** =C		n.d.

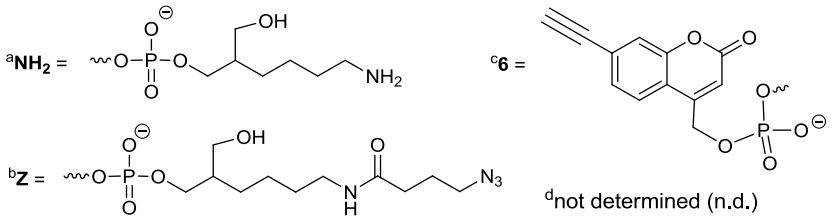

2.2.2. Thermal Stability Study

The efficiency of DNA-templated chemical reactions depends on formation of a stable DNA duplex. The sequence selectivity relies on the mismatch discrimination of the modified ODN probes. In order for coumarin or azide group to be useful as part of a probe to specifically detect a complementary sequence, they must maintain the mismatch discrimination ability of DNA probes. Therefore, the melting temperatures (T_m) of ODNs bearing alkyne-modified coumarin or azide unit has been examined (Table 2-2). The specific sequences were designed to target codon 248 in exon 7 of the p53 gene. The p53 gene is often mutated in human cancer, and there is a high frequency of A $\rightarrow$ G transition at codon 248.[37] Initially, the ODN probe (ODN **4**) was designed to utilize "click" reaction to cross-link target sequence and to discriminate between matched (dG, ODN **5**) and mismatched sequence (dA, ODN **6**). The coumarin moiety increased the duplex stability (ODN **2** • ODN **5**) with a ΔT_m of 3.6 °C relative to duplex not containing coumarin moiety (ODN **1** • ODN **2**), while Azide group slightly decreased the duplex stability (ODN **1** • ODN **2**) (ΔT_m = - 0.4 °C). However, the duplex (ODN **4** • ODN **5**) containing a coumarin moiety opposite to an azide unit showed extra stability (ΔT_m = 4.6 °C). The introduction of a coumarin moiety or an azide group in the ODN probes do not affect mismatch discrimination of dC toward dA (ΔT_m = -17.4). These data suggest that azide

and coumarin moiety can be utlized as reporters for designing ODN probes for detecting tumor's mutated DNA.

Table 2-2. Duplex thermal stability [a]

Duplexes	T_m (°C)	ΔT_m [c] (°C)
5'-d(GCC TC C GGT TCA) (ODN **2**) 3'-d(CGG AGG ACC AGT) (ODN **1**)	53.1 ± 0.3	0
5'-d(GCC TC C GGT TCA**Z**) (ODN **4**) 3'-d(CGG AGG ACC AGT) (ODN **1**)	52.7 ± 0.4	-0.4
5'-d(GCC TC C GGT TCA) (ODN **2**) 3'-d(CGG AGG CCA AGT**6**) (ODN **5**)	56.7 ± 0.4	+3.6
5'-d(GCC TC C GGT TCA**Z**) (ODN **4**) 3'-d(CGG AGG CCA AGT**6**) (ODN **5**)	57.7 ± 0.8	+4.6
5'-d(GCC TC C GGT TCA**Z**) (ODN **4**) 3'-d(CGG AGA CCA AGT**6**) (ODN **6**)	40.3 ± 0.3	-17.4

[a] Measured in 0.1 M NaCl, 10 mM potassium phosphate buffer (pH 7.0) with 4 μM + 4 μM single-strand concentration.

2.3. Fluorogenic DNA Interstrand Cross-Linking via Click Reaction

2.3.1. Efficiency of Click Reaction

Cross-linked DNA duplexes have been used in many fields such as DNA repair, gene regulation, reversible control of DNA hybridization, and as aptamers and decoys to sequester DNA-binding proteins, and in nanotechnology for the assembly of stable DNA

nanoarrays (Chapter 1). Both Brown and Seela groups have used "click" chemistry to cross-link complementary DNA strands through modified nucleobases or sugar moieties.[38-39] In this work, we used a fluorogenic "click" reaction for building covalently fluorescent cross-linked DNA constructs, which can be a useful tool in nanotechnology and in biological applications. ODN **4** containing an azide group at the 3'-terminus and ODN **5** bearing an alkyne-modified courmarin at the 5'-terminus have been used for this study (Figure 2-4A). All click reactions were performed in 100 mM NaCl and 10 mM potassium phosphate buffer (pH = 7) to ensure complete formation of the duplexes. Initially, we used gel-electrophoresis to examine the cross-linking efficiency. ODN **4** was ^{32}P-labeled at the 5'-terminus. The cross-linking reaction was performed in the presence of Cu[I]/THPTA (Tris-(hydroxypropyltriazolylmethyl)amine) at room temperature. The Cu[I] was generated in situ from $CuSO_4$ and sodium ascorbate and bound with a water-soluble ligand THPTA which greatly reduced the degradation of ODNs and also increased the "click" reaction yield.[40] The click reaction was performed at room temperature under different conditions: lane 1, the reaction was carried out in the absence of the catalyst; lanes 2-4, the reactions were carried out in the presence of 80 mM THPTA/4 mM $CuSO_4$/40 mM Na-ascorbate for different time; lane 5, the reaction was performed with 40 mM THPTA/2 mM $CuSO_4$/20 mM Na-ascorbate (Figure 2-4). The DNA interstrand cross-linking (ICL) reaction between ODN 4 and ODN 5 was highly efficient with a yield of about 90% within 0.5 hour at room temperature (Figure 2-4B, lane 2). A control reaction was performed in the absence of $CuSO_4$/sodium ascorbate/THPTA and no cross-linking product (~ 0.3%, close to background) was observed (Figure 2-4B, Lane 1). We also observed that less catalyst led to a lower yield

(79%, Figure 2-4B, Lane 5). The rate of DNA ICL formation at room temperature followed first-order kinetics (k_{ICL} = (1.1 ± 0.2) × 10^{-3} s^{-1}, $t_{1/2}$ = 10.5 min, Figure 2-4C). Cross-linked product (ODN **15**) was purified by gel electrophoresis and characterized by MALDI-TOF.

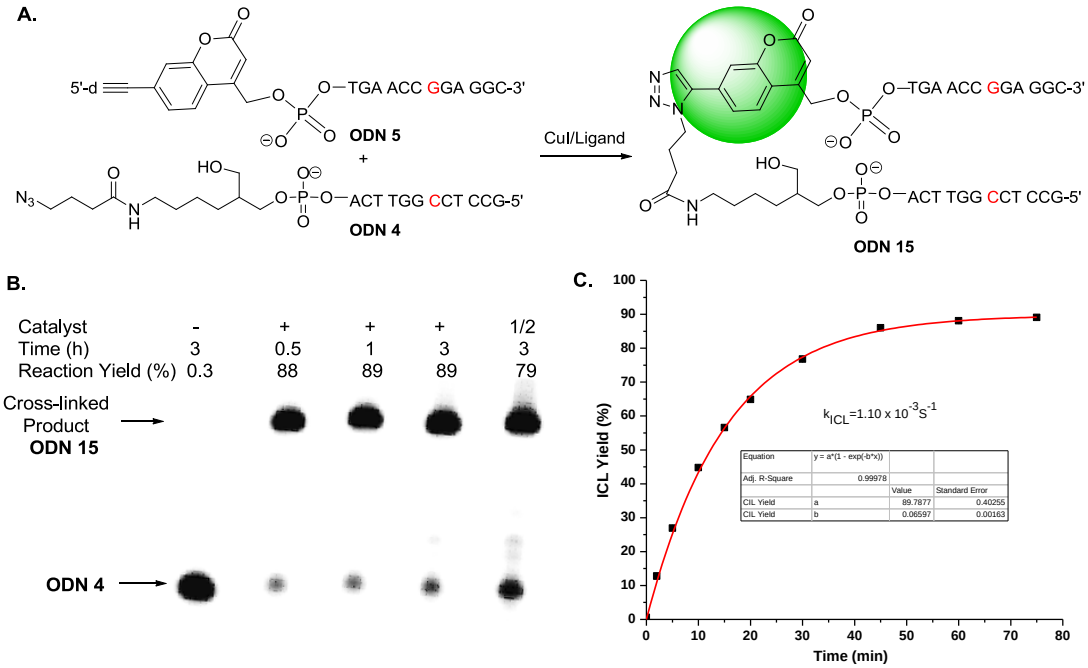

Figure 2-4. The fluorogenic ICL reaction between ODN **4** and ODN **5** [The fluorogenic click reaction (A), phosphorimage autoradiogram of denaturing PAGE analysis (B), and kinetic study (C). ([ODN **4**] = 50 nM, [ODN **5**] = 75 nM).].

2.3.2. Detection of ICL via Fluorescence Assay

To confirm the enhanced fluorescence after the fluorogenic click reaction, the isolated cross-linking product (ODN **15**) as well as the DNA ICL reaction was also examined by fluorescence spectroscopy. In comparison with a mixture of unreacted ODN **4** and ODN **5** (10 μM), ODN **15** showed 5 times fluorescence enhancement (Figure 2-5A). This is

consistent with the results observed by Fahrni and coworker that an alkyne group at the position-7 quenched the fluorescence of coumarin moiety, while the formation of a triazole moiety restored its fluorescence.[36] The results indicated that the restored fluorescence was not quenched by duplex DNA or only to a very small extent. Therefore, alkyne-modified coumarin can be a good reporter group for a DNA-templated fluorogenic reaction. Finally, we were able to use the fluorescence spectroscopy to detect DNA ICL formation. The DNA precipitations and gel-filtration on an Illustra G-25 column were carried out to remove the catalyst and salts. The fluorescence of the reaction mixture was measured before and after "click" reaction. The enhanced fluorescence intensity was observed upon the addition of the catalyst (80 mM THPTA/4 mM $CuSO_4$/40 mM Na-ascorbate) (Figure 2-5B). Thus, the DNA cross-linking reaction can be monitored by fluorescence spectroscopy.

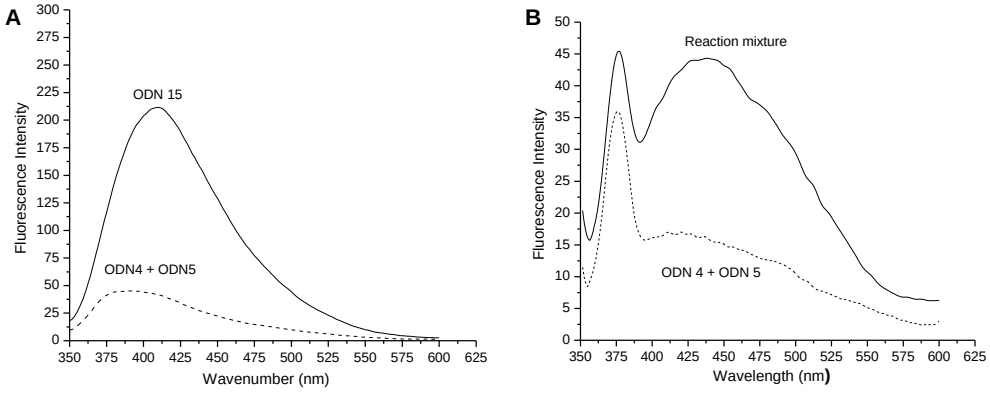

Figure 2-5. Monitoring fluorogenic ICL reaction via fluorescence assay [Fluorescence emission of the cross-linking product ODN **15** and a mixture of unreacted ODN **4** and ODN **5** in water (A, 10 μM, λ_{ex} = 330 nm, λ_{em} = 410 nm, slit width = 10 nm); Fluorescence emission of a reaction mixture of ODN **4** (0.4 μM) and ODN **5** (0.4 μM) in

or without the presence of 80 mM THPTA/4 mM $CuSO_4$/40 mM Na-ascorbate for 1 hour (B, 0.4 μM, λ_{ex} = 330 nm, λ_{em} = 410 nm, slit width = 10 nm).].

2.3.3. Selectivity of Fluorogenic DNA Interstrand Cross-Linking

Then, we examined the selectivity of the DNA-templated fluorogenic "click" reaction, which depended on the reaction temperature and duplex stability. At room temperature, ICL product was also observed with a mismatched duplex DNA (ODN **4** • ODN **6**) that contains a dA opposite to dC (Figure 2-6A). The cross-linking yield is comparable with that obtained with a fully matched DNA duplex (ODN **4** • ODN **5**) (Figure 2-6B, lanes 2 and 4). The matched duplex (ODN **4** • ODN **5**) formed efficient ICL with a yield of 89% while similar efficiency (86%) was observed for the mismatched duplex (ODN **4** • ODN **6**) at room temperature. However, the selectivity (~ 10:1) was achieved when the reaction was performed at the melting temperature of the mismatched duplex (ODN **4** • ODN **6**, 45 °C, Table 2-2) (Figure 2-6B, lanes 2 and 4). The matched duplex (ODN **4** • ODN **5**) produced efficient ICL with a yield of 83% while very little cross-linked product (< 8%) was observed for the mismatched duplex (ODN **4** • ODN **6**). These data showed that DNA-templated fluorogenic "click" reaction is sequence-specific and has the potential to be used for DNA detection.

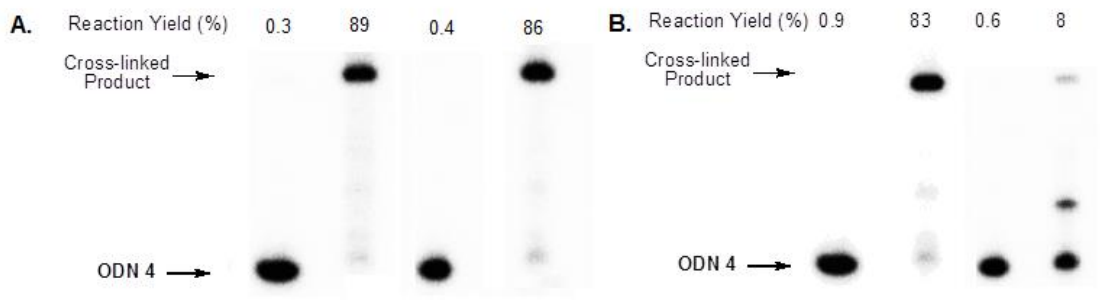

Figure 2-6. Single-nucleotide-specific "click" cross-linking reaction (room temperature (A) and 45 °C (B)) [lane 1, the matched DNA duplex ODN **4** • ODN **5** in the absence of the catalyst; lane 2, the matched DNA duplex ODN **4** • ODN **5** in the presence of 80 mM THPTA/4 mM $CuSO_4$/40 mM Na-ascorbate; lane 3, the mismatched DNA duplex ODN **4** • ODN **6** in the absence of the catalyst (THPTA/$CuSO_4$/Na-ascorbate); lane 4, the mismatched DNA duplex ODN **4** • ODN **6** in the presence of 80 mM THPTA/4 mM $CuSO_4$/40 mM Na-ascorbate. The "click" reactions were performed for 30 min at different temperatures with [ODN **4**] = 50 nM and [ODN **5**] = [ODN **6**] = 75 nM.].

2.4. Single Nucleotide Discrimination via the Fluorogenic Click Ligation Reaction

2.4.1. Optimization of Probes

Our preliminary experiments demonstrated that the fluorogenic "click" reaction can be used to detect DNAs at single nucleotide resolution. However, DNA cross-linking reaction has some limitations in real application for DNA detection because it requires both probe and target be modified with either azide or alkyne moiety. The targets are difficult to be modified with azide or alkyne at the specific position. The above problem can be overcome by developing a template-directed fluorogenic "click" ligation reaction because one can use two modified probes that are complementary to a native target. The

designed templates (ODN **12a-d**) contain sequences from the region around codon 248 in exon 7 of the p53 gene that is often mutated in human cancers.[27] Template ODN **12b** contains the genetic sequence in normal human cells, while ODN **12a** contains the mutated nucleic acid G existing in cancer cells. Detection of the tumor's mutated nucleic acids can be achieved if a DNA-templated fluorogenic "click" ligation reaction capable of single nucleotide discrimination is available. Because we expected to develop DNA probes that would enable a sequence-specific fluorogenic "click" ligation reaction therefore allowing for the detection of tumor's mutated DNA sequence (ODN **12a**). The identification of such DNA probes requires systematic design of suitable length of ODN, optimization of the distance between two probes, reaction conditions, and work-up procedures.

Initially, a 12-mer probe (ODN **4**) containing azide unit was employed, which is complementary to the 3'-terminal part of the templates. Another 12-mer probe (ODN **11**) containing an alkyne-modified coumarin at the 5'-terminus has been designed to pair with the 5'-terminal part of ODN **12a**. There is no gap between two substrates (ODN **4** and ODN **11**). An efficient ligation reaction was observed in the presence of the target **12a (**tumor's mutated nucleic acid) with a ligation yield of 89%. The "click" ligation was complete within 3 hours at 28 °C and followed first-order kinetics with a rate constant (k_L) of $(2.9 + 0.4) \times 10^{-4}$ s^{-1} (Figure 2-7A). Apart from the formation of ligation product, a byproduct (DNA*) was observed. This byproduct is most likely caused by the side reaction between azide-modified DNA and the ligand, as it was not formed in the absence of the ligand in ICL click reactions (Figure 2-6, lane 1). However, the selectivity was not achieved when the "click" reaction was performed at room temperature. The mismatched

template (ODN **12b**) also produced 84% ligated product (Figure 2-7B). The excellent selectivity was achieved when the reaction temperature was increased to 45 °C which is above the melting temperature of the mismatched duplex (40 °C for ODN **4** • ODN **12a**) (Table 2-2) (Figure 2-7C). In order for the detection method being carried out in mild condition, we expected that the fluorogenic "click" ligation reaction should show sequence-selectivity at room temperature. Therefore, the length of probes has been optimized.

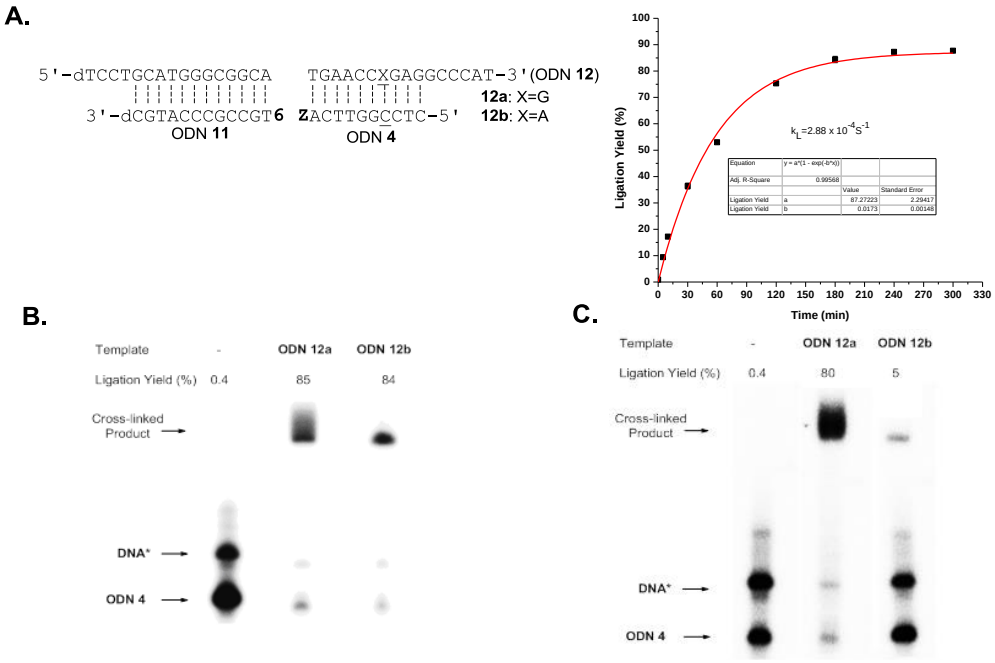

Figure 2-7. The selectivity of "click" ligation reactions using probe ODN **4** [Kinetic study for the "click" ligation reactions with ODN **4** and ODN **11** in the presence of matched template ODN **12a** at room temperature (A); Phosphorimage autoradiogram of denaturing PAGE analysis of the "click" ligation reactions with ODN **4** and ODN **11** at room temperature (B) and 45 °C (C) (lane 1, in the absence of the template; lane 2, in the presence of matched template **12a**; lane 3, in the presence of the mismatched template

12b; **and** the ligation reaction was carried out in the presence of 80 mM THPTA/4 mM $CuSO_4$/40 mM Na-ascorbate for 3 h).].

Two sets of probes have been designed, one with 8-nucleotides (ODN **8**) and another with 9-nucleotides (ODN **10**). The melting temperatures of the DNA duplexes were determined (Table 2-3). Both ODN **8** and ODN **10** formed a stable duplex with a fully matched ODN **14a** with a melting temperature of 37.5 °C and 44.1 °C respectively, while their mismatched duplexes showed a melting temperature of lower than room temperature (<15 °C for duplexes ODN **8** • **14b**, ODN **8** • **14c**, ODN **8** • **14d** and < 21.5 °C for duplexes ODN **10** • **14b**, ODN **10** • **14c**, ODN **10** • **14d**). These data indicated that both probes can discriminate matched template (ODN **14a**) from mismatched templates (ODN **14b-d**) at room temperature with a ΔT_m of more than 22 °C. Thus, a sequence-specific "click" ligation reaction was expected to achieve by using ODN **8** or ODN **10**.

Table 2-3. Duplex melting temperatures (Tm) of ODN probes[a].

Duplexes	T_m (°C)	Duplexes	T_m (°C)
5'-dTGAACCGGAG-3' (ODN **14a**) 3'-dZCTTGGCCT (ODN **8**)	37.5 ± 0.5	5'-dTGAACCGGAG-3' (ODN **14a**) 3'-dZCTTGGCCTC (ODN **10**)	44.1 ± 0.6
5'-dTGAACCAGAG-3' (ODN **14b**) 3'-dZCTTGGCCT (ODN **8**)	< 15	5'-dTGAACCAGAG-3' (ODN **14b**) 3'-dZCTTGGCCTC (ODN **10**)	21.5 ± 0.5
5'-dTGAACCTGAG-3' (ODN **14c**) 3'-dZCTTGGCCT (ODN **8**)	< 15	5'-dTGAACCTGAG-3' (ODN **14c**) 3'-dZCTTGGCCTC (ODN **10**)	21.2 ± 0.5
5'-dTGAACCCGAG-3' (ODN **14d**) 3'-dZCTTGGCCT (ODN **8**)	< 15	5'-dTGAACCCGAG-3' (ODN **14d**) 3'-dZCTTGGCCTC (ODN **10**)	19.9 ± 0.5

[a] Measured in 0.1 M NaCl, 10 mM potassium phosphate buffer (pH 7.0) with 4 μM + 4 μM single-strand concentration.

Considering the steric hindrance between azide and coumarin moieties, ODN **8** or ODN **10** is designed to be one nucleotide away from ODN **11** (Figure 2-8A). The "click" ligation reaction of ODN **8**/ODN **11** or ODN **10**/ODN **11** was carried out in the presence of ODNs **12a-d**. As we expected, good selectivity was observed for both probes ODN **8** and ODN **10**. The matched template **12a** resulted in more efficient ligation (Figure 2-8B and 2-8C, lane 2), while almost no ligated products were observed in the presence of mismatched templates **12b**-**d** (Figure 2-8B and 2-8C, lanes 3-5). However, ODN **8** resulted in a lower ligation yield (15%) possibly due to the lower melting temperature leading to the inefficient duplex formation (Figure 2-8B). When ODN **10** was employed, almost quantitative yield (90%) was obtained in the presence of the matched template ODN **12a** while the mismatched templates (ODN **12b-d**) produced less than 3% ligation products (Figure 2-8C). The ODN **10** is the best probe for single nucleotide discrimination.

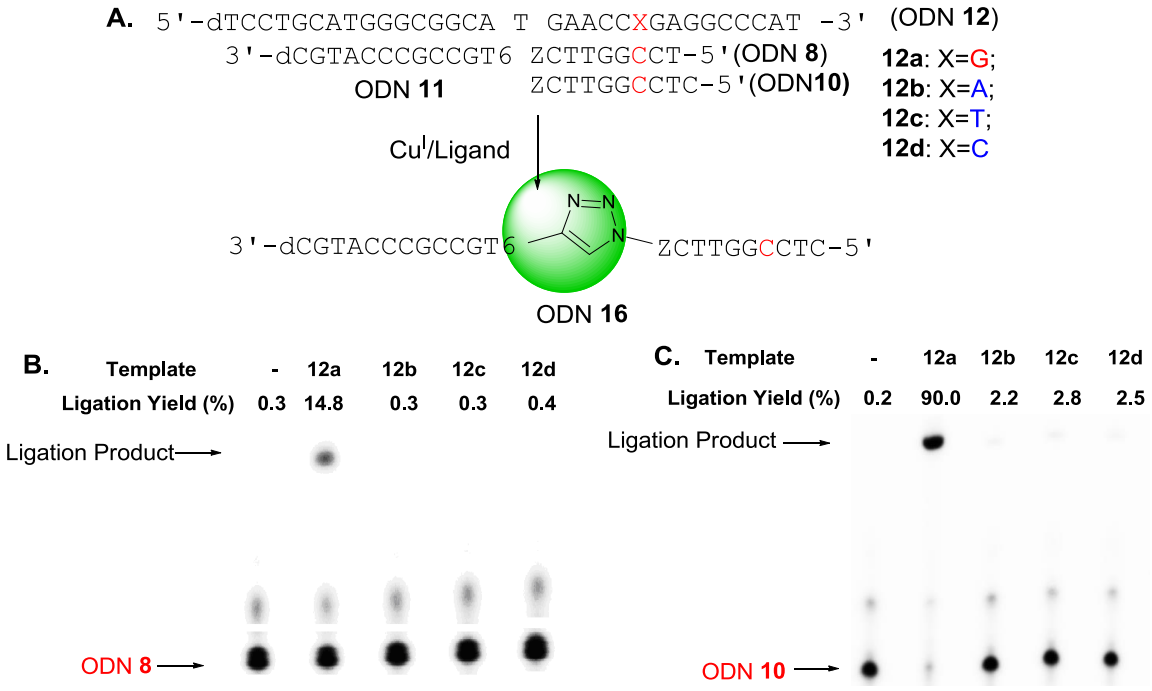

Figure 2-8. Sequence-specific fluorogenic "click" ligation reaction for probes ODN **8** and ODN **10** in the presence of templates **12a-d** [Fluorogenic "click" ligation reaction for probes ODN **8** and ODN **10** (A); Phosphorimage autoradiogram of denaturing PAGE analysis of the "click" ligation reaction between ODN **8** (B) or ODN **10** (C) and ODN **11** ([ODN **8**] = [ODN **10**] = 50 nM, [ODN **11**] = [ODN **12**] = 75 nM). The click reaction was performed at room temperature for 3 h in the presence of 80 mM THPTA/4 mM $CuSO_4$/40 mM Na-ascorbate: lane 1, the reaction was carried out in the absence of the template; lanes 2-4, the reactions were carried out in the presence of templates **12a-d**.].

In addition, ODNs **10**, **11**, and **12a** have been used to optimize the reaction conditions for the template-directed "click" ligation reaction by varying the ratio of THPTA/$CuSO_4$ (Figure 2-9A), the concentration of $CuSO_4$ (Figure 2-9B), and the ratio of $CuSO_4$/Na-ascorbate (Figure 2-9C). The ratio of THPTA/$CuSO_4$ greatly affects the ligation efficiency and the optimum ratio is 20:1. The minimum concentration of $CuSO_4$ for an

efficient “click” ligation is 4 mM and that of Na ascorbate is 8 mM. Finally, the optimum conditions (80 mM THPTA/4 mM $CuSO_4$/40 mM Na-ascorbate, 3 hours, 25-28 °C) have been established, which was used in all following “click” ligation reactions and DNA detections.

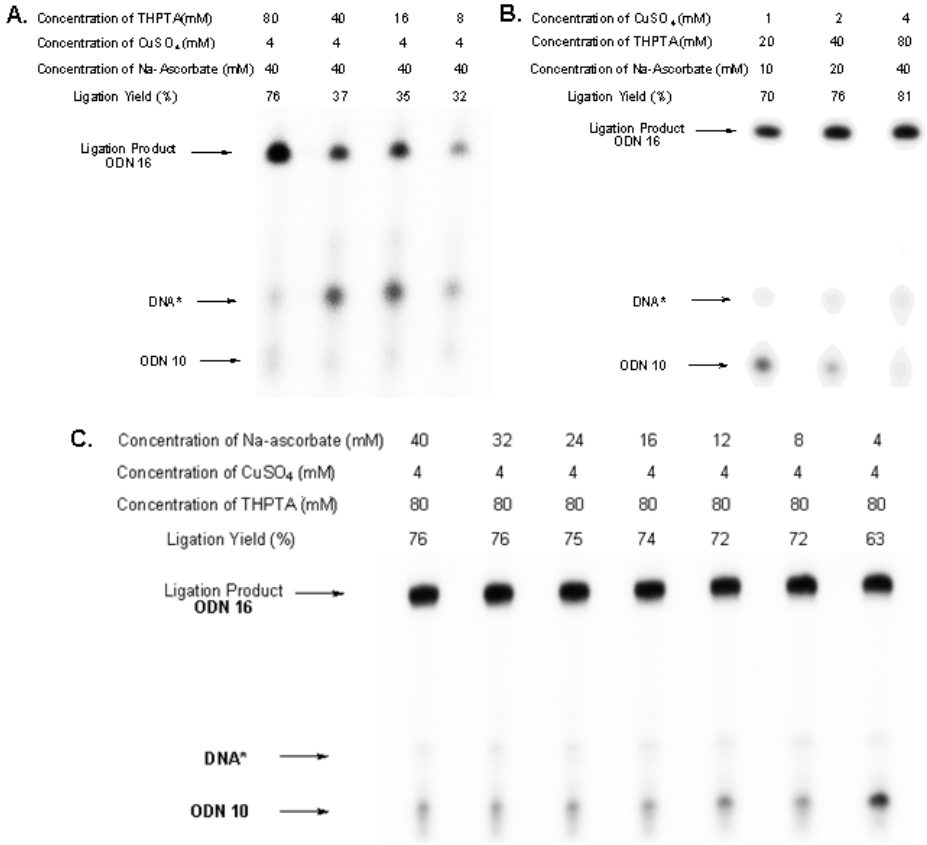

Figure 2-9. Optimizations of the “click” ligation reaction conditions [The effect of THPTA (A), $CuSO_4$ (B), and Na-ascorbate (C). (Phosphorimage autoradiogram of denaturing PAGE analysis of template-directed “click” ligation reactions of ODN **10** and ODN **11** in the presence of matched template ODN **12a** were performed at room temperature for 3 h.)].

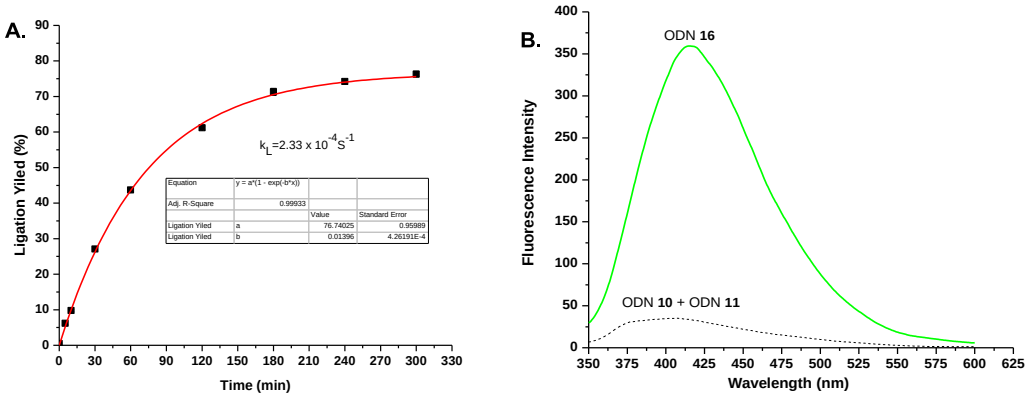

Figure 2-10. Fluorogenic "click" ligation reaction between ODN **10** and ODN **11** in the presence of template **12a** [Kinetic studuy (A); Fluorescence emission of the gel-purified ligation product (10 μM ODN **16**, solid line) and a mixture of unreacted ODN **10** (10 μM) and ODN **11** (10 μM) in water (dashed line) (B, λ_{ex} = 330 nm, slit width = 10 nm; λ_{em} = 410 nm, slit width = 10 nm).].

The rate constant for ligation product formation with ODN **10**/ODN **11** (k_L= (2.3 ± 0.3) × 10^{-4} s^{-1}) was within experimental error of that measured with ODN **4**/ODN **11** where there is no gap existing between two probes (k_L= (2.9 ± 0.4) × 10^{-4} s^{-1}) (Figure 2-10A). These data showed that one nucleotide gap between two probes does not affect the ligation reaction. However, the "click" ligation reaction is about four times more slowly than the "click" cross-linking reaction (k_{ICL} = (1.1 ± 0.2) × 10^{-3} s^{-1}). The ligation product (ODN **16**) was isolated and characterized by MALDI-TOF. The fluorescence of ODN **16** (10 μM) and a mixture of the unreacted ODN **10** (10 μM) and ODN **11** (10 μM) were measured. The fluorescence intensity was enhanced about 11 times (λ_{em} 415 nm) with the formation of ligation product (Figure 2-10B). Therefore, a highly efficient fluorogenic

"click" ligation reaction capable of single nucleotide discrimination at room temperature was achieved by using a 9-mer ODN probe.

2.4.2. Single Nucleotide Discrimination

In cellular application, detecting of a specific mutated gene in a mixture of different DNA templates is important because in most cases not all wild type targets are mutated to an identical gene. Some keep intact and some undergo different mutations. Therefore, the ability to detect a matched template in a mixture of different mismatched templates is important for an ODN probe to be used under cellular conditions. Therefore, the fluorogenic "click" ligation reaction of ODN **10** and **11** was performed in the presence of the mixed templates **12a-d** (Figure 2-11A). The efficient ligation reaction (74%) occurred with a template mixture containing ODN **12a** and other mismatched templates (Figure 2-11A, lane 2), while only trace amount of ligation product was observed for a mixture of ODNs **12b-d** without ODN **12a** (Figure 2-11A, lane 3).

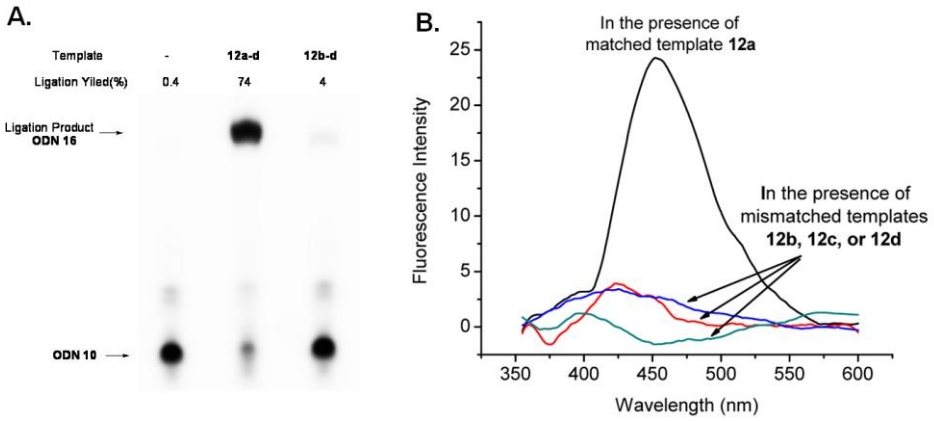

Figure 2-11. Detection of tumor's mutated nucleic acids via fluorogenic ligation reaction [Phosphorimage autoradiogram of denaturing PAGE analysis of the "click" ligation reaction between ODN **10** and ODN **11** in the presence of different templates (A): lane 1,

the reaction was carried out in the absence of templates; lane 2, the reaction was carried out in the presence of a mixture of templates **12a**-**d** ([ODN **10**] = 50 nM, [ODN **11**] = 200 nM, [ODN **12a**] = [ODN **12b**] = [ODN **12c**] = [ODN **12d**] =50 nM); lane 3, the reaction was carried out in the presence of a mixture of templates **12b**-**d** ([ODN **10**] = 50 nM, [ODN **11**] = 150 nM, [ODN **12b**] = [ODN **12c**] = [ODN **12d**] = 50 nM). Click ligation reaction was performed at room temperature for 3 h in the presence of 80 mM THPTA, 4 mM $CuSO_4$, and 40 mM Na-ascorbate. Single nucleotide discrimination via fluorescence: (B) Fluorescence emission spectra of the reaction mixture (about 0.4 μM) in the presence of different templates (ODNs **12a**-**d**) after removal of the catalyst, ligand, and the salts by precipitation and passing through an Illustra G-25 column (λ_{ex} = 330 nm, slit width = 5 nm; λ_{em} = 440 nm, slit width = 15 nm).].

Having established a fluorogenic "click" ligation reaction capable of single nucleotide discrimination, the utility of this reaction for detecting single nucleotide polymorphism and tumor's mutated nucleic acids was demonstrated using a fluorescence assay. The assay conditions were optimized. The templates were hybridized with equal mole of ODN **10** and **11**. Following addition of THPTA/$CuSO_4$/Na-ascorbate to initiate the ligation reaction, the samples were incubated at 25 °C for 3 h. After removal of the catalyst, ligand, and the salts by precipitation and passing through an Illustra G-25 column, the DNA was dissolved in water and the concentration was determined by a Varian CARY-100 BIO UV–VIS spectrophotometer at 260 nm. The fluorescence of 0.4 μM DNA was measured on a Perkin-Elmer LS55 Fluorescence Spectrometer. A control reaction was performed under the same conditions in the absence of templates. The reported fluorescence spectra were subtracted by the background signal from the control

sample. The fluorescence was greatly enhanced in the presence of the matched ODN **12a** (X = G; tumor's mutated DNA) due to the occurrence of the fluorogenic "click" ligation reaction (Figure 2-11B). However, almost no fluorescence was detected in the presence of mismatched templates **12b-d**. The ODN probes **10** and **11** showed 10-20 fold selectivity for the matched versus mismatched target sequences without removing un-reacted probes. Therefore, the fluorogenic "click" ligation reaction can be used for the detection of tumor's mutated nucleic acids under mild condition. It is not necessary to wash away unreacted probes.

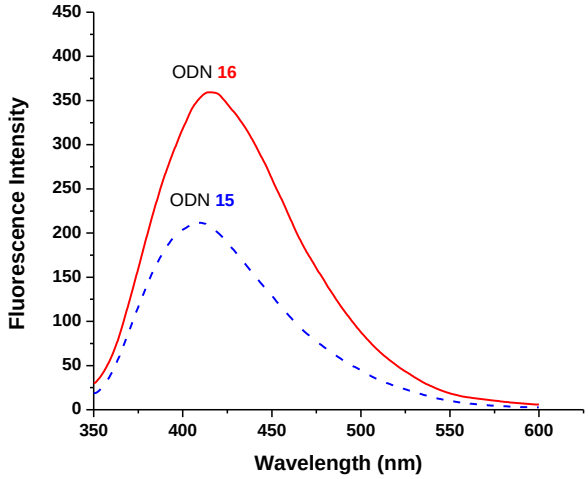

Figure 2-12. Fluorescence spectra of ICL and ligation products [ICL product ODN **15** (10 μM, dashed line) and ligation product ODN **16** (10 μM, solid line) in water (λ_{ex} 330 nm, slit width, 10 nm; λ_{em} 410 nm, slit width, 10 nm.) in water at room temperature.].

Moreover, we found the fluorescence intensity of the ICL product ODN **15** is lower than the ligation product ODN **16**'s at the same concentration (10 μM) (Figure 2-12). This indicated that the fluorescence quenching slightly occurred with the ICL product. It is highly likely that charge transfer processes occur between nucleobases and the

fluorophore in ODN **15**, which decreases the fluorescence intensity. It is well-known that charge transfer processes decrease or quench the fluorescence of fluorophore.[41] The cross-linking product existing as a duplex (ODN **15**) allows more efficient charge transfer from coumarine moiety to the nucleic acid. However, the ligation product ODN **16** is a single stranded DNA which prohibits DNA charge transfer. Therefore, ODN **16** displayed stronger fluorescence intensity than ODN **15**.

2.5. Preparation of PNA Monomers

Peptide nucleic acid (PNA) shows similar biochemical properties with DNA and can hybridize with complementary DNA strands. Different from DNAs that have sugar and phosphate backbone, PNAs contain repeated N-(2-aminoethyl)-glycine units connected by amide bonds. PNA bind with complementary DNA strands more strongly than that of DNA/DNA strands due to a lack of charge repulsion between the PNA and DNA backbones.[42] Interestingly, better sequence specificity was observed for PNA. Higher affinity exists for matched PNA/DNA duplex, but the mismatched PNA/DNA duplex is usually more destabilizing than the mismatched DNA/DNA duplex. Due to its unique biochemical and biophysical properties, PNA have been used as antigene agents, molecular probes, and biosensors. We expect that coumarin-based PNA probes will provide an alternative way for DNA mutation detection with better selectivity.

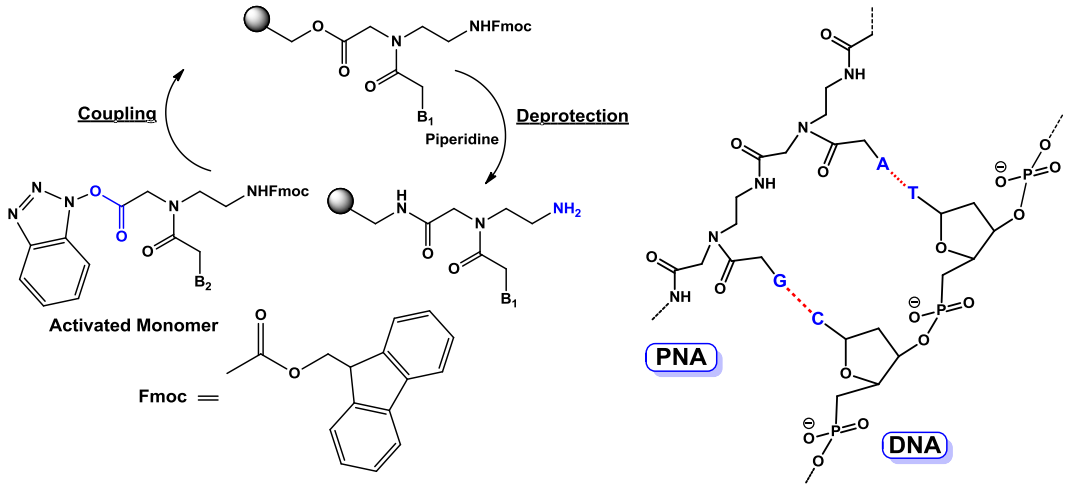

Figure 2-13. Synthesis of PNA and structure of duplex formed by PNA and DNA.

Similar to synthesis of ODN, PNA is usually prepared via automated solid-phase synthesis using 9-fluorenylmethyloxycarbonyl (Fmoc) protected monomers.[42] Two major steps, deprotection and coupling, are involved in PNA synthesis (Figure 2-13). First, the 9-fluorenylmethyloxycarbonyl (Fmoc) protecting group is removed using a solution of 20% piperidine in dimethylformamide. Then, the formed reactive amino group can couple with the activated PNA monomer to form an amide bond. PNA monomers are activated using a benzotriazole uronium salt, such as *O*-(1*H*-benzotriazol-1-yl)-*N*,*N*,*N*',*N*'-tetramethyluronium hexafluorophosphate. Elongation of the peptide chain is achieved after each synthesis cycle. To prepare the PNA probes for DNA mutation detection, the monomers containing alkyne-modified coumarin and azide groups (**14** and **21**) were synthesized using our previously reported procedures (Figure 2-14 and 2-15).[27]

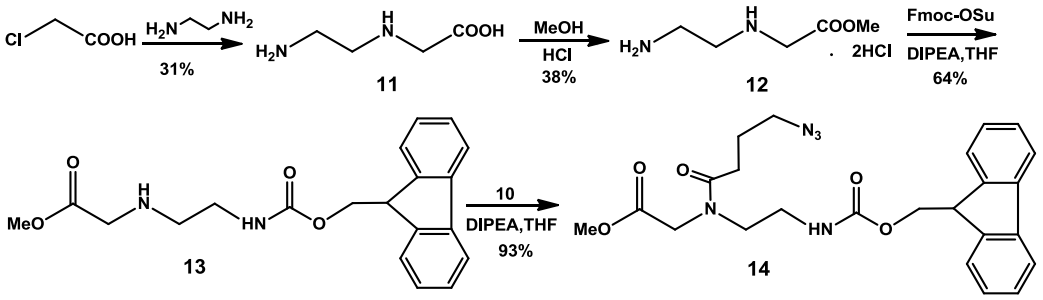

Figure 2-14. Synthesis of azide-based PNA monomer.

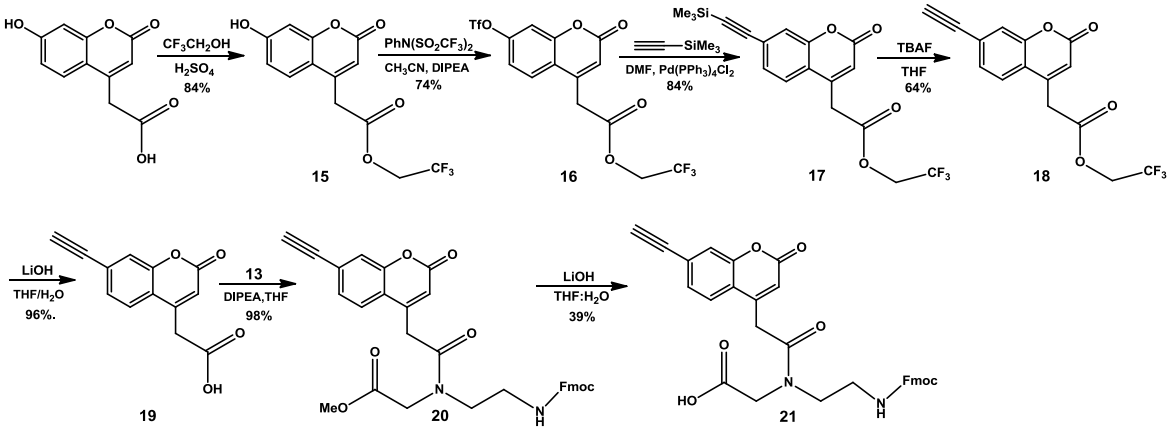

Figure 2-15. Synthesis of coumarin-based PNA monomer.

2.6. Future Study: Copper-Free Click Reaction

The fluorogenic click reaction developed in this work requires the bio-toxic catalyst copper (I) and the ligand THPTA which resulted in strong background signal and side products prohibiting direct detection by fluorescence assay and signal amplification which limits its applications in biochemistry. Bertozzi and co-workers developed a strain-promoted [3 + 2] cycloaddition of azides and cyclooctyne, referred as metal-free 'click' reaction, which occurs readily under physiological conditions without auxiliary reagents.[43-44] Coumarin fusion in biarylazacyclooctynone (**29**) would undergo metal-free fluorogenic reactions with an azide.[45] Therefore, we expect to use a non-fluorescent

coumarin-based biarylazacyclooctynone (**29**) as the probe for developing a fluorogenic ligation reaction capable of signal amplification which may find application for gene mutation detection (Figure 2-16).

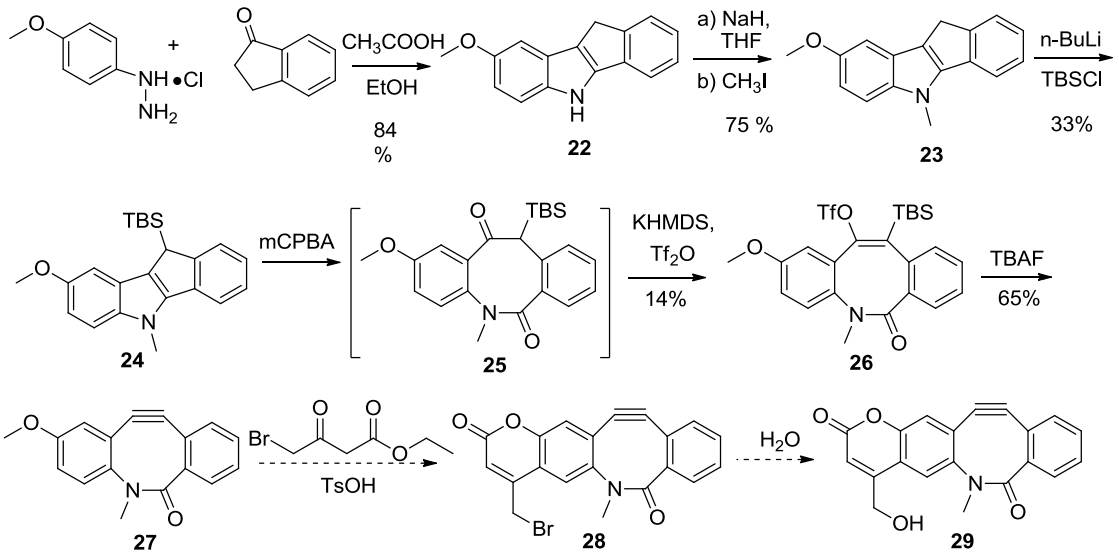

Figure 2-16. Synthesis of coumarin-based biarylazacyclooctynone.

2.7. Experimental Section

Determination of DNA melting temperature. The thermal stability of DNA duplexes was determined on a Varian CARY-100 BIO UV–VIS spectrophotometer with the Cary Win UV Thermal program using a 1.0 cm path-length cell. All measurements were performed in 10 mM potassium phosphate buffer (pH 7), 100 μM ethylenediaminetetraacetic acid (EDTA), and 100 mM NaCl, with 4 μM + 4 μM single strand concentration. The concentrations of the ODNs were determined by measuring the absorbance at 260 nm. The extinction coefficients at 260 nm of the ODNs were calculated from the sum of the extinction coefficients of the monomeric 2'-deoxyribonucleotides. Samples were heated at 1 °C min^{-1} from 4 °C to 80 °C and the

absorbance at 260 nm was measured at 1.0 °C steps. Three independent samples have been determined to get the melting temperatures of DNA duplexes.

PAGE analysis of DNA interstrand cross-link formation via "click" reaction and the kinetic study. The 5'-^{32}P-labeled ODN **4** (500 nM) and its complementary strand ODN **5** or ODN **6** (1.5 eq.) were hybridized in 100 mM NaCl and 10 mM potassium phosphate (pH 7). The "click" cross-linking reaction of DNA duplexes (50 nM) was carried out in the optimized conditions (80 mM Tris-(3-hydroxypropyltriazolylmethyl)amine (THPTA), 4 mM $CuSO_4$, and 40 mM Na-ascorbate) at the designed temperature. A control reaction was performed without adding the catalyst and the ligand. Aliquots were taken at the prescribed times and immediately quenched with the equal volumes of 95% formamide loading buffer, and stored at -20°C until subjecting to 20% denaturing PAGE analysis. For kinetics study, three independent samples were studied with the same procedures mentioned above.

PAGE analysis of template-directed "click" ligation reaction and the kinetic study. The 5'-^{32}P-labeled ODN **8** (ODN **10** or ODN **4**) (500 nM), ODN **11** (750 nM), and templates (ODN **12a-d**, 750 nM) were hybridized in 100 mM NaCl and 10 mM potassium phosphate (pH 7). The "click" ligation of DNA duplexes (50 nM) was performed in the same buffer (10 mM pH 7 potassium phosphate, 100 mM NaCl) under the optimized conditions (80 mM THPTA/4 mM $CuSO_4$/40 mM Na-ascorbate) at the designed temperature. A control reaction was carried out in the absence of templates. Aliquots were taken at the prescribed times and immediately quenched with the equal volume of 95% formamide loading buffer, and stored at -20 °C until subjecting to 20%

denaturing PAGE analysis. For kinetics study, three independent samples were studied with the same procedures mentioned above.

Isolation of the interstrand cross-link product. ODN **4** (20 μM) and its complementary strand ODN **5** (1.5 eq.) were hybridized in 100 mM NaCl and 10 mM potassium phosphate buffer (pH 7). The cross-linking reaction of DNA duplex (10 μM, 200 μL) was carried out in 10 mM potassium phosphate (pH 7) and 100 mM NaCl in the presence of 80 mM THPTA/4 mM $CuSO_4$/40 mM Na-ascorbate at room temperature for 1 hour. Then, 2 M NaCl solution (200 μL) and cold ethanol (1.2 mL) were added, the mixture was incubated at -80 °C for 30 mins and DNA was precipitated by centrifugation at 15000 g for 6 min at room temperature. ODN **15** was purified by 20% denaturing PAGE. The band containing the cross-linked product was cut, crushed, and eluted with 200 mM NaCl, 20 mM EDTA (2.0 mL). The crude product was further purified by C18 column eluting with H_2O (3 × 1.0 mL) followed by MeOH:H_2O (3:2, 1.0 mL). ODN **15** was characterized by MALDI-TOF and fluorescence spectroscopy. Its fluorescence (10 μM) was measured in water on a Perkin-Elmer LS55 Fluorescence Spectrometer.

Detection of interstrand cross-linking by fluorescence spectroscopy. The "click" reaction of DNA duplexes (0.2 μM, 200 μL) was performed in 10 mM potassium phosphate (pH 7) and 100 mM NaCl in the presence of 80 mM THPTA/4 mM $CuSO_4$/40 mM Na-ascorbate for 1 hour. The reaction mixture was precipitated by adding 2.0 M NaCl (30 μL), cold ethanol (690 μL), and keeping at -80 °C for 30 min. The DNA precipitates were collected by centrifugation at 15000 g for 6 mins at room temperature. The precipitation procedures were repeated twice. Finally, the DNA precipitates were dissolved in 50 μL H_2O and subjected to gel-filtration on an Illustra G-25 column (GE

Healthcare) to remove the catalyst and salts. The final product was dissolved in 100 μL water for fluorescence measurement.

Isolation of "click" ligation products. ODN **10** (20 μM), ODN **11** (1.5 eq.), and ODN **12a** (1.5 eq.) were hybridized in 100 mM NaCl and 10 mM potassium phosphate (pH 7). The "click" ligation of DNA duplexes (10 μM, 170 μL) were carried out in 10 mM potassium phosphate (pH 7) and 100 mM NaCl under the optimized conditions (80 mM THPTA/4 mM $CuSO_4$/40 mM Na-ascorbate, room temperature, 3 hours). The reaction mixture was precipitated by adding 2.0 M NaCl (30 μL), cold ethanol (600 μL), and keeping at -80 °C for 30 min. The precipitates were dissolved in 50 μL H_2O and 50 μL loading buffer (10 mM EDTA, 95% formamide). The ligation products were purified by 20% denaturing PAGE. The band containing ligated product was cut, crushed, and eluted with 200 mM NaCl, 20 mM EDTA (2.0 mL). The crude product was further purified by C18 column eluting with H_2O (3 × 1.0 mL) followed by MeOH:H_2O (3:2, 1.0 mL). The ligation product was characterized by MALDI-TOF. The fluorescence of ODN **16** (10 μM) was measured in water on a Perkin-Elmer LS55 Fluorescence Spectrometer.

Detection of SNPs in p53 tumor suppressor gene with DNA-templated fluorogenic "click" reaction. ODN **10** (0.4 μM) and ODN **11 (**1.5 eq.) were hybridized with DNA templates (ODNs **12a-d**, 1.5 eq.) in 100 mM NaCl and 10 mM potassium phosphate (pH 7). The "click" ligation reaction of DNA duplexes (0.2 μM, 200 μL) was carried out in 10 mM potassium phosphate (pH 7) and 100 mM NaCl under the optimized conditions (80 mM THPTA/4 mM $CuSO_4$/40 mM Na-ascorbate, room temperature, 3 hours). After 3 times' precipitations (30 μL 2 M NaCl/690 μL ethanol, -80 °C, 30 min), the DNA precipitates were dissolved in 50 μL water and subjected to gel-filtration on an Illustra G-

25 column (GE Healthcare). The DNA was reprecipitated, dissolved in 100 μL water, and the fluorescence was determined.

Ethyl 4-bromoacetoacetate (1). To a mixture of ethyl acetoacetate (2.97 g, 22.9 mmol) and acetic acid (10 mL), Br_2 (3.66 g, 22.9 mmol) in acetic acid (10 mL) was added dropwise. The mixture was stirred for 8 h at room temperature and extracted with methylene chloride (25 mL x 3). The combined organic layer was washed with water (20 mL x 3) and brine (20 mL x 2), then dried over anhydrous Na_2SO_4 and concentrated under reduced pressure. The crude product was purified by flash chromatography on silica gel (EtOAc:Hexane = 1:10) providing compound **1** as a colorless oil (2.88 g, 14.85 mmol, 65%) (**keto form**). ^{1}H NMR (300 MHz, $CDCl_3$): δ 4.21 - 4.24 (q, *J* = 7.2 Hz, 2 H), 4.06 (s, 2 H), 3.71 (s, 2 H), 1.28 - 1.33 (t, *J* = 7.1 Hz, 3 H). (**enol form**) ^{1}H NMR (300 MHz, $CDCl_3$): δ 12.05 (s, 1 H), 5.29 (s, 1 H), 4.21 - 4.24 (q, *J* = 7.0 Hz, 2 H), 3.86 (s, 2 H), 1.28-1.33 (t, *J* = 7.0 Hz, 3 H).

4-Bromomethyl-7-hydroxychromen-2-one (2). To a mixture of 1, 3-dihydroxybenzene (1.50 g, 13.7 mmol) and **1** (2.88 g, 13.7 mmol) in benzene (10 mL), a catalytic amount of conc. H_2SO_4 was added. The mixture was stirred vigorously at room temperature for 8 h. Then, water (50 mL) was added. The resulting precipitate was filtered off and dried under vacuum. The crude product was purified by flash chromatography on silica gel (EtOAc:Hexane = 1:1) affording compound **2** as a white solid (0.69 g, 2.71 mmol, 20 %). ^{1}H NMR (DMSO-d_6, 300 MHz): δ 10.70 (s, 1 H), 7.71, 7.74 (d, *J* = 8.4 Hz, 1 H), 6.84, 6.87 (d, *J* = 8.4 Hz, 1 H), 6.75 (s, 1 H), 6.48 (s, 1 H), 4.82 (s, 2 H).

7-Hydroxy-4-hydroxymethylchromen-2-one (3). A suspension of bromide **2** (600 mg, 2.35 mmol) in 50 mL water was heated under refluxing for 8 h. After cooling to room temperature, the mixture was extracted with EtOAc (25 mL x 3). The combined organic layers were washed with water (20 mL x 2) and brine (20 mL x 2), then dried over anhydrous Na_2SO_4 and evaporated to dryness. The crude product was purified by flash chromatography on silica gel (EtOAc:Hexane = 4:1) yielding **3** as a white solid (408 mg, 2.13 mmol, 90%). ^{1}H NMR (DMSO-d_6, 300 MHz): δ 4.69, 4.71 (d, *J* = 5.1 Hz, 2 H), 5.56 - 5.60 (t, *J* = 5.1 Hz, 1 H), 6.24 (s, 1 H), 6.73 (s, 1 H), 6.76, 6.79 (d, *J* = 8.7 Hz, 1 H), 7.51, 7.54 (d, *J* = 8.7 Hz, 1 H), 10.51 (s, 1 H).

4-Hydroxymethyl-2-oxo-2H-chromen-7-yl trifluoromethanesulfonate (4). A reaction mixture of *N*-phenylbis(trifluoromethanesulfonimide) (200 mg, 0.56 mmol), **3** (360 mg, 1.88mmol), and *N*, *N*-diisopropylethylamine (0.43 mL, 2.5 mmol) in CH_3CN (20 mL) was stirred at room temperature for 3 h. The mixture was extracted with EtOAc (25 mL x 3). The combined organic layers were washed with water (20 mL x 2) and brine (20 mL x 2), then dried over anhydrous Na_2SO_4 and concentrated under reduced pressure. The residue was purified by flash chromatography on silica gel (Hexane:EtOAc = 1:1) yielding **4** as a white solid (452 mg, 1.40 mmol, 74%). ^{1}H NMR ($CDCl_3$, 300 MHz): δ 4.93 (s, 2 H), 6.71 (s, 1 H), 7.23, 7.26 (d, *J* = 9.0 Hz, 1 H), 7.33 (s, 1 H), 7.64, 7.67 (d, *J* = 9.0 Hz, 1 H).

7-(Trimethylsilylethylethynyl)-4-hydroxylcoumarin (5). A mixture containing **4** (370 mg, 1.14 mmol), dichloro(triphenylphosphine)-palladium (42 mg, 0.06 mmol), CuI (11.6 mg, 0.06 mmol), trimethylsilylacetylene (0.54 mL, 3.82 mmol), triethylamine (0.36 mL, 2.7 mmol), and *N*,*N*-diisopropylethylamine (0.25 mL, 1.8 mmol) in DMF (15 mL) was

flushed with argon for 10 min and stirred at 40 °C for 3 hours. The mixture was diluted with EtOAc (40 mL), washed with water (30 mL x 2) and brine (30 mL), dried over anhydrous Na_2SO_4, and concentrated under reduced pressure. The crude product was purified by flash chromatography on silica gel (Hexane:EtOAc = 1:1) providing **5** as a white solid (281 mg, 1.03 mmol, 90%). ^{1}H NMR ($CDCl_3$, 300 MHz): δ 0.30 (s, 9 H), 4.92 - 4.94 (q, *J* = 8.4 Hz, 2 H), 6.65 (s, 1 H), 7.34 (d, 1 H), 7.34 - 7.46 (m, 2 H).

7-Ethynyl-4-hydroxymethylchromen-2-one (6). To a solution of **5** (163 mg, 0.6 mmol) in methanol (25 mL), 1.0 M tetrabutylammomium fluoride in THF (2 mL) was added. The reaction mixture was stirred at 60 °C for 30 min. After cooling to room temperature, water was added until precipitation occurred. The crude product was filtered off and purified on silica gel (hexane:EtOAc = 1 : 1) yielding **6** as a white solid (90 mg, 0.45 mmol, 75%). ^{1}H NMR (DMSO-d_6, 300 MHz): δ 4.51 (s, 1 H), 4.76,4.78 (d, *J* = 5.4 Hz, 2 H), 5.68-5.72 (t, *J* = 5.1 Hz, 1 H), 6.49 (s, 1 H), 7.42, 7.45 (d, *J* = 8.4 Hz, 1 H), 7.54 (s, 1 H), 7.70, 7.73 (d, *J* = 8.4 Hz, 1 H).

7-Ethynyl-4-hydroxymethylchromen-2-*O*-(2-cyanoethyl-N,N-diisosopropyl)-Phosphoramidite (7). To a solution of **6** (20 mg, 0.1 mmol) in dichloromethane (2 mL), *N*,*N*-diisopropylethylamine (DIPEA) (33.6 µL, 0.18 mmol) and 2-cyanoethyl-*N*,*N*-diisopropylchlorophosphoramidite (33.6 µL, 0.15 mmol) were added under an atmosphere of argon. The reaction mixture was stirred at room temperature for 3 h and diluted with EtOAc (30 mL). The organic layer was washed with water (20 mL x 2) and saturated aqueous NaCl (20 mL), and dried over anhydrous sodium sulfate. The solvent was removed under reduced pressure. The crude product was purified by column chromatography (EtOAc:hexane:Et_3N = 66:33:1) yielding **7** as a white solid (28 mg,

70%). ^{31}P ($CDCl_3$, 300 MHz): δ 149.38. ^{1}H NMR ($CDCl_3$, 300 MHz): δ 7.50 (d, *J* = 8.1 Hz, 1 H), 7.46 (s, 1 H), 7.28 (d, *J* = 8.1 Hz, 1 H), 6.61 (s, 1 H), 4.87 (t, *J* = 6.3 Hz, 1 H), 3.66-3.99 (m, 4 H), 3.28 (s, 1 H), 2.67 (t , *J* = 6.3 Hz, 1 H), 1.25 (d, 12 H). ^{13}C NMR ($CDCl_3$): δ 160.4, 153.2, 151.7, 151.6, 127.9, 125.6, 120.6, 117.8, 117.6, 113.3, 82.0, 61.6, 61.3, 58.5, 58.2, 43.6, 43.4, 24.7, 20.6, 20.5.

Methyl 4-azidobutyrate (8). To a solution of methyl 4-bromobutyrate (2.7 g, 15 mmol) in DMF (4 mL), sodium azide (1.95 g, 30 mmol) was added. The mixture was heated at 80 °C overnight and was diluted with ethyl acetate (50 mL). The organic layer was washed with $NaHCO_3$ (20 mL x 3), water (20 mL x 3), and brine (20 mL), and dried over anhydrous Na_2SO_4. The solvent was removed under vacuum to yield **8** as a pale yellow liquid (1.32 g, 62%). ^{1}H NMR ($CDCl_3$, 300 MHz): δ 3.66 (s, 3 H), 3.32 (t, *J* = 7.8 Hz, 3 H), 2.38 (t, *J* = 7.5 Hz, 2 H), 1.86 (m, 2 H).

5-Azidovaleric acid (9). To a mixture of LiOH (20 mmol in 5 mL water) and MeOH (15 mL), **8** (1.29 g, 9 mmol) was added. The suspension was stirred overnight. MeOH was removed under vacuum. The resulting residue was diluted by ethyl acetate (50 mL) and washed with 1.0 M HCl (20 mL x 3), water (20 mL x 3) and brine (20 mL). The organic layer was dried over anhydrous Na_2SO_4 and evaporated to dryness under vacuum yielding **9** as a pale yellow liquid (0.89 g, 76%). ^{1}H NMR ($CDCl_3$, 300 MHz): δ 3.38 (t, *J* = 6.6 Hz, 3 H), 2.48 (t, *J* = 7.2 Hz, 2 H), 1.90 (m, 2 H).

Succinimidyl 5-azidovalerate (10). To a mixture of **9** (180 mg, 1.40 mmol) and *N*-hydroxysuccinimide (173 mg, 1.50 mmol) in CH_2Cl_2 (20 mL), 1-(3-dimethylaminopropyl)-3-ethylcarbodiimide hydrochloride (EDC; 287 mg, 1.50 mmol) was added. The mixture was stirred at room temperature for 20 h. Then, H_2O (20 mL)

was added. The organic layer was washed with H_2O (20 mL x 3) and brine (20 mL), dried over Na_2SO_4, and evaporated to afford **10** as a white solid (277 mg, 87%). ^{1}H NMR ($CDCl_3$): δ 3.45 (t, *J* = 6.6 Hz, 2 H), 2.87 (s, 4 H), 2.73 (t, *J* = 7.2 Hz, 2 H), 2.00 (m, 4 H).

***N*-(2-Aminoethyl)glycine (11)**. To the cooled ethylenediamine (30 mL) in an ice bath (0 °C), solid chloroacetic acid (5.0 g, 52.9 mmol) was added in ten portions allowing for complete dissolution between each addition. The reaction mixture was then stirred overnight at room temperature. The unreacted ethylenediamine was removed under vacuum. The remaining paste was triturated with DMSO and then filtered, and the solid cake was washed with DMSO and then diethyl ether. The white solid was dried under vacuum affording *N*-(2-Aminoethyl)glycine (**11**) (1.91 g, 31%). ^{1}H NMR (300 MHz, D_2O-*d2*): *δ* 3.12 (s, 2H), 2.90 (t, *J* = 7.8 Hz, 2H), 2.80 (t, *J* = 7.8 Hz, 2H).

Methyl *N*-(2-aminoethylglycinate)dihydrochloride (12). The mixture containing *N*-(2-Aminoethyl)- glycine (750 mg, 6.36 mmol) methanol (12 mL) , HCl (38%, 2.5 mL) and 2.5 mL benzene was refluxed for 12 h. White solid can be obtained by cooling the mother liquor to -20 °C and then washed with diethyl ether (3x20 mL). Removed the remaining solvent in vacuum to yield the salt **12** (1.18 g, 90%) as a white solid. ^{1}H NMR (300 MHz, DMSO-*d*6): *δ* 8.46 (br s, 3H), 4.07 (s, 2H), 3.76 (s, 3H), 3.27 (m, 2H), 3.21 (m, 2H).

Methyl 2-(2-{[(9*H*-Fluoren-9-yl)methoxy]carbonylamino}ethylamino)-acetate (13). A solution of **12** (410 mg, 2.0 mmol) and Fmoc-OSu (910 mg, 2.4 mmol) in THF was cooled to 0°C. After the addition of DIPEA (1.05 mL), the mixture was stirred at 0°C for 30min and then at room temperature for 4h. The reaction mixture was poured into ethylacetate/$NaHCO_3$ saturated solution (1:1, 60mL). The organic phase was washed with brine (3 x 25 mL) and dried over anhydrous Na_2SO_4. The solvent was then removed

under reduced pressure. The crude product was purified by flash column chromatography on silica gel using 10:90 hexane:ethylacetate mixture as eluent to obtain **13** as a white solid. Yield: 198 mg, 64%. ^{1}H NMR (300 MHz, DMSO-*d6*): δ 7.49 (d, J = 7.5, 1H), 7.41 (d, J = 8.4, 1H), 7.28 (d, J = 7.5, 1H), 6.46 (s, 1H), 4.55 (d, J = 8.4, 2 H), 4.21 (s, 2H), 3.95 (s, 1H).

Methyl 2-(2-{[(9*H*-Fluoren-9-yl)methoxy]carbonylamino}ethyl)- 5-azidovaleric acetamido acetate (14). The mixture of EDCI (75mg, 0.39 mmol), HOBt (53mg, 0.39mmol), 5-azidovaleric acid (38.7 mg, 0.3 mmol) and DCM (3 mL) was stirred for 30min. The solution of **13** (71 mg, 0.2 mmol in 1 mL DCM) was added. The reaction mixture was stirred at room temperature for 8h. The reaction mixture was poured into ethylacetate (50mL). The organic phase was washed with 10% KH_2PO_4 (3 × 30 mL), $NaHCO_3$ (20 mL), brine (2x20 mL) and dried over anhydrous Na_2SO_4. The solvent was then removed under reduced pressure. The crude product was purified by flash column chromatography on silica gel using a 1:2 hexane:ethylacetate mixture as eluent to afford **14** (86 mg, 93 %) as a colorless liquid. ^{1}H NMR (300 MHz, $CDCl_3$-*d*): δ 7.77 (d, J = 7.2 Hz, 2 H), 7.60 (d, J = 7.2 Hz, 2 H), 7.40 (t, J = 7.2 Hz, 2 H), 7.31 (t, J = 7.5 Hz, 2 H), 4.38 (t, J = 7.5 Hz, 1 H), 4.23 (d, J = 6.6 Hz, 1 H), 4.02 (s, 2 H), 3.80 (s, 3 H), 3.53 (t, J = 5.7 Hz, 2 H), 3.37 (t, J = 6.3 Hz, 2 H), 3.29 (t, J = 6.3 Hz, 2 H), 2.32 (m, 2 H), 1.89 (m, 2 H). ^{13}C NMR (CDCl3): δ 172.6, 171.0, 156.5, 143.9, 143.8, 141.3, 127.7, 127.0, 125.1, 125.0, 120.0, 67.0, 52.7, 52.4, 50.7, 49.3, 49.0, 47.3, 47.2, 39.5, 29.6, 24.2. HRMS (TOF-MS-ESI): calcd. for C24H27N5O5Na $[M+Na]^+$ 488.1910; found 488.1903.

(7-Hydroxy-2-oxo-2H-chromen-4-yl)-acetic acid 2,2,2-trifluoroethyl ester (15). The mixture containing 7-hydroxycoumarine-4-acetic acid (1.03 g, 4.7 mmol), 2,2,2-trifluoro

ethanol (40 mL) and H_2SO_4 (4.2 mL) was refluxed overnight. After cooling to room temperature, the methanol was removed under vacuum followed by the addition of ethylacetate (40mL). The organic layer was washed with $NaHCO_3$ (3 × 20 mL), brine (3 × 20 mL) and dried over anhydrous Na_2SO_4. The solvent was evaporated under vacuum to obtain compound **15** as a white solid. Yield: 1.19 g, 84.2 %. ^{1}H NMR (300 MHz, DMSO-*d6*): δ 10.62 (s, 1H), 7.51 (d, *J* = 8.7, 1H), 6.78 (q, *J* = 2.4, J =8.7, 1H), 6.74 (d, *J* = 2.4, 1H), 6.29 (s, 1H), 4.80 (q, *J* = 9.0, 2 H), 4.13 (s, 2H).

(2-Oxo-7-trifluoromethanesulfonyloxy-2H-chromen-4-yl)-acetic acid 2,2,2-trifluoroethyl ester (16). The solution of **15** (630 mg, 2.1 mmol), N-phenyl-bis(trifluoromethanesulfonimide) (830 mg, 2.3 mmol) and N,N-diisopropylethylamine (0.50 mL, 2.75 mmol) in acetonitrile (30 mL) was stirred at room temperature for 4 h. Then, the reaction mixture was dilute in ethylacetate (30 mL). The organic layer was washed with water (2 × 15 mL), brine (1 × 15 mL) and dried over anhydrous Na_2SO_4. The solvent was removed under reduced pressure. The crude product was purified by column chromatography using a 70:30 hexane:ethylacetate mixture as eluent to afford **16** as a yellowish solid. Yield: 680 mg, 74.4 %.1H NMR (300 MHz, DMSO-*d6*): δ 7.91 (d, *J* = 9.0,1H), 7.80 (d, *J* = 2.4,1H),6.70 (s, 1H), 7.54 (q, *J* = 2.4, 1H),4.78 (q, *J* = 9.0, 2 H), 4.28 (s, 2H).

(2-Oxo-7-trimethylsilanylethynyl-2H-chromen-4-yl)-acetic acid 2,2,2-trifluoroethyl ester (17). Dichlorobis(triphenylphosphine)-palladium (II) (45.5 mg, 0.065 mmol), CuI (12.6 mg, 0.065 mmol), triethylamine (0.39 mL, 2.92 mmol) and (trimethylsilyl)acetylene (0.29 mL, 2.0 mmol) were added to a solution of **16** (587 mg, 1.33 mmol) in dry DMF (18 mL) under argon atmosphere. The reaction mixture was

heated at 40°C for 3 hours. After cooling to room temperature, the mixture was diluted with EtOAc, washed with water (2 × 30 mL) and brine (30 mL), dried over anhydrous Na_2SO_4, and concentrated under reduced pressure. The crude product was purified by flash column chromatography using a 70:30 hexane:ethylacetate mixture as eluent to provide **17** as an orange solid. Yield: 400 mg, 84 %. ^{1}H NMR (300 MHz, DMSO-*d6*): δ 7.75 (d, J = 8.4, 1H), 7.42 (br s, 2H), 6.55 (s, 1H), 4.76 (q, J = 9.0, 2 H), 4.20 (s, 2H), 0.26 (s, 9H).

(7-Ethynyl-2-oxo-2H-chromen-4-yl)-acetic acid 2,2,2-trifluoroethyl ester (18). To a solution of **17** (380 mg, 1.0 mmol) in THF (20 mL) tetrabutylammonium fluoride (3.5 mL 1M in THF, 3.5 mmol) was added. The mixture was heated at 50°C for 2 h. After cooling to room temperature, the mixture was dilute in ethylacetate (30 mL) and washed with water (20 mL) and brine (3 × 20 mL) and dried over anhydrous Na_2SO_4. The solvent was then removed under reduced pressure. The crude product was purified by flash column chromatography using 70:30 hexane:ethylacetate mixture as eluent to yield **18** as a yellow solid. Yield: 198 mg, 64 %. ^{1}H NMR (300 MHz, DMSO-*d6*): δ 7.49 (d, J = 7.5, 1H), 7.41 (d, J = 8.4, 1H), 7.28 (d, J = 7.5, 1H), 6.46 (s, 1H), 4.55 (d, J = 8.4, 2 H), 4.21 (s, 2H), 3.95 (s, 1H).

(7-Ethynyl-2-oxo-2H-chromen-4-yl)-acetic acid (19). To a solution of **18** (150 mg, 0.48 mmol) in the mixture of tetrahydrofuran (20 mL) and water (10 mL), lithium hydroxide monohydrate (338 mg, 14 mmol) was added. The mixture was stirred at 40°C for 20 h. After cooling to the room temperature, water (30 mL) was added. The mixture was acidified to pH 1 and extracted with ethylacetate (3 × 10 mL). The combined organic phases were washed with brine (2 × 15 mL) and dried over anhydrous Na_2SO_4. The

solvent was removed under vacuum to obtain **19** as an orange solid. Yield: 106 mg, 96.1 %. 1H NMR (300 MHz, DMSO-*d6*): δ 12.89 (s, 1H), 7.71 (d, *J* = 8.4, 1H), 7.55 (s, 1H), 7.45 (d, *J* = 8.1, 1H), 6.56 (s, 1H), 4.53 (s, 1H), 3.94 (s, 2H).

Methyl 2-(2-{[(9*H*-Fluoren-9-yl)methoxy]carbonylamino}ethyl)- (7-ethynyl-2-oxo-2H-chromen-4-yl) -acetamido acetate (20). The mixture containing EDCI (75 mg, 0.39 mmol), HOBt (53mg, 0.39mmol), **19** (68 mg, 0.3 mmol) and DCM (3 mL) was stirred for 30min. The solution of **13** (71 mg, 0.2 mmol in 1 mL DCM) was added. The reaction mixture was stirred at room temperature for 18h and then poured into ethylacetate (50mL). The organic layer was washed with 10% KH_2PO_4 (2 × 30 mL), $NaHCO_3$ (20 mL), brine (2 × 20 mL) and dried over anhydrous Na_2SO_4. The solvent was then removed under vacuum. The crude product was purified by flash column chromatography using a 1:2 hexane:ethylacetate mixture as eluent to afford **20** as a yellowish solid. Yield: 110 mg, 98 %. ^{1}H NMR (300 MHz, $CDCl_3$-*d*): δ 7.32-7.80 (m, 11 H), 6.29 (d, *J* = 7.2, 1 H), 4.44 (d, *J* = 9.3, 2H), 4.08-4.22 (m, 3H), 3.84 (s, 3H), 3.80 (s, 2H), 3.60 (s, 2H), 3.42 (d, *J* = 5.1, 2H), 3.26 (s, 1 H). ^{13}C NMR (300 MHz, $CDCl_3$-*d*): δ 170.4, 169.9, 168.7, 159.8, 156.7, 153.3, 148.5, 143.8, 141.3, 128.0, 127.1, 125.7, 125.0, 124.6, 120.5, 119.5, 117.6, 82.0, 80.6, 67.0, 53.0, 52.6, 49.7, 48.8, 47.2, 39.4, 37.3, 36.4, 29.7. HRMS (TOF-MS-ESI): calcd. for C33H28N2O7Na $[M+Na]^+$ 587.1794; found 587.1756.

2-[*N*-(2-{[(9*H*-Fluoren-9-yl)methoxy]carbonylamino}ethyl)- (7-ethynyl-2-oxo-2H-chromen-4-yl) –acetamido acetic Acid (21). To the solution of ethyl ester **20** (28 mg, 0.05 mmol) in THF (1 mL), NaOH aq. (0.25 M, 2 mL, 10 equiv.) was added. The mixture was stirred at 0 °C for about 40 min. Cold H_2O (10 mL) was added to the reaction mixture, which was first extracted with Et_2O (3 × 10 mL) and then acidified to pH 6 with

$KHSO_4$ (at 0 °C, the flask was placed in an ice bath). The aqueous solution was extracted with EtOAc (3 × 25 mL), and the combined organic layers were washed with $NaHCO_3$ (25 mL) and brine (2 × 25 mL), and dried over anhydrous Na_2SO_4. The solvent was removed under vacuum providing the monomer **21** (11 mg, 39.3%) as an off-yellow solid. ^{1}H NMR (300 MHz, $CDCl_3$-*d*): δ 7.22-7.69 (m, 11H), 6.29 (s, 1H), 4.22 (d, *J* = 6.3, 1H), 3.86-4.15 (m, 5H), 3.46 (s, 2H), 3.34 (s, 2H), 3.21 (s, 1H). ^{13}C NMR (300 MHz, $CDCl_3$-*d*): *δ* 171.7, 167.5, 161.8, 157.4, 153.3, 144.1, 143.9, 141.6, 141.5, 129.4, 128.0, 127.5, 125.6, 120.3, 118.9, 82.5, 81.0, 67.4, 47.4, 47.3, 42.2, 40.0, 30.0, 14.4. HRMS (TOF-MS-ESI): calcd. for C32H26N2O7Na $[M+Na]^+$ 573.1638; found 573.1617.

8-Methoxy-5,10-dihydroindeno[1,2-b]indole (**22**). To a suspension of 4-methoxyphenylhydrazine•HCl (9.60 g, 55 mmol) and 1-indanone (7.29 g, 55 mmol) in ethanol (175 mL), acetic acid (0.20 mL) was added to the flask fitted with a condenser and the reaction mixture is heated at 85 °C for overnight. The solution will become red and light tan precipitate was formed. After cooling to 0 °C with ice-bath, the mixture was filtered. The solid precipitate was washed with ice-cold ethanol (10 mL) and hexane (30 mL), and then dried under vacuum to afford product **22** as a light tan solid (10.9 g, 84%), which is pure in NMR and used without further purification.

8-Methoxy-5-methyl-5,10-dihydroindeno[1,2-b]indole (**23**). Two methods were used for preparation of compound **10**. Method A: To a suspension of **22** (1.70 g, 7.2 mmol) in anhydrous acetone (30 mL) immersed in an ice-bath, KOH (2.0 g, 56 mmol) was added. After stirring dark solution for 5 min at 0 °C, CH_3I (1 mL, 36 mmol) was added. The solution was stirred at 0 °C for another 1 h, and then heated to room temperature prior to addition of another 1 mL CH_3I (36 mmol). The reaction was kept stirring at room

temperature for overnight and then 60 mL 1 M HCl and 30 mL water was added. The mixture was extracted with ethyl acetate (50 mL × 3), and collected organic phases were washed with water (30 mL × 2), brine (20 mL), and then dried over by anhydrous sodium sulfate. The solvent was evaporated under reduced pressure. Upon purification by silica gel column chromatography (EtOAc:hexane = 1:5, R_f = 0.62), the product was isolated as a white solid (1.22 g, 67%). Method B: A dried flask charged with a solution of **22** (1.88 g, 8.0 mmol) in anhydrous THF (30 mL) was cooled to 0 °C using an ice-bath, NaH (60% in oil, 0.48 g, 12 mmol) was added slowly at three times. After stirring dark at room temperature for 0.5 h, the solution was cooled to 0 °C. CH_3I (2 mL, 72 mmol) was added and reaction solution was heated to room temperature and stirred for overnight. The reaction is carefully quenched by adding saturated NH_4Cl (20 mL) and water (40 mL), and mixture was extracted with ethyl acetate (50 mL × 3). The combined organic phases were washed with water (30 mL × 2), brine (20 mL), and then dried over by anhydrous sodium sulfate. Evaporation of the solvents under reduced pressure and purification by flash column chromatography on silica gel yields methylated indole **23** as a white solid (1.50 g, 75%).

10-(Tert-butyldimethylsilyl)-8-methoxy-5-methyl-5,10-dihydroindeno[1,2-b]indole (**24**). A dried flask charged with a solution of **23** (2.49 g, 10 mmol) in anhydrous THF (30 mL) was cooled to 0 °C via immersing in an ice-bath. The n-BuLi (2.5 M in hexane, 6 mL, 15 mmol) was carefully added by syringe pump over 20 min. The dark red reaction mixture was stirred at 0 °C for another 30 min, and then TMSCl (2.26 g dissolved in 10 mL anhydrous THF, 15 mmol) was slowly added over 40 min. The reaction mixture was warmed to room temperature by removing the ice bath and stirred at room temperature

for 6 h. The reaction is carefully quenched via slowly addition of saturated NH_4Cl (20 mL) and water (40 mL), and mixture was extracted with ethyl acetate (50 mL × 3). The combined organic layers were washed with water (30 mL × 2), brine (20 mL), and then dried over by anhydrous sodium sulfate. The solvent was evaporated under reduced pressure and the residue was subjected to column chromatography on silica gel (gradient hexane:EtOAc = 20:1 to 10:1, R_f = 0.70 in EtOAc:hexane = 1:3) yielding compound **24** (decomposition is observed on TLC plate) as a yellowish solid (1.20 g, 33%).

(Z)-11-(tert-butyldimethylsilyl)-2-methoxy-5-methyl-6-oxo-5,6-dihydrodibenzo [b,f]azocin-12-yl trifluoromethanesulfonate (**26**). Meta-Chloroperoxybenzoic acid (m-CPBA, 77%, 4.5 g, 20 mmol) was added to ice-cold solution of **24** (1.82 g, 5 mmol) in dichloromethane (40 mL) and saturated aqueous $NaHCO_3$ (8 mL) at three times over 10 min. The dark red mixture was maintained at 0 °C for additional 30 min and then warmed to room temperature. After another 1.5 h, ice cold 1M NaOH (30 mL) was slowly added to quench the reaction. The mixture was extracted with dichloromethane (50 mL × 2), and collected organic phases were washed with water (30 mL × 2), brine (20 mL), and then dried over by anhydrous sodium sulfate. Evaporation of solvent under reduced pressure afford crude intermediate 11-(tert-butyldimethylsilyl)-2-methoxy-5-methyldibenzo[b,f]azocine-6,12(5H,11H)-dione as a red oil (It will decompose into starting material in dichloromethane upon 12 h), which was immediately brought on to next step.

To the red solution of crude intermediate (5 mmol assuming 100% yield) in anhydrous THF (30 mL) at -78 °C in acetone-dry ice bath, potassium hexamethyldisilazide (0.7 M in toluene, 7.8 mL, 5.5 mmol) was slowly added via syringe yielding a dark red solution.

After stirring for 30 min at -78 °C, triflic anhydride (1 mL, 8 mmol) was added and stirred for additional 30 min at -78 °C. The reaction mixture was diluted with 50 mL anhydrous ether and carefully quenched via slowly addition of saturated NH_4Cl (20 mL) and water (40 mL). The mixture was subsequently extracted with ethyl acetate (50 mL × 2), and collected organic phases were washed with water (30 mL × 2), brine (20 mL), and then dried over by anhydrous sodium sulfate. The solvent was removed by vacumm affording crude product, which was purified by column chromatography on silica gel (R_f = 0.33) to yield desired product as a yellowish solid (380 mg, 14%).

Biarylazacyclooctynone (**27**). To a solution of **26** (211 mg, 0.4 mmol) in THF (20 mL), TBAF (1 M in THF, 4 mL, 4 mmol) was added. After stirring resulting red solution at room temperature for 6h, reaction mixture was diluted with 50 mL ethyl acetate. The mixture was subsequently extracted with ethyl acetate (40 mL × 2), and collected organic phases were washed with water (30 mL × 2), brine (20 mL), and then dried over by anhydrous sodium sulfate. The solvent was evaporated by vacumm. Upon purification by column chromatography on silica gel (EtOAc:hexane = 1:1, R_f = 0.55), the product was isolated as a yellowish solid (68 mg, 65%).

2.8. References

[1] Part of this chapter was published in Sun, H., Peng, X. Template directed fluorogenic oligonucleotide ligation using "click" chemistry: detection of single nucleotide polymorphism in the human p53 tumor suppressor gene. *Bioconjugate Chem.* **2013**, *24,* 1226-1234.

[2] Haliassos, A., Chomel, J. C., Grandjouan, S., Kruh, J., Kaplan, J. C., Kitsis, A. Detection of minority point mutations by modified PCR technique: a new approach for a sensitive diagnosis of tumor-progression markers. *Nucleic Acids Res.* **1989**, *17*, 8093-8099.

[3] Anker, P., Mulcahy, H., Chen, X. Q., Stroun, M. Detection of circulating tumor DNA in the blood (plasma/serum) of cancer patients. *Cancer Metastasis Rev.* **1999**, *18*, 65-73.

[4] Schimanski, C., Linnemann, U., Berger, M. R. Sensitive detection of K-ras mutations augments diagnosis of colorectal cancer metastases in the liver. *Cancer Res.* **1999**, *59*, 5169-5175.

[5] Yamaguchi, Y., Watanabe, H., Yrdiran, S., Ohtsubo, K., Motoo, Y., Okai, T., Sawabu, N. Detection of mutations of p53 tumor suppressor gene in pancreatic juice and its application to diagnosis of patients with pancreatic cancer: comparison with K-ras mutation. *Clin. Cancer Res.* **1999**, *5*, 1147-1153.

[6] Maekawa, M., Nagaoka, T., Taniguchi, T., Higashi, H., Sugimura, H., Sugano, K., Yonekawa, H., Satoh, T., Horii, T., Shirai, N., *et al.* Three-dimensional microarray compared with PCR-single-strand conformation polymorphism analysis/DNA sequencing for mutation analysis of K-ras codons 12 and 13. *Clin. Chem.* **2004**, *50*, 1322-1327.

[7] Oefner, P. J., Underhill, P. A. Comparative DNA sequencing by denaturing high-performance liquid chromatography (DHPLC). *Am. J. Hum. Genet.* **1995**, *57,* A266.

[8] Kapoor, A., Jones, M., Shafer, R. W., Rhee, S. Y., Kazanjian, P., Delwart, E. L. Sequencing-based detection of low-frequency human immunodeficiency virus type 1 drug-resistant mutants by an RNA/DNA heteroduplex generator-tracking assay. *J. Virol.* **2004**, *78*, 7112-7123.

[9] Eng, C., Brody, L. C., Wagner, T. M., *et al.* Interpreting epidemiological research: blinded comparison of methods used to estimate the prevalence of inherited mutations in BRCA1. *J. Med. Genet.* **2001**, *38*, 824-833.

[10] Sidransky, D. Nucleic acid-based methods for the detection of cancer. *Science* **1997**, *278*, 1054-1058.

[11] Chen, Y. F., Wang, J. Y., Wu, C. H., *et al.* Detection of circulating cancer cells with K-ras oncogene using membrane array. *Cancer Lett.* **2005**, *229*, 115-122.

[12] Dabritz, J., Hanfler, J., Preston, R., Stieler, J., Oettle, H. Detection of Ki-ras mutations in tissue and plasma samples of patients with pancreatic cancer using PNA-mediated PCR clamping and hybridisation probes. *Br. J. Cancer* **2005**, *92*, 405-412.

[13] Chen, C. Y., Shiesh, S. C., Wu, S. J. Rapid detection of K-ras mutations in bile by peptide nucleic acid-mediated PCR clamping and melting curve analysis: comparison with restriction fragment length polymorphism analysis. *Clin. Chem.* **2004**, *50*, 481-489.

[14] Chou, L. S., Lyon, E., Wittwer, C. T. A comparison of high-resolution melting analysis with denaturing high-performance liquid chromatography for mutation scanning: cystic fibrosis transmembrane conductance regulator gene as a model. *Am. J. Clin. Pathol.* **2005**, *124*, 330-338.

[15] Mori, S., Sugahara, K., Uemura, A., Akamatsu, N., Tutsumi, R., Kuroki, T., Hirakata, Y., Atogami, S., Hasegawa, H., *et al.* Rapid, simple, and accurate detection of K-ras mutations from body fluids using real-time PCR and DNA melting curve analysis. *Labmedicine* **2006**, *37*, 286-289.

[16] Landegren, U., Kaiser, R., Sanders, J., Hood, L. A ligase-mediated gene detection technique. *Science* **1988**, *241*, 1077-1080.

[17] Silverman, A. P., Kool, E. T. Detecting RNA and DNA with templated chemical reactions. *Chem. Rev.* **2006**, *106*, 3775-3789.

[18] Grossmann, T. N., Strohbach, A., Seitz, O. Achieving turnover in DNA-templated reactions. *ChemBioChem.* **2008**, *9*, 2185-2192.

[19] Sando, S., Kool, E. T. Imaging of RNA in bacteria with self-ligating quenched probes. *J. Am. Chem. Soc.* **2002**, *124*, 9686-9687.

[20] Silverman, A. P., Baron, E. J., Kool, E. T. RNA-templated chemistry in cells: discrimination of escherichia, shigella, and salmonella bacterial strains with a new two-color FRET strategy. *ChemBioChem.* **2006**, *7*, 1890-1894.

[21] Rostovtsev, V. V., Green, L. G., Fokin, V. V., Sharpless, K. B. A stepwise huisgen cycloaddition process: copper (I)-catalyzed regioselective 'ligation' of azides and terminal alkynes. *Angew. Chem. Int. Ed.* **2002**, *41*, 2596-2599.

[22] Marti, A. A., Jockusch, S., Stevens, N., Ju, J., Turro, N. J. (2007) Fluorescent hybridization probes for sensitive and selective DNA and RNA detection. *Acc. Chem. Res*. **2007**, *40*, 402-409.

[23] Jockusch, S., Marti, A. A., Turro, N. J., Li, Z., Li, Z., Ju, J., Stevens, N., Akins, D. L. Spectroscopic investigation of a FRET molecular beacon containing two

fluorophores for probing DNA/RNA sequences. *Photochem. Photobiol. Sci.* **2006**, *5*, 493-498.

[24] Nwe, K., Brechbiel, M. W. Growing applications of "click chemistry" for bioconjugation in contemporary biomedical research. *Cancer Biother. Radiopharm.* **2009**, *24*, 289-302.

[25] Franzini, R. M., Kool, E. T. Improved templated fluorogenic probes enhance the analysis of closely related pathogenic bacteria by microscopy and flow cytometry. *Bioconjugate Chem.* **2011**, *22*, 1869-1877.

[26] Kumar, R., El-Sagheer, A., Tumpane, J., Lincoln, P., Wilhelmsson, L. M., Brown, T. Template-directed oligonucleotide strand ligation, covalent intramolecular DNA circularization and catenation using click chemistry. *J. Am. Chem. Soc.* **2007**, *129*, 6859-6864.

[27] Peng, X., Li, H., Seidman, M. A template-mediated click–click reaction: PNA-DNA, PNA-PNA (or peptide) ligation, and single nucleotide discrimination. *Eur. J. Org. Chem.* **2010**, *22*, 4194-4197.

[28] Seela, F., Sirivolu, V. R. Pyrrolo-dC oligodeoxynucleotides bearing alkynyl side chains with terminal triple bonds: synthesis, base pairing and fluorescent dye conjugates prepared by the azide-alkyne ''click'' reaction. *Org. Biomol. Chem.* **2008**, *6*, 1674-1687.

[29] Seela, F., Sirivolu, V. R., Chittepu, P. Modification of DNA with octadiynyl side chains: synthesis, base pairing, and formation of fluorescent coumarin dye conjugates of four nucleobases by the alkyne–azide ''click'' reaction. *Bioconjugate Chem.* **2008**, *19*, 211-224.

[30] Berndl, S., Herzig, N., Kele, P., Lachmann, D., Li, X., Wolfbeis, O. S., Wagenknecht, H. A. Comparison of a nucleosidic vs non-nucleosidic postsynthetic ''click'' modification of DNA with base-labile fluorescent probes. *Bioconjugate Chem.* **2009**, *20*, 558-564.

[31] Choy, G., O'Connor, S., Diehn, F. E., Costouros, N., Alexander, H. R., Choyke, P., Libutti, S. K. Comparison of noninvasive fluorescent and bioluminescent small animal optical imaging. *Biotechniques* **2003**, *35*, 1022-1026.

[32] Beatty, K. E., Xie, F., Wang, Q., Tirrell, D. A. Selective dye-labeling of newly synthesized proteins in bacterial cells. *J. Am. Chem. Soc.* **2005**, *127*, 14150-14151.

[33] Beatty, K. E., Liu, J. C., Xie, F., Dieterich, D. C., Schuman, E. M., Wang, Q., Tirrell, D. A. Fluorescence visualization of newly synthesized proteins in mammalian cells. *Angew. Chem., Int. Ed.* **2006**, *45*, 7364-7367.

[34] Neef, A. B., Schultz, C. Selective fluorescence labeling of lipids in living cells. *Angew. Chem., Int. Ed.* **2009**, *48*, 1498-1500.

[35] Droumaguet, C. L., Wang, C., Wang, Q. Fluorogenic click reaction. *Chem. Soc. Rev.* **2010**, *39*, 1233-1239.

[36] Zhou, Z., Fahrni, C. J. A fluorogenic probe for the copper(I)-catalyzed azide-alkyne ligation reaction: modulation of the fluorescence emission via $^{3}(n, \pi^*)$-$^{1}(\pi, \pi^*)$ inversion. *J. Am. Chem. Soc.* **2004**, *126*, 8862-8863.

[37] Mancuso, T., Aguilar, F., Pescarolo, M. P., Clerico, L., Russo, P., Parodi, S. Mutation frequencies at codon 248 of the p53 tumor suppressor gene are not increased in colon cancer cell lines with the RER^{+} phenotype. *Nucleic Acids Res.* 1997, *25*, 3643-3648.

[38] Kocalka, P., El-Sagheer, A. H., Brown, T. Rapid and efficient DNA strand cross-linking by click chemistry. *ChemBioChem.* **2008**, *9*, 1280-1285.

[39] Xiong, H., Seela, F. Stepwise "Click" Chemistry for the Template Independent Construction of a Broad Variety of Cross-linked Oligonucleotides: Influence of Linker Length, Position and Linking Number on DNA Duplex Stability. *J. Org. Chem.* **2011**, *76*, 5584-5597.

[40] Kanan, M. W., Rozenman, M. M., Sakurai, K., Snyder, T. M., Liu, D. R. Reaction discovery enabled by DNA-templated synthesis and in vitro selection. *Nature* **2004**, *431*, 545-549.

[41] Garo, F., Häner, R. 2,1,3-Benzothiadiazole-modified DNA. *Eur. J. Org. Chem.* **2012**, *14*, 2801-2808.

[42] Nielsen, P. E., Egholm, M. An introduction to peptide nucleic acid. *Curr. Issues Mol. Biol.* **1999**, *1*, 89-104.

[43] Jewetta, J. C., Bertozzi, C. R. Cu-free click cycloaddition reactions in chemical biology. *Chem. Soc. Rev.* **2010**, 39, 1272-1279.

[44] Gordon, C. G., Mackey, J. L., Jewett, J. C., Sletten, E. M., Houk, K. N., Bertozzi, C. R. Reactivity of biarylazacyclooctynones in copper-free click chemistry. *J. Am. Chem. Soc.* **2012**, *134*, 9199-9208.

[45] Jewetta, J. C., Bertozzi, C. R. Synthesis of a fluorogenic cyclooctyne activated by Cu-free click chemistry. *Org. Lett.* **2011**, *13*, 5937-5939.

2.9. Appendices A: Characterization of Compounds

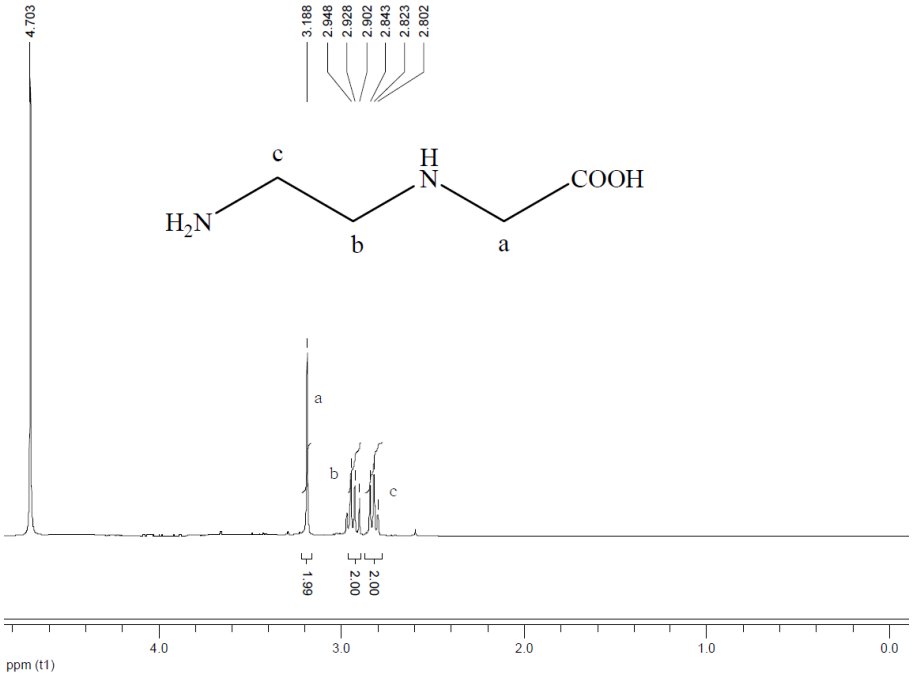

^{1}H NMR (300 MHz, D_2O-*d2*) spectra of **11**.

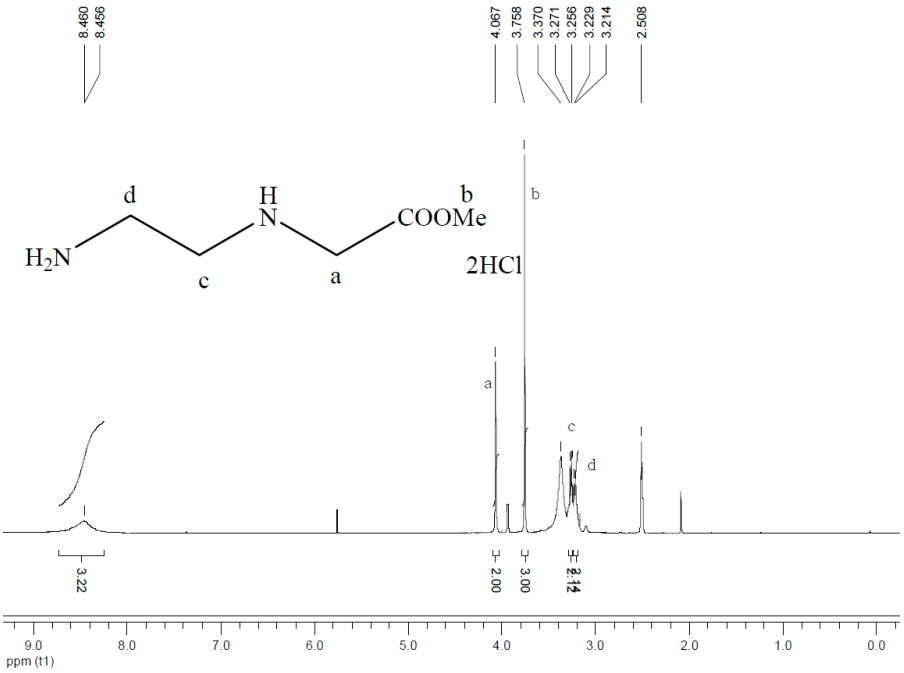

^{1}H NMR (300 MHz, DMSO-*d*6) spectra of **12**.

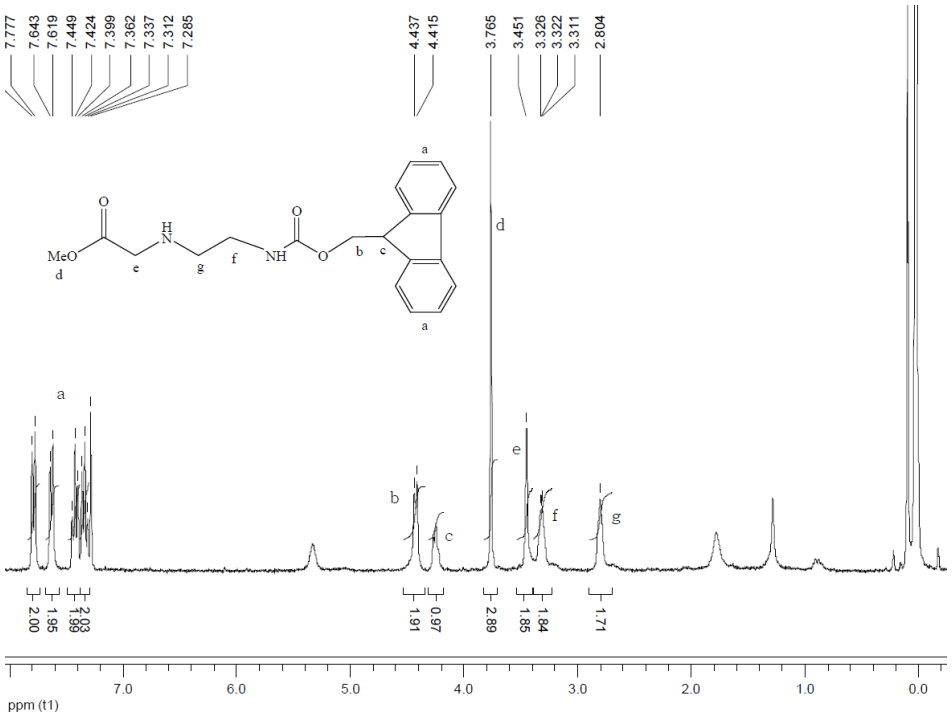

^{1}H NMR (300 MHz, DMSO-*d6*) spectra of **13**.

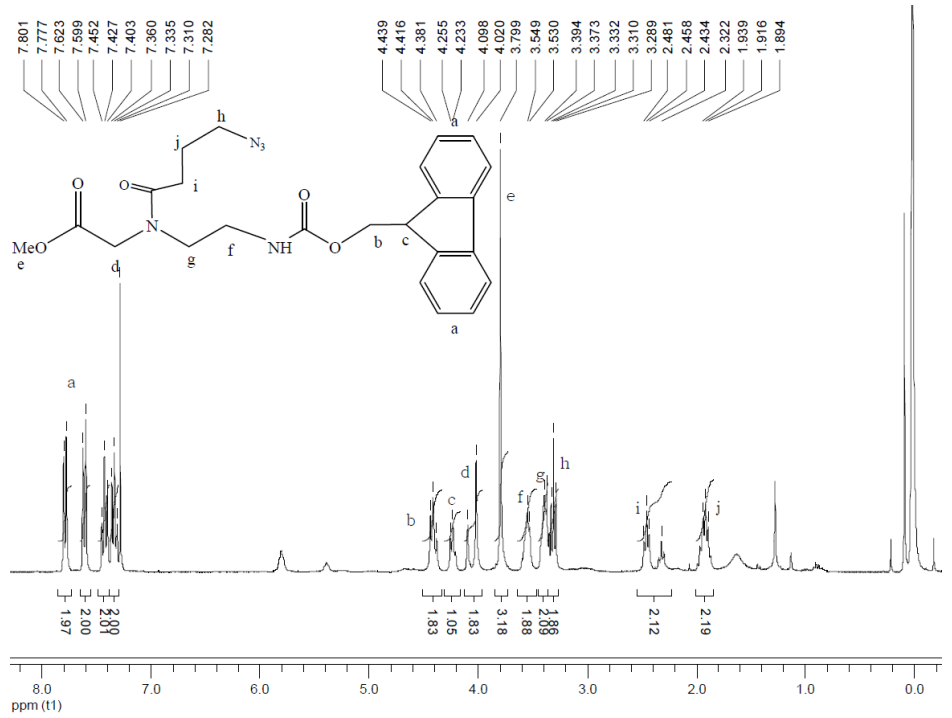

^{1}H NMR (300 MHz, $CDCl_3$-*d*) spectra of **14**.

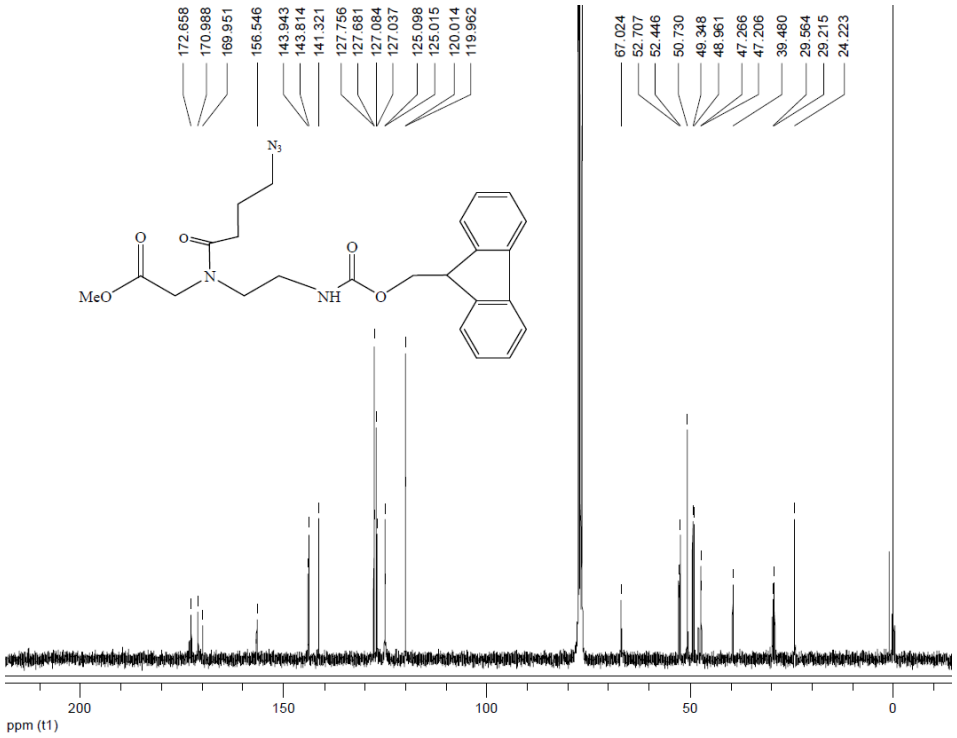

^{13}C NMR (300 MHz, $CDCl_3$-*d*)spectra of **14**.

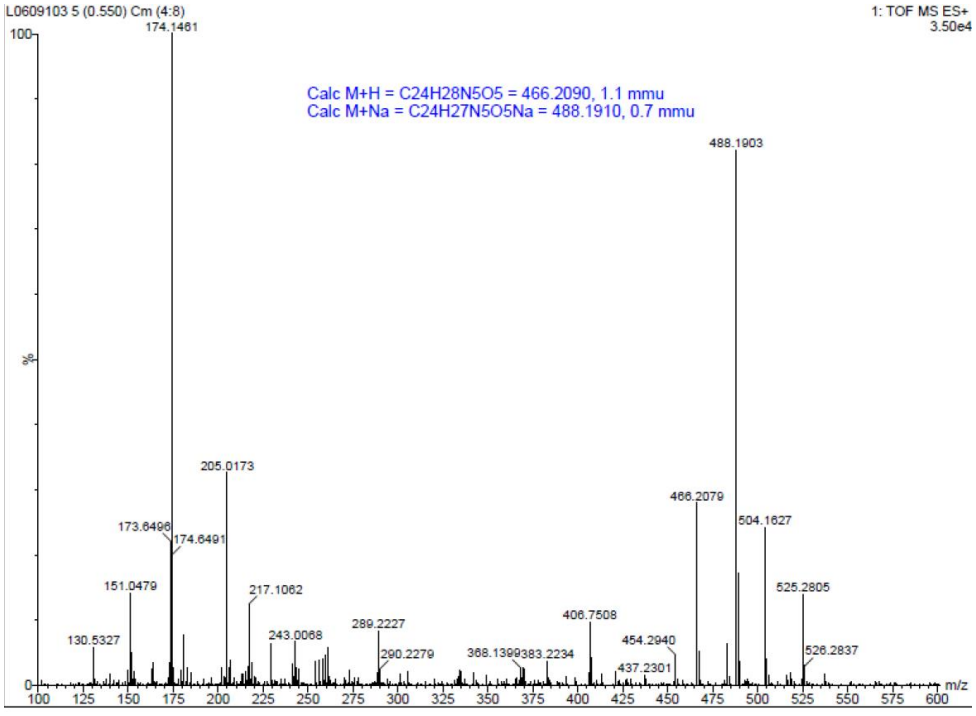

HRMS (TOF-MS-ESI) spectra of **14**.

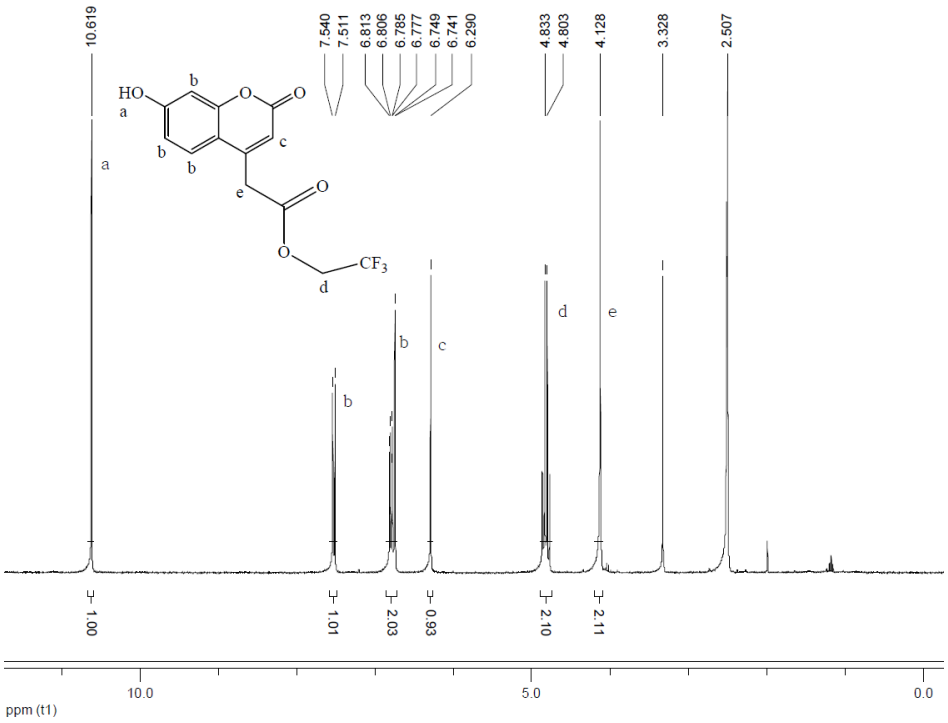

^{1}H NMR (300 MHz, DMSO-*d6*) spectra of **15**.

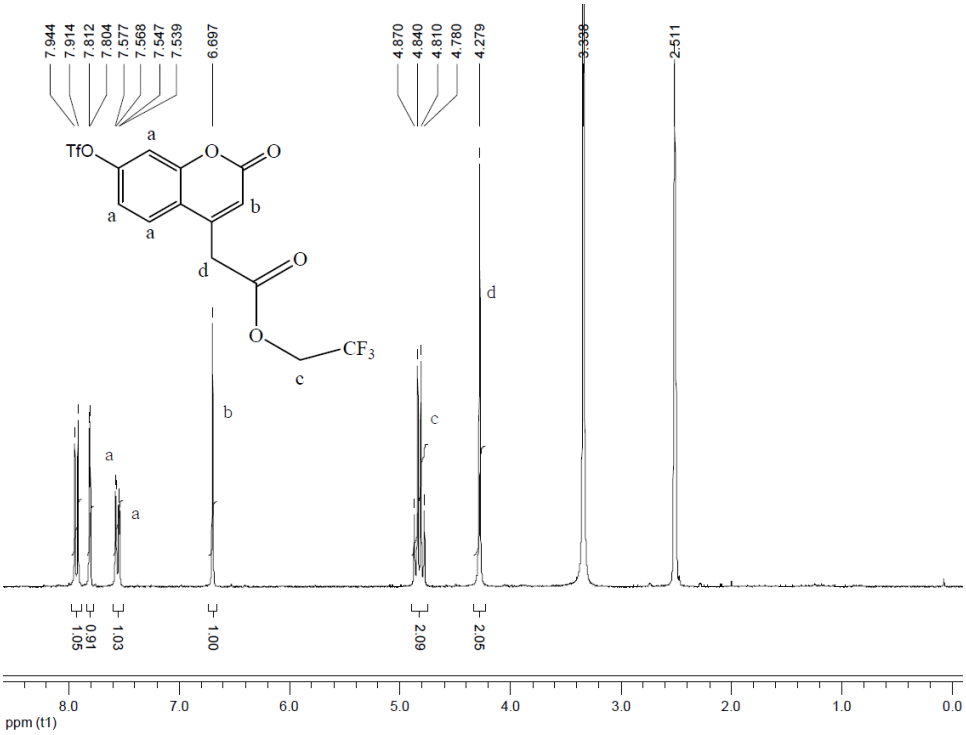

^{1}H NMR (300 MHz, DMSO-*d6*) spectra of **16**.

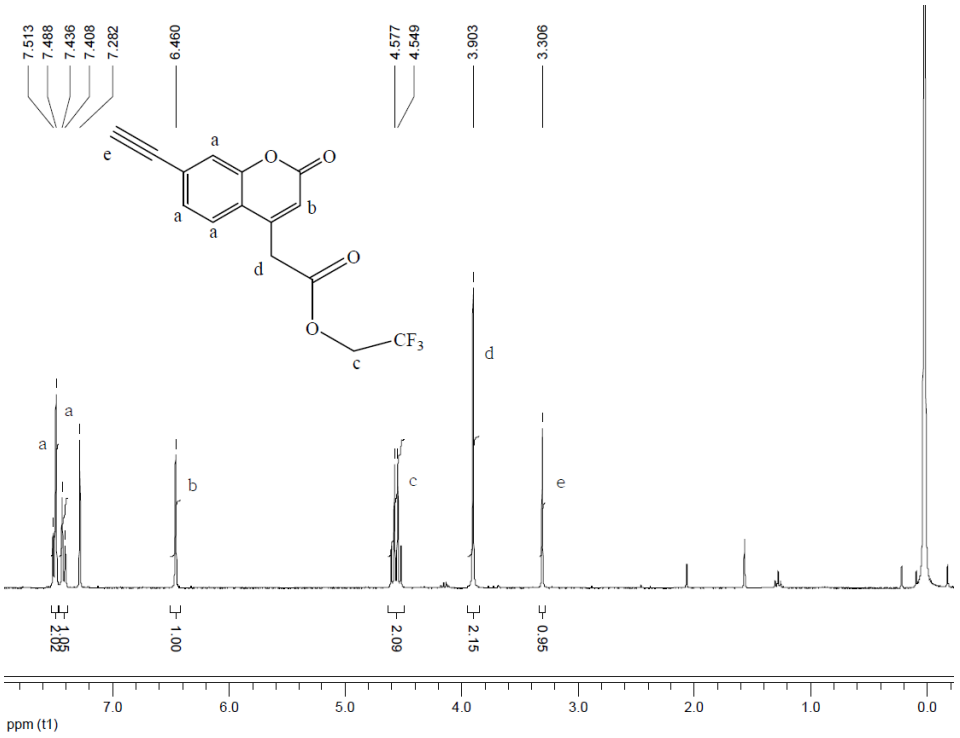

^{1}H NMR (300 MHz, DMSO-*d6*) spectra of **18**.

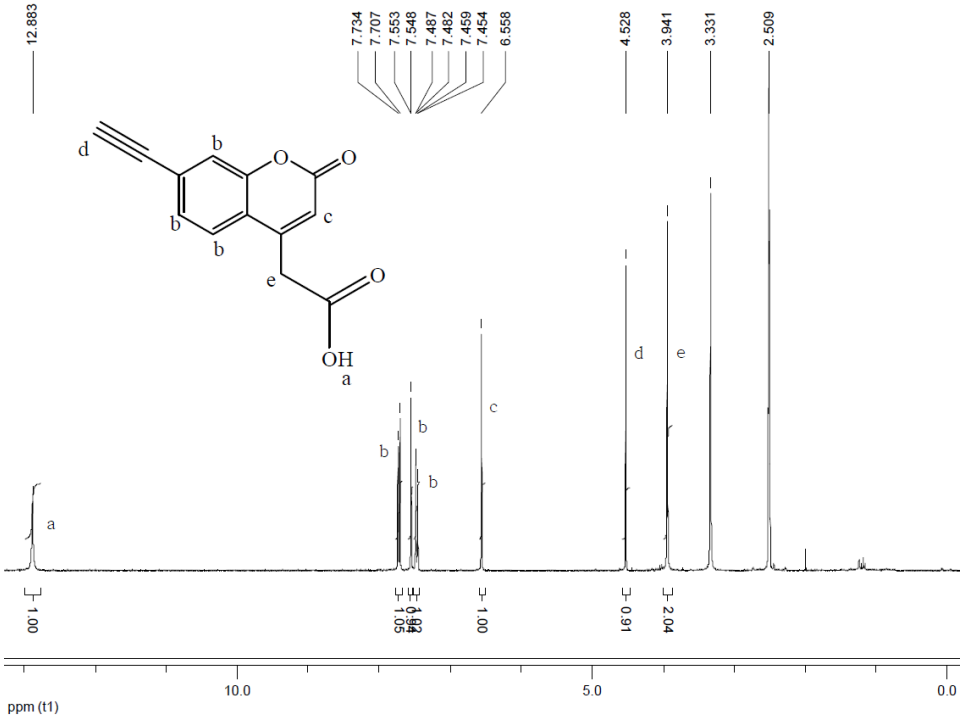

^{1}H NMR (300 MHz, DMSO-*d6*) spectra of **19**.

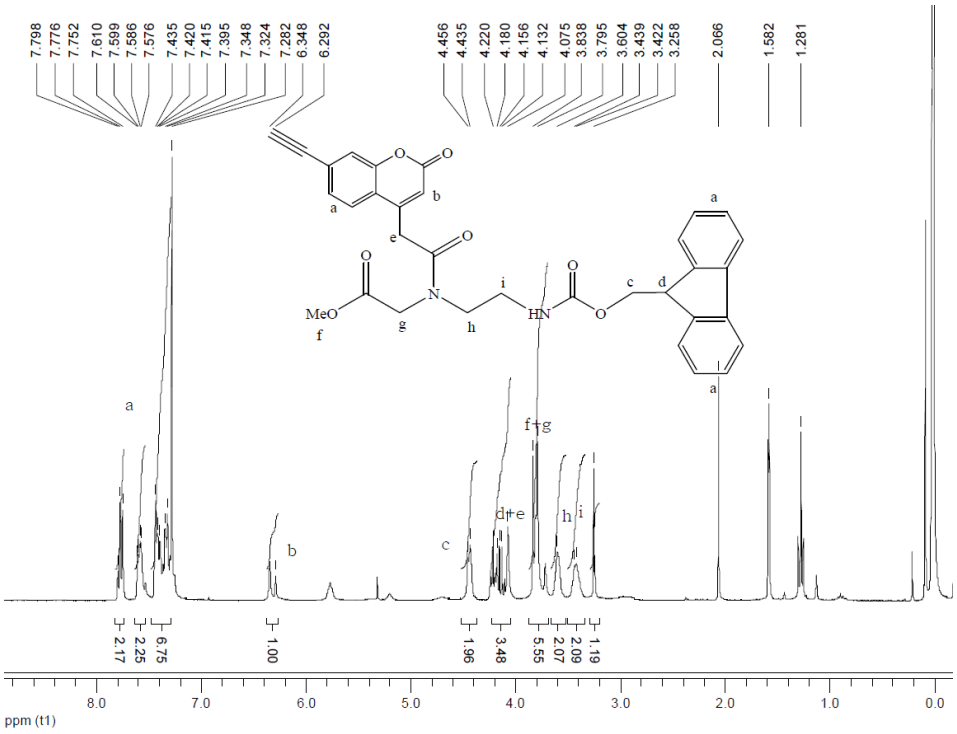

^{1}H NMR (300 MHz, $CDCl_3$-*d*) spectra of **20**.

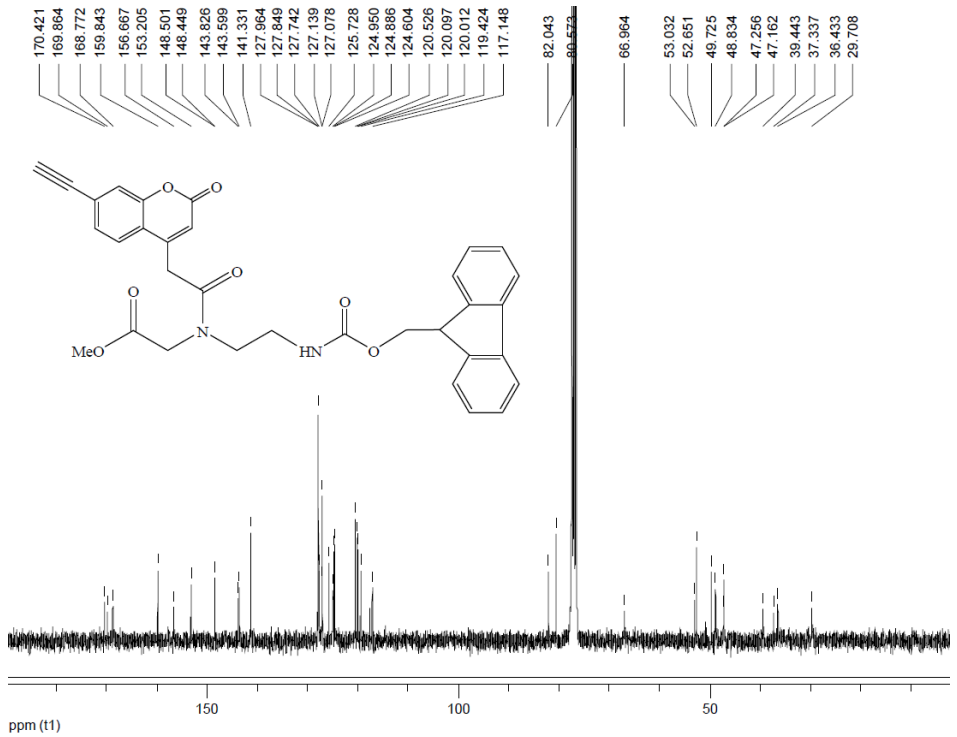

^{13}C NMR (300 MHz, $CDCl_3$-*d*) spectra of **20**.

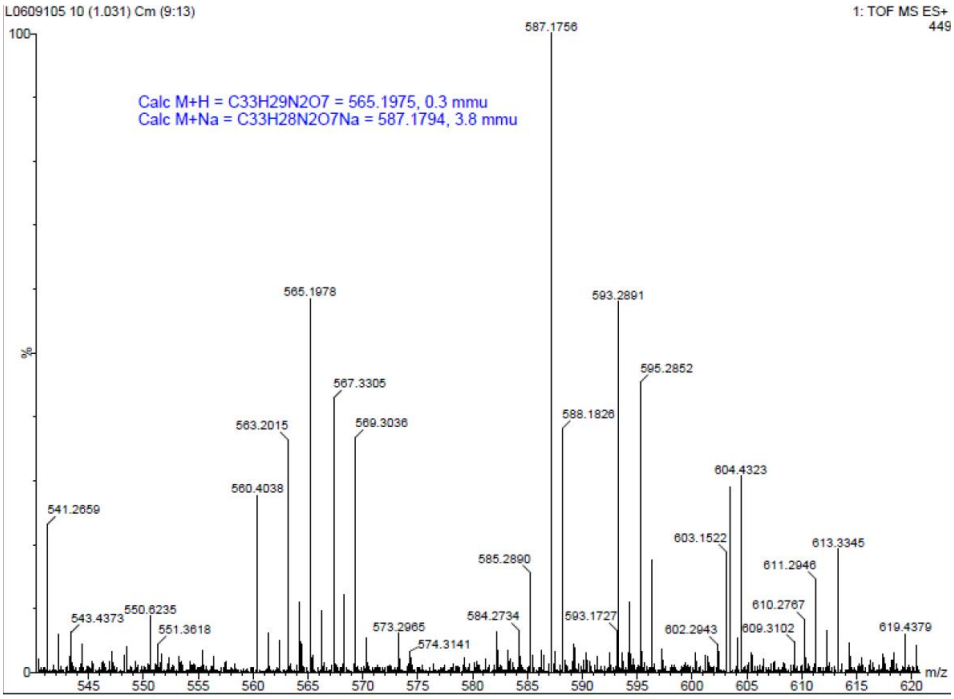

HRMS (TOF-MS-ESI) spectra of **20**.

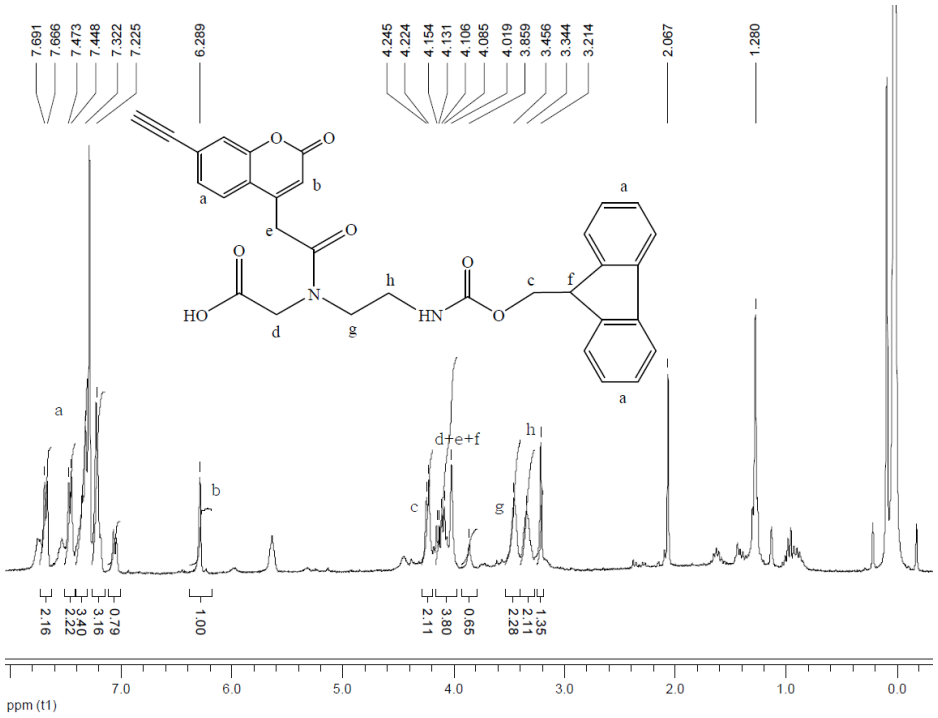

^{1}H NMR (300 MHz, $CDCl_3$-*d*) spectra of **21**.

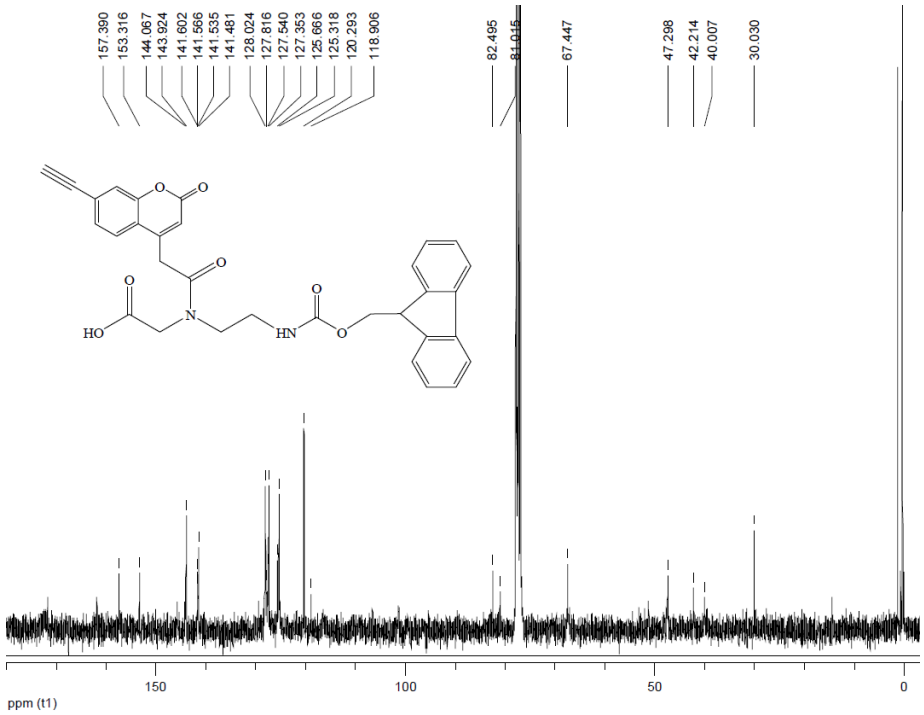

^{13}C NMR (300 MHz, $CDCl_3$-*d*) spectra of **21**.

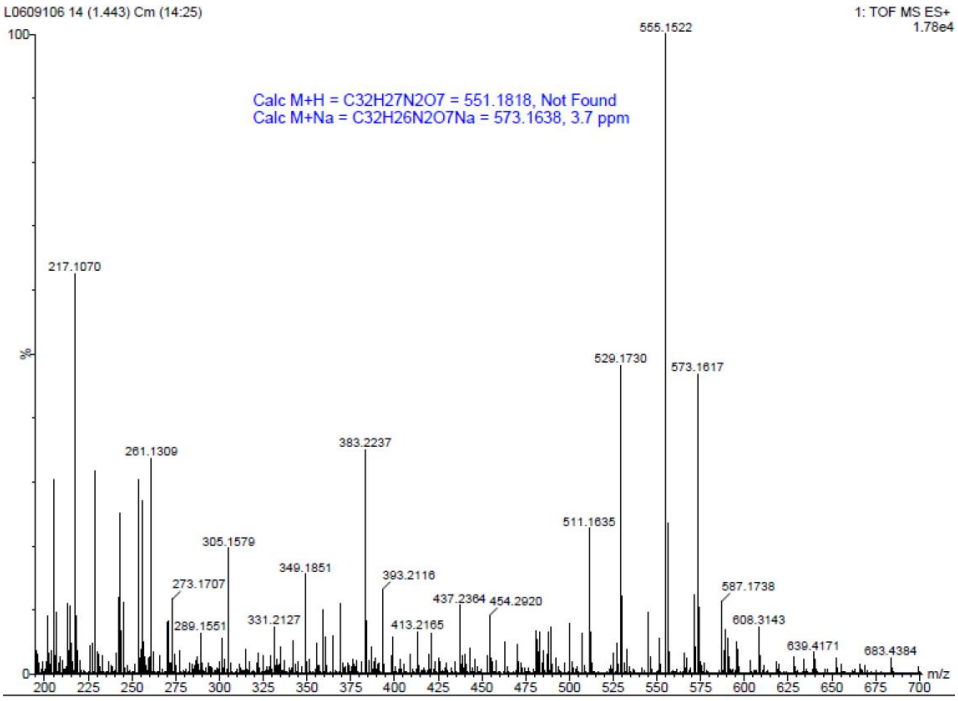

HRMS (TOF-MS-ESI) spectra of **21**.

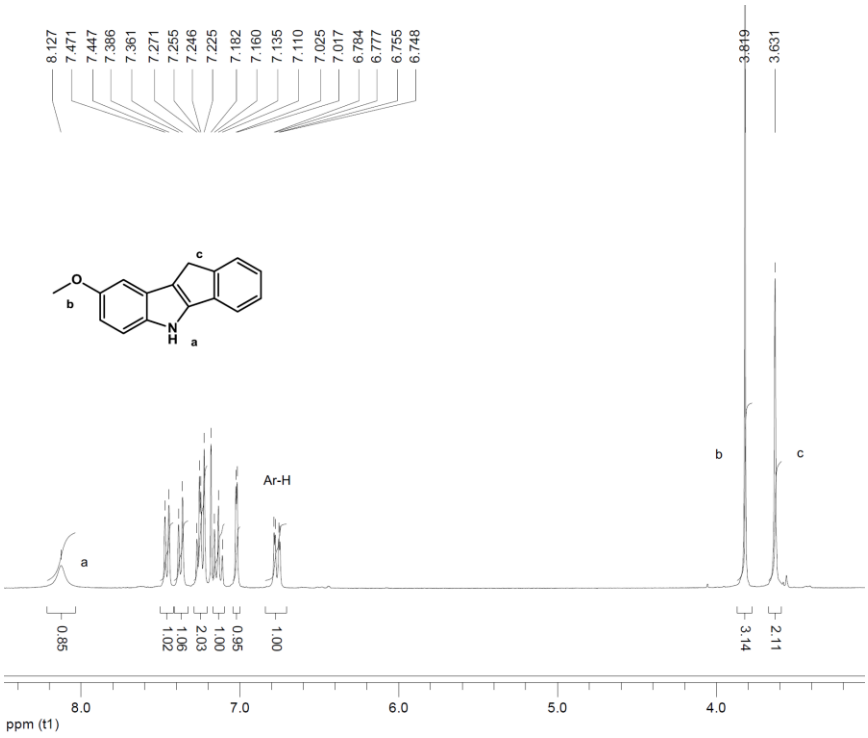

^{1}H NMR (300 MHz, $CDCl_3$-*d*) spectra of **22**.

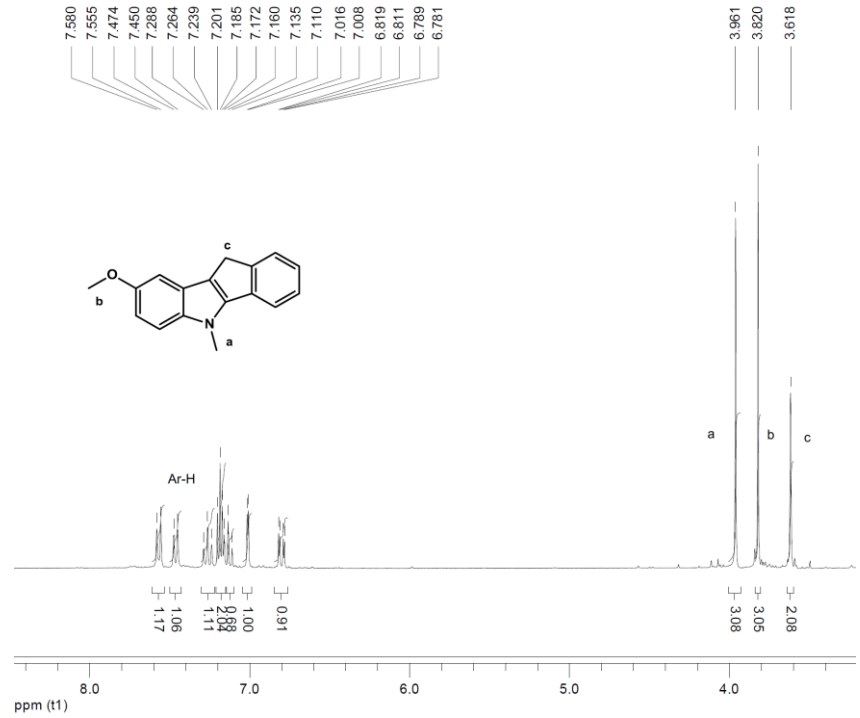

^{1}H NMR (300 MHz, DMSO-*d6*) spectra of **23**.

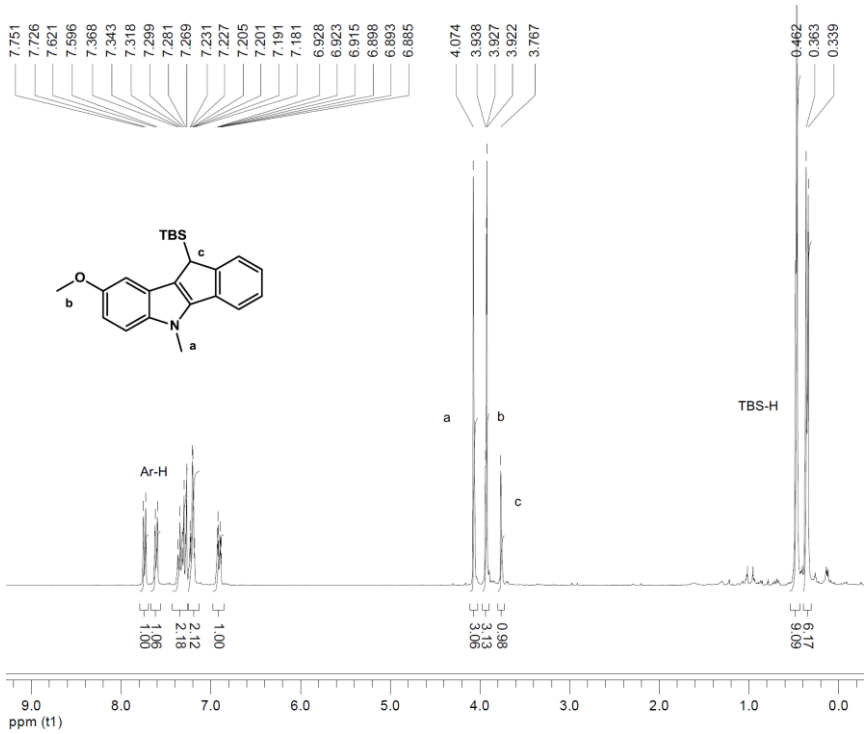

^{1}H NMR (300 MHz, $CDCl_3$-*d*) spectra of **24**.

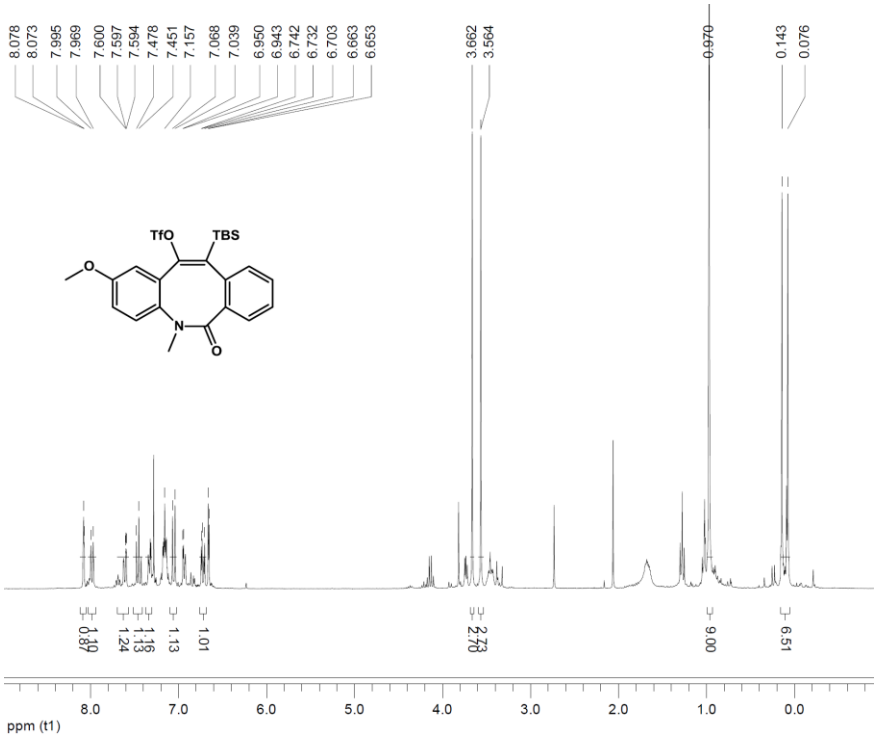

^{1}H NMR (300 MHz, $CDCl_3$-*d*) spectra of **26**.

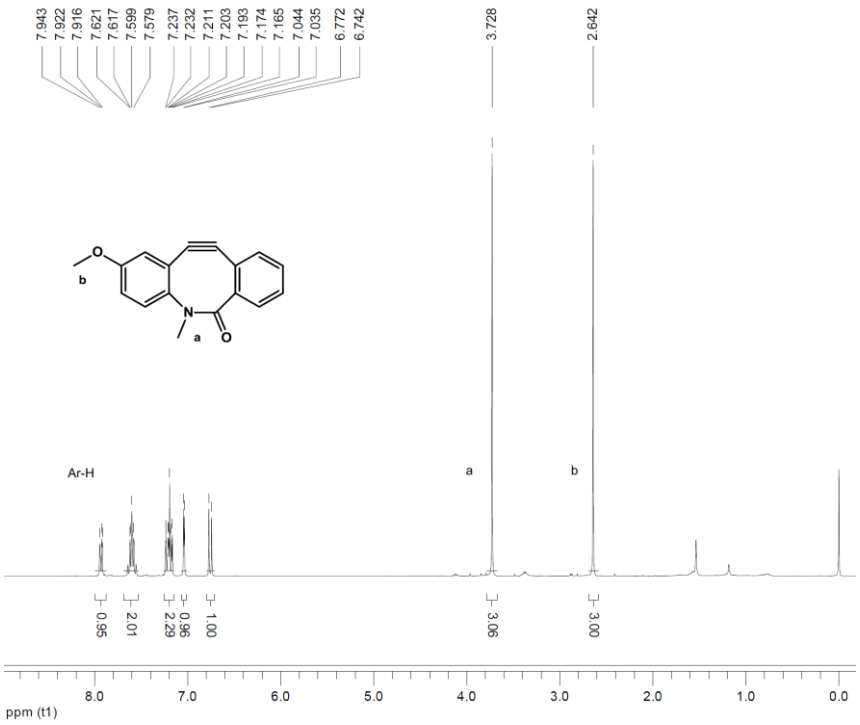

^{1}H NMR (300 MHz, $CDCl_3$-*d*) spectra of **27**.

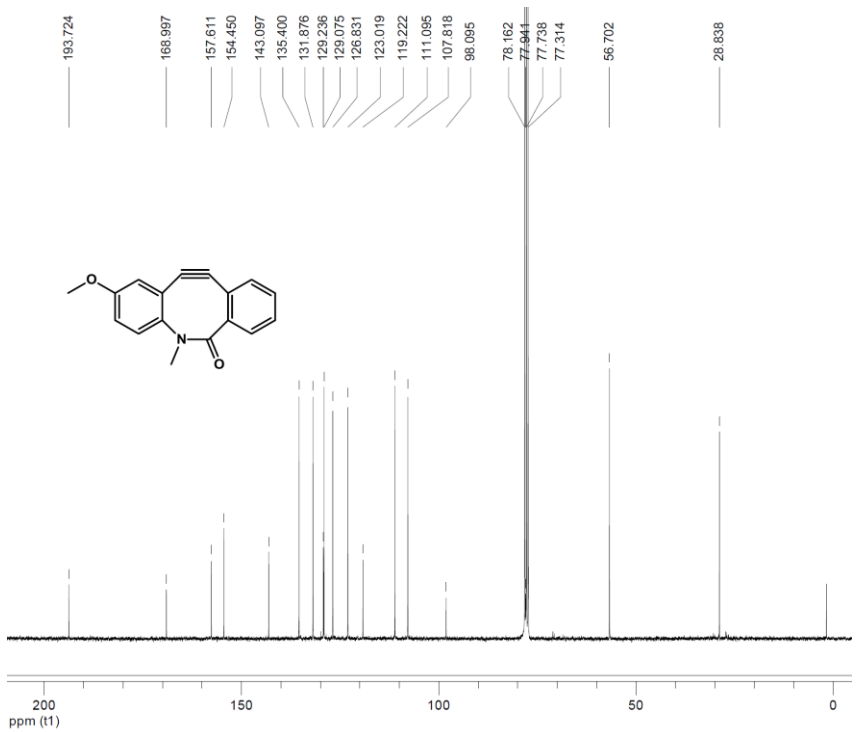

^{1}H NMR (300 MHz, $CDCl_3$-*d*) spectra of **27**.

Chapter 3. Site-Specific Fluorescence Labeling of Natural DNA

3.1. Introduction

Fluorescence-labeled ODNs have been widely utilized in the life sciences, particularly in genetic analysis, genome screening and high-throughput DNA sequencing, because of the simplicity and versatility they provide.[1-2] Lots of fluorophores, such as coumarins, phenanthridine derivatives and fluorescein analogues, are commercially available for the construction of fluorescent ODNs via biochemical approaches.[3] However, most only allow one ODN to be associated with a single fluorophore, leading to low sensitivity for real-time imaging.

The chemically functionalized ODNs conjugated with multiple fluorescent reporters via post-conjugation methods can yield sufficiently bright signals for sensitive image. For example, the alkyne-modified uridine nucleosides can be incorporated into ODNs at multiple sites to afford ODNs containing alkyne reporters (Chapter 1). After the fluorogenic "click" reactions with 7-hydoxyl-3-azidocoumarin, the resulting ODNs showed highly strong fluorescence (Chapter 1).[4] However, preparation of the modified ODNs used in biological study is hard via artificial gene synthesis, due to the low efficiency for synthesizing long ODNs.[5] It is well known that the total yield is less than 10% for 200 mers ODN in DNA solid phase synthesis, even though the yield is around 99% for each step. The PCR perceives high efficiency in DNA synthesis, but the modified nucleosides, which can tune the base pairing properties, are hard to be used in PCR.[6]

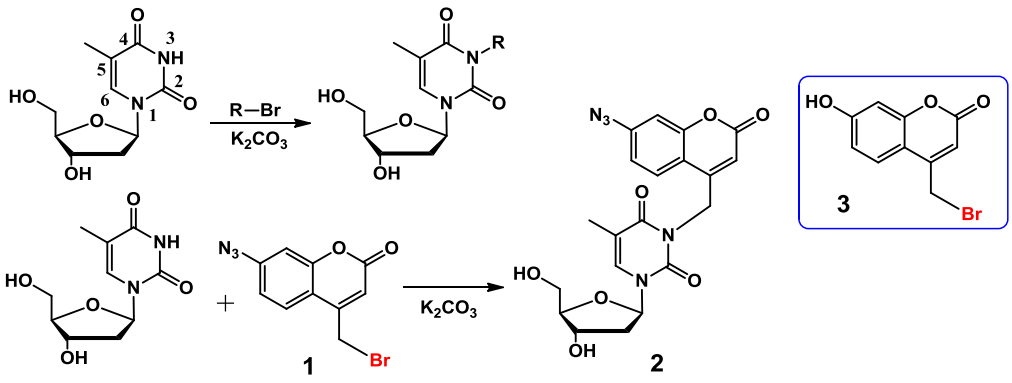

Figure 3-1. N3-alkylation of thymidine and uridine.

One strategy to overcome the problem is functionalization of natural DNA using fluorescent reporters. Recently, selective N-3 alkylation of thymidine using alkyl halide was reported (Figure 3-1).[7] And the formed N3-substituted thymidine showed bioactivity in mice, such as potent antinociceptive effects.[8] Moreover, Helm used 7-azido-4-(bromomethyl)coumarin (**1**) as an alkylation agent to selectively react with the uridine forming **2** in natural RNA, which affords a simple and effective method for introduction of multiple fluorophores in single RNA.[9] We expect that the thymidine (T) in natural DNA with similar structure as uridine can react with 7-hydroxy-4-(bromomethyl) coumarin (**3**) to afford the highly fluorescent DNA for bioanalysis.

3.2. Synthesis of Fluorescent Tags for DNA Labeling

At first, the coumarin derivative **3** with a bromo-methyl group at the position-4 was designed and synthesized as the alkylation agent (Figure 3-2). It is well known that the coumarin derivatives have wide applications as fluorogenic reporters because their fluorescence intensity can be tuned by varying the electronic properties of the substituents at the aromatic rings. Furthermore, they are easy to prepare and are biocompatible.[10] The coumarin derivative **3** with a bromomethyl group was chosen as the

fluorescent alkylation agent for DNA multiple labeling. The selective bromination of **4** in the presence of acetic acid yielded compound **5**. After the Pechmann condensation between resorcinol and **5**, the 7-hydroxy-4-(bromomethyl) coumarin (**3**) was obtained.

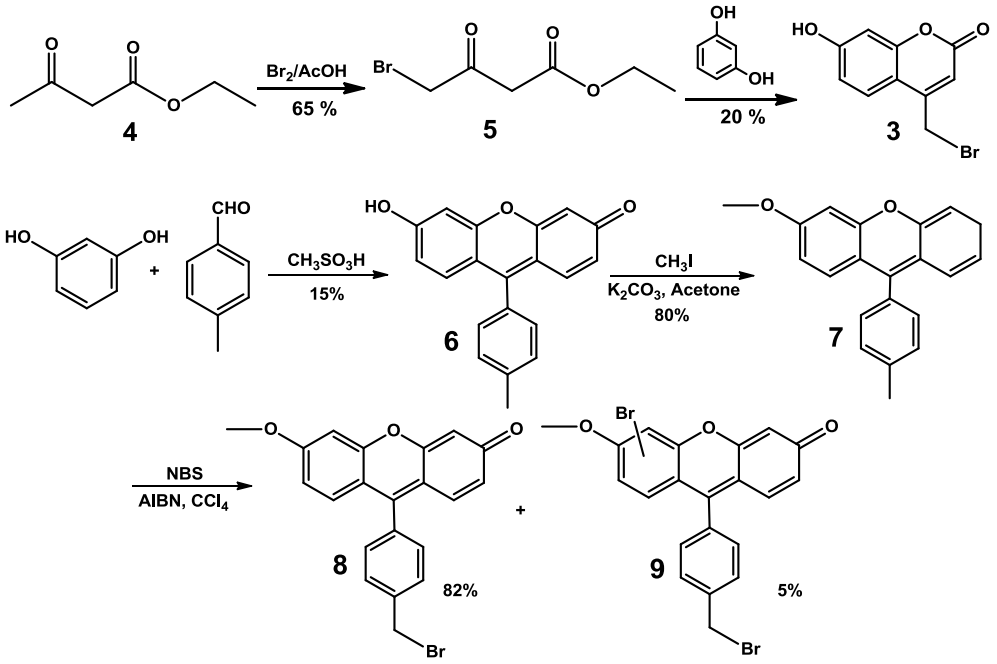

Figure 3-2. Preparation of alkylation agents **3** and **8**.

In addition, fluorescein moiety **8** with a bromomethyl group was also designed and synthesized (Figure 3-2). The fluorescein, a highly fluorescent molecule, has better fluorescence properties (strong fluorescence in longer wavelength) and has been used as fluorophores in biological experiments.[11] The fluorescein **6** was prepared via the acid-catalyzed condensation of resorcinol with 4-methylbenzaldehyde. As the hydroxyl group has the ability to destroy radicals or intermediates in radical substitution reaction, fluorescein **7** obtained from methylation of **6** was used for the bromination reaction.[12] Finally, the desired alkylation agent **8** and the byproduct **9** with the additional bromo-group at the benzene ring were obtained at reasonable yields.

3.3. Reactivity of Labeling Agents towards Nucleic Acids

After synthesizing coumarin and fluorescein derivatives with a bromo-methyl group, the selective alkylation ability of compounds **3** and **8** towards thymidine was confirmed in the monomer reactions. The fluorescent reporter **3** with the bromo-methyl group has the potential for electrophilic reactions and was employed in the monomer reactions to study its reactivity towards canonical nucleosides dA, dG, dT, and dC. In the presence of K_2CO_3, a new compound was observed with dT, while no new compounds were observed for dC, dA, or dG. The N3-alkylation product **10** was isolated and characterized by ^{1}H NMR and ^{13}C NMR. This indicated that coumarin **3** can selectively react with thymidine, other than the other canonical nucleosides (Figure 3-3). The selectivity of the reaction arises from the stability of the negative ion intermediate formed wih dT. The existence of two carbonyl groups in T can efficiently stabilize the intermediate via conjugated π system, which results in the selective reaction with T (Figure 3-3). Compound **8** can also selectively react with thymidine under the same conditions, except that DMF was used as the solvent, to afford compound **11** at a yield of 7%. The structure of N3-substituded product **11** was also confirmed by NMR. Both reaction yields were low, but excess alkylation reagents (100-1000 times) improved the labeling efficiency, which is commonly used in bioorthogonal labeling reactions.[13]

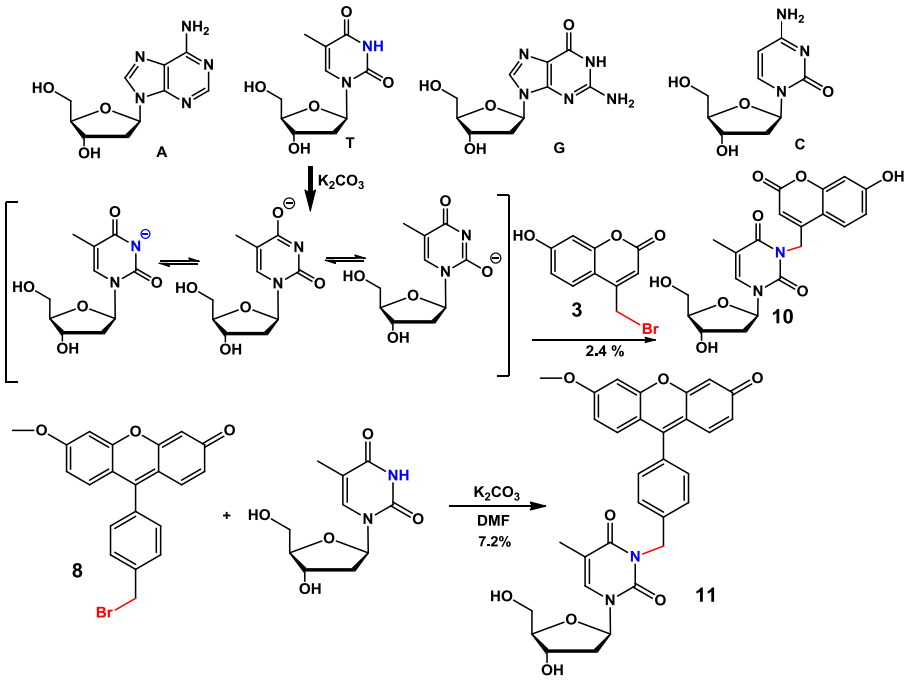

Figure 3-3. N3-akylation of thymidine with **3** and **8**.

More importantly, the alkylation of non-fluorescent thymidine with coumarin **3** can form a highly fluorescent product **10**. Compound **10** preserves the thymidine's absorbance at 260 nm, also shows a new UV absorbance peak at 330 nm arising from the incorporation of coumarin moiety (Figure 3-4). The obvious fluorescence enhancement has been observed for **10** compared with the monomer dT (Figure 3-4). No fluorescence was observed for dT, but the formed alkylation product **10** exhibited similar fluorescent signals as coumarin **3**. Interestingly, no fluorescence enhancement was observed for **11**, and the fluorescein **8** shows very weak fluorescent signal. The possible reasons for this are: 1) Intermolecular electron transfer in fluorescein **8** or **11** can quench their fluorescence; 2) The fluorescein conjugates sometimes are unstable under intense illumination, leading to a rapid reduce in fluorescent signal.[14] These results established the potential utility of coumarin **3** for selectively N3-labelling of thymidine, which

provides a novel strategy for construction of highly fluorescent DNA in sensitive detection.

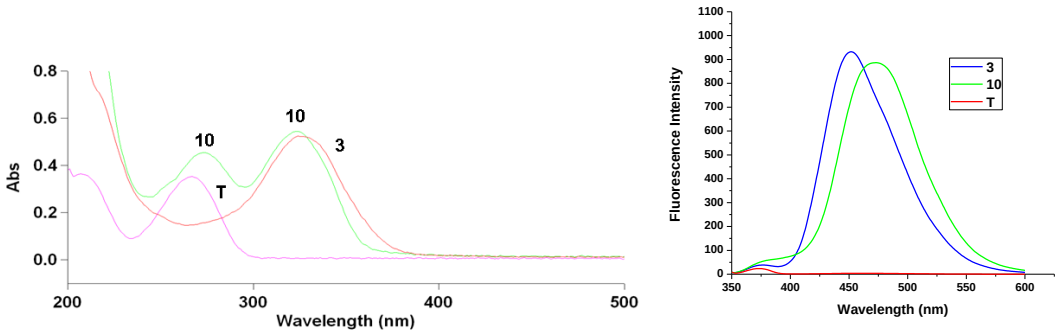

Figure 3-4. Excitation and emission spectra of T, **3** and **10**.

3.4. Optimization of the Reaction Condition for DNA Labeling

We have optimized the conditions for directly post-labeling DNA using coumarin **3**, especially the effects of solvents. As the products are highly fluorescent and starting material dT is non-fluorescent in monomer reactions, fluorescence spectra was employed to detect the reaction. The ODN-**T12** containing 12 dT bases has been used for optimizing solvents, such as methanol, ethanol, acetone, and acetonitrile (Figure 3-5). The reaction mixture containing ODN-**T12**, coumarin **3** and K_2CO_3 in different anhydrous solvents were heated at 37°C for 2 days. After removing unreacted reporters, the fluorescence of the resulting ODNs, consisting of coumarin-conjugated product (ODN-**CT12**), was tested. Obvious fluorescence enhancement was observed when menthol was used as the solvent. It indicated methanol is the best solvent for labeling. This can be explained by two possible factors: the solubility of ODN-**T12**, coumarin **3** and K_2CO_3, and the stability of the intermediate in the solvent. The solubility of ODN-**T12**, coumarin **3** and K_2CO_3 in methanol is better than in other solvents; therefore the

reaction in methanol is more efficient. In addition, the solubility of ODN-**T12** and K_2CO_3 in water is very good, but water is too acidic to stabilize the intermediate-a Lewis base. It is the reason that the solvent containing water is not good for this reaction.

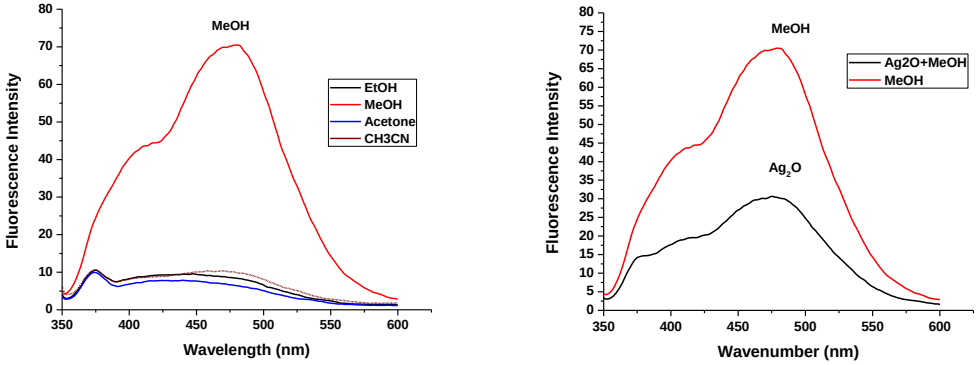

Figure 3-5. Fluorescence spectra of resulting ODNs under different conditions.

Moreover, the effect of Ag_2O on the reaction was studied following the same procedure. Generally, Ag_2O is considered to accelerate the reaction and afford higher efficiency, but co-precipitation of Ag_2O and ODN-**T12** was observed. Therefore, the addition of Ag_2O did not increase the yield of the reaction as expected.[15]

3.5. Sequence-Depentent DNA Labeling

The coumarin **3** is site-specific for labelling DNA containing dT. The ODN-**A12**, ODN-**T12**, ODN-**G12**, and ODN-**C12** containing 12 dA, 12 dT, 12 dG, and 12 dC respectively were utilized in the labeling reactions (Figure 3-6). Only ODN-**T12** led to the great fluorescence enhancement after treatment with **3**, which indicated that the reaction of **3** with dT is a good way for site-specifically post-labelling of DNA. However, the high fluorescence was observed with ODN-**G1** without treatment with **3**, which arised from formation of G-quadruplex structures.[16]

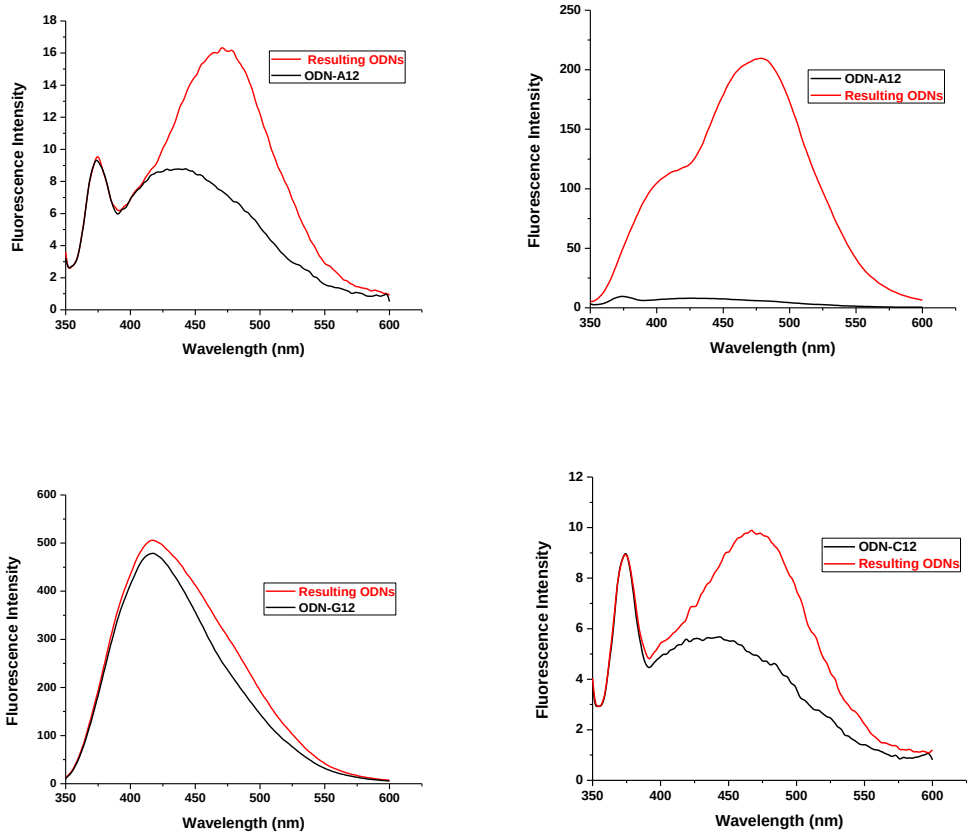

Figure 3-6. Fluorescence spectra of resulting ODNs after the labeling for ODN-**A12**, **T12**, **G12**, and **T12**.

3.6. Future Study

Our work has demonstrated the efficiency of post-labelling natural ODN using coumarin **3**. Our future study will focus on cellular DNA labeling and functionalization of labeling agents for bio-detection. We expect that the coumarin **3** can selectively react with dT in cellular DNA to afford the highly fluorescent DNA for bio-study. In addition, some functional groups can be introduced in the alkylation agents yielding the functionalized DNA, which can offer possible advantages in water-solubility, cost, and simplicity. For example, excessive H_2O_2 in cells contributes to the development and progression of

cancer and other diseases.[17] Many aryl boronates probes have been discovered for H_2O_2-responsive image, but most suffer from low solubility in water, leading to low sensitivity.[18] We hope that the non-fluorescent boronate-coumarin **16** can be introduced into water-soluble ODNs, and its fluorescence can be restored upon reaction with H_2O_2(Figure 3-7).

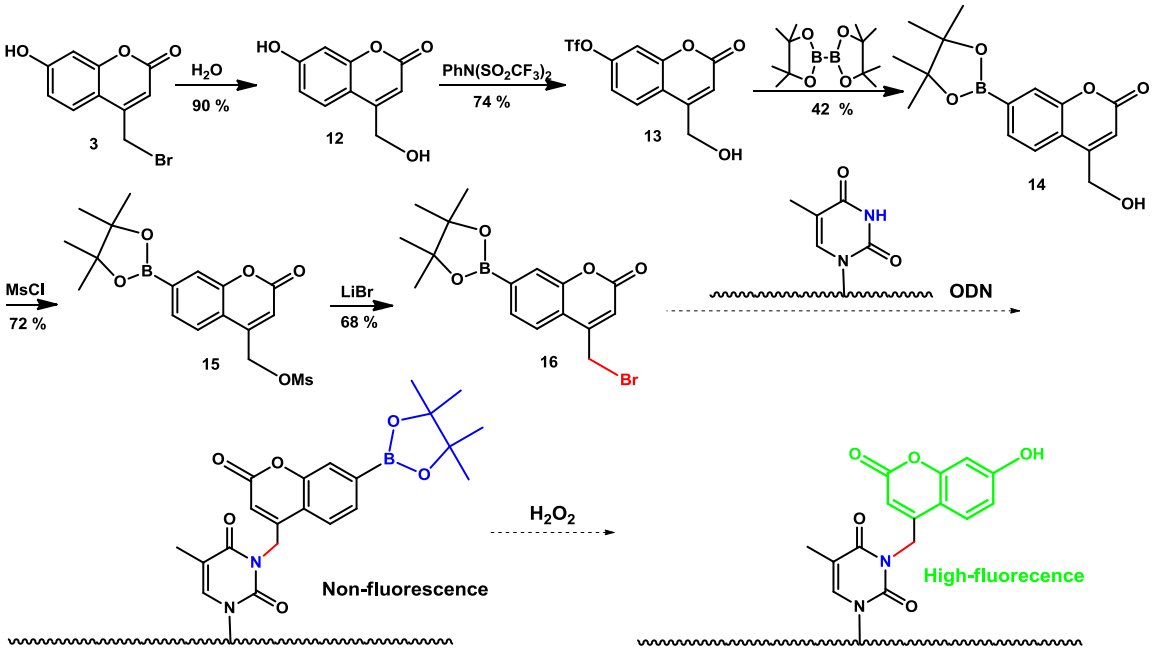

Figure 3-7. Preparation of alkylation agent **14** for detection of H_2O_2.

3.7. Experimental Section

Optimizing solvents for DNA post-labeling reaction. 15 nmol ODN-**T12**, 0.8 μmol **3** and 0.8 μmol K_2CO_3 were dissolved in 200 μL different anhydrous solvents. After heating at 37°C for 2 days, solvents were removed under reduced pressure. Precipitated for 3 times using a mixture of ethanol and NaCl solution (1M) at the ratio of 3:1 and went through the G-25 column to remove the unreacted reporters and salts. Finally, the

resulted ODNs solutions with the concentration of 10 μM were prepared for the fluorescence measurement.

Selectivity of post-labeling using coumarin 3. ODNs (20 nmol) were incubated with coumain **3** (2.54 mg, 1.0 μmol) and K_2CO_3 (1.38 mg, 1.0 μmol) in 0.5 mL methanol at 37°C for 2 days. Precipitated for 3 times using the mixture of ethanol and NaCl solution (1M) at the ratio of 3:1 and went through the G-25 column to remove the unreacted reporters and salts. The resulting ODNs were dissolved in pure water at the concentration of 2 μM for the fluorescence test.

6-Hydroxy-9-(p-tolyl)-3H-xanthen-3-one (**6**). To the suspension of resorcinol (4.4 g, 40 mmol), in methanesulfonic acid (60 mL), 4-methylbenzaldehyde (2.35 mL, 20 mmol) was added. The reaction mixture was stirred at 85°C for 24 h. After cooling to room temperature, the reaction mixture was poured into 3 volumes of saturated sodium acetate solution. A dark-red precipitate was formed and collected by filtration. The crude product was purified by silica gel column chromatography (CH_2Cl_2:MeOH = 9:1) for two times yielding the product as a dark-red solid (907 mg, 15%).

6-Methoxy-9-(p-tolyl)-3H-xanthen-3-one (**7**). To the suspension of 6-hydroxy-9-(p-tolyl)-3H-xanthen-3-one (**6**, 604 mg, 2 mmol) and K_2CO_3 (600 mg, 4.34 mmol) in acetone (30 mL), iodemethane (0.825 mL, 12.5 mmol) was added. The reaction mixture was stirred at 50°C for 24h. After cooling to the room temperature, the solvents were removed under reduced pressure. The residue was diluted with ethyl acetate (50 mL), washed with 1 M HCl (30 mL), and brine (20 mL), and then dried over by anhydrous Na_2SO_4. The solvent was removed under vacuum. The crude product was purified by the

silica gel column chromatography (EtOAc) to provide the product **7** as a red solid (632 mg, 80%).

9-(4-(Bromomethyl)phenyl)-6-methoxy-3H-xanthen-3-one (**8**). *N*-Bromosuccinimide (214 mg, 2 mmol) and azobisisobutyronitrile (8.2 mg, 0.05 mmol) were added to the solution of 6-methoxy-9-(p-tolyl)-3H-xanthen-3-one (**7**, 316 mg, 1 mmol) in carbon tetrachloride (15 mL). The reaction mixture was refluxed for overnight. After evaporation of the solvent, the residue was diluted with dichloromethane (40 mL), washed with water (30 mL × 2) and brine (20 mL), and then dried over by anhydrous Na_2SO_4. The solvent was removed under reduced pressure. The crude product was purified by the silica gel column chromatography (EtOAc:Hexane = 1:1) to provide the product **8** as a red solid (283 mg, 82%) and the byproduct **9** as a dark-red solid (26 mg, 5%).

C3T (**10**). To the solution of **3** (153 mg, 0.60 mmol) in methanol (10 mL), thymine (121 mg, 0.50 mmol) and K_2CO_3 (69 mg, 0.50 mmol) was added. The mixture was stirred at 45 °C for about 36h. The mixture was filtered, and the filtrate was concentrated in vacuum. The residue was purified by flash column chromatography on silica gel (gradient CH_2Cl_2:MeOH = 98:2 to 95:1) to afford coumarin-N3-cojugated-thymidine **10** (**C3T**, 5 mg, 2.4 %) as a yellowish solid. ^{1}H NMR (300 MHz, DMSO-*d6*): *δ.* 7.93 (s, 1 H), 7.80, 7.78 (d, *J* = 8.7, 1 H), 6.88, 6.84(d, *J* = 8.7, 1 H), 6.77 (s, 1 H), 6.23, 6.21, 6.18 (t, *J* = 6.6, 1 H), 5.67 (s, 1 H), 5.26 (s, 1 H), 5.16 (s, 2 H), 5.09 (s, 1 H), 4.28 (s, 1 H), 3.80 (s, 1 H), 3.63-3.60 (m, 2 H), 2.22-2.14 (m, 2 H), 1.88 (s, 1 H). ^{13}C NMR (300 MHz, DMSO-*d6*):*δ.* 163.0, 161.9, 160.6, 155.4, 151.5, 150.8, 136.2, 126.3, 113.6, 110.2, 108.9, 106.4, 102.9, 87.9, 85.6, 70.6, 61.6, 13.4.

1-((2R,4S,5R)-4-hydroxy-5-(hydroxymethyl)tetrahydrofuran-2-yl)-3-(4-(6-methoxy-3-oxo-3H-xanthen-9-yl)benzyl)-5-methylpyrimidine-2,4(1H,3H)-dione (**11**). To a suspension of thymidine (73 mg, 0.3 mmol), K_2CO_3 (50 mg, 0.36 mmol) and KI (60 mg, 0.36 mmol) in DMF (20 mL), fluorescein moiety: 9-(4-(bromomethyl)phenyl)-6-methoxy-3H-xanthen-3-one (**8**, 120 mg, 0.30 mmol) was added. The reaction mixture was stirred at 50°C for 2d. After cooling to the room temperature, 30 mL water was added. The mixture was extracted with ethyl acetate (30 mL × 3), and collected organic phases were washed with water (30 mL × 2), brine (20 mL), and then dried over by anhydrous sodium sulfate. The solvent was evaporated under reduced pressure. Upon purification by column chromatography on silica gel (DCM:MeOH = 99:1 to 95:5, R_f = 0.25 using DCM:MeOH = 95:5), the product **11** was isolated as a dark-red solid (12 mg, 7.2%). ^{1}H NMR (300 MHz, $CDCl_3$-d): δ. ^{13}C NMR (300 MHz, $CDCl_3$-d):

4-hydroxymethyl-7-(4,4,5,5-tetramethyl-1,3,2-dioxaborolan-2-yl)-2*H*-chromen-2-one (14). 4-Hydroxymethyl-2-oxo-2H-chromen-7-yl trifluoromethanesulfonate (**13**, 324 mg, 1 mmol), bis(pinacolato)-diboron (508 mg, 2 mmol), $Pd(dppf)Cl_2{\cdot}CH_2Cl_2$ (82 mg, 0.1 mmol) and potassium acetate (295 mg, 3 mmol) were added to the dried round-bottom flask and flushed with argon. The reaction contents were dissolved in 10 mL 1, 4-dioxane and stirring at 60°C for overnight. After cooling to the room temperature, the reaction mixture was extracted with ethyl acetate (10 mL × 3). The combined organic layer was washed with water (10 mL × 3), and brine (20 mL), then dried (Na_2SO_4) and concentrated under reduced pressure. The crude product was purified by flash chromatography on silica gel (1 : 1 hexane : EtOAc) providing **14** as a white solid (126 mg, 42%). ^{1}H NMR (300 MHz, DMSO-*d6*): δ 7.73 (d, J = 7.8, 1 H), 7.60 (d, J = 8.4, 1

H), 7.54 (s, 1 H),6.52 (s, 1 H), 5.72 (t, *J* = 5.4, 1 H), 4.20 (m, 2 H), 1.32 (s, 12 H). ^{13}C NMR (300 MHz, DMSO-*d6*): δ 160.4, 156.5, 152.8, 130.1,124.4, 122.2, 120.1, 112.4, 84.8, 59.4, 25.1. HRMS (TOF-MS-ESI): calcd. for C16H21BO5 $[M+H]^+$ 303.1398; found 303.1389.

[7-(4,4,5,5-tetramethyl-1,3,2-dioxaborolan-2-yl)-2-oxo-2H-chromen-4-yl]methyl methane –sulfonate (15). 4-Hydroxymethyl-7-(4,4,5,5-tetramethyl-1,3,2-dioxaborolan-2-yl)-2*H*-chromen-2-one (**14**, 121 mg, 0.4 mmol), methanesulfonyl chloride (37 μL, 0.48 mmol), Et_3N (84 μL, 0.6 mmol) and 10 mL dichloromethane were added to the dried round-bottom flask flushed with argon. The reaction mixture was stirring at 0°C for 1h and then washed with water (10 mL × 3), and brine (20 mL). The organic phase was dried (Na_2SO_4) and concentrated under reduced pressure. The crude product was purified by flash chromatography on silica gel (hexane : EtOAc = 1 : 1) providing **15** as a white solid (113 mg, 74%). ^{1}H NMR (300 MHz, $CDCl_3$-*d*): δ 7.81 (s, 1 H), 7.75 (d, *J* = 7.8, 1 H), 7.60 (d, *J* = 7.8, 1 H), 6.63 (s, 1 H), 5.43 (d, *J* = 0.6, 2 H), 3.17 (s, 3 H), 1.39 (s, 12 H). ^{13}C NMR (300 MHz, $CDCl_3$-*d*): δ 159.9, 153.0, 146.5, 130.5,123.5, 122.4, 118.4, 115.4, 84.6, 64,8, 38.3, 31.5, 24.9.

4-Bromomethyl-7-(4,4,5,5-tetramethyl-1,3,2-dioxaborolan-2-yl)-2*H*-chromen-2-one (16). Lithium bromide (174 mg, 2.0 mmol) was added to the solution of [7-(4,4,5,5-tetramethyl-1,3,2-dioxaborolan -2-yl)-2-oxo-2H-chromen-4-yl]methyl methane-sulfonate (**15**, 76 mg, 0.2 mmol) in anhydrous acetone (10 mL) and the reaction mixture was refluxing for overnight. After cooling to room temperature, the acetone was removed under reduced pressure. The crude product was purified by flash chromatography on silica gel (hexane : EtOAc = 1 : 1) providing **16** as a white solid (58 mg, 80%). ^{1}H NMR

(300 MHz, $CDCl_3$-*d*): δ 7.73-7.79 (3 H), 6.58 (s, 1 H), 4.53 (s, 2 H), 1.39 (s, 12 H). ^{13}C NMR (300 MHz, $CDCl_3$-*d*): δ 160.2, 153.4, 149.7, 130.2,123.6, 123.4, 119.2, 117.2, 84.5, 26.6, 24.9. HRMS (TOF-MS-ESI): calcd. for C16H20BO4Br $[M+H]^+$ 365.0554; found 365.0550.

3.8. References

[1] Ranasinghe, R. T., Brown, T. Fluorescence based strategies for genetic analysis. *Chem. Commun.* **2005**, *44,* 5487-5502.

[2] Eggleston, A. K., Rahim, N. A., Kowalczykowski, S. C. A helicase assay based on the displacement of fluorescent, nucleic acid-binding ligands. *Nucl. Acids Res.* **1996**, *24*, 1179-1186.

[3] Proudnikov, D., Mirzabekov, A. Chemical methods of DNA and RNA fluorescent labeling. *Nucl. Acids Res.* **1996**, *24*, 4535-4542.

[4] Gierlich, J., Burley, G. A., Gramlich, P. M., Hammond, D. M., Carell, T. Click chemistry as a reliable method for the high-density postsynthetic functionalization of alkyne-modified DNA. *Org. Lett.* **2006**, *8*, 3639-3642.

[5] Tsuchiya, Y., Morioka, K., Shirai, J., Yoshida, K., Inumaru, S. Comparison of artificial synthesis methods of gene. *Nucleic Acids Symp Ser. (Oxf)* **2006**, *50*, 275-276.

[6] Gonzalez, J. M., Portillo, M. C., Belda-Ferre, *P*., Mira, A. Amplification by PCR artificially reduces the proportion of the rare biosphere in microbial communities. *Plos One* **2012**, *7*, e29973.

[7] Colombeau, L., Teste, K., Hadj-Bouazza, A., Chaleix, V., Zerrouki, R., Kreamer, M., Sainte Catherine, O. Synthesis and biological activity of chloroethyl pyrimidine nucleosides. *Nucleos. Nucleot. Nucl. Acid.* ***2008****, 27,* 110-120.

[8] Shimizu, T., Kimura, T., Funahashi, T., Watanabe, K., Ho, I. K., Yamamoto, I. Synthesis of N3-substituted uridine and related pyrimidine nucleosides and their antinociceptive effects in mice. *Chem. Pharm. Bull.* **2005**, *53*, 313-318.

[9] Kellner, S., Seidu-Larry, S., Burhenne, J., Motorin, Y., Helm, M. A multifunctional bioconjugate module for versatile photoaffinity labeling and click chemistry of RNA. *Nucl. Acids Res.* **2011**, *39,* 7348-7360.

[10] Behl, G., Sikka, M., Chhikara, A., Chopra, M. PEG-coumarin based biocompatible self-assembled fluorescent nanoaggregates synthesized via click reactions and studies of aggregation behavior. *J Colloid Interface Sci.* **2014**, *416*, 151-160.

[11] Ueno, T., Urano, Y., Setsukinai, K., Takakusa, H., Kojima, H., Kikuchi, K., Ohkubo, K., Fukuzumi, S., Nagano, T. Rational principles for modulation fluorescence properties of fluorescein. *J. Am. Chem. Soc.* **2004**, *126*, 14079-14085.

[12] Aksoya, L., Kolaya, E., Ağılönüa, Y., Aslana, Z., Kargıoğlub, M. Free radical scavenging activity, total phenolic content, total antioxidant status, and total oxidant status of endemic Thermopsis turcica. *Saudi J Biol Sci* **2013**, *20*, 235-239.

[13] Shieh P., Bertozzi, C. R. Design strategies for bioorthogonal smart probes. *Org. Biomol. Chem.* **2014**, *12*, 9307-9320.

[14] Song, L., Varma, C. A. G. O., Verhoeven, J. W., Tanke, H. J. Influence of the triplet excited state on the photobleaching kinetics of fluorescein in microscopy. *Biophys. J.* **1996**, *70*, 2959-2968.

[15] Chen, J., Cammers-Goodwin, A. 2-(Fluorophenyl)pyridines by the Suzuki-Miyaura method: Ag_2O accelerates coupling over undesired *ipso*-substitution (SNAr) of fluorine. *Tetrahedron Lett.* **2003**, *44*, 1503-1506.

[16] Zhang, L., Er, J. C., Ghosh, K. K., Chung, W. J., Yoo, J., Xu, W., Zhao, W., Phan, A. T., Chang, Y. T. Discovery of a structural-element specific G-quadruplex "light-up" probe. *Sci. Rep.* **2014**, *4*, 3776.

[17] Carroll, V., Michel, B. W., Blecha, J., VanBrocklin, H., Keshari, K., Wilson, D., Chang, C. J. A boronate-caged [^{18}F]FLT probe for hydrogen peroxide detection using positron emission tomography. *J. Am. Chem. Soc.* **2014**, *136*, 14742-14745.

[18] Lippert, A. R., Van de Bittner, G. C., Chang, C. J. Boronate oxidation as a bioorthogonal reaction approach for studying the chemistry of hydrogen peroxide in living systems. *Acc. Chem. Res.* **2011**, *44*, 793-804.

3.9. Appendices B: Characterization of Compounds

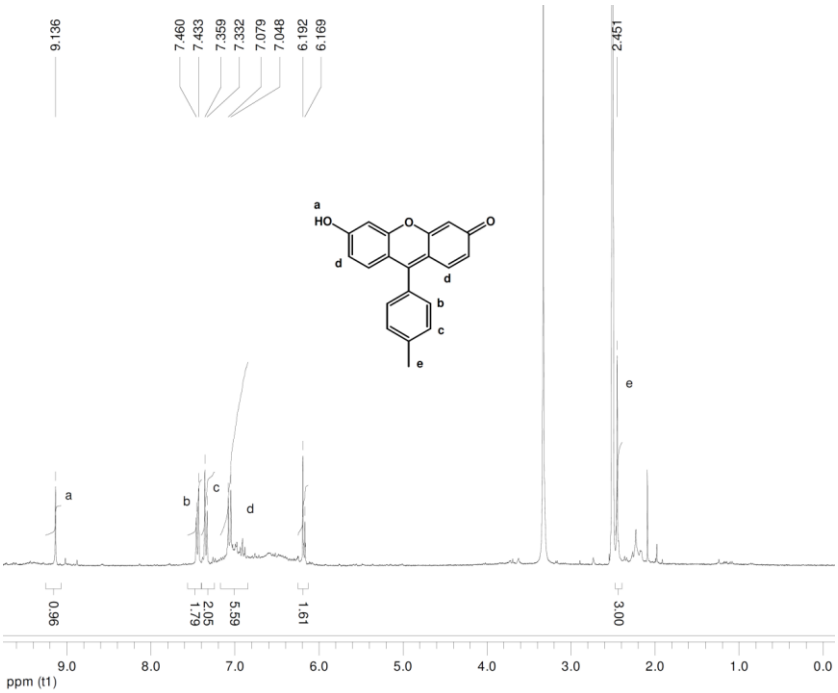

^{1}H NMR (300 MHz, DMSO-*d6*) spectra of **6**.

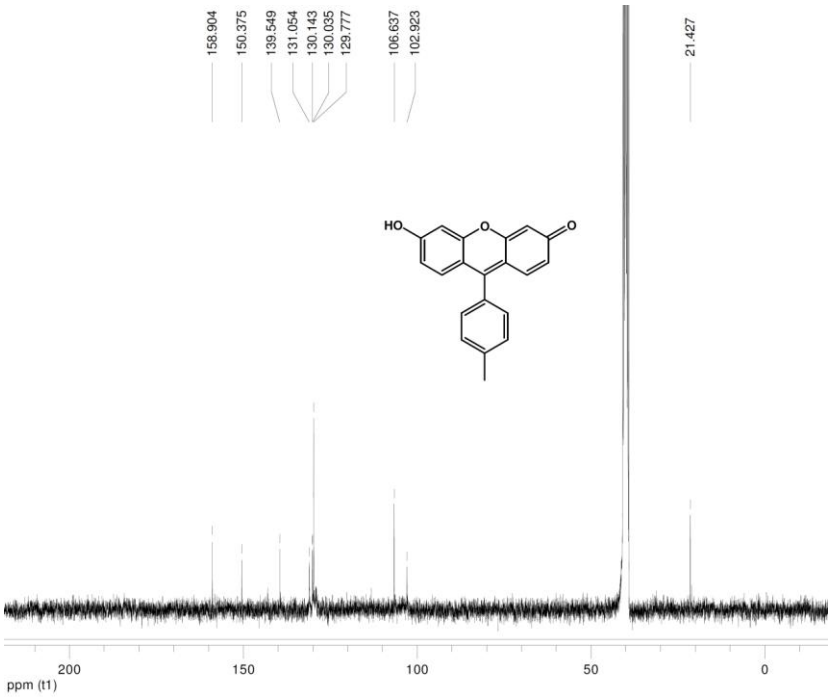

^{13}C NMR (300 MHz, DMSO-*d6*) spectra of **6**.

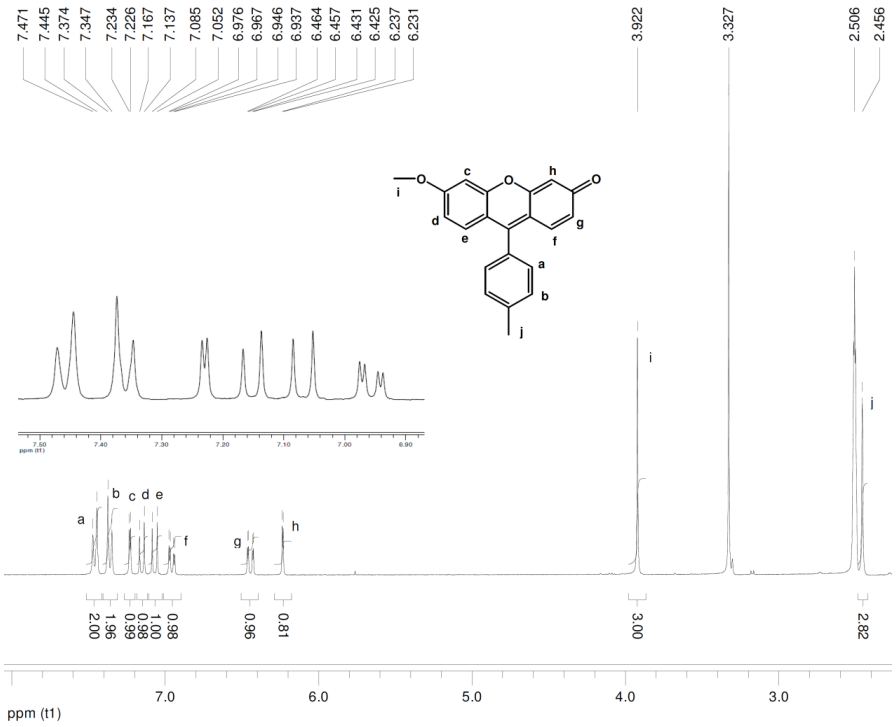

^{1}H NMR (300 MHz, DMSO-*d6*) spectra of **7**.

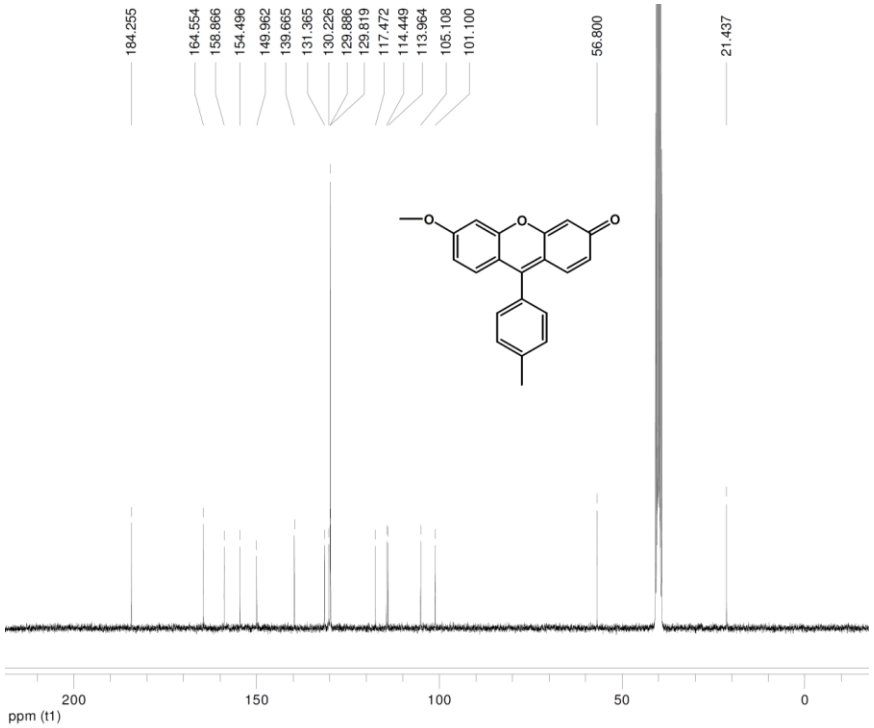

^{13}C NMR (300 MHz, DMSO-*d6*) spectra of **7**.

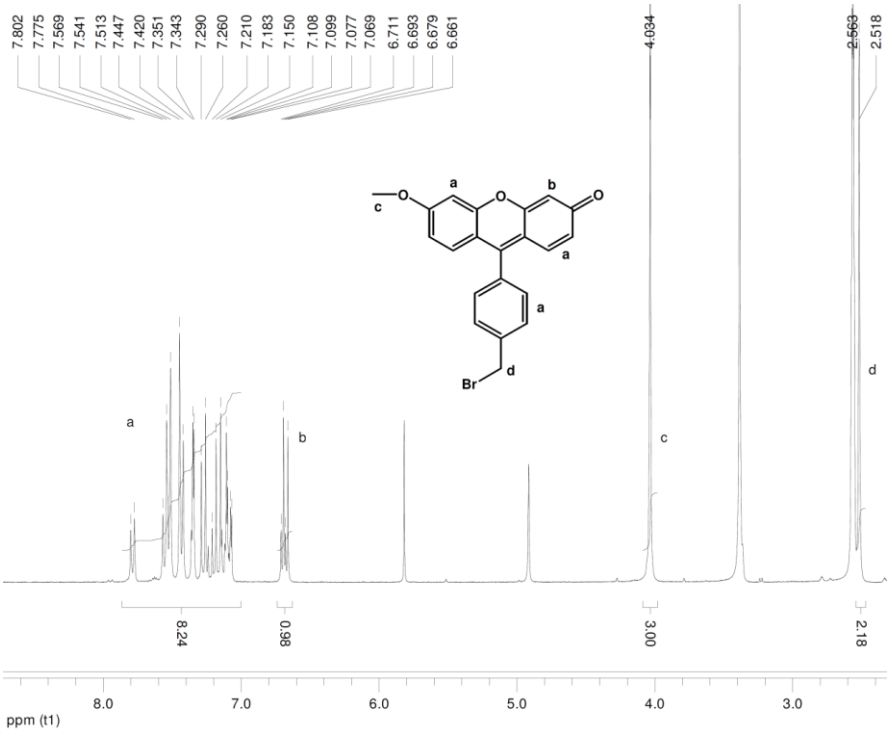

^{1}H NMR (300 MHz, DMSO-*d6*) spectra of **8**.

^{13}C NMR (300 MHz, DMSO-*d6*) spectra of **8**.

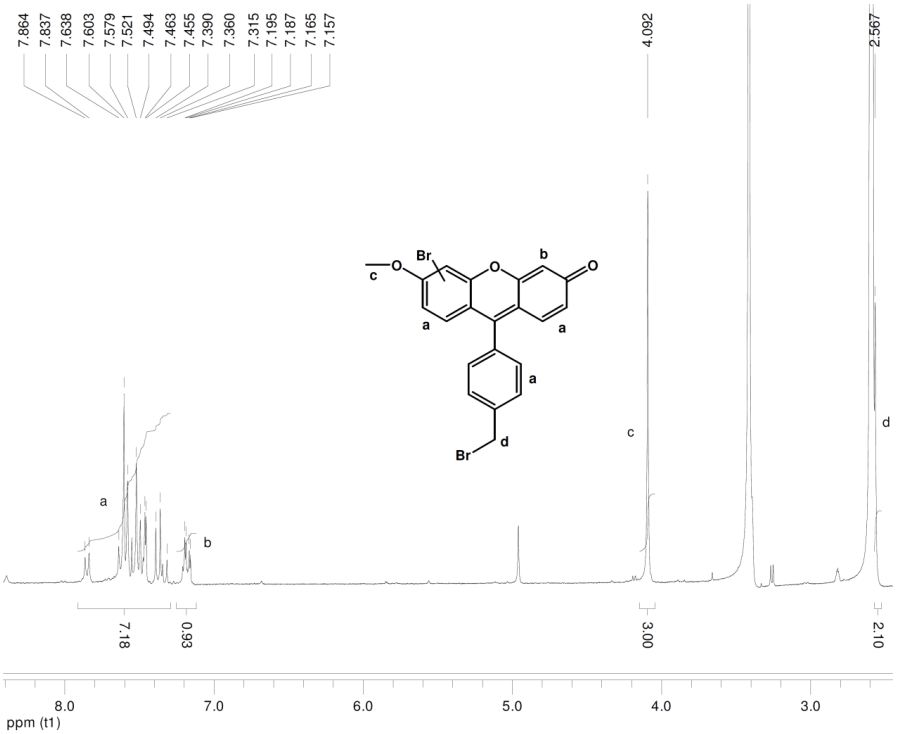

^{1}H NMR (300 MHz, DMSO-*d6*) spectra of **9**.

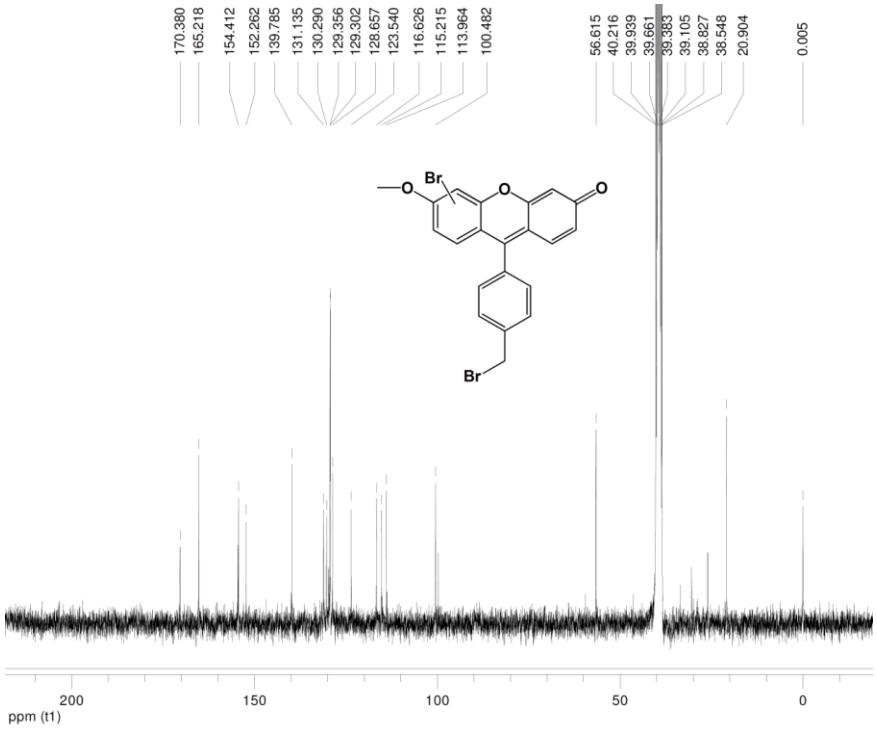

^{13}C NMR (300 MHz, DMSO-*d6*) spectra of **9**.

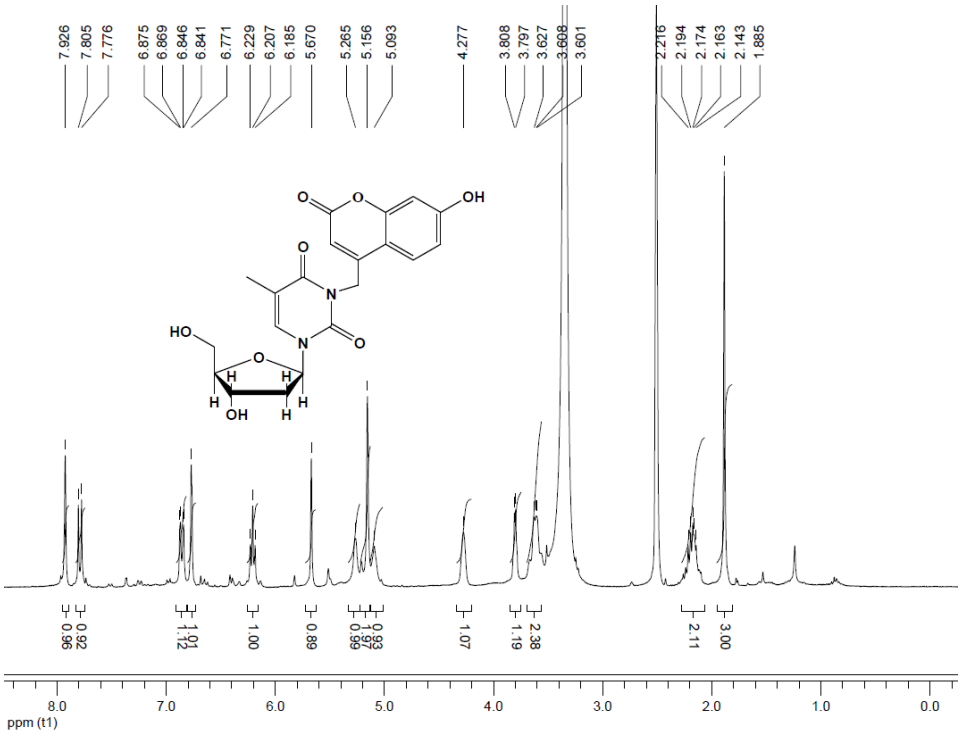

^{1}H NMR (300 MHz, DMSO-*d6*) spectra of **10**.

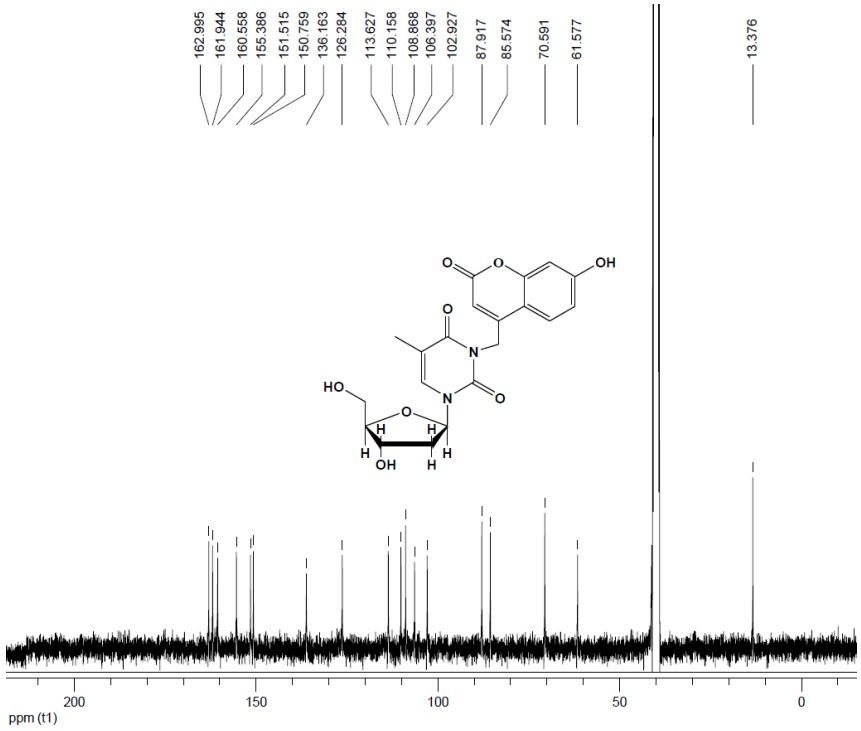

^{13}C NMR (300 MHz, DMSO-*d6*) spectra of **10**.

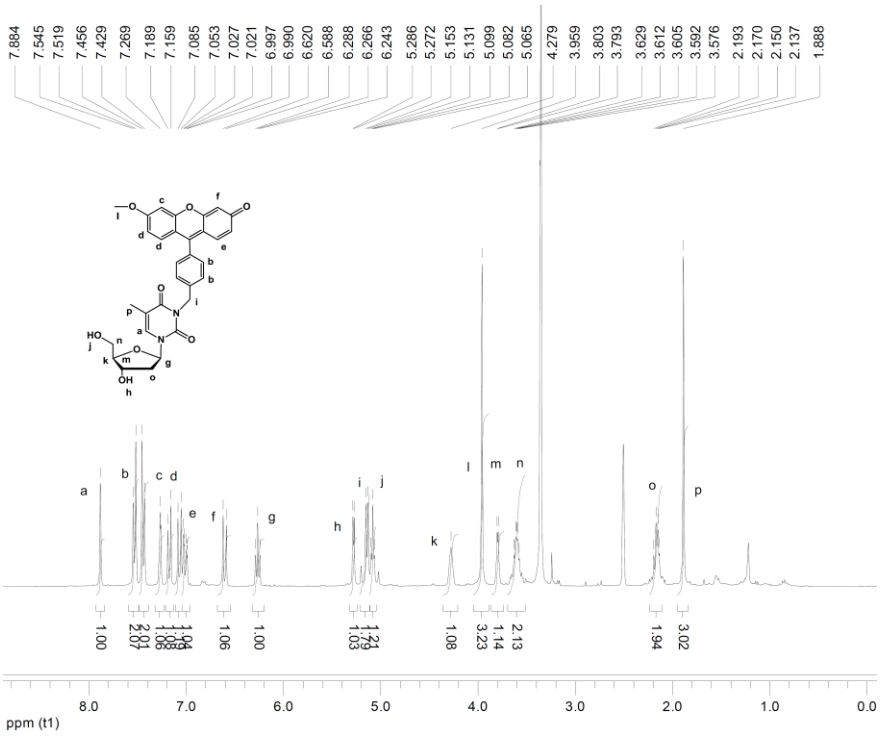

^{1}H NMR (300 MHz, DMSO-*d6*) spectra of **11**.

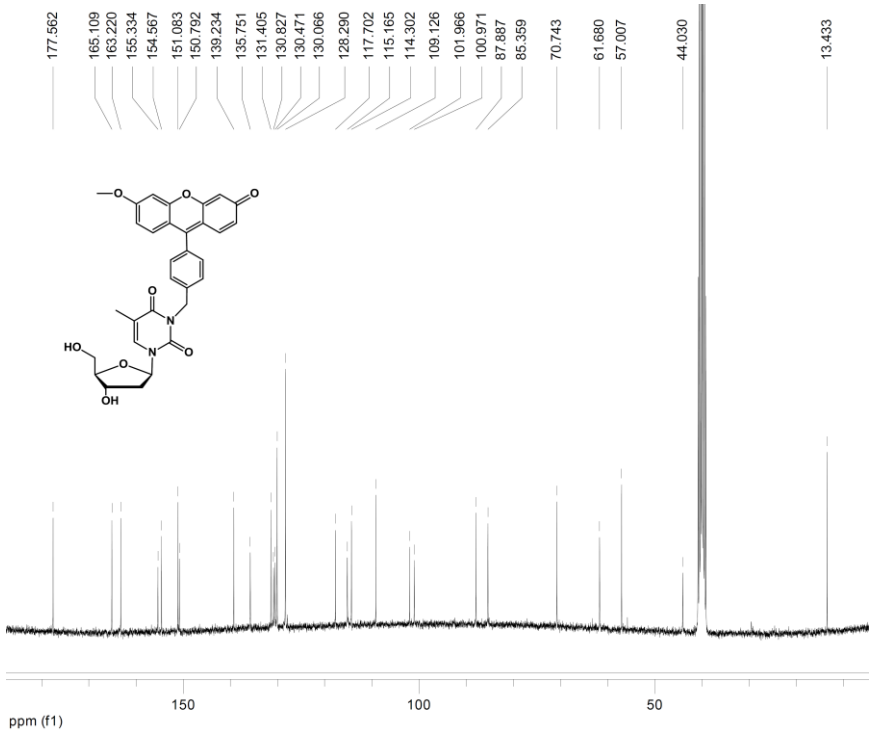

^{13}C NMR (300 MHz, DMSO-*d6*) spectra of **11**.

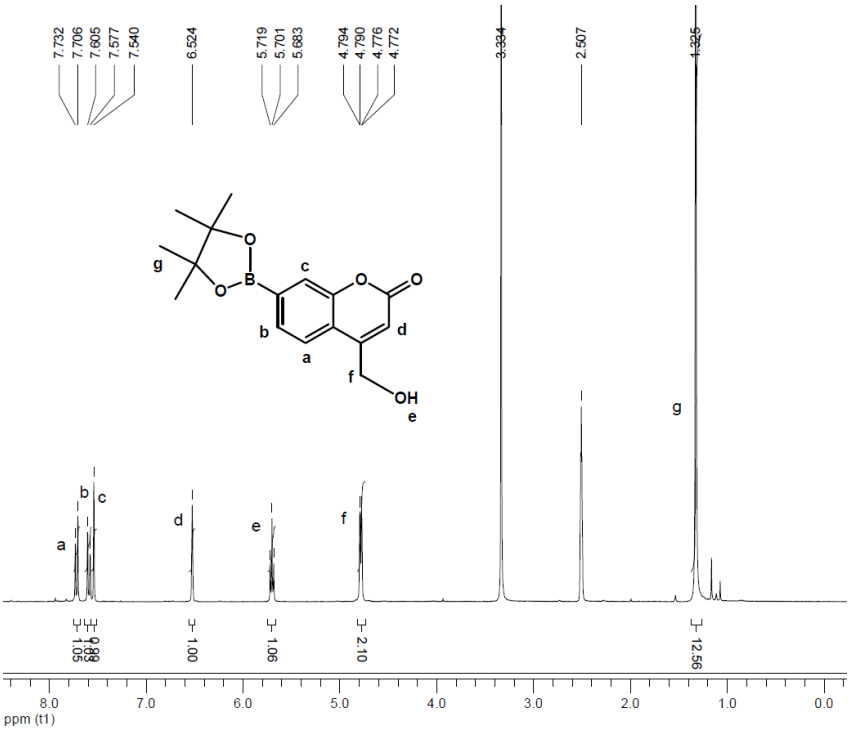

^{1}H NMR (300 MHz, DMSO-*d6*) spectra of **14**.

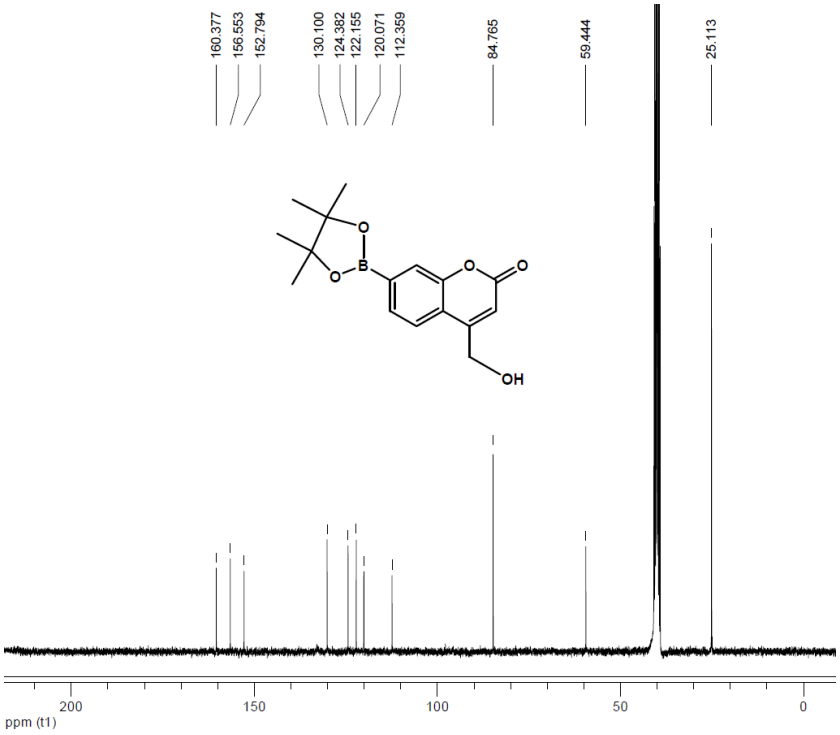

^{13}C NMR (300 MHz, DMSO-*d6*) spectra of **14**.

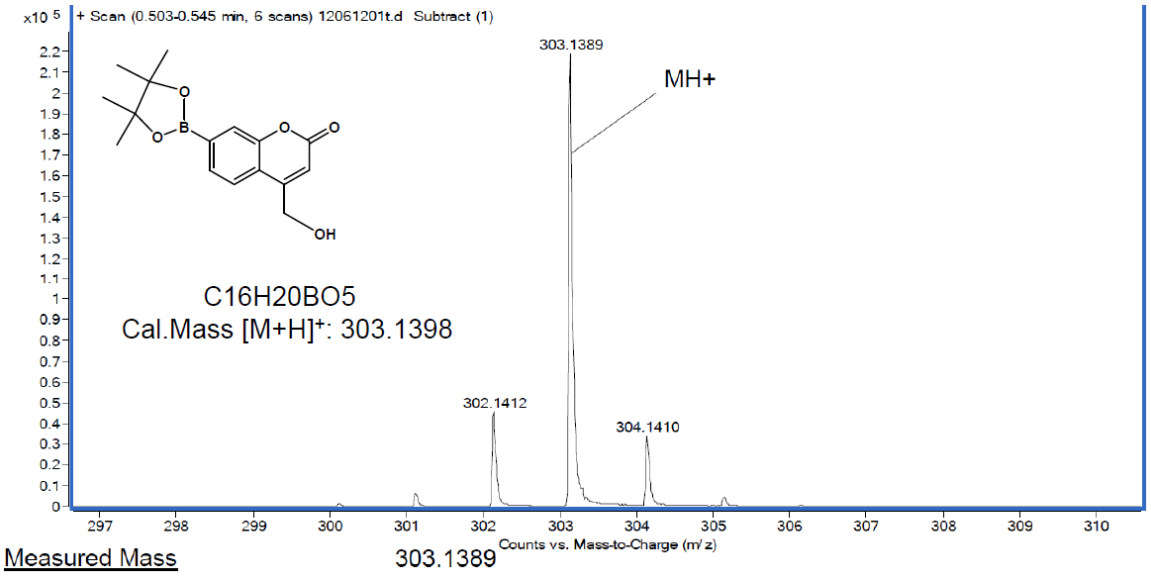

HRMS (TOF-MS-ESI) spectra of **14**.

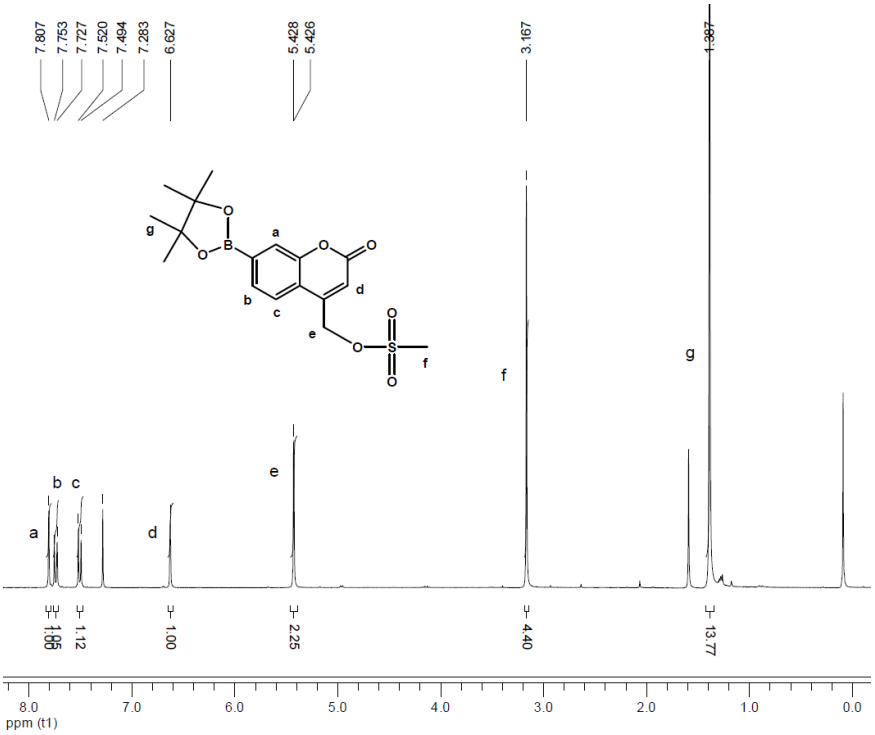

^{1}H NMR (300 MHz, $CDCl_3$-*d*) spectra of **15**.

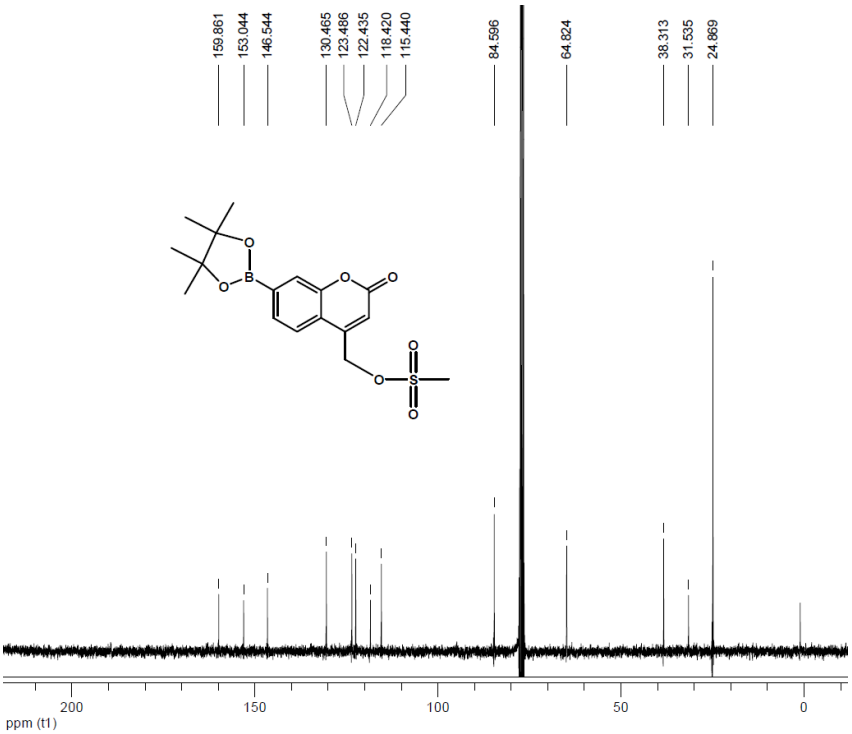

^{13}C NMR (300 MHz, $CDCl_3$-*d*) spectra of **15**.

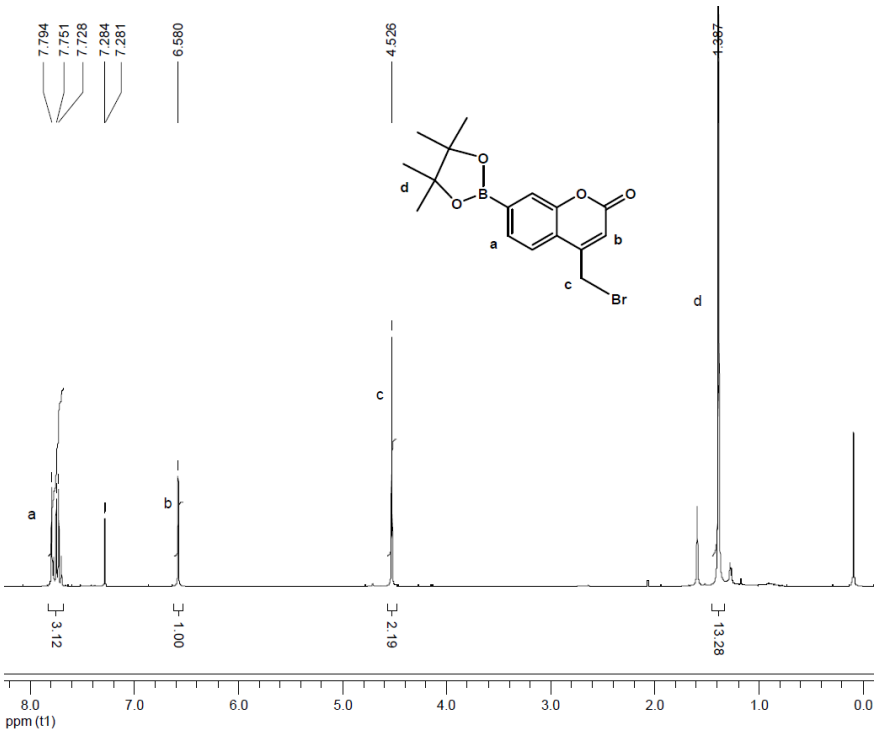

^{1}H NMR (300 MHz, $CDCl_3$-*d*) spectra of **16**.

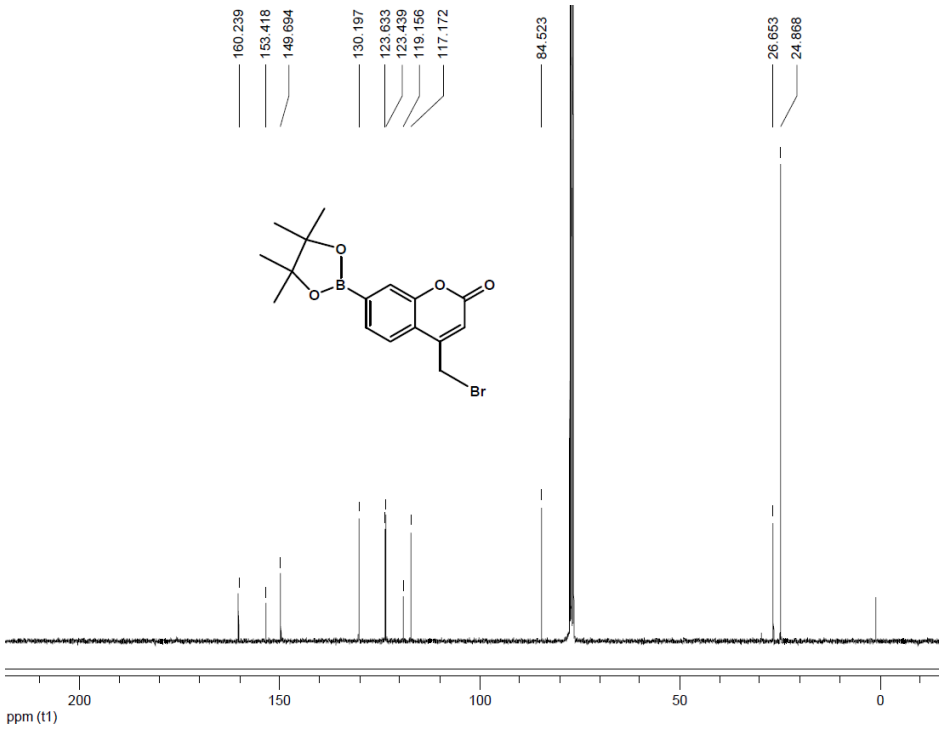

^{13}C NMR (300 MHz, $CDCl_3$-*d*) spectra of **16**.

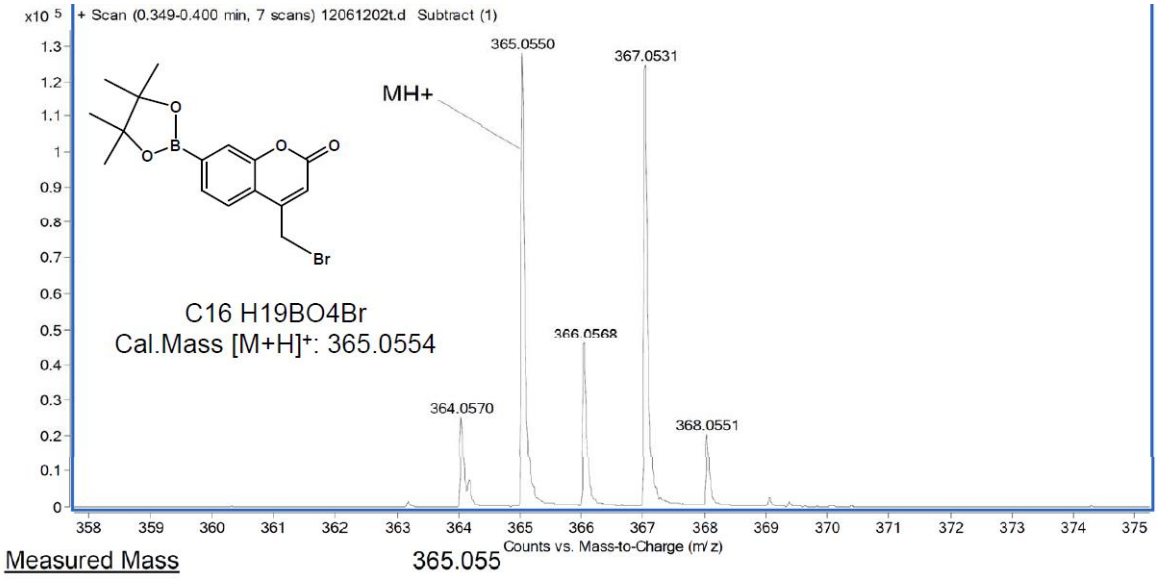

HRMS (TOF-MS-ESI) spectra of **16**.

Chapter 4. Photo-Reversible DNA Interstrand Cross-Linking by Coumarin[1]

4.1. Introduction

Unlike the normal Watson-Crick base pair interactions, chemical bonds formed in DNA interstrand cross-link (ICL) reactions can inhibit DNA replication and gene expression by preventing separation of two ODN strands. Therefore, DNA cross-linking agents have been widely applied in cancer therapy, study of DNA repair and gene regulation, and protein-DNA binding.[2-7] The cross-linking agents and modified DNA constructs are commonly used in DNA ICL reactions. A number of bifunctional chemical reagents have been developed as powerful DNA cross-linking agents including mitomycins, azinomycins, synthetic aziridinomitosenes, bizelesin, nitrogen mustard derivatives, cis-platinum-like organometallics, and psoralens.[8-11] Recently, H_2O_2 or photo-induced quinone methide-based cross-linking agents have been reported.[12-17] In addition to bifunctional reagents capable of reacting with two ODN strands, the modified ODNs containing certain functional groups have also been used for DNA-templated cross-linking reactions. Instead of much excessive chemical reagents (most more than 100 times) used in ICL formation, only equivalent modified DNA constructs are required for efficient DNA ICL formation. ICL formation via modified ODNs can be achieved via click chemistry, photo-generated radicals or carbens, and photo-induced cycloaddition.[18-26] However, most ICL formation is irreversible. Reversible DNA cross-linking agents offer opportunities for development of anticancer agents with selectivity. For example, the anticancer drug ecteinascidin 743-induced reversible alkylation reactions allow for

migration of the drug to the alkylating sites therefore achieving sequence-selective anticancer activity.[27] More recently, the reversible property of quinone methides afforded a novel strategy for cell-compatible target selective alkylation. It invovled strand exchange and cross-link migration leading to dynamic cross-linking.[28, 29]

Many photoresponsive molecules induce reversible photochemical reactions which have wide application in polymer sciences, such as light switchable coatings and drug delivery,[30-32] and studies of reversible DNA cross-linking and manipulation.[33-36] For instance, psoralens can form reversible ICLs and have been utilized for DNA damage and repair study, for therapeutic gene modulation, and as photoactive probes of nucleic acid structure and function.[37, 38] Coumarin molecules, with similar structure scaffold as psoralens, enable photoreversible dimerization via a photoinduced [2 + 2] cycloaddition reaction and subsequent photocleavage at a different wavelength. They have been widely applied in polymeric research, such as electroluminescence studies, light and energy harvesting, construction of liquid crystalline polymers and photoactive surfaces, and photoreversible polymerization, chain extension, and cleavage.[39] Besides its polymer applications, coumarin analogues are also used as medicines or as fluorescent tags in the field of biology science and fluoroprobes for labelling protein and nucleic acids.[40] However, to the best of our knowledge, no detailed reports on the photoactivity of coumarin towards biomolecules such as DNA, RNA, and proteins are avaible.

Recently, we reported a coumarin-modified thymidine allowing for reversible ICL formation with dT upon 350 nm irradiation at a yield of 69%.[41] The fluorescence of coumarin was quenched with formation of ICL, but low efficiency and possible intramolecular reaction limited its application for on-line fluorescence detection of ICL

formation. We propose that the cross-linking efficiency will increase with optimization of suitable linkers between the coumarin moiety and ODNs. Coumarin moieties containing suitable linkers would also allow for direct incorporation into ODNs at any positions instead of conjugating to thymidine in our previous report. Moreover, real-time detection of ICL progress can be achieved if coumarin-containing DNA duplexes generate quantitative ICL formation. Usually, traditional DNA ICL analysis methods involved radiolabeling with ^{32}P, ^{14}C, or ^{3}H, which is considered to be health and safety hazards. In addition, they are offline and time-consuming. The fluorescence-based method allow for a safe real-time monitoring ICL process, which will undoubtedly facilitate its bio-application. The primary focus of this chapter involves investigation of the coumarin-dT reactions and the quantitative, fluorescence-detectable, sequence-dependent, and photo-switchable DNA ICL formation via coumarin moieties.

4.2. Coumarin-Containing ODNs for ICL Study

4.2.1. Synthesis of the Coumarin Derivatives

The substitutions at the position-7 of coumarin have great influence in its photoactivity and the electron donating groups enhance the coumarins' photoreactivity.[42] 7-Hydroxy-2H-chromen-2-one (**3**) with a hydroxyl group at the position-7 was chosen as the basic scaffold to build its derivatives. Seven coumarin analogues **1-7** with modifications at the position-4 (**2**) or 7 (**3-7**) were designed and synthesized, which allowed us to investigate the effects of the linkers and the ICL reaction sites of coumarin on DNA cross-linking efficiency (Figure 4-1). Compounds **2** and **3** containing a hydroxyl group at the position-4 and 7 respectively, allow for studying the effects of the phosphorous position on the cross-linking efficiency. Compounds **3-6**, bearing different linkers at position-7, are

capable of investigation of the linker-length effect. The coumarin **7** with a linker containing two hydroxyl groups allows for flexible incorporation into DNA at any positions. Synthesis of **1** or **2** involved methylation of **3** or **14** using methyl iodide, and compounds **4**, **5,** and **7** containing three different linker units at the position-7 were prepared via Williamson ether synthesis starting from coumarin **3** (Figure 4-1). Compound **6** was synthesized by Huisgen 1,3-dipolar cycloaddition between 3-azidopropan-1-ol and 7-ethynyl-4-methyl-2H-chromen-2-one (**15**) (Figure 4-1D).

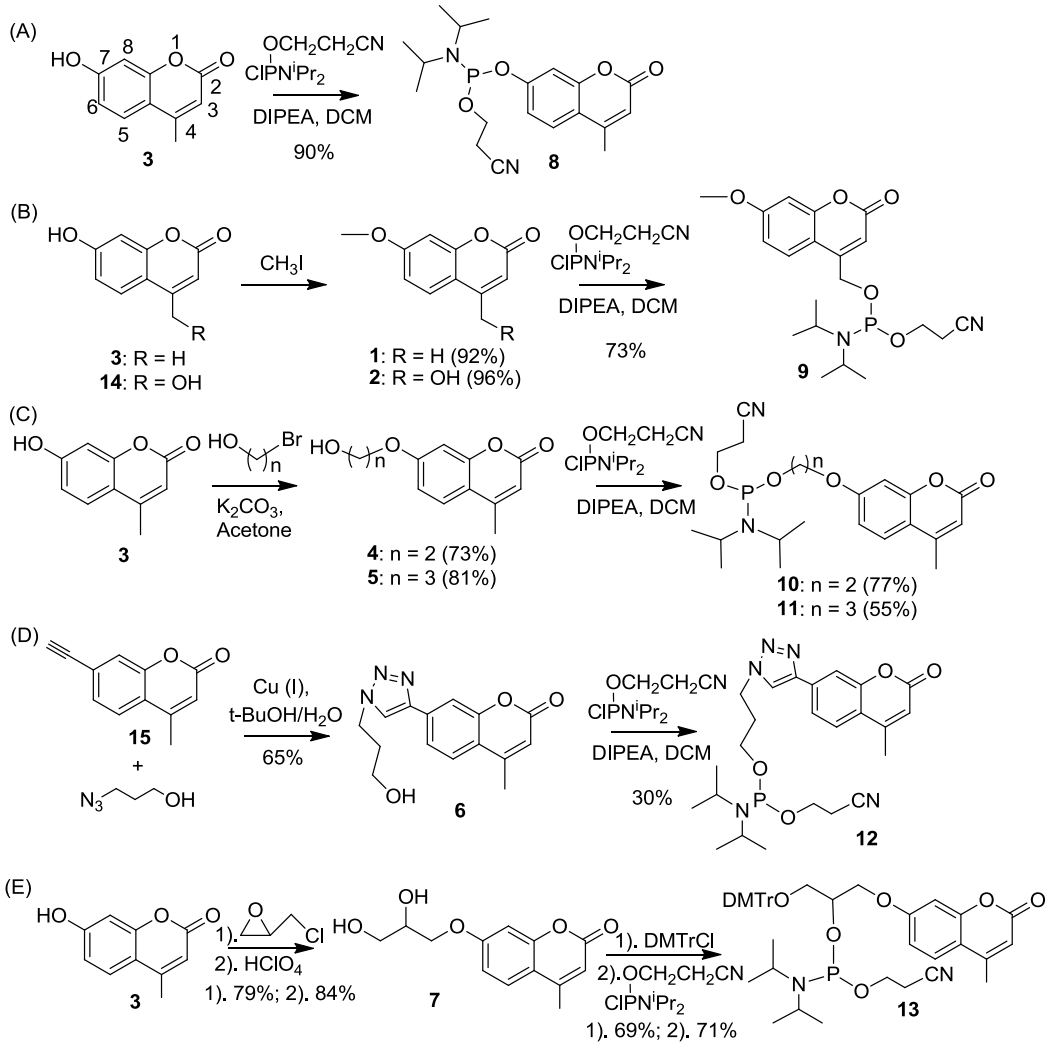

Figure 4-1. Preparation of phosphoramidites **8**-**13**.

Compounds **2**-**6** were converted to the corresponding phosphoramidites **8**-**12** using standard method. The phosphoramidite **12** was prepared with light-protection due to its photo-sensitivity. Compound **7** was converted to the phosphoramidite **13** under standard conditions after introduction of DMTr residue. The phosphoramidites **8**-**13** were directly incorporated into ODNs via automated DNA solid-phase synthesis with > 98% coupling yields.

4.2.2. Preparation of the ODNs

The ODNs were prepared via standard automated DNA synthesis techniques in a 1.0 μmole scale using commercial 1000Å CPG-succinyl-nucleoside supports. The ^{i}Pr-Pac-dA and ^{i}Pr-Pac-dG phosphoramidites were used for synthesis of coumarin-containing ODNs. The commercially available β-cyanoethyl phosphoramidites with phenoxyacetyl (Pac) protecting groups on the exocyclic amines of dA and dG allowed for a very mild deprotection condition minimizing decomposition of the functionalized ODNs **2b**-**10b**, **11**, and **13b** (Table 4-1).

Table 4-1. List of coumarin-containing ODNs.

Entry	ODN sequence	Mass (*Calcd.*)	Mass (*Found*)
ODN **2b**	3′- dACC CGC CGT AT**2**	3546.2	3546
ODN **3b**	3′- dACC CGC CGT AT**3**	3516.2	3516
ODN **4b**	3′- dACC CGC CGT AT**4**	3560.2	3560
ODN **5b**	3′- dACC CGC CGT AT**5**	3574.2	3574
ODN **6b**	3′- dACC CGC CGT AT**6**	3625.3	3625
ODN **7a**	3′- dACC CGC CGT A**A4**	3569.2	3569

ODN **8a**	3′- dACC CGC CGT A**G4**	3585.2	3585
ODN **9a**	3′- dACC CGC CGT A**C4**	3545.2	3545
ODN **10b**	3′- dGGCTAA**7**AACGC	3663.4	3663.4
ODN **11**	3′- dCCG CCG TAC TT **4**	3551.2	3551
ODN **13b**	3′- dACCCGCCGTAA**7**AA	4225.8	4225.4

Deprotection of the nucleobases and phosphate moieties as well as cleavage of the linker for normal ODNs were performed with a mixture containing 40% aq. $MeNH_2$ and 28% aq. NH_3 (1:1) at room temperature for 2 h. Coumarin-containing ODNs were deprotected and cleaved using 28% aq. NH_3 at room temperature for 2 h. All crude ODNs were purified by 20% denaturing polyacrylamide gel electrophoresis and identified by MALDI-TOF-MS after treatment with C-18 column. The quantification of ODNs in water was achieved using UV–VIS spectrophotometer at 260 nm.

4.2.3. Thermal Stability Study

After successfully incorporating coumarin analogues into ODNs, we investigated the effect of coumarin on duplex thermal stability by measuring the UV-melting temperatures (T_M) of ds DNAs containing coumarins **2**-**6** (Table 4-2). Introduction of coumarin moieties enhanced the stability of the duplexes with a ΔT_M of 1.1 - 3.1 °C relative to when natural 2'-deoxyadenosine (dA) was present. This is possibly due to increased π-π stacking and/or increased lipophilicity (Chapter 2).[43-45] In addition, the linkers and their position play an important role in this. More obvious T_M increase was observed when coumarin was conjugated with ODNs via position-4 (ds DNA-**2**, ΔT_M = 2.0 °C) than via position-7 (ds DNA-**3**, ΔT_M = 1.1 °C). The flexible linker unit at the position-7 further

enhances the duplex stability by about 3.0 °C (ds DNA-**4**, ΔT_M = 2.9 °C; ds DNA-**5**, ΔT_M = 3.1 °C), but the triazole moiety in **6** with less flexibility in stacking and decreased lipophilicity seems less favorable for duplex stability (ds DNA-**6**) than an alkyl chain (ds DNA-**5**).

Table 4-2. Melting Temperatures of ds DNA-**1**-**6**.[a]

Entry	Duplex	T_m (°C)	ΔT_m (°C)
ds DNA-**1**	5'-d(TGG GCG GCA TAT) (ODN **1a**) 3'-d(ACC CGC CGT ATA) (ODN **1b**)	57.8 ± 0.1	
ds DNA-**2**	5'-d(TGG GCG GCA TAT) (ODN **1a**) 3'-d(ACC CGC CGT AT**2**) (ODN **2b**)	59.8 ± 0.1	2.0
ds DNA-**3**	5'-d(TGG GCG GCA TAT) (ODN **1a**) 3'-d(ACC CGC CGT AT**3**) (ODN **3b**)	58.9 ± 0.7	1.1
ds DNA-**4**	5'-d(TGG GCG GCA TAT) (ODN **1a**) 3'-d(ACC CGC CGT AT**4**) (ODN **4b**)	60.7 ± 1.0	2.9
ds DNA-**5**	5'-d(TGG GCG GCA TAT) (ODN **1a**) 3'-d(ACC CGC CGT AT**5**) (ODN **5b**)	60.9 ± 0.8	3.1
ds DNA-**6**	5'-d(TGG GCG GCA TAT) (ODN **1a**) 3'-d(ACC CGC CGT AT**6**) (ODN **6b**)	59.2 ± 1.2	1.4

[a] Measured in a buffer containing 0.1 M NaCl, 10 mM potassium phosphate (pH 7), and 4 μM of each single-stranded ODN.

4.3. Structure Determination of Coumarin-dT Adducts

4.3.1. LC-MS Analysis for Monomer Reaction

Initially, we studied the photoreactivity of coumarin **1** towards canonical nucleosides dA, dG, dT, and dC. As the hydroxyl group has the ability to destroy radicals or intermediates in photo-induced cycloaddition reaction, coumarin **1** obtained by methylation of **3** was used for the monomer reaction.[46] The 350 nm UV light is chosen for the reaction, because it is compatible with living cells and inert to biological components. LC-MS was used to detect the reaction products. A new compound with a molecular ion peak at 455.4 (corresponding to *syn*- and *anti*-cyclobutane **1**-dT dimmers **17** and **18**) was observed in the presence of dT after 350 nm irradiation for 2 days. However, coumarin-nucleoside adducts were not formed when **1** reacted with dC, dA, or dG, while only a coumarin-coumarin dimmer was detected in LC-MS mass spectrum (Figure 4-2). This indicated that coumarin has good photo reactivity toward thymidine but not with dA, dC, and dG.

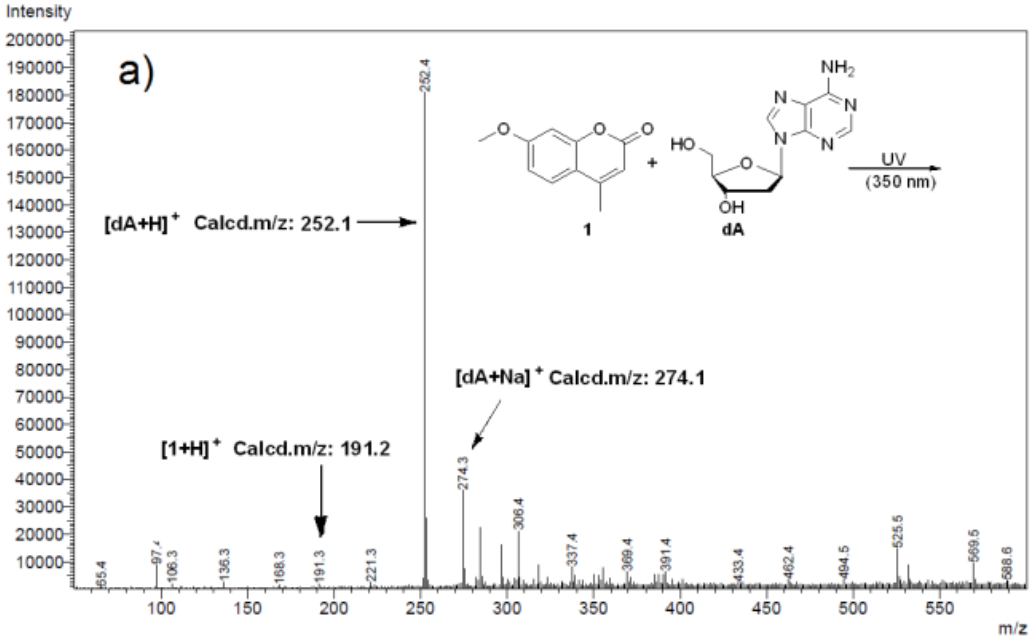
Intensity
a)
[dA+H]+ Calcd.m/z: 252.1
[dA+Na]+ Calcd.m/z: 274.1
[1+H]+ Calcd.m/z: 191.2
252.4
274.3
306.4
191.3
1
dA
UV
(350 nm)
m/z

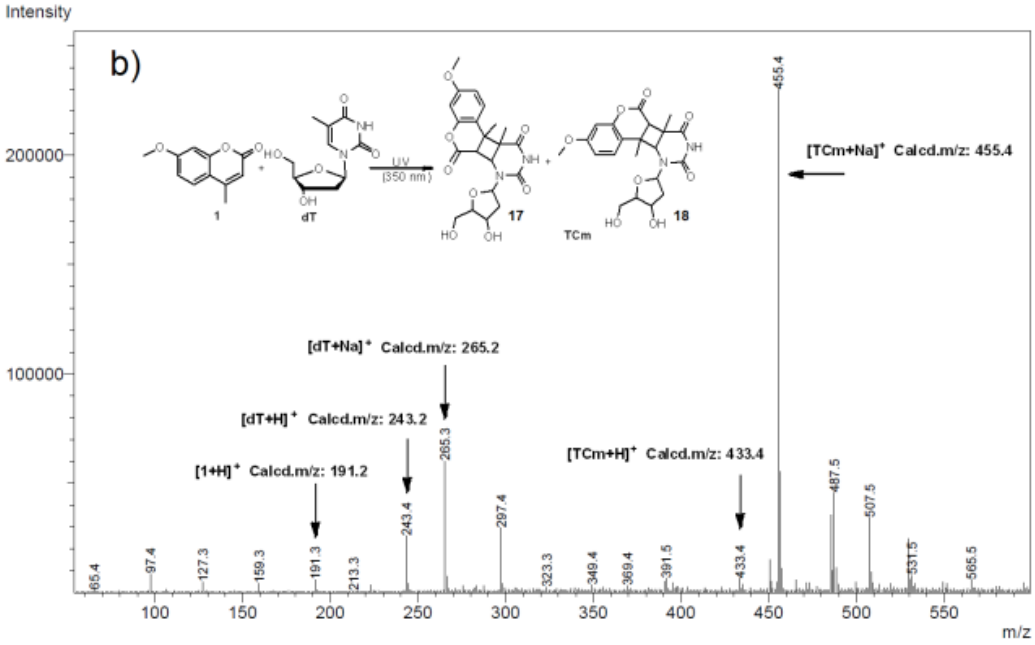
Intensity
b)
[TCm+Na]+ Calcd.m/z: 455.4
[dT+Na]+ Calcd.m/z: 265.2
[dT+H]+ Calcd.m/z: 243.2
[1+H]+ Calcd.m/z: 191.2
[TCm+H]+ Calcd.m/z: 433.4
455.4
265.3
243.4
191.3
433.4
1
dT
17
TCm
18
UV
(350 nm)
m/z

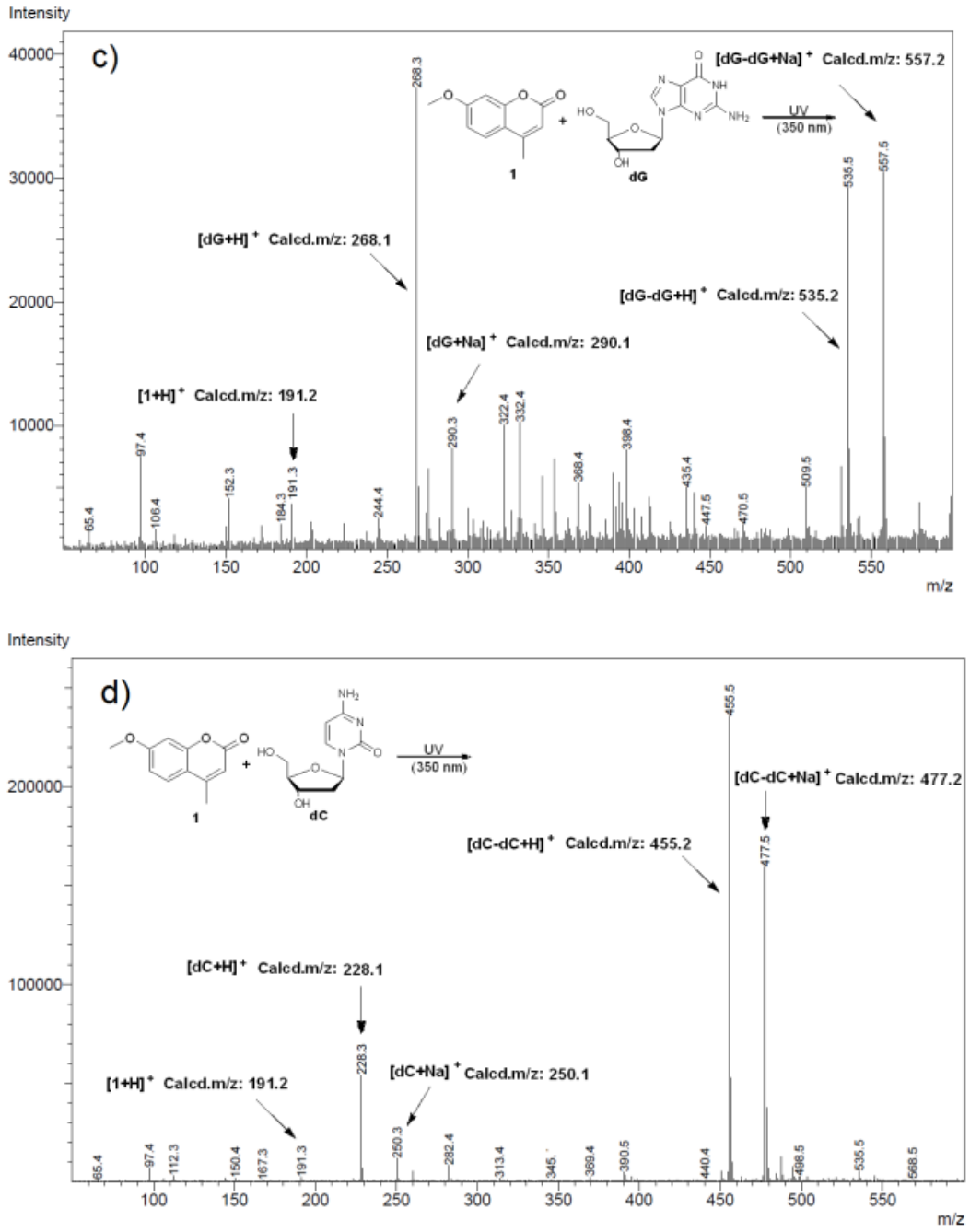

Figure 4-2. LC-MS analysis of photochemical reaction of **1** and nucleosides.

4.3.2. [2+2] Cycloaddition between **1** and dT

The [2+2] cycloaddition reaction occurred between dT and **1** upon 350 nm irradiation yielding the products **17**, **18**, and a coumarin dimmer **19**, which were isolated and

characterized by ^{1}H NMR, ^{13}C NMR, and HRMS. The structure of the isomers **17** and **18** was determined by two-dimensional nuclear magnetic resonance spectroscopy (H-H COSY). They were formed by a [2+2] cycloaddition reaction between 3, 4 double bond of **1** and 5, 6 double bond of dT, while the syn-adduct **17** was the predominant product (yield: 15% for **17** and 9% for **18**) (Figure 4-3). Compound **19** was also isolated. Formation of cyclobutane products **17**-**19** quenches the fluorescence of coumarin due to the disruption of conjugated π system of coumarin (Figure 4-3). Almost no fluorescence for products **17** and **18** was observed. In DNA-templated reaction, only non-fluorescent **17** and **18** would be generated as cycloaddition products and all observed fluorescence would result from unreacted coumarin. This allows us to real-time detect the dT-**1** cycloaddition reaction process using fluorescence spectra.

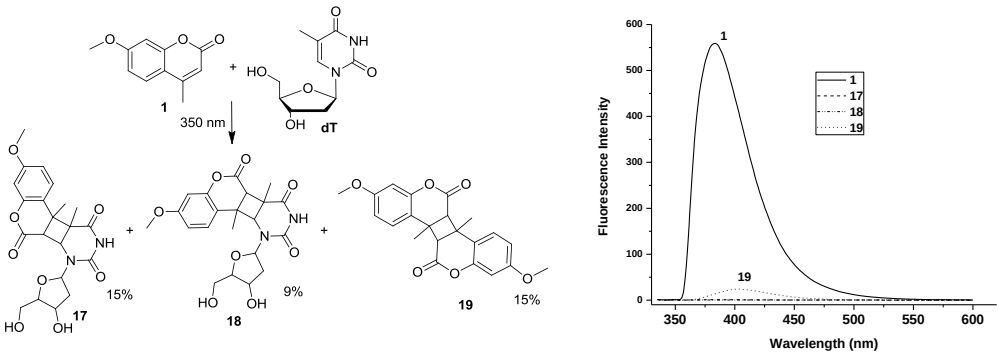

Figure 4-3. Cycloaddition between **1** and dT, and Fluorescence emission spectra of **1** and Products (Coumarin **1** and dimmers **17**-**19**, 10 μM in water with < 1% menthol, λ_{ex} = 325 nm, slit width = 15 nm; λ_{em} = 385 nm, slit width = 2.5 nm).

4.4. The Effect of the Linker and Flanking Sequences on ICL

4.4.1. Linker Effect on Cross-Linking Efficiency

Six double stranded (ds) DNAs (**1**-**6**) were designed to investigate the coumarin's photoreactivity towards dT (Table 4-2). The ds DNA-**2**-**6** contain coumarin analogues opposing dT, while ds DNA-**1** with a natural A:T base pair serves as a control. Upon photo-irradiation at 350 nm, ds DNA-**2**-**6** generated a new band with lower migration than the original ODNs. The resulting products were verified as the ICL adducts by HRMS (Figure 4-4). No ICL band was observed for ds DNA-**1** and higher ICL yield was obtained with ds DNA-**3** (86%, lane 3) than ds DNA-**2** (3%, lane 2). This result indicated that the coumarin's photoactivity in DNA depends on the linker's position. The coumarins attached to ODN by position-7, allowed a favorable conformation for formation of a highly efficient transition state between 3, 4 double bond of coumarin and dT, while coumarin incorporated into ODN via position-4 induces steric hindrance. This is further confirmed by the result that better reactivity was observed for ds DNA-**3**-**6** with coumarins conjugated with ODNs at the position-7 (Figure 4-4).

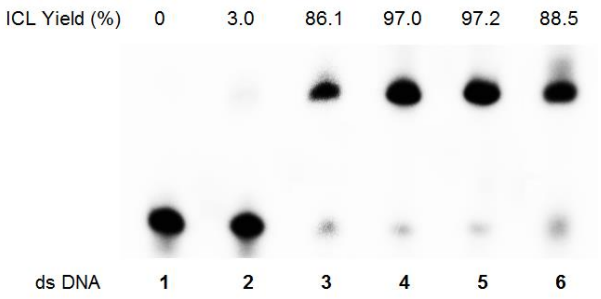

Figure 4-4. PAGE analysis of ICL formation for ds DNA-**1**-**6** (100 nM ds DNA-1-6 was irradiated at 350 nm for 2 h; ODN **1a** was 5'-[^{32}P]-labeled).

Moreover, the length and flexibility of linkers also played an important role in the ICL formtion. Almost quantitative ICL was formed for ds DNA-**4** and **5** with an adaptable chain between the phosphate group and coumarin. The ds DNA-**3** showed less ICL

efficiency due to the lack of linker. Installation of a triazole ring in **6** reduced its photoactivity in ds DNA-**3**, possibly due to the electron transfer in the excitation state of coumarin. In addition, duplexes containing coumarin with a flexible linker at the 7-position proceeded at a faster rate for ICL formation. The photo-induced cycloaddition reaction in DNA followed first-order kinetics. ICL generation with ds DNA-**4** (50.4 ± 3.8×10^{-4} s^{-1}) and DNA-**5** (53.9 ± 4.1 $\times10^{-4}$ s^{-1}) is about 5 times faster than those for ds DNA-**3** (9.5 ± 1.6 $\times10^{-4}$ s^{-1}) and **6** (9.8 ± 1.1×10^{-4} s^{-1}) (Table 4-3). Finally, coumarin **4** with high efficiency was employed for further study.

Table 4-3. ICL formation rates for ds DNA-**1**-**6**.

Entry	k (10^{-4} s^{-1})	$t_{1/2}$ (min)
ds DNA-**2**	*n.d.*	*n.d.*
ds DNA-**3**	9.5 ± 1.6	12.4 ± 2.0
ds DNA-**4**	50.4 ± 3.8	2.3 ± 0.2
ds DNA-**5**	53.9 ± 4.1	2.3 ± 0.2
ds DNA-**6**	9.8 ± 1.1	11.9 ± 1.2

n.d.: not determined.

4.4.2. Flanking Sequence-Dependent Cross-Link Formation

As electron transfer in photochemical reactions affects the reactivity of photoactive compounds, the flanking bases play the most important role in the electron transfer, which affects ICL effciency.[47] The ds DNA-**7**, **4**, **8**, and **9** with coumarin **4** flanked by dA, dT, dG, and dC respectively, were designed for this study (Figure 4-5). The efficient electron transfer would lead to nucleobase-specific fluorescence quenching, which can be directly observed from fluorescence emission spectra.

ds DNA-**7**

ODN **7a**: 3'-dTTTACGGCGGGT

ODN **7b**: 5'-d**4**AATGCCGCCCA

ds DNA-**8**

ODN **8a**: 3'-dTCTACGGCGGGT

ODN **8b**: 5'-d**4**GATGCCGCCCA

ds DNA-**4**

ODN **1a**: 3'-dTATACGGCGGGT

ODN **4b**: 5'-d**4**TATGCCGCCCA

ds DNA-**9**

ODN **9a**: 3'-dTGTACGGCGGGT

ODN **9b**: 5'-d**4**CATGCCGCCCA

ds DNA-**10**

ODN **10a**: 3'-dGCGTTTTTAGCC

ODN **10b**: 5'-dCGCAA**7**AATCGG

ds DNA-**11a-d**

ODN **11a-d**: 3'-d**X**AAGTACGGCGGGTACG

ODN **11**: 5'-d**4**TTCATGCCGCC

a: X = T;
b: X = C;
c: X = A;
d: X = G

ds DNA-**12**

ODN **12a**: 3'-dTTTTTACGGCGGGTACCCGGATTCCAAGTACGGCTAGTACGTCCTTGACA

ODN **7b**: 5'-d**4**AATGCCGCCCA

ds DNA-**13**

ODN **12a**: 3'-dTTTTTACGGCGGGTACCCGGATTCCAAGTACGGCTAGTACGTCCTTGACA

ODN **13b**: 5'-dAA**7**AATGCCGCCCA

Figure 4-5. List of ds DNAs used in the study.

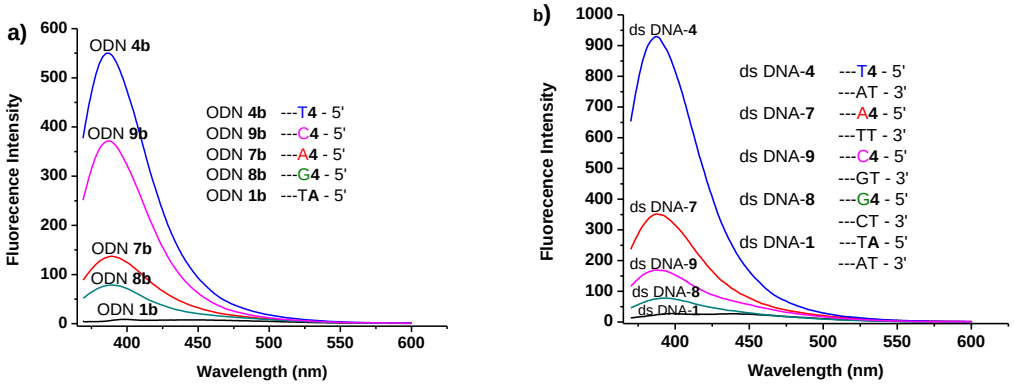

Figure 4-6. Fluorescence intensity of **4** when flanked by different bases: (a) fluorescence emission spectra of 10 μM single stranded ODNs; (b) fluorescence emission spectra of 10 μM duplexes (measured in 100 mM NaCl and 10 mM pH 7 phosphate buffer solution with λ_{ex} = 350 nm, slit width = 10 nm; λ_{em} = 390 nm, slit width = 10 nm).

The ODNs (**7b** and **8b**) containing **4** adjacent to a purine nucleoside (A and G) showed a greatly reduced fluorescence intensity compared to those (**4b** and **9b**) with **4** flanking to a

pyrimidine nucleoside (T and C) (Figure 4-6a). Interestingly, hybridization of DNAs enhances the fluorescence of ds DNA-**4** and **7** with an A:T base pair adjacent to **4**:T, and quenches the fluorescence of ds DNA-**9** and **8** with a G:C pair next to **4**:T (Figure 4-6b). This can be explained by the large excited state reduction potential of coumarin **4** (2.10 V, Figure 4-7), which is capable of oxidizing the adjacent nucleobase.[48] The sequence of the fluorescence quenching efficiency is in the order of dG > dA > dC ≈ dT, which is consistent with the order of nucleobase oxidation potentials ($E_{O,CV}$: G (1.25), A (1.72), C (1.87), and T (1.90)).[49] Therefore, more efficient photo-induced electron transfer occurred when **4**:T base pair was next to G:C base pairs than next to A:T pair. The efficiency of cross-link formation is consistent with this trend.

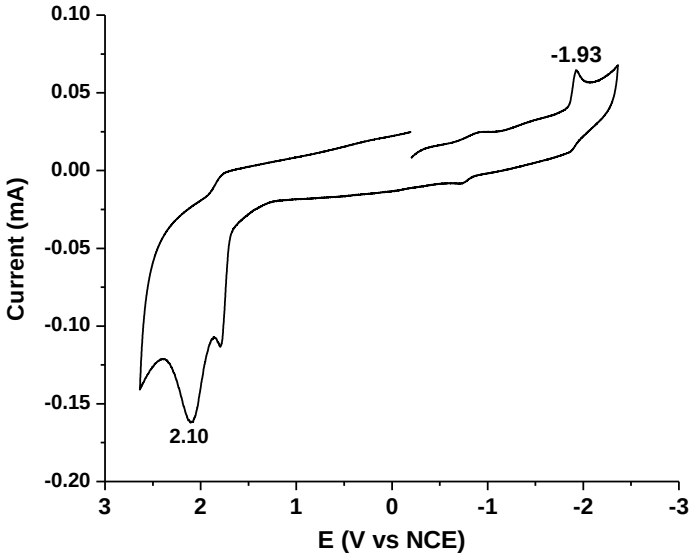

Figure 4-7. Cyclic voltammogram of coumarin **4** (0.1 M TBA PF_6 in acetonitrile). The scan was initiated at 0.20 V vs NCE with a scan rate of 100 mV s^{-1}.

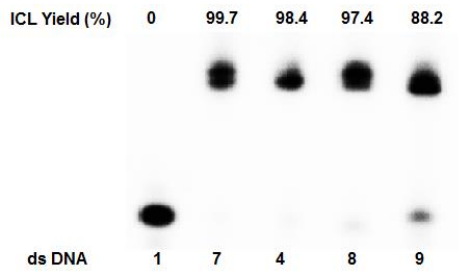

Figure 4-8. PAGE analysis of ICL generation for ds DNA-**1**, **4**, and **7**-**9** (100 nM ds DNA-**1**, **4**, and **7**-**9** were irradiated at 350 nm for 2 h; ODNs without coumarin were 5'-[^{32}P]-labeled).

Although DNA ICLs were efficiently generated when **4** was flanked by all four bases, lower ICL yields were observed when **4** was flanked by dG or dC than by dA, or dT (ds DNA-**8**: 97%, **9**: 88% vs ds DNA-**4**: 98%, **7**: 100%) (Figure 4-8). Moreover, the ICL formation reaction for ds DNA-**8** or **9** with **4**/dT flanked by G:C, proceeded ~ 10 times slower than when **4**/dT was flanked by a T:A pair (ds DNA-**4** and **7**) (Table 4-4). Photo-induced cross-linking reaction for ds DNA-**4** and ds DNA-**7** was complete within 10 min at a yield of more than 95%, while 120 min was needed for ds DNA-**8** and **9**.

4.5. ICL Detection via Fluorescence Assay

4.5.1. Design Principle

Moreover, there is a promising demand for methods to on-line monitor cross-linking reactions.[1-2] Even HPLC, ^{32}P-labelled approach, and MS-associated techniques are among the most used strategies, but they do not allow real-time detection of the ICL progress. Fluorescence assay relies on sensitive fluorescence change during the process and can serve as a promising way for real-time detection of the cross-linking process, which will efficiently reduce the costs and time associated with ICL determination. A

successful fluorescence-based detection requires no substantial background fluorescence before or after the reaction, due to the fact that it is hard to determine the source of background emission. Our monomer reaction proved that formation of cycloaddition products efficiently quenches the fluorescence of coumarin producing no background emission. In addition coumarin **4** induces quantitative ICL generation which makes it possible for ICL detection using fluorescence assay. The fluorescence intensity of ds DNA-**4** before and after photoirradiation at 350 nm for 1h was determined. Almost no fluorescence emission was observed after efficient formation of cyclobutane adducts (98%) **20** (Figure 4-9).

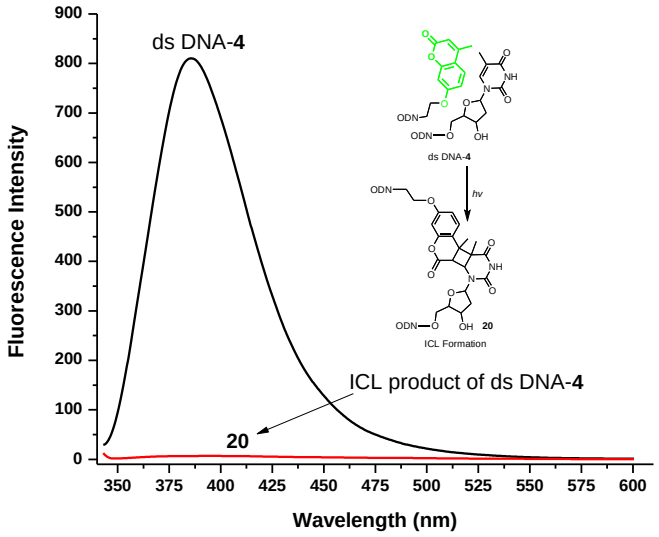

Figure 4-9. Fluorescence spectra of ds DNA-**4** before and after photoirradiation (10 μM, measured in 100 mM NaCl and 10 mM pH 7 phosphate buffer solution with λ_{ex} = 325 nm, slit width = 15 nm; λ_{em} = 390 nm, slit width = 10 nm).

In addition, the fluorescence intensity was linearly correlated with the fluorophore concentration at the μM level (Self-quenching can occur at high concentration of mM

level).[50] As the ICL product is non-fluorescent, the fluorescence intensity observed in the reaction mixture arises from the unreacted DNA duplexes. Based on these facts, a reasonable equation ICL yield = $[I_0\text{-}I/I_0\text{-}I_{60}]$*Y was proposed, where I_0 is the fluorescence intensity of the unreacted ds DNA at 0 min, I is the fluorescence intensity of ds DNA upon photoirradiation for the designed time, I_{60} is the fluorescence intensity of ds DNA after 60 min irradiation, and Y is the ICL yield after 60 min irradiation. The I_0-I stands for the reduced fluorescence intensity after desired time, and I_0-I_{60} means decreased fluorescence intensity when the ICL yield is Y after irradiation for 60 min.

4.5.2. Fluorescence Assay for Monitoring ICL Formation

The fluorescence of ds DNA-**4** reduced steadily upon ICL generation (Figure 4-10a). Almost no fluorescence emission was observed when 98% ICL was yielded with 10 μM ds DNA-**4** upon 60 min photoirradiation at 350 nm. The equation showed in Figure 4-10a was used to calculate the ICL yield at the designed time. The rate constants measured by fluorescence assay ($k_{\text{cal.-4}}$ 4.66 ± 0.27×10^{-3} s^{-1}) were within the experimental error of those measured using traditional ^{32}P-labelling method (5.04 ± 0.38×10^{-3} s^{-1}) (Table 4-4).

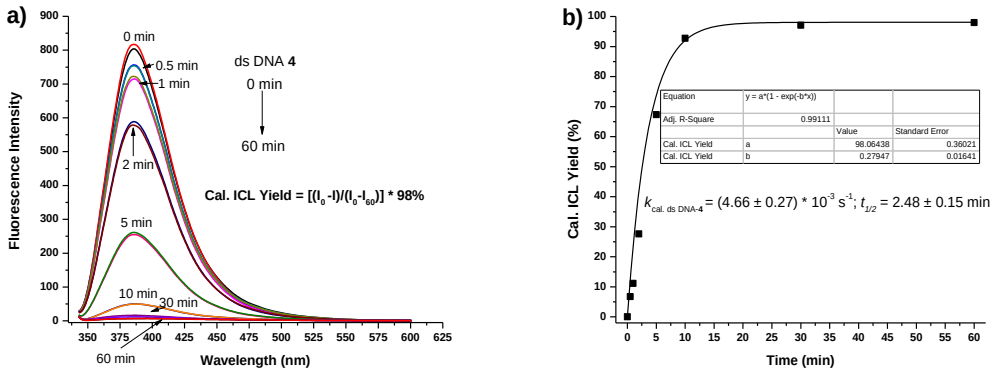

Figure 4-10. ICL formation rate of ds DNA-**4** via fluorescence assay: (a) fluorescence emission spectra of two independent samples containing 10 μM ds DNA-**4** which were irradiated at 350 nm for the desired time (λ_{ex} = 325 nm, slit width = 15 nm; λ_{em} = 385 nm, slit width = 10 nm); (b) rate of DNA cross-linking formation.

Table 4-4. Rate of ICL formation or cleavage for ds DNA-**4**, and **7**-**9**.

(ds DNA-**4** and 7-**9**: 3'-d**T**Y**T**ACGGCGGGT ● 5'-d**4**X**A**TGCCGCCCA)

Entry	X:Y	*k* (ICL Formation, 10^{-4} s^{-1})		$t_{1/2}$ (min)		k_c (Cleavage, 10^{-3} s^{-1})	$t_{1/2}$ (min)
		p.d.	*f.d.*	*p.d.*	*f.d.*		
ds DNA-**7**	A:T	42.0 ± 4.0	31.7 ± 0.4	2.7 ± 0.2	3.6 ± 0.1	4.6 ± 0.2	2.5 ± 0.1
ds DNA-**4**	T:A	50.4 ± 3.8	46.6 ± 2.7	2.3 ± 0.2	2.5 ± 0.2	4.0 ± 0.5	2.9 ± 0.4
ds DNA-**8**	G:C	5.8 ± 0.2	6.8 ± 0.2	20.0 ± 0.8	16.9 ± 0.6	17.1 ± 0.1	0.7 ± 0.0
ds DNA-**9**	C:G	4.1 ± 0.1	5.1 ± 1.2	28.1 ± 1.0	22.8 ± 5.5	12.2 ± 1.2	1.0 ± 0.2

p.d.: determined by radioactive ^{32}P-labelling method; *f.d.*: determined by fluorescence assay.

The reliability of this approach was further verified by applying this method to calculate the rate constants of cross-linking generation for ds DNA-**7**-**9** (Figures 4-10, 4-10 and 4-12). The results obtained by the fluorescence assay are consistent with those measured by ^{32}P-labelling method (Table 4-5). This is the first example allowing rapid, direct, and

efficient real-time monitoring of the DNA cross-linking progress by a non-invasive method other than traditionally-used harmful ^{32}P-labelling techniques in biochemical research. The novel method can serve as an effective way in biology for DNA cross-linking study and afford real-time detection without disrupting native cell environment.

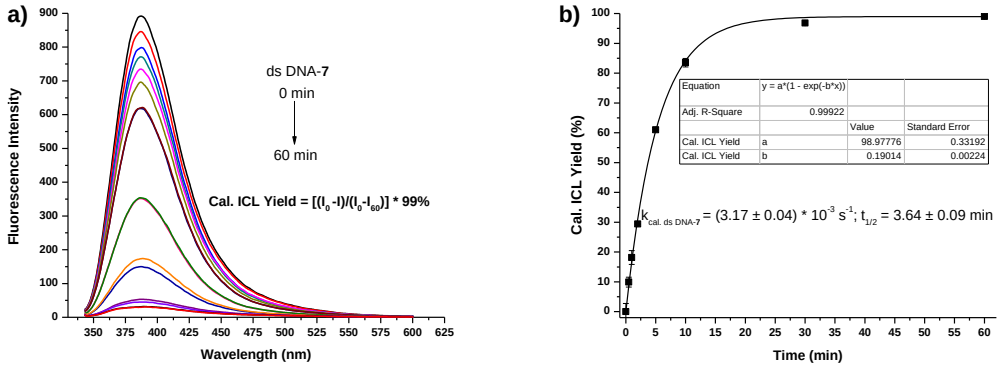

Figure 4-11. ICL formation rate of ds DNA-**7** via fluorescence assay: (a) fluorescence emission spectra of two independent samples containing 10 μM ds DNA-**7** which were irradiated at 350 nm for the desired time (measurement was carried out in a mixture of 100 mM NaCl and 10 mM pH 7 phosphate buffer solution with λ_{ex} = 325 nm, slit width = 15 nm; λ_{em} = 385 nm, slit width = 10 nm); (b) rate of DNA cross-linking formation (fluorescence intensities at 385 nm were used for calculating ICL yield).

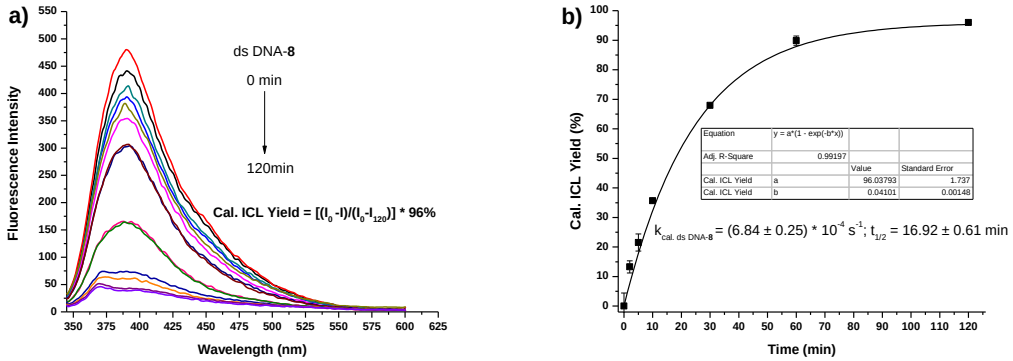

Figure 4-12. ICL formation rate of ds DNA-**8** via fluorescence assay: (a) fluorescence emission spectra of two independent samples containing 10 μM ds DNA-**8** upon irradiation at 350 nm at the desired time (measurement was carried out in a mixture of 100 mM NaCl and 10 mM pH 7 phosphate buffer solution; λ_{ex} = 325 nm, slit width = 5 nm; λ_{em} = 390 nm, slit width = 15 nm) and (b) rate of DNA cross-linking formation (fluorescence intensities at 390 nm were used for calculating ICL yield).

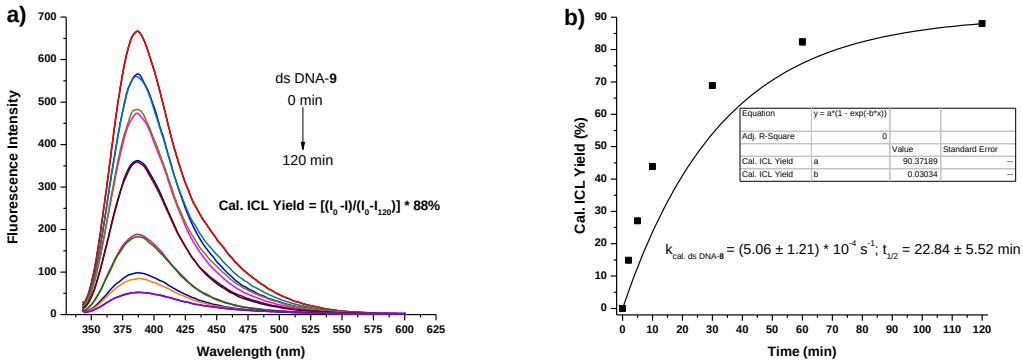

Figure 4-13. ICL formation rate of ds DNA-**9** via fluorescence assay: (a) fluorescence emission spectra of two independent samples containing 10 μM ds DNA-**9** upon irradiation at 350 nm at the desired time (measurement was carried out in a mixture of 100 mM NaCl and 10 mM pH 7 phosphate buffer solution; λ_{ex} = 325 nm, slit width = 10

nm; λ_{em} = 390 nm, slit width = 10 nm) and (b) rate of DNA cross-linking formation (fluorescence intensities at 387 nm were used for calculating ICL yield).

4.6. Photoreversible DNA Cross-linking

The coumarin-induced cross-linking in polymers can be cleaved into the original strands upon photoirridiation at a short wavelength. The dT-coumarin cyclobutane products were also decomposed into coumarin **1** and thymidine during HRMS mass measurement due to the use of high voltage electrons. Similar cleavage reaction was observed when [2+2] cycloaddition products were irradiated at 254 nm for 2 days, which was confirmed by NMR. Photocleavage reaction was also observed for DNA cross-linked products formed with ds DNA-**4** and **7-9** upon irradiation at 254 nm. Due to the electron transfer, the cleavage of the cross-linking proceeded at a very fast rate and is sequence-dependent. The reaction followed first-order kinetics and was finished within 15 min. The G:C base pair next to the cross-linking site facilitated the cleavage reaction possibly due to more efficient electron transfer. The cleavage reaction rate for the ICL products formed with ds DNA-**8** and **9** is larger than that of ds DNA-**4** and **7** (Table 4-4). The ODN strands obtained from the cleavage reaction of the ICL products efficiently form the ICL products again upon photo irradiation at 350 nm. This reversible behavior was still observed after three cycles of 350 nm/254 nm irradiation and ds DNA-**4** can still generate cross-linking at a yield of 80% (Figure 4-14a). Similarly, this process was detected via fluorescence spectra. Formation of DNA cross-linking products quenches the fluorescence but cleavage of the cross-linked product regenerate the fluorescence due to generation of the original single stranded ODNs. The results measured by fluorescence spectra were consistent with results using ^{32}P-labelling method (Figure 4-14b). Similar

study was performed with ds DNA-**7** which showed similar result. This further proved generality of this phenomenon (Figure 4-15).

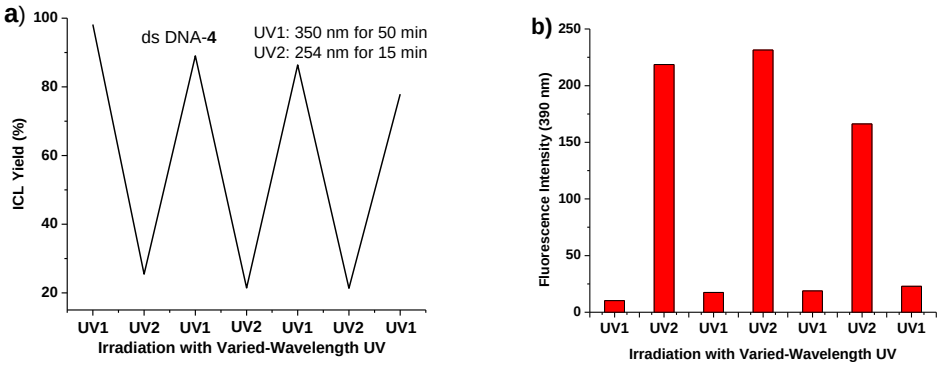

Figure 4-14. Photoreversible process for ds DNA-**4** over three cycles (photoirradiation at 350 nm for 50 min (UV1) and 254 nm for 15 min (UV2)): (a) ICL yields obtained from phosphorimage autoradiogram of denaturing PAGE analysis of 100 nM ds DNA-**4** (ODN **1a** was 5'-[^{32}P]-labeled); (b) fluorescence intensity at 390 nm of 10 μM ds DNA-**4** (λ_{ex} = 325 nm, slit width = 15 nm; λ_{em} = 390 nm, slit width = 10 nm).

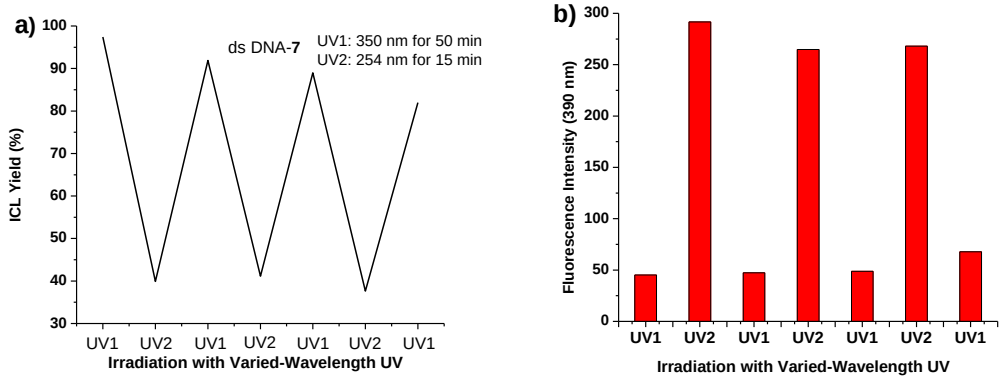

Figure 4-15. Photoreversible process for ds DNA-**7** over three cycles (photoirradiation at 350 nm for 50 min (UV1) and 254 nm for 15 min (UV2)): (a) ICL yields obtained from phosphorimage autoradiogram of denaturing PAGE analysis of 100 nM ds DNA-**7** (ODN

7a was 5'-[^{32}P]-labeled) and (b) fluorescence intensity at 390 nm of 10 μM ds DNA-**7** (λ_{ex} = 325 nm, slit width = 10 nm; λ_{em} = 390 nm, slit width = 10 nm).

4.7. Mutation Detection

The coumarin-induced ICL formation quenches the fluorescence of coumarin, which can be directly detected. Different reactivity of coumarin towards dA, dT, dG, and dC makes it useful for detecting single nucleotide polymorphisms (SNPs) via fluorescence assay. The probe ODN **11** containing the coumarin moiety **4** and the templates ODN **11a-d** were designed for this study. Templates ODN **11a-d** contain sequences of codon 248 in exon 7 of the p53 gene, which always mutates in human cancers and a T to C nucleotide transition is frequently observed.[44] ODN **11a** contains the wild-type genetic sequence with the nucleotide T at the 3'-termius, while ODN **11b** associating with cancer contains the mutated C nucleotide at the 3'-terminus. ODN **11c** and **11d** were other minor transition types in p53 gene with A and G respectively. Upon photoirradiation at 350 nm for 1 h, DNA ICL was observed for ds DNA-**11a-d** with varied efficiency (92% for ds DNA-**11a**, 81% for ds DNA-**11b**, 10% for ds DNA-**11c**, and 7% for ds DNA-**11d**) (Figure 4-16).

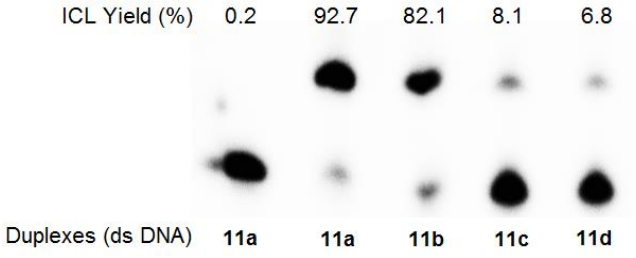

Figure 4-16. PAGE analysis of ICL formation for ds DNA-**11a-d** (ODNs without coumarin was 5'-[^{32}P]-labeled, and lane 1 is the control reaction without photo irradiation.).

Varied DNA cross-linking efficiency obtained with different DNA duplexes was also detected via fluorescence assay. The greatly decreased fluorescence was observed for DNA-**11a** and DNA-**11b** after UV irritation at 350 nm for 1 h, and much less decrease was observed for DNA-**11c** and DNA-**11d**. The difference of fluorescence intensity before and after UV irritation at 350 nm for 1 h was shown in figure 4-17. The ds DNA-**11b** showed the highest difference of the fluorescence intensity at 385 nm before and after cross-linking reaction, while less difference was observed for ds DNA-**11a** and very little difference for DNA-**11c-d**. In this way, coumarin-containing ODNs are potentially useful for detecting single nucleotide polymorphisms via fluorescence assay.

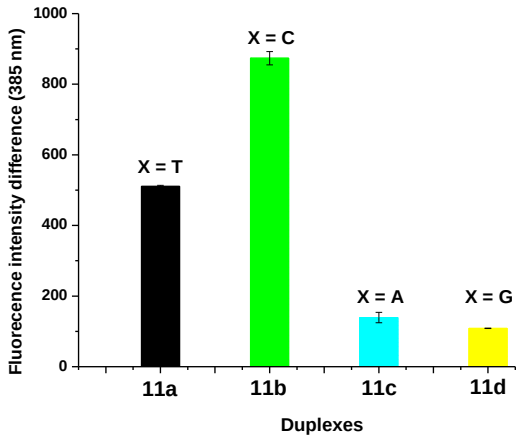

Figure 4-17. Decreased fluorescence intensity at 385 nm for ds DNA-**11a-d** (after UV irritation at 350 nm for 1 h with 10 μM ds DNA-**11a-d**; λ_{ex} = 325 nm, slit width = 6 nm; λ_{em} = 385 nm, slit width = 14 nm).

In addition, ICL formation for ds DNA-**11a** ($9.17 \pm 1.01 \times 10^{-4}$ s^{-1}) and **11b** ($7.50 \pm 0.56 \times 10^{-4}$ s^{-1}) is much faster and more efficient than that for ds DNA-**11c** ($8.3 \pm 0.9 \times 10^{-5}$ s^{-1}) and **11d** ($9.7 \pm 0.8 \times 10^{-5}$ s^{-1}) (Table 4-6). The ICL products formed from ds DNA-**11a** and **11b** can be quickly reversed into the single strands with a rate constant of 6.6 ±

0.3×10^{-3} s^{-1} and $4.35 \pm 0.65\times10^{-2}$ s^{-1} respectively upon photoirridiation at 254 nm, while the ICL products generated from ds DNA-**11c** and **11d** were not cleaved into the single strands upon photoirradiation for 1h.

Table 4-5. Rate of ICL formation or cleavage for ds DNA-**11a-d**.

ODN **11a-d**: 3'-dXAAGTACGGCGGGTACG

ODN **11**: 5'-d**4**TTCATGCCGCC

Entry	X	k (ICL, 10^{-5} s^{-1})	$t_{1/2}$ (min)	k_c(Cleavage, 10^{-3} s^{-1})	$t_{1/2}$ (s)
ds DNA-**11a**	T	91.7 ± 10.1	12.6 ± 1.6	6.6 ± 0.3	105.0 ± 4.2
ds DNA-**11b**	C	75.0 ± 5.6	15.5 ± 1.2	43.5 ± 6.5	16.3 ± 2.4
ds DNA-**11c**	A	8.3 ± 0.9	141.2 ± 15.7	*n.d.*	*n.d.*
ds DNA-**11d**	G	9.7 ± 0.8	120.4 ± 10.3	*n.d.*	*n.d.*

n.d. : not determined.

4.8. The Effect of Incorporation Site on ICL Formation

DNA duplexes containing coumarins at the 5'-terminal site showed perfect photoreversibility. In order to know the generality of this property and demonstrate the versatility of coumarin analogues in biochemical applications, we investigated the photoproperties of the coumarins incorporated at the internal positions of ODNs. To address this issue, the diol-based coumarin **7** was designed and prepared. After introduction of DMTr group in **16**, the phorsphoramidite **13** was synthesized via standard method. The ODN-**10b** and **13b** containing compound **7** at the internal sites were prepared in a similar way as the other modified ODNs by using **13**. Compound **7** at the internal site (ds DNA-**10**) induced almost quantitative ICL generation (97%) upon 350

nm irradiation (Figure 4-18, lane 2). In addition, the ICL products generated with ds DNA-**10** were split into the original single-stranded ODNs after photoirradiation at 254 nm with good efficiency (cleavage percentage 84%) (Figure 4-18, lane 3). Kinetic study showed that both cross-link formation and cleavage were very effective and fast, and were complete within 15 min (Table 4-6).

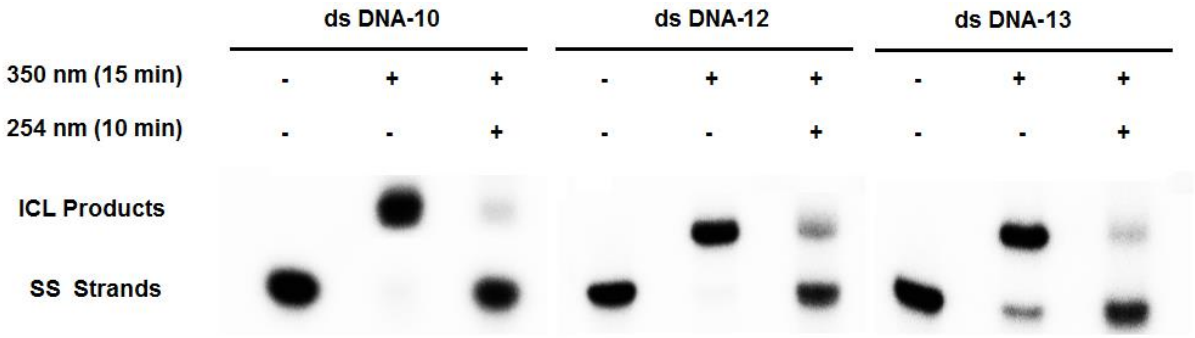

Figure 4-18. PAGE analysis of ICL formation and cleavage of ds DNA-**10**, **12**, and **13** (100 nM ds DNA were irradiated at 350 nm or 254 nm; ODNs without coumarin were 5'-[^{32}P]-labelled.).

After having established the chemistry and generality of coumarin-induced photo-reversible DNA cross-linking, we studied the photoactivity of coumarins toward a longer DNA template. This provided a more realistic illustration of how coumarin analogues might be applied in cellular DNA. The ODN-**7b** with terminal coumarin **4** and a 50-mer matched template ODN-**12a** were employed. Almost quantitative DNA cross-link was formed for the terminal coumarin **4** in ds DNA-**12** (98%, Figure 4-18, lane 5) upon photoirradiation at 350 nm, and a reasonable ICL yield (84%, Figure 4-18, lane 8) was achieved for ds DNA-**13** with the internal coumarin **7**. Lower ICL yield for compound **7** may result from less flexibility in ds DNA-**13** than **4** in ds DNA-**12.** The formed ICL products for ds DNA-**12** and **13** can be efficiently reverted to the original single-stranded

ODNs upon 254 nm irradiation. Moreover, both ICL formation and cleavage reactions for ds DNA-**12** and **13** are fast and efficient. The steric hindrance arising from the long ODN template ODN-**12a** promoted the cleavage reaction rate for ds DNA-**12** and **13** than when a shorter DNA template was used, such as ds DNA-**10** (Table 4-6). The generality and versatility of coumarin-induced cross-linking proved its potential as a powerful and versatile tool in biochemical research.

Table 4-6. Rate of ICL formation or cleavage for ds DNA-**10**, **12**, and **13**.

Entry	k (ICL Formation, 10^{-3} s^{-1})	$t_{1/2}$ (min)	k_c (Cleavage, 10^{-2} s^{-1})	$t_{1/2}$ (min)
ds DNA-**10**	3.99 ± 0.32	2.91 ± 0.23	0.57 ± 0.04	2.02 ± 0.13
ds DNA-**12**	6.27 ± 0.62	1.86 ± 0.18	1.67 ± 0.19	0.70 ± 0.08
ds DNA-**13**	1.55 ± 0.14	7.51 ± 0.66	1.42 ± 0.03	0.82 ± 0.02

4.9. Experimental Section

LC-MS analysis of photoinduced reaction between coumarin 1 and canonical nucleosides. The reaction mixtures containing 30 nmol deoxyribonucleosides (dA: 7.5 mg, dT: 7.2 mg, dG: 8.0 mg, or dC: 6.8 mg) and coumarin **1** (5.7 mg, 30 nmol) in methanol (1- 6 mL, depending on solubility) were placed in four vials, respectively. After UV irradiation at 350 nm for two days, the mixtures were diluted to the desired concentration for LC-MS analysis.

Preparation of DNA cross-linked products for MALDI-TOF-MS analysis. Interstrand cross-linking reactions were performed using 10 μM coumarin-containing oligonucleotides, which were annealed with 1.0 equiv. of the complementary strands by

heating to 80 ^{o}C for 3 min in a buffer containing 10 mM pH 7 potassium phosphate buffer and 100 mM NaCl, followed by slowly cooling to room temperature overnight. The DNA duplexes were irradiated with the UV light at 350 nm for the desired time to make sure that the reactions were complete. Then 2 M NaCl solution (200 μL) and cold ethanol (1.2 mL) were added to the reaction mixture which was incubated at -80 °C for 30 mins. ODNs were precipitated by centrifugation at 15000 g for 6 min at room temperature. The crude DNA was further purified via C18 column eluting with H_2O (3 × 1.0 mL) followed by MeOH:H_2O (3:2, 1.0 mL) to remove salts. The afforded ODNs were dried and characterized by MALDI-TOF-MS at the University of California-Riverside Mass Spectrometry Lab.

Determination of DNA duplexes' thermal stability. All measurements were carried out in 10 mM potassium phosphate buffer (pH 7), 100 μM ethylenediaminetetraacetic acid (EDTA), and 100 mM NaCl, with 4 μM + 4 μM single strand concentration. Samples were heated at 1 °C min^{-1} from 20 °C to 80 °C and the absorbance of DNA at 260 nm was measured at 1.0 °C steps. At least two independent samples have been tested to get the melting temperatures of DNA duplexes.

PAGE analysis of interstrand cross-link formation and kinetic study using ^{32}P-labelling method. ODNs (0.1 μM) without coumarin were 5'-^{32}P-labeled and hybridized with 1.5 equiv. of the complementary strands in 100 mM NaCl and 10 mM potassium phosphate (pH 7). The DNA duplexes were irradiated at 350 nm to form ICLs (a control reaction was carried out without photoirradiation). Aliquots were taken at the prescribed time and immediately quenched with the equal volume of 95% formamide loading buffer,

and stored at -20 °C until subjecting to 20% denaturing PAGE analysis. For kinetics study, three independent samples were used with the same procedures mentioned above.

Kinetic study of DNA interstrand cross-link formation using fluorescence assay. Coumarin-modified ODNs (10 μM) were hybridized with 1.0 equiv. of the complementary strands in 100 mM NaCl and 10 mM potassium phosphate (pH 7). The DNA duplexes were irradiated at 350 nm and the fluorescence was measured at the prescribed time. The equations used for calculation of the ICL yields were shown in each figure. For kinetics study, two independent samples were used.

PAGE analysis of photo-induced (254 nm) cleavage reactions of DNA ICL products and kinetic study. The reactions were carried out with photoirradiation at 254 nm using two or three independent samples. Aliquots were taken at the prescribed time and immediately quenched with the equal volume of 95% formamide loading buffer, and stored at -20 °C until subjecting to 20% denaturing PAGE analysis.

7-Hydroxy-4-methyl-2H-chromen-2-*O*-(2-cyanoethyl-*N*, *N*-diisopropyl)-phosphoramidite (**8**). To a solution of 7-hydroxy-4-methyl-2H-chromen-2-one (**3**, 88 mg, 0.5 mmol) in dichloromethane (10 mL), *N*, *N*-diisopropylethylamine (DIPEA) (156 μL, 0.9 mmol), and 2-cyanoethyl-*N*, *N*-diisopropylchlorophosphoramidite (167 μL, 0.75 mmol) were added under an atmosphere of argon. The reaction mixture was stirred at room temperature for 3 h and diluted with dichloromethane (50 mL). The organic layer was washed with $NaHCO_3$ (20 mL) and saturated aqueous NaCl (20 mL), and dried over anhydrous sodium sulfate. The solvent was removed under reduced pressure. Upon purification by column chromatography (EtOAc:hexane:Et_3N = 59:40:1), the product was isolated as a white solid (**8**, 170 mg, 90%).^{31}P NMR (300 MHz, $CDCl_3$-*d*): δ 147.48. ^{1}H

NMR (300 MHz, $CDCl_3$-*d*): δ 7.50-7.53 (m, 1H), 7.00-7.02 (dd, *J* = 1.5 Hz, 2H), 6.18 (s, 1H), 3.93-4.01 (m, 2H), 3.71-3.79 (m, 2H), 2.69-2.73 (t, *J* = 6.3 Hz, 3H), 1.18-1.27 (dd, *J* = 6.6 Hz, 1H). ^{13}C NMR (300 MHz, $CDCl_3$-*d*): δ 161.1, 157.7, 157.6, 154.8, 152.4, 125.5, 117.3, 116.5, 116.4, 115.0, 112.7, 107.5, 107.3, 59.3, 59.0, 44.0, 43.8, 24.7, 24.6, 24.5, 24.4, 20.4, 20.3, 18.7. HRMS-ESI (+) (*m/z*): $[M+H]^+$ calcd. for $C_{19}H_{26}N_2O_4P$, 377.1625; found: 377.1633.

4-Methyl-7-methoxy-2H-chromen-2-one (**1**). Iodomethane (1.3 mL, 20 mmol) was added to a suspension of 7-hydroxy-4-methyl-2H-chromen-2-one (**3**, 704 mg, 4 mmol) and K_2CO_3 (600 mg, 3.34 mmol) in acetone (50 mL). The reaction mixture was stirred at 50°C overnight. After cooling to the room temperature, the solvent was removed under reduced pressure. The residue was diluted with ethyl acetate (50 mL), washed with 1 M HCl (30 mL), H_2O (30 mL) and brine (20 mL), and then dried over anhydrous sodium sulfate. The solvent was removed under vacuum providing the product **1** as a white solid (699 mg, 92%). ^{1}H NMR (300 MHz, $CDCl_3$-*d*): δ 7.60-7.65 (m, 1H), 7.01-7.02 (t, *J* = 1.8 Hz, 1H), 6.93-6.98 (m, 2H), 6.25,6.28 (t, *J* = 1.8 Hz, 1H), 3.86 (s, 3H), 2.37 (s, 3H).

4-(Hydroxymethyl)-7-methoxy-2H-chromen-2-one (**2**). To a suspension of 7-hydroxy-4-(hydroxylmethyl)-2H-chromen-2-one (**14**, 384 mg, 2 mmol) and K_2CO_3 (300 mg, 2.17 mmol) in acetone (30 mL), iodomethane (0.65 mL, 10 mmol) was added. The reaction mixture was stirred at 50°C overnight. After cooling to the room temperature, the solvent was removed under reduced pressure. The residue was diluted with ethyl acetate (50 mL), washed with 1 M HCl (30 mL), and brine (20 mL), and then dried over anhydrous sodium sulfate. The solvent was removed under vacuum providing **2** as a white solid (394 mg, 96%). ^{1}H NMR (300 MHz, $CDCl_3$-*d*): δ 7.61-7.64 (m, 1H), 7.01-7.02 (t, *J* = 1.8 Hz,

1H), 6.92-6.97 (m, 1H), 6.30,6.31 (t, *J* = 1.5 Hz, 1H), 5.60-5.64 (m, 1H), 4.73-4.75 (t, *J* = 1.5 Hz, 2H), 3.85, 3.86 (d, *J* = 1.8 Hz, 3H).

4-(Hydroxymethyl)-7-methoxy-2H-chromen-2-*O*-(2-cyanoethyl-*N*, *N*-diisopropyl)-phosphor-amidite (**9**). Compound **2** (103 mg, 0.5 mmol) was dissolved in dichloromethane (8 mL) under an atmosphere of argon. *N, N*-diisopropylethylamine (DIPEA) (156 µL, 0.9 mmol) was then added dropwise, followed by 2-cyanoethyl-*N, N*-diisopropylchlorophosphoramidite (167 µL, 0.75 mmol). The reaction mixture was stirred at room temperature for 3 h, then diluted by dichloromethane (30 mL), washed with $NaHCO_3$ (20 mL), and brine (20 mL), and dried over anhydrous sodium sulfate. The solvent was removed under reduced pressure. Upon purification by column chromatography (EtOAc:hexane:Et_3N = 40:59:1), the product **9** was isolated as a white solid (148 mg, 73%).^{31}P NMR (300 MHz, $CDCl_3$-*d*): δ 149.96. ^{1}H NMR (300 MHz, $CDCl_3$-*d*): δ 7.44-7.47 (m, 1H), 6.84-6.88 (dd, *J* = 3.0 Hz, 2H), 6.44-6.45 (d, *J* = 1.5 Hz, 1H), 4.84-4.90 (m, 2H), 3.85-3.95 (m, 5H), 3.68-3.71 (dd, *J* = 3.6 Hz, 2H), 2.66-2.71 (t, *J* = 6.3 Hz, 2H), 1.22-1.25 (dd, *J* = 2.4 Hz, 12H). ^{13}C NMR (300 MHz, $CDCl_3$-*d*): δ 162.6, 161.5, 155.4, 152.5, 152.4, 124.5, 117.6, 112.4, 110.9, 109.5, 101.1, 61.7, 61.5, 58.5, 58.2, 55.8, 43.5, 43.3, 24.8, 24.7, 24.6, 20.5, 20.4. HRMS-ESI (+) (*m/z*): $[M+H]^+$ calcd. for $C_{20}H_{28}N_2O_5P$, 407.1730; found: 407.1745.

7-(2-Hydroxyethoxy)-4-methyl-2H-chromen-2-one (**4**). To a suspension of 7-hydroxy-4-methyl-2H-chromen-2-one (**3**, 704 mg, 4 mmol), KI (1.65 g, 10 mmol) and K_2CO_3 (900 mg, 6.51 mmol) in acetone (60 mL), 2-bromoethanol (1.42 mL, 20 mmol) was added. The reaction mixture was stirred at 50°C for 48 h. After cooling to the room temperature, the solvents were removed under reduced pressure. The residue was diluted with ethyl

acetate (80 mL), washed with 1 M HCl (40 mL), and brine (20 mL), and then dried over anhydrous Na_2SO_4. The solvent was removed under reduced pressure. The crude product was purified by column chromatography (EtOAc) yielding **4** as a white solid (642 mg, 73%). ^{1}H NMR (300 MHz, $CDCl_3$-*d*): δ 7.67, 7.70 (d, *J* = 9.3 Hz, 1H), 6.96, 6.99 (d, *J* = 6.6 Hz, 2H), 6.21 (s, 1H), 4.90-4.93 (t, *J* = 5.4 Hz, 1H), 4.09-4.12 (t, *J* = 5.4 Hz, 2H), 3.72-3.77 (dd, *J* = 5.1 Hz, 2H), 2.40 (s, 3H).

7-(3-Hydroxypropoxy)-4-methyl-2H-chromen-2-one (**5**). To a suspension of **3** (704 mg, 4 mmol), KI (1.65 g, 10 mmol) and K_2CO_3 (900 mg, 6.51 mmol) in acetone (60 mL), 3-bromo-1-propanol (0.54 mL, 6 mmol) was added. The reaction mixture was stirred at 50°C for 36 h. After cooling to the room temperature, the solvent was removed under reduced pressure. The residue was diluted with ethyl acetate (80 mL), washed with 1 M HCl (40 mL), and brine (20 mL), and then dried over anhydrous Na_2SO_4. The solvent was removed under reduced pressure to afford **5** as a white solid (760 mg, 81%). ^{1}H NMR (300 MHz, $CDCl_3$-*d*): δ 7.49, 7.52 (d, *J* = 8.7 Hz, 1H), 6.83-6.90 (m, 2H), 6.14 (s, 1H), 4.18-4.22 (t, *J* = 6.0 Hz, 2H), 3.87-3.92 (dd, *J* = 5.4 Hz, 2H), 2.41 (s, 3H), 2.06-2.14 (m, 2H).

7-(2-Hydroxyethoxy)-4-methyl-2H-chromen-2-*O*-(2-cyanoethyl-*N*, *N*-diisopropyl)-phosphoramidite (**10**). To a solution of **4** (110 mg, 0.5 mmol) in dichloromethane (10 mL), *N*, *N*-diisopropylethylamine (DIPEA) (156 μL, 0.9 mmol) and 2-cyanoethyl-*N*, *N*-diisopropylchlorophosphoramidite (167 μL, 0.75 mmol) were added under an atmosphere of argon. The reaction mixture was stirred at room temperature for 3 h and diluted with EtOAc (50 mL). The organic layer was washed with $NaHCO_3$ (20 mL) and saturated aqueous NaCl (20 mL), and dried over anhydrous sodium sulfate. The solvent was

removed under reduced pressure. The crude product was purified by column chromatography (EtOAc:hexane:Et_3N = 49:50:1) yielding **10** as a white solid (162 mg, 77%). ^{31}P ($CDCl_3$-*d*, 300 MHz): δ 149.28. ^{1}H NMR ($CDCl_3$-*d*, 300 MHz): δ 7.41, 7.44 (d, *J* = 8.7 Hz, 1H), 6.75-6.82 (t, *J* = 8.7 Hz, 2H), 6.06 (s, 1H), 4.12-4.15 (t, *J* = 4.5 Hz, 2H), 3.88-4.00 (m, 2H), 3.75-3.80 (m, 2H), 3.52-3.60 (m, 2H), 2.55-2.59 (t, *J* = 6.3 Hz, 2H), 2.32 (s, 3H), 1.11, 1.13 (d, *J* = 6.6 Hz, 12H). ^{13}C NMR (300 MHz, $CDCl_3$-*d*): δ 161.8, 161.2, 155.2, 152.6, 125.6, 117.6, 113.7, 112.6, 112.0, 101.6, 68.6, 68.5, 61.9, 61.6, 58.6, 43.2, 43.1, 24.7, 24.6, 20.4, 20.3, 18.7. HRMS-ESI (+) (*m/z*): $[M+H]^+$ calcd. for $C_{21}H_{30}N_2O_5P$, 421.1887; found: 421.1899.

7-(3-Hydroxypropoxy)-4-methyl-2H-chromen-2-*O*-(2-cyanoethyl-*N*, *N*-diisopropyl)-phosphoramidite (**11**). To a solution of **5** (117 mg, 0.5 mmol) in dichloromethane (10 mL), *N*, *N*-diisopropylethylamine (DIPEA) (156 μL, 0.9 mmol) and 2-cyanoethyl-*N*, *N*-diisopropylchlorophosphoramidite (167 μL, 0.75 mmol) were added under an atmosphere of argon. The reaction mixture was stirred at room temperature for 3 h and diluted with dichloromethane (30 mL). The organic layer was washed with $NaHCO_3$ (20 mL) and saturated aqueous NaCl (20 mL), and dried over anhydrous sodium sulfate. The solvent was removed under reduced pressure. The residue was purified by column chromatography (EtOAc:hexane:Et_3N = 49:50:1) providing **11** as a white solid (120 mg, 55%). ^{31}P ($CDCl_3$-*d*, 300 MHz): δ 147.89. ^{1}H NMR ($CDCl_3$-*d*, 300 MHz): δ 7.40, 7.43 (d, *J* = 8.7 Hz, 1H), 6.75-6.81 (m, 2H), 6.06 (s, 1H), 4.06-4.10 (t, *J* = 6.0 Hz, 2H), 3.72-3.80 (m, 2H), 3.49-3.57 (m, 2H), 2.33 (s, 3H), 2.03-2.07 (t, *J* = 6.0 Hz, 2H), 1.10, 1.11 (t, *J* = 2.1 Hz, 12H). ^{13}C NMR (300 MHz, $CDCl_3$-*d*): δ 162.1, 161.3, 155.3, 152.5, 125.5, 117.6, 113.6, 112.6, 111.9, 101.5, 65.1, 60.0, 59.8, 58.4, 58.2, 43.2, 43.0, 30.8, 30.7, 24.7, 24.6,

20.4, 20.3, 18.7. HRMS-ESI (+) (*m/z*): $[M+H]^+$ calcd. for $C_{22}H_{32}N_2O_5P$, 435.2043; found: 435.2055.

7-(1-(3-Hydroxypropyl)-1H-1,2,3-triazol-5-yl)-4-methyl-2H-chromen-2-one (**6**). To a suspension of 7-ethynyl-4-methyl-2H-chromen-2-one (**15**, 184 mg, 1 mmol), 3-azidopropan-1-ol (152 mg, 1.5 mmol) and Copper(II) sulfate (pentahydrate) (50 mg, 0.2 mmol) in a mixture of water (10 mL) and tert-butyl alcohol (10 mL), sodium ascorbate (119 mg, 0.6 mmol) was added and stirred at room temperature overnight. After addition of water (20 mL) to mixture, extract with ethyl acetate (20 mL × 3). The organic phases were collected, washed with water (20 mL × 2) and brine (20 mL), and then dried over anhydrous Na_2SO_4. The solvent was removed under reduced pressure and the white residue was purified by column chromatography (EtOAc) to afford **6** as a white solid (186 mg, 65%). ^{1}H NMR (300 MHz, $CDCl_3$-*d*): δ 8.79 (s, 1H), 7.81-7.86 (m, 3H), 6.39 (s, 1H), 4.70-4.73 (t, *J* = 5.1 Hz, 1H), 4.47-4.52 (t, *J* = 6.9 Hz, 2H), 3.43-3.49 (dd, *J* = 6.0 Hz, 2H), 2.45 (s, 3H), 2.00-2.08 (m, 2H). ^{13}C NMR (300 MHz, $CDCl_3$-*d*): δ 160.2, 154.0, 153.5, 145.3, 134.8, 126.6, 123.4, 121.4, 119.4, 114.5, 57.9, 47.5, 33.2, 18.5. HRMS-ESI (+) (*m/z*): $[M+H]^+$ calcd. for $C_{15}H_{16}N_3O_3$, 286.1192; found: 286.1186.

2-Cyanoethyl (3-(4-(4-methyl-2-oxo-2H-chromen-7-yl)-1H-1,2,3-triazol-1-yl)propyl) diisopropyl- phosphoramidite (**12**). To a suspension of **6** (143 mg, 0.5 mmol) in dichloromethane (10 mL), *N*, *N*-diisopropylethylamine (DIPEA) (156 μL, 0.9 mmol) and 2-cyanoethyl-*N*, *N*-diisopropylchlorophosphoramidite (167 μL, 0.75 mmol) were added under an atmosphere of argon. The reaction mixture was protected from light by aluminum foil, stirred at room temperature for 3 h, and diluted with dichloromethane (30 mL). The organic layer was washed with 1M $NaHCO_3$ (20 mL) and saturated aqueous

NaCl (20 mL), and dried over anhydrous sodium sulfate in the dark room. The solvent was removed under reduced pressure. The crude product was purified by column chromatography (EtOAc:hexane:Et_3N = 49:50:1) in the dark room yielding **12** as a white solid (73 mg, 30%). ^{31}P ($CDCl_3$-*d*, 300 MHz): δ 148.06. ^1H NMR ($CDCl_3$-*d*, 300 MHz): δ 7.92 (s, 1H), 7.76-7.78 (d, *J* = 8.1 Hz, 1H), 7.63 (s, 1H), 7.56-7.58 (d, *J* = 8.4 Hz, 1H), 6.19 (s, 1H), 4.49-4.54 (t, *J* = 6.9 Hz, 2H), 3.48-3.86 (m, 6H), 2.57-2.61 (t, *J* = 6.0 Hz, 2H), 2.38 (s, 3H), 2.20-2.24 (t, *J* = 6.0 Hz, 2H), 1.09-1.13 (dd, *J* = 4.2 Hz, 12H). ^{13}C NMR (300 MHz, $CDCl_3$-*d*): δ 159.8, 152.9, 151.2, 144.9, 133.4, 124.2, 120.5, 118.5, 116.8, 113.8, 112.5, 59.0, 58.8, 57.4, 57.1, 46.3, 42.2, 42.0, 30.6, 30.5, 23.7, 23.6, 19.6, 19.5, 17.6. HRMS-ESI (+) (*m/z*): $[M+H]^+$ calcd. for $C_{24}H_{33}N_5O_4P$, 486.2278; found: 486.2285.

7-(2,3-Dihydroxypropoxy)-4-methyl-2H-chromen-2-one (**7**). To a suspension of 7-hydroxy-4-methyl-2H-chromen-2-one (**3**, 1.76 g, 10 mmol) and KOH (1.12 g, 20 mmol) in ethanol (50 mL), epichlorohydrin (8.0 mL, 102 mmol) and KI (166 mg, 1 mmol) was added. The reaction mixture was stirred at 70°C for overnight. After cooling to the room temperature, the solvent was removed under vacuum. The residue was submitted to flash chromatography (CH_2Cl_2:MeOH = 98:2, the product has similar R_f value with starting material and is hard to be separated using EtOAc and hexane) to afford 4-methyl-7-(oxiran-2-ylmethoxy)-2H-chromen-2-one as a white solid (1.83 g, 79%). ^1H NMR (300 MHz, $CDCl_3$-*d*): δ 7.42-7.45 (d, *J* = 9.0 Hz, 1H), 6.81-6.85 (dd, *J* = 2.4 Hz, 1H), 6.76 (d, *J* = 2.4 Hz, 1H), 6.08 (s, 1H), 4.25-4.29 (d, *J* = 2.7 Hz, 1H), 3.88-3.93 (q, *J* = 6.0 Hz, 1H), 3.30-3.35 (m, 1H), 2.86-2.89 (t, *J* = 4.5 Hz, 1H), 2.71-2.74 (q, *J* = 2.7 Hz, 1H), 2.33 (s, 3H). The solution of 4-methyl-7-(oxiran-2-ylmethoxy)-2H-chromen-2-one (1.16 g, 5

mmol) in 6% perchloric acid (40 ml) was stirred at room temperature for overnight. Then, the pH of the solution was adjusted to 8 via addition of Na_2CO_3. After stirring for 2 h, ethyl acetate (80 mL) was added and stirred for 20 h. The organic layer was washed with water (20 mL) and saturated aqueous NaCl (20 mL), and dried over anhydrous sodium sulfate. The solvent was removed under reduced pressure to afford 7-(2,3-Dihydroxypropoxy)-4-methyl-2H-chromen-2-one **7** (1.05 g, 84%) as a viscous liquid which was solidified into a white solid upon standing. ^{1}H NMR (DMSO-d_6): δ 7.66-7.68 (d, J = 8.4 Hz, 1H), 6.95-6.99 (m, 2H), 6.20 (s, 1H), 5.04-5.06 (d, J = 5.1 Hz, 1H), 4.72-4.76 (t, J = 5.4 Hz, 1H), 4.10-4.14 (dd, J = 3.9 Hz, 1H), 3.96-4.01 (m, 1H), 3.80-3.85 (m, 1H), 3.44-3.48 (t, J = 5.4 Hz, 2H), 3.04 (s, 3H).

7-(3-(Bis(4-methoxyphenyl)(phenyl)methoxy)-2-hydroxypropoxy)-4-methyl-2H-chromen-2-one (**16**). To the solution of compound **7** (0.50 g, 2.0 mmol) in pyridine (8 mL), 4, 4'-dimethoxytriphenylmethyl chloride (0.81 g, 2.4 mmol) was added. The mixture was stirred at room temperature for overnight. The reaction mixture was quenched with MeOH (5 mL) and concentrated under reduced pressure. Upon purification by column chromatography (EtOAc:Et_3N = 99:1), 7-(3-(bis(4-methoxyphenyl)(phenyl)methoxy)-2-hydroxypropoxy)-4-methyl-2H-chromen-2-one **16** was isolated as a white foam (0.76 g, 69%). ^{1}H NMR (DMSO-d_6): δ 7.67-7.70 (d, J = 8.7 Hz, 1H), 7.39-7.41 (d, J = 7.5 Hz, 2H), 7.19-7.32 (m, 7H), 6.85-6.96 (m, 6H), 6.22 (s, 1H), 5.24-5.26 (d, J = 5.4 Hz, 1H), 4.00-4.19 (m, 3H), 3.73 (s, 6H), 3.08-3.10 (d, J = 5.7 Hz, 2H), 2.4 (s, 3H). ^{13}C NMR (300 MHz, $CDCl_3$-d): δ 162.2, 160.7, 158.5, 155.2, 153.9, 145.4, 136.2, 130.2, 128.2, 127.1, 126.9, 113.6, 113.0, 111.6, 101.7, 85.8, 70.6, 68.4,

64.6, 55.5, 18.6. HRMS-ESI (+) (*m/z*): $[M+H]^+$ calcd. for $C_{34}H_{33}O_7$, 553.2226; found: 553.2216.

1-(Bis(4-methoxyphenyl)(phenyl)methoxy)-3-((4-methyl-2-oxo-2H-chromen-7-yl)oxy)-propan-2-yl (2-cyanoethyl) diisopropylphosphoramidite (**13**). To a solution of compound **16** (226 mg, 0.50 mmol) in anhydrous CH_2Cl_2 (5 mL) under argon atmosphere, *N*, *N*-diisopropylethylamine (DIPEA) (156 µL, 0.9 mmol) was then added dropwise, followed by 2-cyanoethyl-*N*, *N*-diisopropylchlorophosphoramidite (167 µL, 0.75 mmol). The reaction mixture was stirred at room temperature for 3 h, then diluted by dichloromethane (30 mL), washed with $NaHCO_3$ (20 mL), and brine (20 mL), and dried over anhydrous sodium sulfate. The solvent was removed under reduced pressure. Upon purification by column chromatography (EtOAc:hexane:Et_3N = 40:59:1), the product **13** was isolated as a white foam (266 mg, 71%). ^{31}P ($CDCl_3$-*d*, 300 MHz): δ 149.99, 149.67. ^1H NMR (DMSO-d_6): δ 7.12-7.43 (m, 10H), 6.71-6.80 (m, 6H), 6.06 (s, 1H), 4.02-4.26 (m, 3H), 3.42-3.75 3.16-3.31 (m, 2H), 2.49-2.60 (m, 1H), 2.37-2.41 (m, 1H), 2.32 (s, 3H), 1.07-1.13 (m, 9H), 0.96-0.98 (d, J = 6.6 Hz, 3H). ^{13}C NMR (300 MHz, $CDCl_3$-*d*): δ 160.8, 160.2, 157.5, 154.2, 151.5, 143.6, 134.9, 129.1, 127.2, 126.8, 125.8, 124.6, 116.6, 112.7, 112.1, 111.5, 111.4, 111.0, 100.7, 85.2, 70.9, 70.7, 70.5, 70.3, 68.3, 68.1, 62.4, 57.5, 57.2, 54.2, 42.3, 42.1, 29.7, 23.4, 19.3, 19.1, 17.7. HRMS-ESI (+) (*m/z*): $[M+H]^+$ calcd. for $C_{43}H_{50}N_2O_8P$, 753.3305; found: 753.3295.

Synthesis of coumarin-dT and coumarin-coumarin dimmers. A solution of 4-methyl-7-methoxy-2H-chromen-2-one (**1**, 38 mg, 0.2 mmol) and dT (146 mg, 0.6 mmol) in methanol (200 mL) was irritated with UV light at 350 nm for 3 days at room temperature.

After removing solvent under reduced pressure, products were isolated upon purification by column chromatography.

7-(4-Hydroxy-5-(hydroxymethyl)tetrahydrofuran-2-yl)-3-methoxy-10a,10b-dimethyl-6b,7,10a,10b-tetrahydro-6H-chromeno[4',3':3,4]cyclobuta[1,2-d]pyrimidine-6,8,10(6aH,9H)-trione (**17**). (CH_2Cl_2:MeOH = 95:5, a yellowish oil, 13 mg, 15%). ^{1}H NMR (300 MHz, DMSO-d_6): δ 7.18, 7.21 (d, J = 8.7 Hz, 1H), 6.70-6.73 (m, 1H), 6.51-6.53 (t, J = 2.4 Hz, 1H), 5.88 (m, 1H), 4.78, 4.82 (d, J = 9.3 Hz, 1H), 4.19-4.21 (t, J = 2.4 Hz, 1H), 4.04 (s, 3H), 3.64 (s, 2H), 3.28, 3.31 (d, J = 9.3 Hz, 1H), 1.99-2.06 (m, 2H), 1.56 (s, 3H), 1.27 (s, 3H). ^{13}C NMR (300 MHz, DMSO-d_6): δ 172.4, 164.7, 159.8, 151.5, 151.3, 128.7, 116.5, 111.2, 101.7, 87.3, 85.7, 83.3, 70.8, 62.0, 55.8, 52.3, 52.4, 46.9, 22.8, 22.6, 18.3, 17.9. HRMS-ESI (+) (*m/z*): $[M+H]^+$ calcd. for $C_{21}H_{25}N_2O_8$, 433.1605; found: 433.1612.

10-(4-Hydroxy-5-(hydroxymethyl)tetrahydrofuran-2-yl)-3-methoxy-6b,10b-dimethyl-8,10,10a,10b-tetrahydro-6H-chromeno[3',4':3,4]cyclobuta[1,2-d]pyrimidine-6,7,9(6aH,6bH)-trione (**18**). (CH_2Cl_2:MeOH = 95:5, a yellowish oil, 8 mg, 9.2%). ^{1}H NMR (300 MHz, DMSO-d_6): δ 10.65 (s, 1H), 7.20, 7.23 (d, J = 8.7 Hz, 1H), 6.79-6.82 (m, 1H), 6.65, 6.66 (d, J = 2.4 Hz, 1H), 5.97-6.02 (m, 1H), 5.06, 5.08 (d, J = 3.6 Hz, 1H), 4.50 (s, 1H), 4.03-4.10 (m, 3H), 3.78 (s, 3H), 3.16-3.18 (m, 3H), 1.77 (m, 2H), 1.36 (s, 3H), 1.01 (s, 3H). ^{13}C NMR (300 MHz, DMSO-d_6): δ 172.5, 163.8, 160.0, 151.7, 130.9, 114.3, 111.2, 102.6, 87.3, 84.1, 71.7, 62.1, 55.9, 52.7, 52.2, 50.3, 49.1, 42.7, 42.0, 37.9, 27.1, 20.4. HRMS-ESI (+) (*m/z*): $[M+H]^+$ calcd. for $C_{21}H_{25}N_2O_8$, 433.1605; found: 433.1615.

3,9-Dimethoxy-6b,12b-dimethyl-12a,12b-dihydrocyclobuta[1,2-c:3,4-c']dichromene-6,12(6aH,6bH)-dione (**19**). (CH_2Cl_2:MeOH = 99:1, a white solid, 5.6 mg, 15%). ^{1}H NMR (300 MHz, $CDCl_3$-*d*): δ 6.97-7.04 (m, 2H), 6.70-6.73, 5.98-5.99 (m, 2H), 6.56-6.00 (m, 2H), 3.76, 3.60 (s, 6H), 3.35, 3.31(s, 2H), 1.60, 1.18 (s, 6H). ^{13}C NMR (300 MHz, $CDCl_3$-*d*): δ 165.0, 163.7, 159.3, 150.7, 149.3, 127.0, 126.5, 114.0, 112.8, 111.0, 110.7, 101.4, 100.8, 54.6, 54.2, 45.6, 44.0, 40.0, 30.7, 25.4. HRMS-ESI (+) (*m/z*): $[M+H]^+$ calcd. for $C_{22}H_{21}O_6$, 381.1338; found: 381.1346.

4.10. References

[1] Part of this chapter was published in Sun, H., Fan, H., Peng, X. Quantitative DNA interstrand cross-link formation by coumarin and thymine: structure determination, sequence effect, and fluorescence detection. *J. Org. Chem.* **2014**, *79*, 11359-11369.

[2] Noll, D. M., McGregor Mason, T., Miller, P. S. Formation and repair of interstrand cross-links in DNA. *Chem. Rev.* **2006**, *106*, 277-301.

[3] Rajski, S. R., Williams, R. M. DNA cross-linking agents as antitumor drugs. *Chem. Rev.* **1998**, *98*, 2723-2796.

[4] Mishina, Y., He, C. Probing the structure and function of the Escherichia coli DNA alkylation repair AlkB protein through chemical cross-linking. *J. Am. Chem. Soc.* **2003**, *125*, 8730 -8731.

[5] Verdine, G. L., Norman, D. P. G. Covalent trapping of protein-DNA complexes. *Annu. Rev. Biochem.* **2003**, *72*, 337-366.

[6] Banerjee, A., Santos, W. L., Verdine, G. L. Structure of a DNA glycosylase searching for lesions. *Science* **2006**, *311*, 1153-1157.

[7] Duguid, E. M., Mishina, Y., He, C. How do DNA repair proteins locate potential base lesions? A chemical crosslinking method to investigate O6-alkylguanine-DNA alkyltransferases. *Chem. Biol.* **2003**, *10*, 827-835.

[8] Wolkenberg, S. E., Boger, D. L. Mechanisms of in situ activation for DNA-targeting antitumor agents. *Chem. Rev.* **2002**, *102*, 2477-2495.

[9] Jamieson, E. R., Lippard, S. J. Structure, recognition, and processing of cisplatin-DNA adducts. *Chem. Rev.* **1999**, *99*, 2467-249.

[10] Reissner, T., Schneider, S., Schorr, S., Carell, T. Crystal structure of a cisplatin-(1, 3-GTG) cross-link within DNA polymerase η. *Angew. Chem., Int. Ed.* **2010**, *49*, 3077-3080.

[11] Cimino, G. D., Gamper, H. B., Isaacs, S. T., Hearst, J. E. Psoralens as photoactive probes of nucleic acid structure and function: organic chemistry, photochemistry, and biochemistry. *Annu. Rev. Biochem.* **1985**, *54*, 1151-1193.

[12] Verga, D., Nadai, M., Doria, Percivalle, F., C., An-tonio, M. D., Palumbo, M., Richter, S. N., Freccero, M. Photogeneration and reactivity of naphthoquinone methides as purine selective DNA alkylating agents. *J. Am. Chem. Soc.* **2010**, *132*, 14625-14637.

[13] Di Antonio, M., Doria, F., Richter, S. N., Bertipaglia, C., Mella, M., Sissi, C., Palumbo, M., Freccero, M. Quinone methides tethered to naphthalene diimides as selective G-quadruplex alkylating agents. *J. Am. Chem. Soc.* **2009**, *131*, 13132-13141.

[14] Wang, P., Liu, R., Wu, X., Ma, H., Cao, X., Zhou, P., Zhang, J., Weng, X., Zhang, X., Qi, J., Zhou, X., Weng, L. A potent, water-soluble and photoinducible DNA cross-linking agent. *J. Am. Chem. Soc.* **2003**, *125*, 1116-1117.

[15] Cao, S., Wang, Y., Peng, X. ROS-inducible DNA cross-linking agent as a new anticancer prodrug building block. *Chem. Eur. J.* **2012**, *18*, 3850-3854.

[16] Cao, S., Christiansen, R., Peng, X. Substituent effects on oxidation-induced formation of quinone methides from arylboronic ester precursors. *Chem. Eur. J.* **2013**, *19*, 9050-9058.

[17] Kuang, Y., Balakrishnan, K., Gandhi, V., Peng, X. Hydrogen peroxide inducible DNA cross-linking agents: targeted anticancer prodrugs. *J. Am. Chem. Soc.* **2011**, *133*, 19278-19281.

[18] Pujari, S. S., Xiong, H., Seela, F. Cross-linked DNA generated by "bis-click" reactions with bis-functional azides: site independent ligation of oligonucleotides via nucleobase alkynyl chains. *J. Org. Chem.* **2010**, *75*, 8693-8696.

[19] Kocalka, P., El-Sagheer, A. H., Brown, T. Rapid and efficient DNA strand cross-linking by click chemistry. *ChemBioChem.* **2008**, *9*, 1280-1285.

[20] Xiong, H., Seela, F. Cross-linked DNA: site-selective “Click” ligation in duplexes with bis-azides and stability changes caused by internal cross-links. *Bioconjugate Chem.* **2012**, *23*, 1230-1243.

[21] Hong, I. S., Greenberg, M. M. Efficient DNA interstrand cross-link formation from a nucleotide radical. *J. Am. Chem. Soc.* **2005**, *127*, 3692-3693.

[22] Peng, X., Pigli, Y., Rice, P. A., Greenberg, M. M. Protein binding has a large effect on radical mediated DNA damage. *J. Am. Chem. Soc.* **2008**, *130*, 12890-12891.

[23] Kuang, Y., Sun, H., Blain, J. C., Peng, X. Hypoxia-selective DNA interstrand cross-link formation by two modified nucleosides. *Chem. Eur. J.* **2012**, *18*, 12609-12613.

[24] Qiu, Z., Lu, L., Jian, X., He, C. A diazirine-based nucleoside analogue for efficient DNA interstrand photocross-linking. *J. Am. Chem. Soc* **2008**, *130*, 14398-14399.

[25] Cahova, H., Jäschke, A. Nucleoside-sased diarylethene photoswitches and their facile incorporation into photoswitchable DNA. *Angew. Chem. Int. Ed.* **2013**, *52*, 3186-3190.

[26] Thazhathveetil, A. K., Liu, S. T., Indig, F. E., Seidman, M. M. Psoralen conjugates for visualization of genomic interstrand cross-links localized by laser photoactivation. *Bioconjug. Chem.* **2007**, *18*, 431-437.

[27] Zewail-Foote, M., Hurley, L. H. Differential Rates of Reversibility of Ecteinascidin 743−DNA Covalent Adducts from Different Sequences Lead to Migration to Favored Bonding Sites. *J. Am. Chem. Soc.* **2001**, *123*, 6485-6495.

[28] Liu, Y., Rokita, S. E. Inducible alkylation of DNA by a quinone methide-peptide nucleic acid conjugate. *Biochemistry*, **2012**, *51*, 1020-1027.

[29] Wang, H., Wahi, M. S., Rokita, S. E. Immortalizing a transient electrophile for DNA cross-linking. *Angew. Chem. Int. Ed. Engl.* **2008**, *47*, 1291-1293.

[30] Weinert, E. E., Dondi, R., Colloredo-Melz, S., Frankenfield, K. N., Mitchell, C. H., Freccero, M., Rokita, S. E. Substituents on quinone methides strongly modulate formation and stability of their nucleophilic adducts. *J. Am. Chem. Soc.* **2006**, *128*, 11940-11947.

[31] Browne, W. R., Feringa, B. L. Light switching of molecules on surfaces. *Annu. Rev. Phys. Chem.* **2009**, *60*, 407-428.

[32] Chung, J. W., Lee, K., Neikirk, C., Nelson, C. M., Priestley, R. D. Photoresponsive coumarin-stabilized polymeric nanoparticles as a detectable drug carrier. *Small* **2012**, *8*, 1693-1700.

[33] Majumdar, A., Muniandy, P. A., Liu, J., Liu, J. L., Liu, S. T., Cuenoud, B., Seidman, M. M. Targeted gene knock in and sequence modulation mediated by a psoralen-linked triplex-forming oligonucleotide. *J. Biol. Chem.* **2008**, *283*, 11244-11252.

[34] Shahid, K. A., Majumdar, A., Alam, R., Liu, S. T., Kuan, J. Y., Sui, X., Cuenoud, B., Glazer, P. M., Miller, P. S., Seidman, M. M. Targeted cross-linking of the human beta-globin gene in living cells mediated by a triple helix forming oligonucleotide. *Biochemistry* **2006**, *45*, 1970-1978.

[35] Takasugi, M., Guendouz, A., Chassignol, M., Decout, J. L., Lhomme, J., Thuong, N. T., Helene, C. Sequence-specific photo-induced cross-linking of the two strands of double-helical DNA by a psoralen covalently linked to a triple helix-forming oligonucleotide. *Proc Natl Acad Sci U S A* **1991**, *88*, 5602-5606.

[36] Fujimoto, K., Yamada, A., Yoshimura, Y., Tsukaguch, T., Sakamoto, T. Details of the ultrafast DNA photo-cross-linking reaction of 3-cyanovinylcarbazole nucleoside: cis–trans isomeric effect and the application for SNP-based genotyping. *J. Am. Chem. Soc.* **2013**, *135*, 16161-16167.

[37] Thazhathveetil, A. K., Liu, S. T., Indig, F. E., Seidman, M. M. Psoralen conjugates for visualization of genomic interstrand cross-links localized by laser photoactivation. *Bioconjug Chem.* **2007**, *18*, 431-437.

[38] Cimino, G. D., Gamper, H. B., Isaacs, S. T., Hearst, J. E. Psoralens as photoactive probes of nucleic acid structure and function: organic chemistry, photochemistry, and biochemistry. *Annu. Rev. Biochem.* **1985**, *54*, 1151-1193.

[39] Trenor, S. R., Shultz, A. R., Love, B. J., Long, T. E. Coumarins in polymers: from light harvesting to photo-cross-linkable tissue scaffolds. *Chem. Rev.* **2004**, *104*, 3059-3077.

[40] Musa, M. A., Cooperwood, J. S., Khan, M. O. A review of coumarin derivatives in pharmacotherapy of breast cancer. *Curr Med Chem.* **2008**, *15*, 2664-2679.

[41] Haque, M. M., Sun, H., Liu, S., Wang, Y., Peng, X. Photo-switchable DNA interstrand cross-link formation by a coumarin-modified nucleotide. *Angew. Chem. Int. Ed.* **2014**, *27*, 7001-7005.

[42] Droumaguet, C. L., Wang, C., Wang, Q. Fluorogenic click reaction. *Chem. Soc. Rev.* **2010**, *39*, 1233-1239.

[43] Kool, E. T. Preorganization of DNA: design principles for improving nucleic acid recognition by synthetic oligonucleotides. *Chem. Rev.* **1997**, *97*, 1473-1488.

[44] Sun, H., Peng, X. Template directed fluorogenic oligonucleotide ligation using "click" chemistry: detection of single nucleotide polymorphism in the human p53 tumor suppressor gene. *Bioconjugate Chem.* **2013**, *24*, 1226-1234.

[45] Laing, B. M., Barrow-Laing, L., Harrington, M., Long, E. C., Bergstrom, D. E. Properties of double-stranded oligonucleotides modified with lipophilic substituents. *Bioconjugate Chem.* **2010**, *21*, 1537-1544.

[46] Aksoya, L., Kolaya, E., Ağılönüa, Y., Aslana, Z., Kargıoğlub, M. Free radical scavenging activity, total phenolic content, total antioxidant status, and total oxidant status of endemic Thermopsis turcica. *Saudi J Biol Sci* **2013**, *20*, 235-239.

[47] Chibisov, A. K. Electron transfer in photochemical reactions. *Russ. Chem. Rev.* **1981**, *50*, 615-629.

[48] Seidel, C. A. M., Schulz, A., Sauer, M. H. M. Nucleobase-specific quenching of fluorescent dyes. 1. nucleobase one-rlectron redox potentials and their correlation with static and dynamic quenching efficiencies. *J. Phys. Chem.* **1996**, *100*, 5541-5553.

[49] Heinlein, T., Knemeyer, J. P., Piestert, O., Sauer, M. Photoinduced electron transfer between fluorescent dyes and guanosine residues in DNA-hairpins. *J. Phys. Chem. B* **2003**, *107*, 7957-7964.

[50] Kendall, D. A., MacDonald, R. C. A fluorescence assay to monitor vesicle fusion and lysis. *J. Biol. Chem.* **1982**, *257*, 13892-13895.

Chapter 5. Rearrangement of Coumarin-Induced DNA Intrastrand Cross-Linking to Interstrand Cross-Linking

5.1. Introduction

The coumarin-containing ODNs are capable of cross-linking dT or dC in the complementary ODN strands upon 350 nm irradiation and the coumarin-induced cross-linking is photoreversible upon 254/350 nm irradiation.[1] Moreover, the fluorescence of coumarins is quenched upon ICL formation, which provides a novel method for fast, easy, and real-time detection of DNA cross-linking via fluorescence spectroscopy.[2] This approach can be used in DNA bioanalysis. However, it is not clear whether the intrastrand photocycloaddition reactions compete for interstrand cross-linking. Addressing this important issue will expand its biological application

Psoralens, with similar structure as coumarins, generate DNA ICLs but also side products such as monoadducts. Monoadducts formation is three times that of interstrand cross-links formation.[3] Coumarins also can induce interstrand and interstrand cross-links in DNA-templated reaction. This prompted us to undertake a systematic study to establish a perfect model for studying competition between ICL reaction and ligation reaction. The relation of interstrand and intrastrand photocycloaddition reactions was experimentally studied, but more chemistry was discovered in photoreversible reactions.

5.2. Synthesis of ODNs Containing Coumarin Moieties

Preparation of coumarin analogues **1-3** followed the procedures described in our previous reports.[2] Compound **1** was synthesized from compound **2** via Williamson ether synthesis, and coumarin **2** and **3** were prepared with Pechmann Condensation between resorcinol

and ethyl acetoacetate or Malic acid. Compounds **1** and **2** allowed us to study the effects of dT position and linker on the cross-linking efficiency, while **2** and **3** were used to investigate the effect of methyl group at position-4 on coumarin's photoactivity. Compounds **1**-**3** with a hydroxyl group were converted to the corresponding phosphoramidites **4**-**6** used for solid-phase DNA synthesis (Figure 5-1). All new compounds were confirmed by NMR and HRMS.

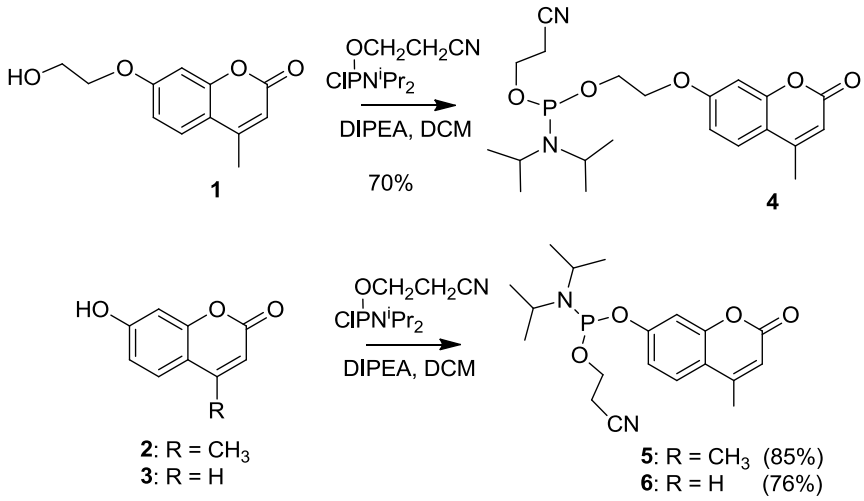

Figure 5-1**.** Synthesis of the phosphoramidites **4**-**6**.

ODNs containing **1**-**3** were synthesized using commercially available β-cyanoethyl phosphoramidites with phenoxyacetyl protecting groups on the exocyclic amines of dA and dG, which allows for a very mild deprotection condition avoiding decomposition of the functionalized ODNs **7b**, **8b**, **11b**, **12b**, **13c**, and **14c** (Figure 5-2). Purification of all ODNs was performed by 20% denaturing polyacrylamide gel electrophoresis.

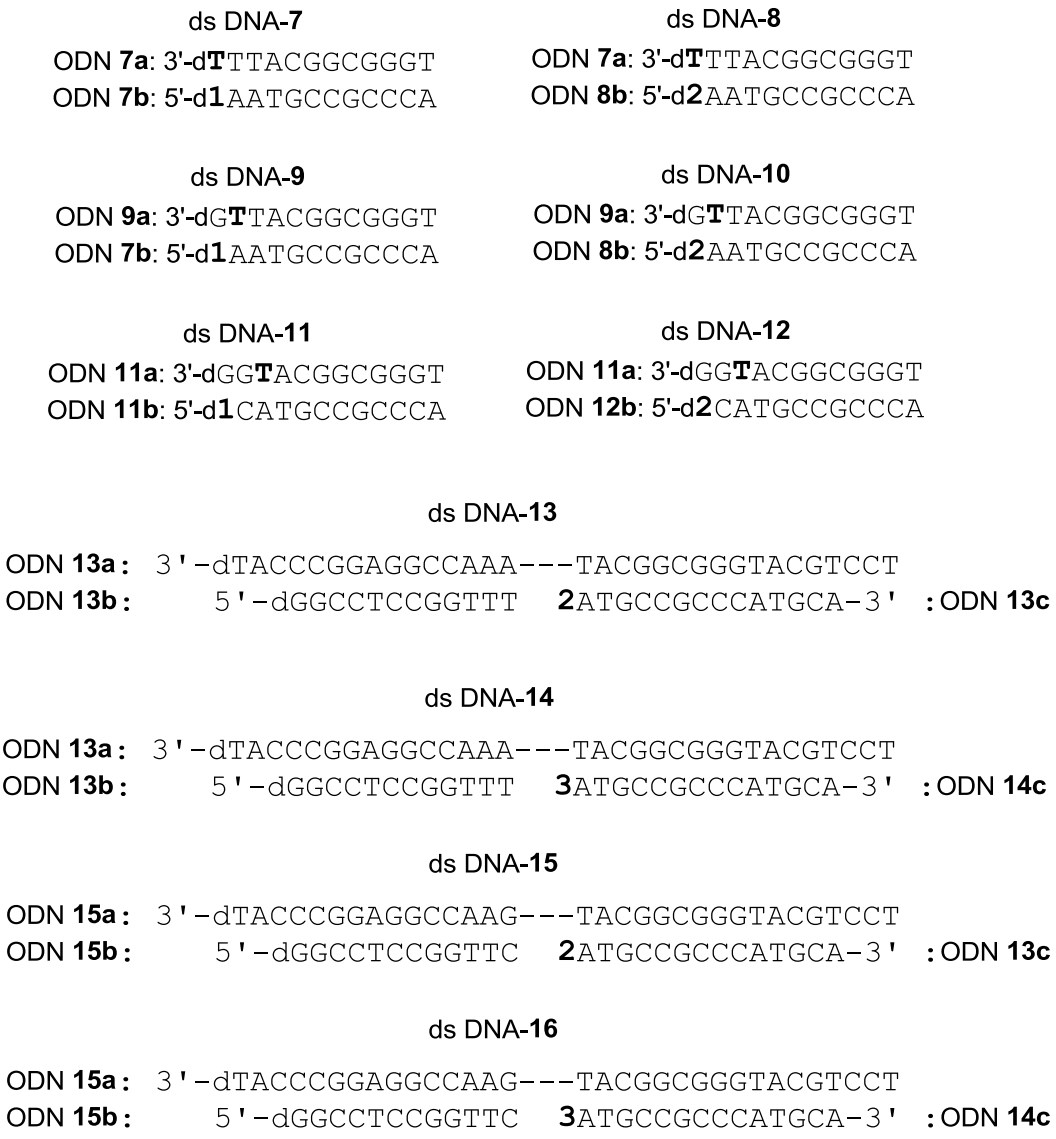

Figure 5-2. Double stranded DNAs used in this study.

5.3. The Effects of dT Position and Linker on the ICL Efficiency

To obtain suitable ligation product for the study, ICL with high efficiency (ICL yield > 90%) should be well controlled in the process. Our previous report verified that the linker of coumarin and flanking sequences played an important role in the ICL formation.[2] Quantitative DNA interstrand cross-link was generated using coumarin moieties with a flexible two-carbon or longer linker, and ICL reaction showed a kinetic preference when

the coumarin was flanked by an A:T base pair as opposed to a G:C pair, due to the efficient photoinduced electron transfer between coumarin and dG. In addition, no cycloaddition reaction was observed between coumarin and dG. Thus, ds DNA **7**-**12** containing coumarin analogues were designed for studying the effect of dT position and linker on ICL efficiency (Figure 5-2). Because coumarins cannot cross-link dG in DNA, duplexes ds DNA-**7**, ds DNA-**9**, and ds DNA-**11** with increasing distance between coumarin **1** and dT in the opposite strand enables the study of the effect of the dT position on ICL formation. While **2** without the linker was introduced in ds DNA-**8**, ds DNA-**10**, and ds DNA-**12** which allow investigation of the linker's effect on ICL formation.

Upon photo-irradiation at 350 nm, ICL products were obtained for all DNA duplexes with different efficiency and rates (Figure 5-3). Almost quantitative DNA ICL formation was observed for ds DNA-**7** (98%) and ds DNA-**9** (97%) containing coumarin **1** with a two-carbon linker, and a slightly lower ICL yield was observed for ds DNA-**11** (78%) resulting from the increased distance between coumarin and dT. However, formation of ICL adducts was less efficient for ds DNA-**8** (89%), ds DNA-**10** (66%), and ds DNA-**12** (50%) bearing coumarin **2**. In addition, decreased ICL yields were observed with increasing distance between dT and **2** (Figure 5-3). The ICL yield ratio for ds DNA-**8**/**10**/**12** is 1/0.74/0.56, while that is 1/0.99/0.80 for ds DNA-**7**/**9**/**11**. This showed that ICL formation induced by **2** is more dependent on the distance/position than **1**. Thus, **2** induced ICL reaction process can be easily handled via careful design of DNA sequences. Kinetic study showed that installation of dG next to coumarin:dT base pair greatly decreased the ICL reaction rate. Introduction of dG in ds DNA-**9** ($6.1 \pm 0.5 \times 10^{-4}$ s^{-1}) and

10 (6.3 ± 0.3 $\times 10^{-5}$ s^{-1}) led to 7 times lower reaction rate than that for ds DNA-**7** (4.2 ± 0.4 $\times 10^{-3}$ s^{-1}) and **8** (4.8 ± 0.4 $\times 10^{-4}$ s^{-1}) (Table 5-1). Further rate reduce was observed for ds DNA-**11** (1.6 ± 0.1 $\times 10^{-4}$ s^{-1}) and **12** (8.4 ± 0.4 $\times 10^{-5}$ s^{-1}), due to longer distance between the coumarin and dT. In order to perform well-controlled ICL formation with suitable efficiency and reactivity, coumarins without linker, such as **2** with methyl group and **3** bearing no methyl group at position-4, were chosen for ICL and ligation reaction study, as well as investigation of substitution effect on the reactivity of coumarin.

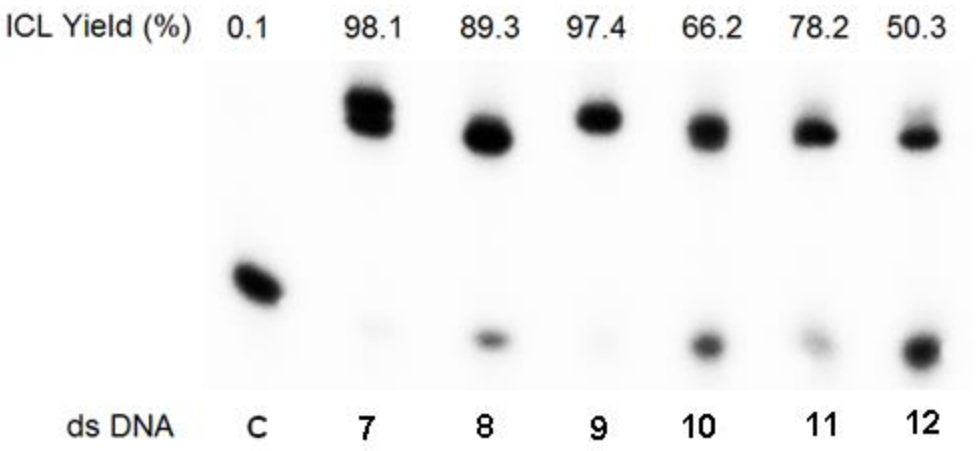

Figure 5-3. PAGE analysis of distance-dependent ICL formation (100 nM ds DNA-**7**-**12** was irradiated at 350 nm; ODNs without coumarins were 5'-[^{32}P]-labeled.).

Table 5-1. ICL reaction rates for ds DNA-**7**-**12**.

Entry	k (10^{-5} s^{-1})	$t_{1/2}$ (min)
ds DNA-**7**	420 ± 40	3 ± 0
ds DNA-**8**	47.8 ± 4.0	24 ± 2
ds DNA-**9**	61.4 ± 5.3	19 ± 2
ds DNA-**10**	6.3 ± 0.3	184 ± 9

ds DNA-**11**	16.2 ± 0.7	67 ± 2
ds DNA-**12**	8.4 ± 0.4	139 ± 6

5.4. Coumarin-Induced ICL and Ligation Reaction

A model was established for the study of coumarin-induced intrastrand and interstrand cross-links. As the intrastrand cycloadditon (cross-links) does not change the length and mass of the ODN strands, it cannot be characterized via commonly used PAGE analysis and mass spectrometry.[4-5] We designed the DNA duplexes that enable the ligation reaction used for analysing the intrastrand cross-links. DNA sequences with less dG near coumarins were deigned to ensure the proper reactivity, such as the ds DNA-**13** and **14** which contain d(AT/T**2**A) and d(AT/T**3**A), respectively. Cycloaddition between coumarin **2** and dT in the opposing strand ODN-**13a** can produce ICL adducts, while the reaction with dT in ODN-**13b** yields the ligation products. Thus, it can be used to study competition between intrastrand cross-linking and interstrand cross-linking reaction. The ICL products and ligation products can be detected via labelling different ODNs with ^{32}P. The 5'-[^{32}P]-labelled ODN-**13a** was used for ICL analysis and 5'-[^{32}P]-labelled ODN-**13b** was employed for ligation reaction study.

As expected, both ICL and ligation products were observed for ds DNA-**13** and **14** upon irradiation at 350 nm. Formation of the ICL and ligation products corresponding to top band in denaturing gel increased with extended reaction time which can be seen from the increased intensity of the top band. The quantitative analysis showed that the ICL and ligation yields after 6 h photoirradiation were 36.7% and 29.3% respectively for ds DNA-**13** containing **2** with methyl group at the position-4, and 34.2% and 34.7% for ds

DNA-**14** bearing **3** without methyl group. No big difference was observed for the total reaction yields, which suggested substitution of methyl group at the position-4 of coumarin has no obvious effect on its cycloaddition reactivity (Figure 5-4). Kinetic study indicated that the ligation reaction proceeded faster than that of ICL reaction with ds DNA-**13**((1.21 ± 0.13) × 10^{-4} s^{-1} for ligation vs. (0.96 ± 0.06) × 10^{-4} for ICL). Similar result was obtained for ds DNA-**14**, which suggested the photoligation was kinetic-controlled (Table 5-2).

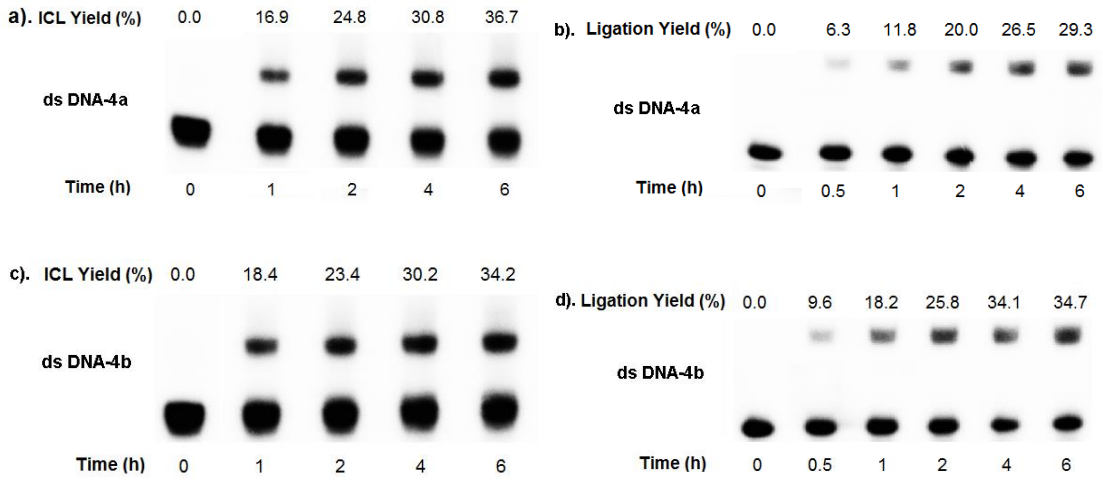

Figure 5-4. PAGE analysis of ICL and ligation reactions for ds DNA-**13** (a,b)/**14** (c,d) [ODN **13a** was 5'-[^{32}P]-labeled for ICL reactions (a) and (c). ODN **13b** was 5'-[^{32}P]-labeled for ligation reactions (b) and (d).100 nM ds DNA were irradiated at 350 nm.].

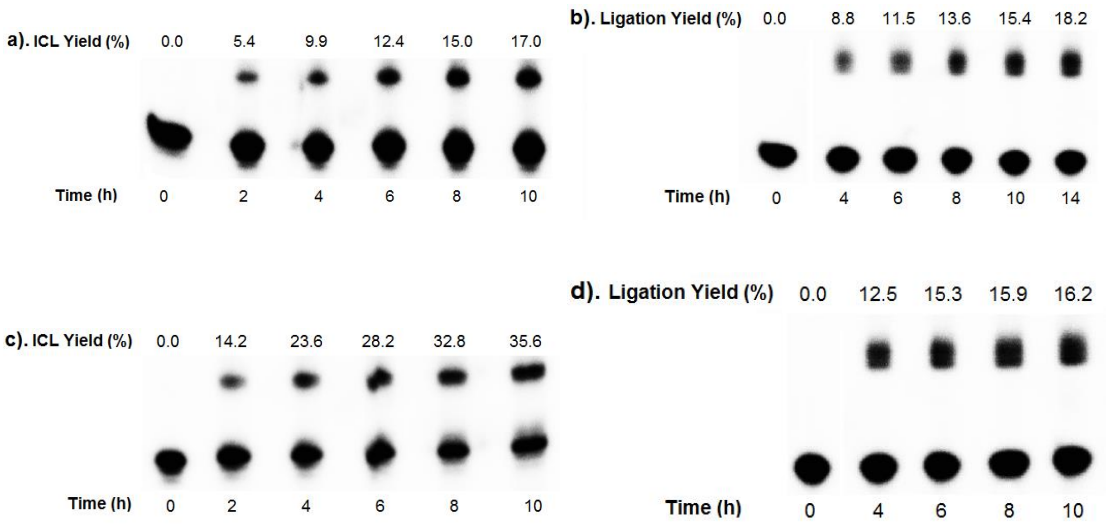

Figure 5-5. PAGE analysis of ICL and ligation reactions for ds DNA-**15** (a,b)/**16** (c,d) [ODN **15a** was 5'-[^{32}P]-labeled for ICL reactions (a) and (c). ODN **15b** was 5'-[^{32}P]-labeled for ligation reactions (b) and (d).100 nM ds DNA were irradiated at 350 nm.].

In addition to a cycloaddition between coumarin and dT, dC also forms cross-linking adducts with the coumarin in DNA. The ds DNA-**15/16** containing d(CT/G**2**A) and d(CT/G**3**A) at central sites respectively were designed to study competition reaction between dT/coumarin ICL reaction and dC/coumarin ligation reaction. The coumarin **3** was more reactive than **2** in this sequence. Lower yields for ICL and ligation products were observed for ds DNA-**15 (ICL:** 17.0% and ligation: 15.4%) than ds DNA-**16** (35.6% for ICL and 16.2% for ligation) after photoirradiation for 10 h (Figure 5-5). Compound **3** has higher absorption coefficient at 350 nm in water (3144 mole^{-1}.cm^{-1}) than **2** (1722 mole^{-1}.cm^{-1}) which may lead to better photoreactivity. Compounds with higher absorption coefficients are more easily to absorb photons forming the excited states for photocycloaddition reactions. On the other hand, lower reaction rate was also observed for ds DNA-**15** than ds DNA-**16** possibly due to electron transfer between

coumarin and dG. The ICL and ligation reactions carried on at a rate of $(3.08 \pm 0.27)\times10^{-5}$ s^{-1} and $(5.48 \pm 0.46)\times10^{-5}$ respectively for ds DNA-**15**, and that were $(5.76 \pm 0.60)\times10^{-5}$ s^{-1} and $(4.20 \pm 0.40)\times10^{-5}$ respectively for ds DNA-**16** (Table 5-2).

Table 5-2. Rates of cross-link formation or cleavage for ds DNA-**13-16**.

Entry	k (ICL Formation, 10^{-5} s^{-1})	$t_{1/2}$ (h)	k_c (ICL Cleavage, 10^{-3} s^{-1})	$t_{1/2}$ (min)
ds DNA-**13**	9.6 ± 0.6	2.01 ± 0.12	5.12 ± 0.27	2.26 ± 0.12
ds DNA-**14**	15.7 ± 0.6	1.22 ± 0.04	4.75 ± 0.34	2.44 ± 0.17
ds DNA-**15**	3.08 ± 0.27	6.30 ± 0.55	8.79 ± 0.71	1.32 ± 0.11
ds DNA-**16**	5.76 ± 0.60	3.37 ± 0.35	3.98 ± 0.33	2.92 ± 0.25
Entry	K (Ligation Formation, 10^{-5} s^{-1})	$t_{1/2}$ (h)	k_c (Ligation Cleavage, 10^{-3} s^{-1})	$t_{1/2}$ (min)
ds DNA-**13**	12.1 ± 1.3	1.61 ± 0.17	5.94 ± 0.45	1.96 ± 0.15
ds DNA-**14**	16.7 ± 1.6	1.16 ± 0.11	9.78 ± 0.43	1.18 ± 0.05
ds DNA-**15**	5.48 ± 0.46	3.54 ± 0.30	6.58 ± 0.79	1.78 ± 0.21
ds DNA-**16**	4.20 ± 0.40	2.70 ± 0.25	6.24 ± 0.66	1.87 ± 0.20

5.5. Rearrangement and Photorelease of the Coumarin Moiety

5.5.1. Rearrangement during Photoswichable Process

The coumarin-induced photocycloadditions with dT and dC are photoreversible. The irradiation at 254 nm of photocycloaddition products gave corresponding single strands

in more than 70% yield. The cleavage reactions followed first-order kinetics and completed within 10 min. The cleavage reactions were much faster than the cross-link reactions (Table 5-2). For example, all cleavage reactions rates are around 5×10^{-4} s^{-1} that is about 30-200 times larger than that for cross-link formation reactions. In addition, cleavage of ligation products proceeded faster than that of ICL products. For instance, the cleavage reaction rate of ligation product formed with ds DNA-**14** is $(9.78 \pm 0.43) \times 10^{-4}$ s^{-1}which is two times that the cleavage rate for ICL products $(4.75 \pm 0.34) \times 10^{-4}$ s^{-1}). It possibly arises from steric hinder, promoting cleavage reaction, in the ligation products, which contain one more coumarin moiety than matched template.

Moreover, rearrangement of the ligation products to the ICL products was observed during the photoswitchable processes. The photoreversible behaviors were observed within three cycles of photoirradiation at 350 nm for 20 h and 254 nm for 10 min (Figure 5-6). Unlike our previous reports that ICL decreased a little after each cycle, the ICL yields increased but the ligation yield decreased upon photoirradiation at 350 nm during each cycle. For example, the ICL yield for ds DNA-**13** increased from 43% in the first cycle to 50% after three cycles of 350 nm/254 nm irradiation, while the ligation yield decreased from 31% to 9% in this process (Figure 5-6a). Similar results were observed for ds DNA-**14** and ds DNA-**15** indicating the rearrangement from kinetic-controlled ligation products to thermo-controlled ICL products. After each cleavage reaction, the free coumarin prefers to react with dT in the complementary strand to form the stable ICL product resulting in the rearrangement. In addition, the ligation cross-linkings containing extra coumarin than complementary strands are unstable in DNA hybridization, which also promoted the migration.[6-7]

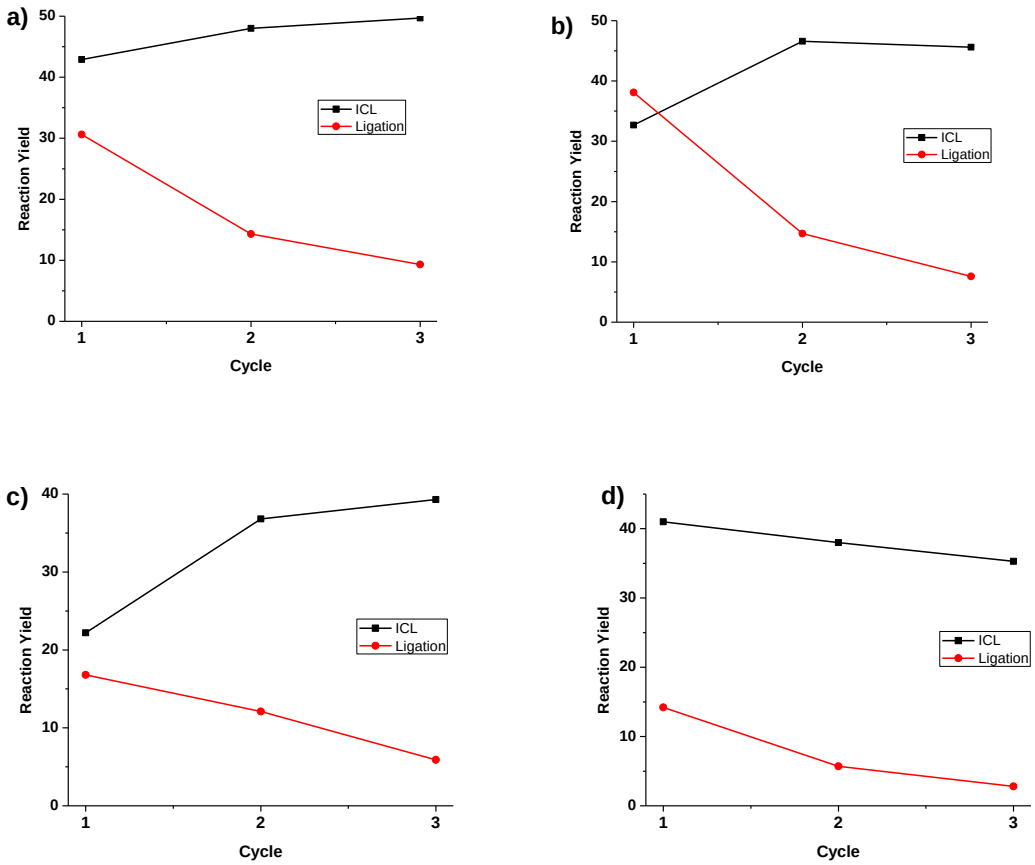

Figure 5-6. Cross-link yields during photoreversible process for ds DNA-**13** (a), ds DNA-**14** (b), ds DNA-**15** (c), and ds DNA-**16** (d) (photoirradiation at 350 nm for 20 h and 254 nm for 10 min for each cycle.).

However, the rearrangement between thermo-dependent cross-links and kinetic-controlled ligation products for ds DNA-**16** was not observed, and both ICL and ligation yields reduced after each cycle (Figure 5-6d). ICL yield for ds DNA-**16** reduced from 41% in the first circle to 35% after three cycles of 350 nm/254 nm irradiation, while the ligation yield decreased from 14% to 3% in this process (Figure 5-6d). One new band migrating faster than the original single strand ODN-**14c** was observed after 3 cycles'

photoreversible reactions. The new band ss DNA* may result from photorelease of coumarin **3** in ODN-**14c**.

5.5.2. Photorelease Reaction

Further study showed that the photorelease of the coumarin moiety only occurred for ODNs containing **3** which was sequence-specific and light-dependent. No obvious photorelease products were observed for coumarin **2**-containing DNA duplexes. The ds DNA-**15** and **16** containing **3** were used to study the photorelease reactions. The ds DNA-**15** and **16** were treated with UV lights at different wavelength for designed time. We found the cycloaddition reaction between dT and coumarin **3** in ds DNA-**15** did not show clear photorelease reaction (Figure 5-7, lanes 2-5). In ds DNA-**16**, the ligation products between **3** and dC produce obvious ss DNA* band upon 254 nm irradiation only after treatment with photoirradiation at 350 nm (Figure 5-7, lanes 6, 7 and 9). This suggests the photorelease reaction only occurs for coumarin **3**-containing DNA duplexes with G:C base pair next to coumarins. No ss DNA* band clearly appear without 350 nm photoirradiation in DNA-**16** (Figure 5-7, lane 8)**.** This indicated that substitution of methyl group of coumarin affect the photorelease reaction in DNA, and G:C base pair and irradiation at 350 nm played an important role in this process. Similar results were observed for coumarin-caged coumpounds at position-4 and 7, but this is the first example for DNA sequence-specific photorelease reaction.[8-10]

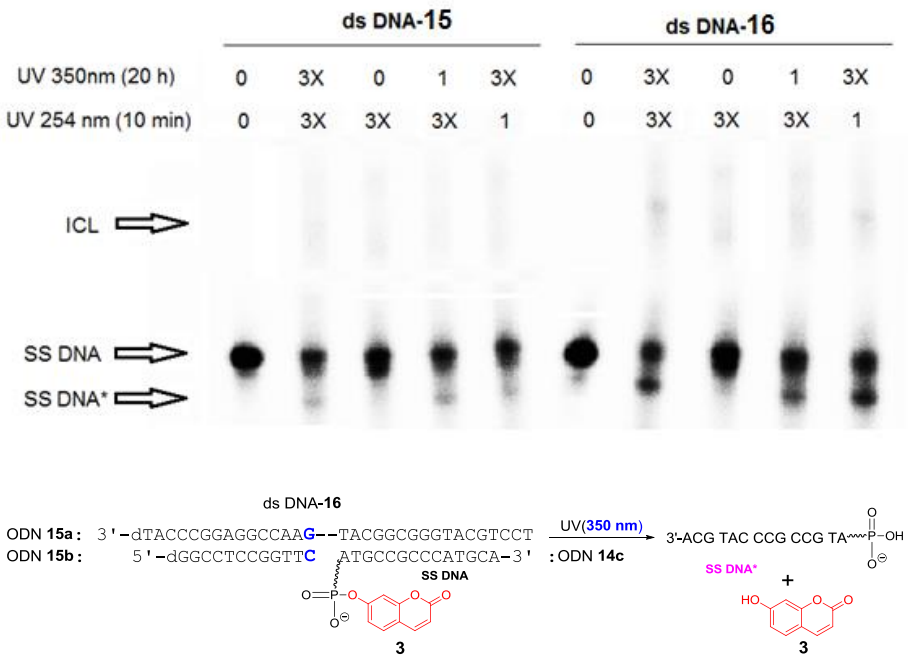

Figure 5-7. Photorelease reaction of **3** for ds DNA-**15**/**16** (they were treated with irradiations at different wavelength for desired time, and ODN **14c** was 3'-[^{32}P]-labelled.).

5.6. Experimental Section

PAGE analysis of DNA ICL and ligation reactions and the kinetic study. The 5'-^{32}P-labeled ODNs (500 nM) and its complementary strands (1.5 eq.) were hybridized in 100 mM NaCl and 10 mM potassium phosphate (pH 7). The DNA duplexes were photoirradiated at 350 nm for desired time. A control reaction was performed without 350 nm photoirradiation. Aliquots were taken at the prescribed times and immediately quenched with the equal volumes of 95% formamide loading buffer, and stored at -20°C until subjecting to 20% denaturing PAGE analysis. For kinetics study, three independent samples were studied with the same procedures mentioned above.

PAGE analysis of photo-induced (254 nm) cleavage reactions of DNA ICL products and kinetic study. The reactions were carried out with photoirradiation at 254 nm using two or three independent samples. Aliquots were taken at the prescribed time and immediately quenched with the equal volume of 95% formamide loading buffer, and stored at -20 °C until subjecting to 20% denaturing PAGE analysis.

Photoirradiation at 350 nm was conducted in Rayonet Photochemical Chamber Reactor (Model RPR-100), and photoirradiation at 254 nm was carried out using Compact UV Lamp (UVGL-25). Fluorescence spectra were recorded on a Perkin-Elmer LS55 Fluorescence Spectrometer using the quartz cell with 10 mm path lengths at room temperature. ^{1}H NMR, ^{13}C NMR, and ^{31}P NMR analysis were performed on a Bruker DRX 300 MHz spectrophotometer. Chemical shifts are reported in ppm relative to Me_4Si (^{1}H and ^{13}C) or H_3PO_4 (^{31}P). Coupling constants (*J*) are reported in Hz.

7-Hydroxy-2H-chromen-2-*O*-(2-cyanoethyl-*N*,*N*-diisopropyl)-phosphoramidite (4). To the solution of 7-hydroxy-2H-chromen-2-one (81 mg, 0.5 mmol) in dichloromethane (10 mL), N,N-diisopropylethylamine (DIPEA) (156 μL, 0.9 mmol) and 2-cyanoethyl-N,N-diisopropyl- chlorophosphoramidite (167 μL, 0.75 mmol) were added under an atmosphere of argon. After stirring at room temperature, the reaction mixture was diluted with dichloromethane (50 mL), washed with $NaHCO_3$ (20 mL) and saturated aqueous NaCl (20 mL). The organic layer was dried over anhydrous sodium sulfate and the solvent was removed under reduced pressure. Upon purification by column chromatography (EtOAc:hexane:Et_3N = 49:50:1, R_f = 0.70), the product was isolated as a white solid (136 mg, 75%). ^{1}H NMR (300 MHz, $CDCl_3$-*d*): *δ*. 7.56, 7.59 (d, *J* = 9.6 Hz, 1H), 7.30, 7.33 (d, *J* = 8.4 Hz, 1H), 6.90-6.94 (m, 2H), 6.20, 6.24 (d, *J* = 9.6 Hz, 1H),

3.87-3.90 (m, 2H), 3.63-3.71 (m, 2H), 2.61-2.85 (t, J = 6.3 Hz, 2H), 1.10-1.19 (d, J = 6.9 Hz, 12H).^{13}C NMR (300 MHz, $CDCl_3$-*d*): δ. 160.00, 158.90, 156.80, 154.34, 142.28, 127.74, 116.25, 115.82, 115.70, 112.96, 106.42, 106.27, 58.25, 58.00, 43.04, 42.86, 23.63, 23.54, 23.45, 23.35, 19.40, 19.30. ^{31}P NMR (300 MHz, $CDCl_3$-*d*): δ. 147.59.

5.7. References

[1] Haque, M. M., Sun, H., Liu, S., Wang, Y., Peng, X. Photo-switchable DNA interstrand cross-link formation by a coumarin-modified nucleotide. *Angew. Chem. Int. Ed.* **2014**, *27*, 7001-7005.

[2] Sun, H., Fan, H., Peng, X. Quantitative DNA interstrand cross-link formation by coumarin and thymine: structure determination, sequence effect, and fluorescence detection. *J. Org. Chem.* **2014**, *79*, 11359-11369.

[3] Cimino, G. D., Gamper, H. B., Isaacs, S. T., Hearst, J. E. Psoralens as photoactive probes of nucleic acid structure and function: organic chemistry, photochemistry, and biochemistry. *Ann. Rev. Biochem.* **1985**, *54*, 1151-1193.

[4] Zimm, B. H., Levene, S. D. Problems and prospects in the theory of gel electrophoresis of DNA. *Q Rev Biophys.***1992**, *25*, 171-204.

[5] Wang, Y., Zhang, Q., Wang, Y. Tandem mass spectrometry for the determination of the sites of DNA interstrand cross-link. *J Am Soc Mass Spectrom.* **2004**, *15*, 1565-1571.

[6] Pérez, C., Leng, M., Malinge, J. M. Rearrangement of interstrand cross-links into intrastrand cross-links in cis-diamminedichloroplatinum(II)-modified DNA. *Nucleic Acids Res.* **1997**, *25*, 896-903.

[7] Malina, J., Kasparkova, J., Farrell, N. P., Brabec, V. Walking of antitumor bifunctional trinuclear Pt^{II} complex on double-helical DNA. *Nucleic Acids Res.* **2011**, *39*, 720-728.

[8] Schade, B., Hagen, V., Schmidt, R., Herbrich, R., Krause, E., Eckardt, T., Bendig, J. Deactivation behavior and excited-state properties of (coumarin-4-yl)methyl derivatives. 1. Photocleavage of (7-methoxycoumarin-4-yl)methyl-caged acids with fluorescence enhancement. *J. Org. Chem.* **1999**, *64*, 9109-9117.

[9] Furuta, T., Tanabe, S., Watanabe, T., Sakyo, J., Matsuba, C. Phototriggers for nucleobases with improved photochemicasl properties. *Org. Lett.* **2007**, *9*, 4717-4720.

[10] Furuta, T., Manabe, K., Teraoka, A., Murakoshi, K., Ohtsubo, A., Suzuki, A. Design, synthesis and photochemistry of modular caging groups for caged nucleotides. *Org. Lett.* **2012**, *14*, 6182-6185.

5.8. Appendices C: Characterization of Compounds

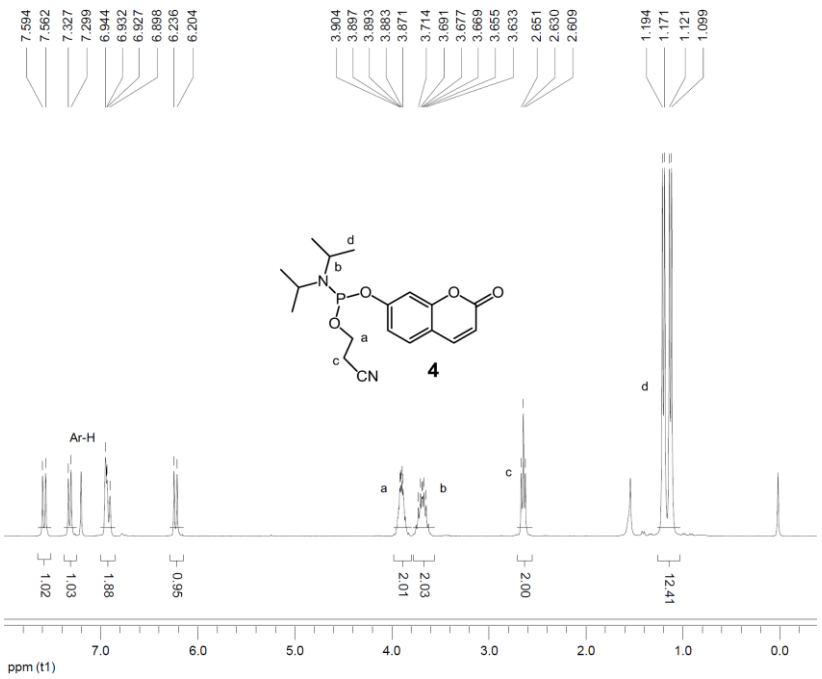

^{1}H NMR spectra of compound **4** (300 MHz, $CDCl_3$-*d*).

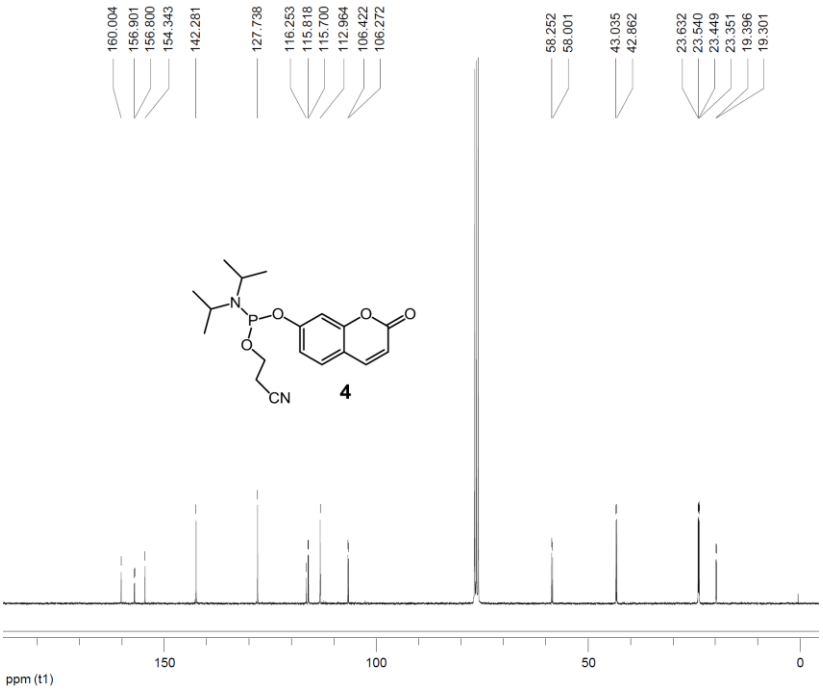

^{13}C NMR spectra of compound **4** (300 MHz, $CDCl_3$-*d*).

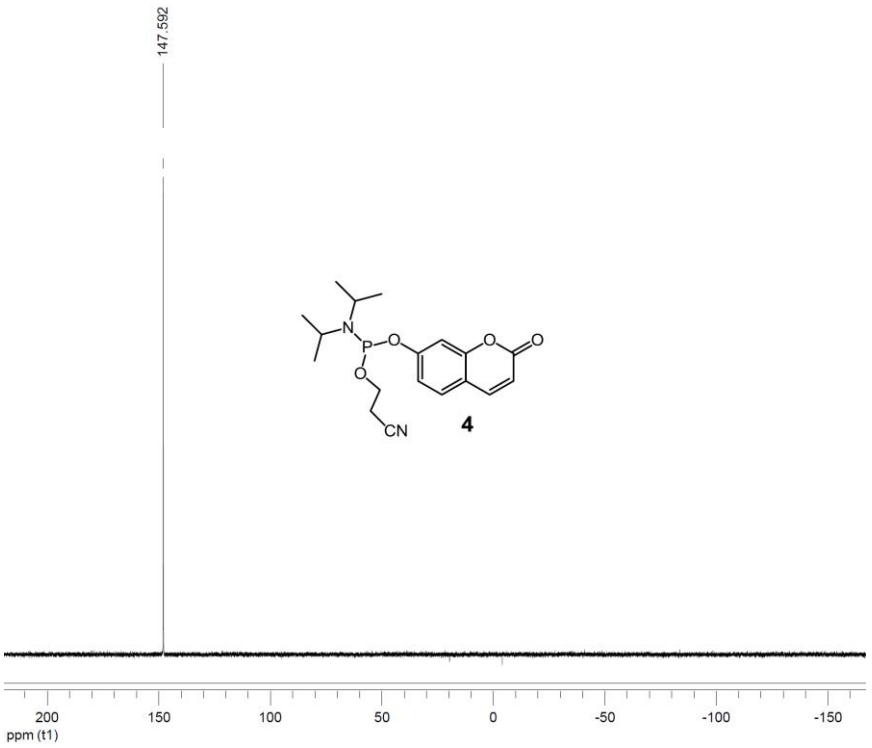

^{31}P NMR spectra of compound **4** (300 MHz, $CDCl_3$-*d*).

Entry	λex (nm)	Abs at λmax	ε (mole^{-1}.cm^{-1})	Abs at 350 nm	ε (mole^{-1}.cm^{-1})
2	320	0.6402	12804	0.0861	1722
3	323	0.565	11300	0.1572	3144

Absorption properties of coumarin **2** and **3**.

CURRICULUM VITAE

Huabing Sun

Place of birth: Yanggu, Shandong, China

Education:

Ph.D, University of Wisconsin-Milwaukee, January 2015

Major: Organic Chemistry, Minor: Physical Chemistry, (Advisor: Prof.Xiaohua Peng)

M.S, Nankai University (China), June 2010

Major: Organic Chemistry, (Advisor: Prof.Jing Li)

B.S, Tianjin University of Science & Technology (China), June 2007

Major: Applied Chemistry, (Advisor: Prof.Fuzhen Tian)

Publications:

Sun, H., Fan, H., Eom, H., Wang, Z., Peng, X. Reversible coumarin-induced DNA interstrand cross-link and ligation reactions: rearrangement and sequence-dependent photorelease. (In preparation)

Sun, H., Fan, H., Peng, X. Quantitative DNA interstrand cross-link formation by coumarin and thymine: structure determination, sequence effect, and fluorescence detection. *J. Org. Chem.* **2014**, *79*, 11359-11369.

Haque, M. M., Sun, H., Liu, S., Wang, Y., Peng, X. Photo-switchable DNA interstrand cross-link formation by a coumarin-modified nucleotide. *Angew. Chem. Int. Ed.* **2014**, *27*, 7001-7005.

Sun, H., Peng, X. Template directed fluorogenic oligonucleotide ligation using "click" chemistry: detection of single nucleotide polymorphism in the human p53 tumor suppressor gene. *Bioconjugate Chem.* **2013**, *24*, 1226-1234.

Zhao, J., Sun, H., Liu, L., Chang, W., Li, J. Synthesis, characterization and potential electrochemical properties of novel Mn-Re dinuclear complexes containing *N*-heterocyclic carbene-carbon disulfide ligands. *Chemical Journal of Chinese Universities* **2013**, *35*, 68-74.

Kuang, Y., Sun, H., Blain, J. C., Peng, X. Hypoxia-selective DNA interstrand cross-link formation by two modified nucleosides. *Chemistry - A European Journal*, **2012**, *18***,** 12609-12613.

Awards:

Sosnovsky Award for Excellence in Graduate Research, UW-Milwaukee, 2014.4.

Distinguished Graduate Student Fellowship, UW-Milwaukee, 2013-2014.

UW-Milwaukee Chancellor's Graduate Fellowship, UW-Milwaukee, 2010.9-Present.

Tianjin Distinguished Students Award, Tianjin, China, 2005.